

# **Gamma-Ray Bursts**



# Contents

<b>1</b>	<b>Topics</b>	<b>79</b>
<b>2</b>	<b>Participants</b>	<b>81</b>
2.1	ICRANet participants . . . . .	81
2.2	Past collaborators . . . . .	81
2.3	Ongoing collaborations . . . . .	82
2.4	Students . . . . .	83
<b>3</b>	<b>Brief summary of recent progresses</b>	<b>85</b>
<b>4</b>	<b>Selected publications before 2005</b>	<b>87</b>
4.1	Refereed journals . . . . .	87
4.2	Conference proceedings . . . . .	93
<b>5</b>	<b>Publications (2005–2014)</b>	<b>97</b>
5.1	Refereed journals . . . . .	97
5.2	Conference proceedings . . . . .	119



# 1 Topics

- The “canonical” GRB: “genuine short” vs long vs “disguised short” GRBs
- GRBs “Disguised by defect” vs. GRBs “Disguised by excess”.
- “Disguised short” GRB host galaxies: correlation between offset and extended afterglow peak luminosity
- The theoretical explanation of the “Amati relation”
- The “Amati relation” as a tool to identify “disguised short” GRBs
- “Genuine short” GRBs: Possible identifications and selection effects
- A modified spectral energy distribution for highly energetic GRBs
- The observed spectra of the P-GRBs
- GRB prompt emission spectra below 5 keV: challenges for future missions
- Interpretation of the ultra high energy emission from GRBs observed by Fermi and AGILE
- Analysis of different families of progenitors for GRBs with different energetics
- GRBs at redshift  $z > 6$
- GRBs originating from a multiple collapse
- Prompt emission and X-ray flares: the clumpiness of CBM
- Microphysical description of the interaction between the fireshell and the CBM
- Theoretical interpretation of the “plateau” phase in the X-ray afterglow
- Emission from newly born neutron stars, or “neo neutron stars”.
- Induced Gravitational Collapse process for GRBs associated with supernovae.

- Redshift estimators for GRBs with no measured redshift.
- Binary Driven Hypernovae (BdHNe) as progenitor of GRBs via Induced Gravitational Collapse.
- GRB light curves as composed of four different episodes.

# 2 Participants

## 2.1 ICRANet participants

- David Arnett
- Carlo Luciano Bianco
- Massimo Della Valle
- Luca Izzo
- Jorge Armando Rueda Hernandez
- Remo Ruffini
- Gregory Vereshchagin
- She-Sheng Xue

## 2.2 Past collaborators

- Andrey Baranov
- Joao Braga (INPE, Brazil)
- Sabrina Casanova (MPIK, Germany)
- Letizia Caito
- Pascal Chardonnet (Université de Savoie, France)
- Guido Chincarini (Universit di Milano “Bicocca”, Italy)
- Demetrios Christodoulou (ETH Zurich, Switzerland)
- Alessandra Corsi (INAF-IASF Roma, Italy)
- Valeri Chechetkin
- Maria Giovanna Dainotti
- Thibault Damour (IHES, France)

- Walter Ferrara
- Federico Frascchetti (CEA Saclay, France)
- Roberto Guida
- Vahe Gurzadyan (Yerevan Physics Institute, Armenia)
- Wen-Biao Han
- Massimiliano Lattanzi (Oxford Astrophysics, UK)
- Vincenzo Liccardo
- Nino Panagia
- Elena Pian
- Giuliano Preparata (Università di Milano, Italy)
- Jay D. Salmonson (Livermore Lab, USA)
- Vineeth Valsan
- Jim Wilson (Livermore Lab, USA)

### 2.3 Ongoing collaborations

- Alexey Aksenov (ITEP, Russia)
- Lorenzo Amati (INAF-IASF Bologna, Italy)
- Riccardo Belvedere (ICRANet-Rio, Brazil)
- Maria Grazia Bernardini (OAB, Italy)
- Sandip Kumar Chakrabarti (S.N. Bose National Centre and Indian Centre for Space Physics, India)
- Alessandro Chieffi (INAF-IASF Roma, Italy)
- Stefano Covino (OAB, Italy)
- Gustavo de Barros (UFRJ, Brazil)
- Filippo Frontera (Università di Ferrara, Italy)
- Dafne Guetta (OAR, Italy)
- Cristiano Guidorzi (OAB, Italy)

- Stanislav Kelner (MEPhI, Russia, and MPIK, Germany)
- Marco Limongi (OAR, Italy)
- Vanessa Mangano (INAF-IASF Palermo, Italy)
- Barbara Patricelli (Astronomy Institute - UNAM, México))
- Ana Virginia Penacchioni (INPE, Brazil)
- Luis Juracy Rangel Lemos (Fundao Universidade Federal do Tocantins, Brazil)
- Ivan Siutsou (ICRANet-Rio, Brazil)
- Susanna Vergani (Dunsink Observatory, Ireland)
- Francesco Vissani (INFN, Italy)
- Elena Zaninoni (ICRANet-Rio, Brazil)

## 2.4 Students

- Cristina Barbarino (IRAP PhD, Italy)
- Maxime Enderli (IRAP PhD, France)
- Milos Kovacevic (IRAP PhD, Serbia)
- Hendrik Ludwig (IRAP PhD, Germany)
- Marco Muccino (IRAP PhD, Italy)
- Giovanni Battista Pisani (IRAP PhD, Italy)
- Yu Wang (IRAP PhD, China)



### 3 Brief summary of recent progresses

Major progresses have been accomplished this year in the following aspects:

- In introducing the new concept of “Binary Driven Hypernovae” (BdHNe) as progenitors of GRBs with an associated supernova.
- In discovering a “nesting” in the late x-ray light curves of BdHN systems.
- In studying the BdHN scenario up to extreme cosmological distances.
- In studying the different properties of short GRBs “genuine” vs. “disguised by excess”.
- In reviewing old BATSE data finding the same characteristic features of BdHN systems.
- In dividing GRBs in two different families, based on their energetics, thanks to the results of the analysis of GRB 130427A, associated with SN 2013cq, within the BdHN scenario.



# 4 Selected publications before 2005

## 4.1 Refereed journals

1. D. Christodoulou, R. Ruffini; "Reversible Transformations of a Charged Black Hole"; *Physical Review D*, 4, 3552 (1971).

A formula is derived for the mass of a black hole as a function of its "irreducible mass", its angular momentum, and its charge. It is shown that 50% of the mass of an extreme charged black hole can be converted into energy as contrasted with 29% for an extreme rotating black hole.

2. T. Damour, R. Ruffini; "Quantum electro-dynamical effects in Kerr-Newman geometries"; *Physical Review Letters*, 35, 463 (1975).

Following the classical approach of Sauter, of Heisenberg and Euler and of Schwinger the process of vacuum polarization in the field of a "bare" Kerr-Newman geometry is studied. The value of the critical strength of the electromagnetic fields is given together with an analysis of the feedback of the discharge on the geometry. The relevance of this analysis for current astrophysical observations is mentioned.

3. G. Preparata, R. Ruffini, S.-S. Xue; "The dyadosphere of black holes and gamma-ray bursts"; *Astronomy & Astrophysics*, 338, L87 (1999).

The "dyadosphere" has been defined as the region outside the horizon of a black hole endowed with an electromagnetic field (abbreviated to EMBH for "electromagnetic black hole") where the electromagnetic field exceeds the critical value, predicted by Heisenberg & Euler for  $e^\pm$  pair production. In a very short time ( $\sim O(\hbar/mc^2)$ ) a very large number of pairs is created there. We here give limits on the EMBH parameters leading to a Dyadosphere for  $10M_\odot$  and  $10^5M_\odot$  EMBH's, and give as well the pair densities as functions of the radial coordinate. We here assume that the pairs reach thermodynamic equilibrium with a photon gas and estimate the average energy per pair as a function of the EMBH mass. These data give the initial conditions for the analysis of an enormous pair-electromagnetic-pulse or "P.E.M. pulse" which naturally leads to relativistic expansion. Basic energy requirements for gamma ray bursts (GRB), including GRB971214 recently observed at  $z=3.4$ , can be accounted for by processes occurring in the dyadosphere. In this letter we do not address the prob-

lem of forming either the EMBH or the dyadosphere: we establish some inequalities which must be satisfied during their formation process.

4. R. Ruffini, J.D. Salmonson, J.R. Wilson, S.-S. Xue; "On the pair electromagnetic pulse of a black hole with electromagnetic structure"; *Astronomy & Astrophysics*, 350, 334 (1999).

We study the relativistically expanding electron-positron pair plasma formed by the process of vacuum polarization around an electromagnetic black hole (EMBH). Such processes can occur for EMBH's with mass all the way up to  $6 \times 10^5 M_{\odot}$ . Beginning with a idealized model of a Reissner-Nordstrom EMBH with charge to mass ratio  $\zeta = 0.1$ , numerical hydrodynamic calculations are made to model the expansion of the pair-electromagnetic pulse (PEM pulse) to the point that the system is transparent to photons. Three idealized special relativistic models have been compared and contrasted with the results of the numerically integrated general relativistic hydrodynamic equations. One of the three models has been validated: a PEM pulse of constant thickness in the laboratory frame is shown to be in excellent agreement with results of the general relativistic hydrodynamic code. It is remarkable that this precise model, starting from the fundamental parameters of the EMBH, leads uniquely to the explicit evaluation of the parameters of the PEM pulse, including the energy spectrum and the astrophysically unprecedented large Lorentz factors (up to  $6 \times 10^3$  for a  $10^3 M_{\odot}$  EMBH). The observed photon energy at the peak of the photon spectrum at the moment of photon decoupling is shown to range from 0.1 MeV to 4 MeV as a function of the EMBH mass. Correspondingly the total energy in photons is in the range of  $10^{52}$  to  $10^{54}$  ergs, consistent with observed gamma-ray bursts. In these computations we neglect the presence of baryonic matter which will be the subject of forthcoming publications.

5. R. Ruffini, J.D. Salmonson, J.R. Wilson, S.-S. Xue; "On the pair-electromagnetic pulse from an electromagnetic black hole surrounded by a baryonic remnant"; *Astronomy & Astrophysics*, 359, 855 (2000).

The interaction of an expanding Pair-Electromagnetic pulse (PEM pulse) with a shell of baryonic matter surrounding a Black Hole with electromagnetic structure (EMBH) is analyzed for selected values of the baryonic mass at selected distances well outside the dyadosphere of an EMBH. The dyadosphere, the region in which a super critical field exists for the creation of  $e+e-$  pairs, is here considered in the special case of a Reissner-Nordstrom geometry. The interaction of the PEM pulse with the baryonic matter is described using a simplified model of a slab of constant thickness in the laboratory frame (constant-thickness approximation) as well as performing the integration of the general relativistic hydrodynamical equations. The validation of the constant-thickness approximation, already presented in a previous paper Ruffini et al. (1999) for a PEM pulse in vacuum, is here generalized to the presence of baryonic matter. It is found that for a baryonic shell of mass-energy less than 1% of the total

energy of the dyadosphere, the constant-thickness approximation is in excellent agreement with full general relativistic computations. The approximation breaks down for larger values of the baryonic shell mass, however such cases are of less interest for observed Gamma Ray Bursts (GRBs). On the basis of numerical computations of the slab model for PEM pulses, we describe (i) the properties of relativistic evolution of a PEM pulse colliding with a baryonic shell; (ii) the details of the expected emission energy and observed temperature of the associated GRBs for a given value of the EMBH mass;  $10^3 M_{\odot}$ , and for baryonic mass-energies in the range  $10^{-8}$  to  $10^{-2}$  the total energy of the dyadosphere.

6. C.L. Bianco, R. Ruffini, S.-S. Xue; "The elementary spike produced by a pure  $e^+e^-$  pair-electromagnetic pulse from a Black Hole: The PEM Pulse"; *Astronomy & Astrophysics*, 368, 377 (2001).

In the framework of the model that uses black holes endowed with electromagnetic structure (EMBH) as the energy source, we study how an elementary spike appears to the detectors. We consider the simplest possible case of a pulse produced by a pure  $e^+e^-$  pair-electro-magnetic plasma, the PEM pulse, in the absence of any baryonic matter. The resulting time profiles show a *Fast-Rise-Exponential-Decay* shape, followed by a power-law tail. This is obtained without any special fitting procedure, but only by fixing the energetics of the process taking place in a given EMBH of selected mass, varying in the range from 10 to  $10^3 M_{\odot}$  and considering the relativistic effects to be expected in an electron-positron plasma gradually reaching transparency. Special attention is given to the contributions from all regimes with Lorentz  $\gamma$  factor varying from  $\gamma = 1$  to  $\gamma = 10^4$  in a few hundreds of the PEM pulse travel time. Although the main goal of this paper is to obtain the elementary spike intensity as a function of the arrival time, and its observed duration, some qualitative considerations are also presented regarding the expected spectrum and on its departure from the thermal one. The results of this paper will be comparable, when data will become available, with a subfamily of particularly short GRBs not followed by any afterglow. They can also be propedeutical to the study of longer bursts in presence of baryonic matter currently observed in GRBs.

7. R. Ruffini, C.L. Bianco, P. Chardonnet, F. Fraschetti, S.-S. Xue; "Relative spacetime transformations in Gamma-Ray Bursts"; *The Astrophysical Journal*, 555, L107 (2001).

The GRB 991216 and its relevant data acquired from the BATSE experiment and RXTE and Chandra satellites are used as a prototypical case to test the theory linking the origin of gamma ray bursts (GRBs) to the process of vacuum polarization occurring during the formation phase of a black hole endowed with electromagnetic structure (EMBH). The relative space-time transformation paradigm (RSTT paradigm) is presented. It relates the observed signals of GRBs to their past light cones, defining the events on the worldline of the

source essential for the interpretation of the data. Since GRBs present regimes with unprecedentedly large Lorentz  $\gamma$  factor, also sharply varying with time, particular attention is given to the constitutive equations relating the four time variables: the comoving time, the laboratory time, the arrival time at the detector, duly corrected by the cosmological effects. This paradigm is at the very foundation of any possible interpretation of the data of GRBs.

8. R. Ruffini, C.L. Bianco, P. Chardonnet, F. Fraschetti, S.-S. Xue; "On the interpretation of the burst structure of Gamma-Ray Bursts"; *The Astrophysical Journal*, 555, L113 (2001).

Given the very accurate data from the BATSE experiment and RXTE and Chandra satellites, we use the GRB 991216 as a prototypical case to test the EMBH theory linking the origin of the energy of GRBs to the electromagnetic energy of black holes. The fit of the afterglow fixes the only two free parameters of the model and leads to a new paradigm for the interpretation of the burst structure, the IBS paradigm. It leads as well to a reconsideration of the relative roles of the afterglow and burst in GRBs by defining two new phases in this complex phenomenon: a) the injector phase, giving rise to the proper-GRB (P-GRB), and b) the beam-target phase, giving rise to the extended afterglow peak emission (E-APE) and to the afterglow. Such differentiation leads to a natural possible explanation of the bimodal distribution of GRBs observed by BATSE. The agreement with the observational data in regions extending from the horizon of the EMBH all the way out to the distant observer confirms the uniqueness of the model.

9. R. Ruffini, C.L. Bianco, P. Chardonnet, F. Fraschetti, S.-S. Xue; "On a possible Gamma-Ray Burst-Supernova time sequence"; *The Astrophysical Journal*, 555, L117 (2001).

The data from the Chandra satellite on the iron emission lines in the afterglow of GRB 991216 are used to give further support for the EMBH theory, which links the origin of the energy of GRBs to the extractable energy of electromagnetic black holes (EMBHS), leading to an interpretation of the GRB-supernova correlation. Following the relative space-time transformation (RSTT) paradigm and the interpretation of the burst structure (IBS) paradigm, we introduce a paradigm for the correlation between GRBs and supernovae. The following sequence of events is shown as kinematically possible and consistent with the available data: a) the GRB-progenitor star  $P_1$  first collapses to an EMBH, b) the proper GRB (P-GRB) and the peak of the afterglow (E-APE) propagate in interstellar space until the impact on a supernova-progenitor star  $P_2$  at a distance  $\leq 2.69 \times 10^{17}$  cm, and they induce the supernova explosion, c) the accelerated baryonic matter (ABM) pulse, originating the afterglow, reaches the supernova remnants 18.5 hours after the supernova explosion and gives rise to the iron emission lines. Some considerations on the dynamical implementation of the paradigm are presented. The concept of induced supernova

explosion introduced here specifically for the GRB-supernova correlation may have more general application in relativistic astrophysics.

10. R. Ruffini, C.L. Bianco, P. Chardonnet, F. Fraschetti, S.-S. Xue; "On the physical processes which lie at the bases of time variability of GRBs"; *Il Nuovo Cimento B*, 116, 99 (2001).

The relative-space-time-transformation (RSTT) paradigm and the interpretation of the burst-structure (IBS) paradigm are applied to probe the origin of the time variability of GRBs. Again GRB 991216 is used as a prototypical case, thanks to the precise data from the CGRO, RXTE and Chandra satellites. It is found that with the exception of the relatively inconspicuous but scientifically very important signal originating from the initial "proper gamma ray burst" (P-GRB), all the other spikes and time variabilities can be explained by the interaction of the accelerated-baryonic-matter pulse with inhomogeneities in the interstellar matter. This can be demonstrated by using the RSTT paradigm as well as the IBS paradigm, to trace a typical spike observed in arrival time back to the corresponding one in the laboratory time. Using these paradigms, the identification of the physical nature of the time variability of the GRBs can be made most convincingly. It is made explicit the dependence of a) the intensities of the afterglow, b) the spikes amplitude and c) the actual time structure on the Lorentz gamma factor of the accelerated-baryonic-matter pulse. In principle it is possible to read off from the spike structure the detailed density contrast of the interstellar medium in the host galaxy, even at very high redshift.

11. R. Ruffini, C.L. Bianco, P. Chardonnet, F. Fraschetti, S.-S. Xue; "On the structures in the afterglow peak emission of gamma ray bursts"; *The Astrophysical Journal*, 581, L19 (2002).

Using GRB 991216 as a prototype, it is shown that the intensity substructures observed in what is generally called the "prompt emission" in gamma ray bursts (GRBs) do originate in the collision between the accelerated baryonic matter (ABM) pulse with inhomogeneities in the interstellar medium (ISM). The initial phase of such process occurs at a Lorentz factor  $\gamma \sim 310$ . The crossing of ISM inhomogeneities of sizes  $\Delta R \sim 10^{15}$  cm occurs in a detector arrival time interval of  $\sim 0.4$  s implying an apparent superluminal behavior of  $\sim 10^5 c$ . The long lasting debate between the validity of the external shock model vs. the internal shock model for GRBs is solved in favor of the first.

12. R. Ruffini, C.L. Bianco, P. Chardonnet, F. Fraschetti, S.-S. Xue; "On the structure of the burst and afterglow of Gamma-Ray Bursts I: the radial approximation"; *International Journal of Modern Physics D*, 12, 173 (2003).

We have recently proposed three paradigms for the theoretical interpretation of gamma-ray bursts (GRBs). (1) The relative space-time transformation (RSTT) paradigm emphasizes how the knowledge of the entire world-line of the source

from the moment of gravitational collapse is a necessary condition in order to interpret GRB data. (2) The interpretation of the burst structure (IBS) paradigm differentiates in all GRBs between an injector phase and a beam-target phase. (3) The GRB-supernova time sequence (GSTS) paradigm introduces the concept of *induced supernova explosion* in the supernovae-GRB association. In the introduction the RSTT and IBS paradigms are enunciated and illustrated using our theory based on the vacuum polarization process occurring around an electromagnetic black hole (EMBH theory). The results are summarized using figures, diagrams and a complete table with the space-time grid, the fundamental parameters and the corresponding values of the Lorentz gamma factor for GRB 991216 used as a prototype. In the following sections the detailed treatment of the EMBH theory needed to understand the results of the three above letters is presented. We start from the considerations on the dyadosphere formation. We then review the basic hydrodynamic and rate equations, the equations leading to the relative space-time transformations as well as the adopted numerical integration techniques. We then illustrate the five fundamental eras of the EMBH theory: the self acceleration of the  $e^+e^-$  pair-electromagnetic plasma (PEM pulse), its interaction with the baryonic remnant of the progenitor star, the further self acceleration of the  $e^+e^-$  pair-electromagnetic radiation and baryon plasma (PEMB pulse). We then study the approach of the PEMB pulse to transparency, the emission of the proper GRB (P-GRB) and its relation to the "short GRBs". Particular attention is given to the free parameters of the theory and to the values of the thermodynamical quantities at transparency. Finally the three different regimes of the afterglow are described within the fully radiative and radial approximations: the ultrarelativistic, the relativistic and the nonrelativistic regimes. The best fit of the theory leads to an unequivocal identification of the "long GRBs" as extended emission occurring at the afterglow peak (E-APE). The relative intensities, the time separation and the hardness ratio of the P-GRB and the E-APE are used as distinctive observational test of the EMBH theory and the excellent agreement between our theoretical predictions and the observations are documented. The afterglow power-law indexes in the EMBH theory are compared and contrasted with the ones in the literature, and no beaming process is found for GRB 991216. Finally, some preliminary results relating the observed time variability of the E-APE to the inhomogeneities in the interstellar medium are presented, as well as some general considerations on the EMBH formation. The issue of the GSTS paradigm will be the object of a forthcoming publication and the relevance of the iron-lines observed in GRB 991216 is shortly reviewed. The general conclusions are then presented based on the three fundamental parameters of the EMBH theory: the dyadosphere energy, the baryonic mass of the remnant, the interstellar medium density. An in depth discussion and comparison of the EMBH theory with alternative theories is presented as well as indications of further developments beyond the radial approximation, which will be the subject of paper II in this series. Future needs for specific

GRB observations are outlined.

13. R. Ruffini, C.L. Bianco, P. Chardonnet, F. Frascchetti, V. Gurzadyan, S.-S. Xue; "On the instantaneous spectrum of gamma ray bursts"; *International Journal of Modern Physics D*, 13, 843 (2004).

A theoretical attempt to identify the physical process responsible for the afterglow emission of Gamma-Ray Bursts (GRBs) is presented, leading to the occurrence of thermal emission in the comoving frame of the shock wave giving rise to the bursts. The determination of the luminosities and spectra involves integration over an infinite number of Planckian spectra, weighted by appropriate relativistic transformations, each one corresponding to a different viewing angle in the past light cone of the observer. The relativistic transformations have been computed using the equations of motion of GRBs within our theory, giving special attention to the determination of the equitemporal surfaces. The only free parameter of the present theory is the "effective emitting area" in the shock wave front. A self consistent model for the observed hard-to-soft transition in GRBs is also presented. When applied to GRB 991216 a precise fit ( $\chi^2 \simeq 1.078$ ) of the observed luminosity in the 2–10 keV band is obtained. Similarly, detailed estimates of the observed luminosity in the 50–300 keV and in the 10–50 keV bands are obtained.

## 4.2 Conference proceedings

1. R. Ruffini; "Beyond the critical mass: The dyadosphere of black holes"; in "Black Holes and High Energy Astrophysics", H. sato, N. Sugiyama, Editors; p. 167; Universal Academy Press (Tokyo, Japan, 1998).

The "dyadosphere" (from the Greek word "duas-duados" for pairs) is here defined as the region outside the horizon of a black hole endowed with an electromagnetic field (abbreviated to EMBH for "electromagnetic black hole") where the electromagnetic field exceeds the critical value, predicted by Heisenberg and Euler for  $e^+e^-$  pair production. In a very short time ( $\sim O(\hbar/mc^2)$ ), a very large number of pairs is created there. I give limits on the EMBH parameters leading to a Dyadosphere for  $10M_\odot$  and  $10^5M_\odot$  EMBH's, and give as well the pair densities as functions of the radial coordinate. These data give the initial conditions for the analysis of an enormous pair-electromagnetic-pulse or "PEM-pulse" which naturally leads to relativistic expansion. Basic energy requirements for gamma ray bursts (GRB), including GRB971214 recently observed at  $z = 3.4$ , can be accounted for by processes occurring in the dyadosphere.

2. R. Ruffini, C.L. Bianco, P. Chardonnet, F. Frascchetti, L. Vitagliano, S.-S. Xue; "New perspectives in physics and astrophysics from the theoretical understanding of Gamma-Ray Bursts"; in "COSMOLOGY AND

GRAVITATION: Xth Brazilian School of Cosmology and Gravitation; 25th Anniversary (1977-2002)", Proceedings of the Xth Brazilian School on Cosmology and Gravitation, Mangaratiba, Rio de Janeiro (Brazil), July - August 2002, M. Novello, S.E. Perez Bergliaffa, Editors; AIP Conference Proceedings, 668, 16 (2003).

If due attention is given in formulating the basic equations for the Gamma-Ray Burst (GRB) phenomenon and in performing the corresponding quantitative analysis, GRBs open a main avenue of inquiring on totally new physical and astrophysical regimes. This program is very likely one of the greatest computational efforts in physics and astrophysics and cannot be actuated using shortcuts. A systematic approach is needed which has been highlighted in three basic new paradigms: the relative space-time transformation (RSTT) paradigm, the interpretation of the burst structure (IBS) paradigm, the GRB-supernova time sequence (GSTS) paradigm. From the point of view of fundamental physics new regimes are explored: (1) the process of energy extraction from black holes; (2) the quantum and general relativistic effects of matter-antimatter creation near the black hole horizon; (3) the physics of ultrarelativistic shock waves with Lorentz gamma factor  $\gamma > 100$ . From the point of view of astronomy and astrophysics also new regimes are explored: (i) the occurrence of gravitational collapse to a black hole from a critical mass core of mass  $M \gtrsim 10M_{\odot}$ , which clearly differs from the values of the critical mass encountered in the study of stars "catalyzed at the endpoint of thermonuclear evolution" (white dwarfs and neutron stars); (ii) the extremely high efficiency of the spherical collapse to a black hole, where almost 99.99% of the core mass collapses leaving negligible remnant; (iii) the necessity of developing a fine tuning in the final phases of thermonuclear evolution of the stars, both for the star collapsing to the black hole and the surrounding ones, in order to explain the possible occurrence of the "induced gravitational collapse". New regimes are as well encountered from the point of view of nature of GRBs: (I) the basic structure of GRBs is uniquely composed by a proper-GRB (P-GRB) and the afterglow; (II) the long bursts are then simply explained as the peak of the afterglow (the E-APE) and their observed time variability is explained in terms of inhomogeneities in the interstellar medium (ISM); (III) the short bursts are identified with the P-GRBs and the crucial information on general relativistic and vacuum polarization effects are encoded in their spectra and intensity time variability. A new class of space missions to acquire information on such extreme new regimes are urgently needed.

3. R. Ruffini, C.L. Bianco, P. Chardonnet, F. Fraschetti, S.-S. Xue; "The EMBH Model in GRB 991216 and GRB 980425"; in Proceedings of "Third Rome Workshop on Gamma-Ray Burst in the Afterglow Era", 17-20 September 2002; M. Feroci, F. Frontera, N. Masetti, L. Piro, Editors; ASP Conference Series, 312, 349 (2004).

This is a summary of the two talks presented at the Rome GRB meeting by C.L. Bianco and R. Ruffini. It is shown that by respecting the Relative Space-Time Transformation (RSTT) paradigm and the Interpretation of the Burst Structure (IBS) paradigm, important inferences are possible: a) in the new physics occurring in the energy sources of GRBs, b) on the structure of the bursts and c) on the composition of the interstellar matter surrounding the source.

4. M.G. Bernardini, C.L. Bianco, P. Chardonnet, F. Frascchetti, R. Ruffini, S.-S. Xue; "A New Astrophysical 'Triptych': GRB030329/SN2003dh/URCA-2"; in "GAMMA-RAY BURSTS: 30 YEARS OF DISCOVERY", Proceedings of the Los Alamos "Gamma Ray Burst Symposium", Santa Fe, New Mexico, 8-12 September 2003, E.E. Fenimore, M. Galassi, Editors; AIP Conference Proceedings, 727, 312 (2004).

We analyze the data of the Gamma-Ray Burst/Supernova GRB030329/SN2003dh system obtained by HETE-2, R-XTE, XMM and VLT within our theory for GRB030329. By fitting the only three free parameters of the EMBH theory, we obtain the luminosity in fixed energy bands for the prompt emission and the afterglow. Since the Gamma-Ray Burst (GRB) analysis is consistent with a spherically symmetric expansion, the energy of GRB030329 is  $E = 2.1 \times 10^{52}$  erg, namely  $\sim 2 \times 10^3$  times larger than the Supernova energy. We conclude that either the GRB is triggering an induced-supernova event or both the GRB and the Supernova are triggered by the same relativistic process. In no way the GRB can be originated from the supernova. We also evidence that the XMM observations, much like in the system GRB980425/SN1998bw, are not part of the GRB afterglow, as interpreted in the literature, but are associated to the Supernova phenomenon. A dedicated campaign of observations is needed to confirm the nature of this XMM source as a newly born neutron star cooling by generalized URCA processes.

5. F. Frascchetti, M.G. Bernardini, C.L. Bianco, P. Chardonnet, R. Ruffini, S.-S. Xue; "The GRB980425-SN1998bw Association in the EMBH Model"; in "GAMMA-RAY BURSTS: 30 YEARS OF DISCOVERY", Proceedings of the Los Alamos "Gamma Ray Burst Symposium", Santa Fe, New Mexico, 8-12 September 2003, E.E. Fenimore, M. Galassi, Editors; AIP Conference Proceedings, 727, 424 (2004).

Our GRB theory, previously developed using GRB 991216 as a prototype, is here applied to GRB 980425. We fit the luminosity observed in the 40–700 keV, 2–26 keV and 2–10 keV bands by the BeppoSAX satellite. In addition the supernova SN1998bw is the outcome of an "induced gravitational collapse" triggered by GRB 980425, in agreement with the GRB-Supernova Time Sequence (GSTS) paradigm. A further outcome of this astrophysically exceptional sequence of events is the formation of a young neutron star generated by the SN1998bw event. A coordinated observational activity is recommended to

further enlighten the underlying scenario of this most unique astrophysical system.

6. A. Corsi, M.G. Bernardini, C.L. Bianco, P. Chardonnet, F. Fraschetti, R. Ruffini, S.-S. Xue; "GRB 970228 Within the EMBH Model"; in "GAMMA-RAY BURSTS: 30 YEARS OF DISCOVERY", Proceedings of the Los Alamos "Gamma Ray Burst Symposium", Santa Fe, New Mexico, 8-12 September 2003, E.E. Fenimore, M. Galassi, Editors; AIP Conference Proceedings, 727, 428 (2004).

We consider the gamma-ray burst of 1997 February 28 (GRB 970228) within the ElectroMagnetic Black Hole (EMBH) model. We first determine the value of the two free parameters that characterize energetically the GRB phenomenon in the EMBH model, that is to say the dyadosphere energy,  $E_{dya} = 5.1 \times 10^{52}$  ergs, and the baryonic remnant mass  $M_B$  in units of  $E_{dya}$ ,  $B = M_B c^2 / E_{dya} = 3.0 \times 10^{-3}$ . Having in this way estimated the energy emitted during the beam-target phase, we evaluate the role of the InterStellar Medium (ISM) number density ( $n_{ISM}$ ) and of the ratio  $\mathcal{R}$  between the effective emitting area and the total surface area of the GRB source, in reproducing the observed profiles of the GRB 970228 prompt emission and X-ray (2-10 keV energy band) afterglow. The importance of the ISM distribution three-dimensional treatment around the central black hole is also stressed in this analysis.

# 5 Publications (2005–2014)

## 5.1 Refereed journals

1. R. Ruffini, C.L. Bianco, P. Chardonnet, F. Fraschetti, V. Gurzadyan, S.-S. Xue; “Emergence of a filamentary structure in the fireball from GRB spectra”; *International Journal of Modern Physics D*, 14, 97 (2005).

It is shown that the concept of a fireball with a definite filamentary structure naturally emerges from the analysis of the spectra of Gamma-Ray Bursts (GRBs). These results, made possible by the recently obtained analytic expressions of the equitemporal surfaces in the GRB afterglow, depend crucially on the single parameter  $R$  describing the effective area of the fireball emitting the X-ray and gamma-ray radiation. The X-ray and gamma-ray components of the afterglow radiation are shown to have a thermal spectrum in the co-moving frame of the fireball and originate from a stable shock front described self-consistently by the Rankine-Hugoniot equations. Precise predictions are presented on a correlation between spectral changes and intensity variations in the prompt radiation verifiable, e.g., by the Swift and future missions. The highly variable optical and radio emission depends instead on the parameters of the surrounding medium. The GRB 991216 is used as a prototype for this model.

2. R. Ruffini, M.G. Bernardini, C.L. Bianco, P. Chardonnet, F. Fraschetti, V. Gurzadyan, M. Lattanzi, L. Vitagliano, S.-S. Xue; “Extracting energy from black holes: ‘long’ and ‘short’ GRBs and their astrophysical settings”; *Il Nuovo Cimento C*, 28, 589 (2005).

The introduction of the three interpretational paradigms for Gamma-Ray Bursts (GRBs) and recent progress in understanding the X- and gamma-ray luminosity in the afterglow allow us to make assessments about the astrophysical settings of GRBs. In particular, we evidence the distinct possibility that some GRBs occur in a binary system. This subclass of GRBs manifests itself in a “tryptich”: one component formed by the collapse of a massive star to a black hole, which originates the GRB; a second component by a supernova and a third one by a young neutron star born in the supernova event. Similarly, the understanding of the physics of quantum relativistic processes during the gravitational collapse makes possible precise predictions about the structure of short GRBs.

3. M.G. Bernardini, C.L. Bianco, P. Chardonnet, F. Fraschetti, R. Ruffini, S.-S. Xue; “Theoretical interpretation of luminosity and spectral properties of GRB 031203”; *The Astrophysical Journal*, 634, L29 (2005).

The X-ray and gamma-ray observations of the source GRB 031203 by INTEGRAL are interpreted within our theoretical model. In addition to a complete spacetime parameterization of the GRB, we specifically assume that the afterglow emission originates from a thermal spectrum in the comoving frame of the expanding baryonic matter shell. By determining the two free parameters of the model and estimating the density and filamentary structure of the ISM, we reproduce the observed luminosity in the 20-200 keV energy band. As in previous sources, the prompt radiation is shown to coincide with the peak of the afterglow, and the luminosity substructure is shown to originate in the filamentary structure of the ISM. We predict a clear hard-to-soft behavior in the instantaneous spectra. The time-integrated spectrum over 20 s observed by INTEGRAL is well fitted. Despite the fact that this source has been considered “unusual”, it appears to us to be a normal low-energy GRB.

4. R. Ruffini, M.G. Bernardini, C.L. Bianco, P. Chardonnet, F. Fraschetti, S.-S. Xue; Evidence for isotropic emission in GRB991216; *Advances in Space Research*, 38, 1291 (2006).

The issue of the possible presence or absence of jets in GRBs is here re-examined for GRB991216. We compare and contrast our theoretically predicted afterglow luminosity in the 2–10 keV band for spherically symmetric versus jetted emission. At these wavelengths the jetted emission can be excluded and data analysis confirms spherical symmetry. These theoretical fits are expected to be improved by the forthcoming data of the Swift mission.

5. R. Ruffini, M.G. Bernardini, C.L. Bianco, P. Chardonnet, F. Fraschetti, R. Guida, S.-S. Xue; “GRB 050315: A step toward understanding the uniqueness of the overall GRB structure”; *The Astrophysical Journal*, 645, L109 (2006).

Using the Swift data of GRB 050315, we are making progress toward understanding the uniqueness of our theoretically predicted gamma-ray burst (GRB) structure, which is composed of a proper GRB (P-GRB), emitted at the transparency of an electron-positron plasma with suitable baryon loading, and an afterglow comprising the so-called prompt emission due to external shocks. Thanks to the Swift observations, the P-GRB is identified, and for the first time we can theoretically fit detailed light curves for selected energy bands on a continuous timescale ranging over 10<sup>6</sup> s. The theoretically predicted instantaneous spectral distribution over the entire afterglow is presented, confirming a clear hard-to-soft behavior encompassing, continuously, the “prompt emission” all the way to the latest phases of the afterglow.

6. C.L. Bianco, L. Caito, R. Ruffini; “Theoretical interpretation of GRB 011121”; *Il Nuovo Cimento B*, 121, 1441 (2006).

GRB011121 is analyzed as a prototype to understand the “flares” recently observed by *Swift* in the afterglow of many GRB sources. Detailed theoretical computation of the GRB011121 light curves in selected energy bands are presented and compared and contrasted with observational BeppoSAX data.

7. R. Ruffini, M.G. Bernardini, C.L. Bianco, P. Chardonnet, F. Frascetti, R. Guida, S.-S. Xue; “GRB 050315: A step toward the uniqueness of the overall GRB structure”; *Il Nuovo Cimento B*, 121, 1367 (2006).

Using the *Swift* data of GRB 050315, we progress on the uniqueness of our theoretically predicted Gamma-Ray Burst (GRB) structure as composed by a proper-GRB (P-GRB), emitted at the transparency of an electron-positron plasma with suitable baryon loading, and an afterglow comprising the so called “prompt emission” as due to external shocks. Thanks to the *Swift* observations, we can theoretically fit detailed light curves for selected energy bands on a continuous time scale ranging over  $10^6$  seconds. The theoretically predicted instantaneous spectral distribution over the entire afterglow confirms a clear hard-to-soft behavior encompassing, continuously, the “prompt emission” all the way to the latest phases of the afterglow. Consequences of the instrumental threshold on the definition of “short” and “long” GRBs are discussed.

8. M.G. Bernardini, C.L. Bianco, L. Caito, P. Chardonnet, A. Corsi, M.G. Dainotti, F. Frascetti, R. Guida, R. Ruffini, S.-S. Xue; GRB970228 as a prototype for short GRBs with afterglow; *Il Nuovo Cimento B*, 121, 1439 (2006).

GRB970228 is analyzed as a prototype to understand the relative role of short GRBs and their associated afterglows, recently observed by *Swift* and HETE-II. Detailed theoretical computation of the GRB970228 light curves in selected energy bands are presented and compared with observational BeppoSAX data.

9. M.G. Dainotti, M.G. Bernardini, C.L. Bianco, L. Caito, R. Guida, R. Ruffini; “GRB060218 and GRBs associated with Supernovae Ib/c”; *Astronomy & Astrophysics*, 471, L29 (2007).

*Context:* The *Swift* satellite has given continuous data in the range 0.3–150 keV from 0 s to  $10^6$  s for GRB060218 associated with SN2006aj. This Gamma-Ray Burst (GRB) which has an unusually long duration ( $T_{90} \sim 2100$  s) fulfills the Amati relation. These data offer the opportunity to probe theoretical models for GRBs connected with Supernovae (SNe).

*Aims:* We plan to fit the complete  $\gamma$ - and X-ray light curves of this long duration GRB, including the prompt emission, in order to clarify the nature of the progenitors and the astrophysical scenario of the class of GRBs associated with SNe Ib/c.

*Methods:* We apply our “fireshell” model based on the formation of a black hole, giving the relevant references. It is characterized by the precise equations of motion and equitemporal surfaces and by the role of thermal emission.

*Results:* The initial total energy of the electron-positron plasma  $E_{e^\pm}^{tot} = 2.32 \times 10^{50}$  erg has a particularly low value, similar to the other GRBs associated with SNe. For the first time, we observe a baryon loading  $B = 10^{-2}$  which coincides with the upper limit for the dynamical stability of the fireshell. The effective CircumBurst Medium (CBM) density shows a radial dependence  $n_{cbm} \propto r^{-\alpha}$  with  $1.0 \lesssim \alpha \lesssim 1.7$  and monotonically decreases from 1 to  $10^{-6}$  particles/cm<sup>3</sup>. This behavior is interpreted as being due to a fragmentation in the fireshell. Analogies with the fragmented density and filling factor characterizing Novae are outlined. The fit presented is particularly significant in view of the complete data set available for GRB060218 and of the fact that it fulfills the Amati relation.

*Conclusions:* We fit GRB060218, usually considered as an X-Ray Flash (XRF), as a “canonical GRB” within our theoretical model. The smallest possible black hole, formed by the gravitational collapse of a neutron star in a binary system, is consistent with the especially low energetics of the class of GRBs associated with SNe Ib/c. We provide the first evidence for a fragmentation in the fireshell. This fragmentation is crucial in explaining both the unusually large  $T_{90}$  and the consequently inferred abnormally low value of the CBM effective density.

10. M.G. Bernardini, C.L. Bianco, L. Caito, M.G. Dainotti, R. Guida, R. Ruffini; “GRB970228 and a class of GRBs with an initial spikelike emission”; *Astronomy & Astrophysics*, 474, L13 (2007).

*Context:* The discovery by *Swift* and HETE-2 of an afterglow emission associated possibly with short GRBs opened the new problematic of their nature and classification. This issue has been further enhanced by the observation of GRB060614 and by a new analysis of the BATSE catalog which led to the identification of a new class of GRBs with “an occasional softer extended emission lasting tenths of seconds after an initial spikelike emission”.

*Aims:* We plan a twofold task: a) to fit this new class of “hybrid” sources within our “canonical GRB” scenario, where all GRBs are generated by a “common engine” (i.e. the gravitational collapse to a black hole); b) to propose GRB970228 as the prototype of the above mentioned class, since it shares the same morphology and observational features.

*Methods:* We analyze *BeppoSAX* data on GRB970228 within the “fireshell” model and we determine the parameters describing the source and the CircumBurst Medium (CBM) needed to reproduce its light curves in the 40–700 keV and 2–26 keV energy bands.

*Results:* We find that GRB970228 is a “canonical GRB”, like e.g. GRB050315, with the main peculiarity of a particularly low average density of the CBM  $\langle n_{cbm} \rangle \sim 10^{-3}$  particles/cm<sup>3</sup>. We also simulate the light curve corresponding

to a rescaled CBM density profile with  $\langle n_{cbm} \rangle = 1$  particle/cm<sup>3</sup>. From such a comparison it follows that the total time-integrated luminosity is a faithful indicator of the nature of GRBs, contrary to the peak luminosity which is merely a function of the CBM density.

*Conclusions:* We call attention on discriminating the short GRBs between the “genuine” and the “fake” ones. The “genuine” ones are intrinsically short, with baryon loading  $B \lesssim 10^{-5}$ , as stated in our original classification. The “fake” ones, characterized by an initial spikelike emission followed by an extended emission lasting tenths of seconds, have a baryon loading  $10^{-4} \lesssim B \lesssim 10^{-2}$ . They are observed as such only due to an underdense CBM consistent with a galactic halo environment which deflates the afterglow intensity.

11. R. Guida, M.G. Bernardini, C.L. Bianco, L. Caito, M.G. Dainotti, R. Ruffini; “The Amati relation in the “fireshell” model”; *Astronomy & Astrophysics*, 487, L37 (2008).

*Context:* The cosmological origin of gamma-ray bursts (GRBs) has been firmly established, with redshifts up to  $z = 6.29$ . They are possible candidates for use as “distance indicators” for testing cosmological models in a redshift range hardly achievable by other cosmological probes. Asserting the validity of the empirical relations among GRB observables is now crucial for their calibration.

*Aims:* Motivated by the relation proposed by Amati and collaborators, we look within the “fireshell” model for a relation between the peak energy  $E_p$  of the  $\nu F_\nu$  total time-integrated spectrum of the afterglow and the total energy of the afterglow  $E_{aft}$ , which in our model encompasses and extends the prompt emission.

*Methods:* The fit within the fireshell model, as for the “canonical” GRB050315, uses the complete arrival time coverage given by the Swift satellite. It is performed simultaneously, self-consistently, and recursively in the four BAT energy bands (15–25 keV, 25–50 keV, 50–100 keV, and 100–150 keV), as well as in the XRT one (0.2–10 keV). It uniquely determines the two free parameters characterizing the GRB source, the total energy  $E_{tot}^{e^\pm}$  of the  $e^\pm$  plasma and its baryon loading  $B$ , as well as the effective CircumBurst Medium (CBM) distribution. We can then build two sets of “gedanken” GRBs varying the total energy of the electron-positron plasma  $E_{tot}^{e^\pm}$  and keeping the same baryon loading  $B$  of GRB050315. The first set assumes the one obtained in the fit of GRB050315 for the effective CBM density. The second set assumes instead a constant CBM density equal to the average value of the GRB050315 prompt phase.

*Results:* For the first set of “gedanken” GRBs we find a relation  $E_p \propto (E_{aft})^a$ , with  $a = 0.45 \pm 0.01$ , whose slope strictly agrees with the Amati one. Such a relation, in the limit  $B \rightarrow 10^{-2}$ , coincides with the Amati one. Instead, no correlation is found in the second set of “gedanken” GRBs.

*Conclusions:* Our analysis excludes the proper GRB (P-GRB) from the prompt emission, extends all the way to the latest afterglow phases, and is independent of the assumed cosmological model, since all “gedanken” GRBs are at

the same redshift. The Amati relation, on the other hand, includes the P-GRB, focuses only on the prompt emission, being therefore influenced by the instrumental threshold that fixes the end of the prompt emission, and depends on the assumed cosmology. This might explain the intrinsic scatter observed in the Amati relation.

12. L. Caito, M.G. Bernardini, C.L. Bianco, M.G. Dainotti, R. Guida, R. Ruffini; “GRB060614: a “fake” short GRB from a merging binary system”; *Astronomy & Astrophysics*, 489, 501 (2009).

*Context:* GRB060614 observations by VLT and by Swift have infringed the traditionally accepted gamma-ray burst (GRB) collapsar scenario that purports the origin of all long duration GRBs from supernovae (SN). GRB060614 is the first nearby long duration GRB clearly not associated with a bright Ib/c SN. Moreover, its duration ( $T_{90} \sim 100$  s) makes it hardly classifiable as a short GRB. It presents strong similarities with GRB970228, the prototype of a new class of “fake” short GRBs that appear to originate from the coalescence of binary neutron stars or white dwarfs spiraled out into the galactic halo. *Aims:* Within the “canonical” GRB scenario based on the “fireshell” model, we test if GRB060614 can be a “fake” or “disguised” short GRB. We model the traditionally termed “prompt emission” and discriminate the signal originating from the gravitational collapse leading to the GRB from the process occurring in the circumburst medium (CBM). *Methods:* We fit GRB060614 light curves in Swift’s BAT (15 – 150 keV) and XRT (0.2 – 10 keV) energy bands. Within the fireshell model, light curves are formed by two well defined and different components: the proper-GRB (P-GRB), emitted when the fireshell becomes transparent, and the extended afterglow, due to the interaction between the leftover accelerated baryonic and leptonic shell and the CBM. *Results:* We determine the two free parameters describing the GRB source within the fireshell model: the total  $e^\pm$  plasma energy ( $E_{tot}^{e^\pm} = 2.94 \times 10^{51}$  erg) and baryon loading ( $B = 2.8 \times 10^{-3}$ ). A small average CBM density  $\sim 10^{-3}$  particles/cm<sup>3</sup> is inferred, typical of galactic halos. The first spikelike emission is identified with the P-GRB and the following prolonged emission with the extended afterglow peak. We obtain very good agreement in the BAT (15 – 150 keV) energy band, in what is traditionally called “prompt emission”, and in the XRT (0.2 – 10 keV) one. *Conclusions:* The *anomalous* GRB060614 finds a natural interpretation within our canonical GRB scenario: it is a “disguised” short GRB. The total time-integrated extended afterglow luminosity is greater than the P-GRB one, but its peak luminosity is smaller since it is deflated by the peculiarly low average CBM density of galactic halos. This result points to an old binary system, likely formed by a white dwarf and a neutron star, as the progenitor of GRB060614 and well justifies the absence of an associated SN Ib/c. Particularly important for further studies of the final merging process are the temporal structures in the P-GRB down to 0.1 s.

13. M.G. Bernardini, C.L. Bianco, L. Caito, M.G. Dainotti, R. Guida, R. Ruffini; "GRB970228 in the "canonical GRB" scenario"; Journal of the Korean Physical Society, 56, 1575 (2010).

Within the "fireshell" model, we define a "canonical GRB" light curve with two sharply different components: the proper-GRB (P-GRB), emitted when the optically thick fireshell of an electron-positron plasma originating from the phenomenon reaches transparency, and the afterglow, emitted due to the collision between the remaining optically thin fireshell and the circumburst medium (CBM). On the basis of the recent understanding of GRB970228 as the prototype for a new class of GRBs with "an occasional softer extended emission lasting tenths of seconds after an initial spikelike emission", we outline our "canonical GRB" scenario, originating from the gravitational collapse to a black hole, with special emphasis on the discrimination between "genuine" and "fake" short GRBs. Furthermore, we investigate how the GRB970228 analysis provides a theoretical explanation for the apparent absence of such a correlation for the GRBs belonging to this new class.

14. L. Caito, M.G. Bernardini, C.L. Bianco, M.G. Dainotti, R. Guida, R. Ruffini; "GRB060614: a preliminary result"; Journal of the Korean Physical Society, 56, 1579 (2010).

The explosion of GRB 060614 produced a deep break in the GRB scenario and opened new horizons of investigation because it can't be traced back to any traditional scheme of classification. In fact, it manifests peculiarities both of long bursts and of short bursts, and above all, it is the first case of a long-duration near GRB without any bright Ib/c associated Supernova. We will show that, in our canonical GRB scenario, this "anomalous" situation finds a natural interpretation and allows us to discuss a possible variation in the traditional classification scheme, introducing a distinction between "genuine" and "fake" short bursts.

15. M.G. Dainotti, M.G. Bernardini, C.L. Bianco, L. Caito, R. Guida, R. Ruffini; "The astrophysical tryptic: GRB, SN and URCA can be extended to GRB060218?"; Journal of the Korean Physical Society, 56, 1588 (2010).

The *Swift* satellite has given continuous data in the range 0.3–150 keV from 0 s to  $10^6$  s for GRB060218 associated with SN2006aj. This GRB is the fourth GRB spectroscopically associated with SNe after the cases of GRB980425-SN1998bw, GRB031203-SN2003lw, GRB 030329-SN2003dh. It has an unusually long duration ( $T_{90} \sim 2100$  s). These data offer the opportunity to probe theoretical models for Gamma-Ray Bursts (GRBs) connected with Supernovae (SNe). We plan to fit the complete  $\gamma$ - and X-ray light curves of this long duration GRB, including the prompt emission, in order to clarify the nature of the progenitors and the astrophysical scenario of the class of GRBs associated to SNe Ib/c. We apply our "fireshell" model based on the formation of a black hole, giving

the relevant references. The initial total energy of the electron-positron plasma  $E_{e^\pm}^{tot} = 2.32 \times 10^{50}$  erg has a particularly low value similarly to the other GRBs associated with SNe. For the first time we observe a baryon loading  $B = 10^{-2}$  which coincides with the upper limit for the dynamical stability of the fireshell. The effective CircumBurst Medium (CBM) density shows a radial dependence  $n_{cbm} \propto r^{-\alpha}$  with  $1.0 \lesssim \alpha \lesssim 1.7$  and monotonically decreases from 1 to  $10^{-6}$  particles/cm<sup>3</sup>. Such a behavior is interpreted as due to a fragmentation in the fireshell. Such a fragmentation is crucial in explaining both the unusually large  $T_{90}$  and the consequently inferred abnormal low value of the CBM effective density. We fit GRB060218, usually considered as an X-Ray Flash (XRF), as a “canonical GRB” within our theoretical model. The smallest possible black hole, formed by the gravitational collapse of a neutron star in a binary system, is consistent with the especially low energetics of the class of GRBs associated with SNe Ib/c. We present the URCA process and the connection between the GRBs associated with SNe extended also to the case of GRB060218.

16. L. Izzo, M.G. Bernardini, C.L. Bianco, L. Caito, B. Patricelli, R. Ruffini; “GRB 090423 at Redshift 8.1: a Theoretical Interpretation”; *Journal of the Korean Physical Society*, 57, 551 (2010).

GRB 090423 is the farthest gamma ray burst ever observed, with a redshift of about 8.1. We present within the fireshell scenario a complete analysis of this GRB. We model the prompt emission and the first rapid flux decay of the afterglow emission as being to the canonical emission of the interaction in the interval  $0 \leq t \leq 440$  s by using accelerated baryonic matter with the circumburst medium. After the data reduction of the Swift data in the BAT (15 - 150 keV) and XRT (0.2 - 10 keV) energy bands, we interpret the light curves and the spectral distribution in the context of the fireshell scenario. We also confirm in this source the existence of a second component, a plateau phase, as being responsible for the late emission in the X-ray light curve. This extra component originates from the fact that the ejecta have a range of the bulk Lorentz  $\Gamma$  factor, which starts to interact each other ejecta at the start of the plateau phase.

17. L. Caito, L. Amati, M.G. Bernardini, C.L. Bianco, G. De Barros, L. Izzo, B. Patricelli, R. Ruffini; “GRB 071227: an additional case of a disguised short burst”; *Astronomy & Astrophysics*, 521, A80 (2010).

*Context:* Observations of gamma-ray bursts (GRBs) have shown an hybridization between the two classes of long and short bursts. In the context of the fireshell model, the GRB light curves are formed by two different components: the *proper* GRB (P-GRB) and the extended afterglow. Their relative intensity is linked to the fireshell baryon loading  $B$ . The GRBs with P-GRB predominance are the short ones, the remainders are long. A new family of *disguised* short bursts has been identified: long bursts with a protracted low instantaneous luminosity due to a low density CircumBurst Medium (CBM). In the 15–150

keV energy band GRB 071227 exhibits a short duration (about 1.8s) spike-like emission followed by a very soft extended tail up to one hundred seconds after the trigger. It is a faint ( $E_{iso} = 5.8 \times 10^{50}$ ) nearby GRB ( $z = 0.383$ ) that does not have an associated type Ib/c bright supernova (SN). For these reasons, GRB 071227 has been classified as a short burst not fulfilling the Amati relation holding for long burst. *Aims:* We check the classification of GRB 071227 provided by the fireshell model. In particular, we test whether this burst is another example of a *disguised* short burst, after GRB 970228 and GRB 060614, and, for this reason, whether it fulfills the Amati relation. *Methods:* We simulate GRB 071227 light curves in the *Swift* BAT 15–50 keV bandpass and in the XRT (0.3–10 keV) energy band within the fireshell model. *Results:* We perform simulations of the tail in the 15–50 keV bandpass, as well as of the first part of the X-ray afterglow. This infers that:  $E_{tot}^{e^\pm} = 5.04 \times 10^{51}$  erg,  $B = 2.0 \times 10^{-4}$ ,  $E_{P-GRB}/E_{aft} \sim 0.25$ , and  $\langle n_{cbm} \rangle = 3.33$  particles/cm<sup>3</sup>. These values are consistent with those of “long duration” GRBs. We interpret the observed energy of the first hard emission by identifying it with the P-GRB emission. The remaining long soft tail indeed fulfills the Amati relation. *Conclusions:* Previously classified as a short burst, GRB 071227 on the basis of our analysis performed in the context of the fireshell scenario represents another example of a *disguised* short burst, after GRB 970228 and GRB 060614. Further confirmation of this result is that the soft tail of GRB 071227 fulfills the Amati relation.

18. M.G. Bernardini, C.L. Bianco, L. Caito, L. Izzo, B. Patricelli, R. Ruffini; “Analysis of GRB060607A within the fireshell model: prompt emission, X-ray flares and late afterglow phase”; *Astronomy & Astrophysics*, submitted to.

*Context:* GRB060607A is a very distant ( $z = 3.082$ ) and energetic event ( $E_{iso} \sim 10^{53}$  erg). Its main peculiarity is that the peak of the near-infrared (NIR) afterglow has been observed with the REM robotic telescope. This NIR peak has been interpreted as the afterglow onset within the fireball forward shock model, and the initial Lorentz gamma factor of the emitting system has been inferred. *Aims:* We analyze GRB060607A within the fireshell model. We emphasize the central role of the prompt emission in determining the initial Lorentz gamma factor of the extended afterglow and we interpret the X-ray flares as produced by the interaction of the optically thin fireshell with overdense CircumBurst Medium (CBM) clumps. *Methods:* We deal only with the *Swift* BAT and XRT observations, that are the basic contribution to the GRB emission and that are neglected in the treatment adopted in the current literature. The numerical modeling of the fireshell dynamics allows to calculate all its characteristic quantities, in particular the exact value of the Lorentz gamma factor at the transparency. *Results:* We show that the theoretically computed prompt emission light curves are in good agreement with the observations in all the *Swift* BAT energy bands as well as the spectra integrated over different time intervals. The flares observed in the decaying phase of the X-ray afterglow are

also reproduced by the same mechanism, but in a region in which the typical dimensions of the clumps are smaller than the visible area of the fireshell and most energy lies in the X-ray band due to the hard-to-soft evolution. *Conclusions:* We show that it is possible to obtain flares with  $\Delta t/t$  compatible with the observations when the three-dimensional structure of the CBM clumps is duly taken into account. We stop our analysis at the beginning of the X-ray plateau phase, since we suppose this originates from the instabilities developed in the collision between different subshells within a structured fireshell.

19. G. de Barros, M. G. Bernardini, C.L. Bianco, L. Caito, L. Izzo, B. Patricelli, R. Ruffini; "On the nature of GRB 050509b: a disguised short GRB"; *Astronomy & Astrophysics*, 529, A130 (2011)

*Context:* GRB 050509b, detected by the *Swift* satellite, is the first case where an X-ray afterglow has been observed associated with a short gamma-ray burst (GRB). Within the fireshell model, the canonical GRB light curve presents two different components: the proper-GRB (P-GRB) and the extended afterglow. Their relative intensity is a function of the fireshell baryon loading parameter  $B$  and of the CircumBurst Medium (CBM) density ( $n_{CBM}$ ). In particular, the traditionally called short GRBs can be either "genuine" short GRBs (with  $B \lesssim 10^{-5}$ , where the P-GRB is energetically predominant) or "disguised" short GRBs (with  $B \gtrsim 3.0 \times 10^{-4}$  and  $n_{CBM} \ll 1$ , where the extended afterglow is energetically predominant). *Aims:* We verify whether GRB 050509b can be classified as a "genuine" short or a "disguised" short GRB, in the fireshell model. *Methods:* We investigate two alternative scenarios. In the first, we start from the assumption that this GRB is a "genuine" short burst. In the second attempt, we assume that this GRB is a "disguised" burst. *Results:* If GRB 050509b were a genuine short GRB, there should initially be very hard emission which is ruled out by the observations. The analysis that assumes that this is a disguised short GRB is compatible with the observations. The theoretical model predicts a value of the extended afterglow energy peak that is consistent with the Amati relation. *Conclusions:* GRB 050509b cannot be classified as a "genuine" short GRB. The observational data are consistent with a "disguised" short GRB classification, i.e., a long burst with a weak extended afterglow "deflated" by the low density of the CBM. We expect that all short GRBs with measured redshifts are disguised short GRBs because of a selection effect: if there is enough energy in the afterglow to measure the redshift, then the proper GRB must be less energetic than the afterglow. The Amati relation is found to be fulfilled only by the extended afterglow excluding the P-GRB.

20. L. Caito, M.G. Bernardini, C.L. Bianco, L. Izzo, B. Patricelli, R. Ruffini; "GRB 071227: another disguised short burst"; *International Journal of Modern Physics D*, 20, 1931 (2011).

Observations of Gamma-ray Bursts (GRBs) put forward in the recent years have revealed, with increasing evidence, that the historical classification be-

tween long and short bursts has to be revised. Within the Fireshell scenario, both short and long bursts are canonical bursts, consisting of two different phases. First, a Proper-GRB (P-GRB), that is the emission of photons at the transparency of the fireshell. Then, the Extended Afterglow, multiwavelength emission due to the interaction of the baryonic remnants of the fireshell with the CircumBurst Medium (CBM). We discriminate between long and short bursts by the amount of energy stored in the first phase with respect to the second one. Within the Fireshell scenario, we have introduced a third intermediate class: the disguised GRBs. They appear like short bursts, because their morphology is characterized by a first, short, hard episode and a following deflated tail, but this last part — coincident with the peak of the afterglow — is energetically predominant. The origin of this peculiar kind of sources is inferred to a very low average density of the environment (of the order of  $10^{-3}$ ). After GRB 970228 and GRB 060614, we find in GRB 071227 a third example of disguised burst.

21. L. Izzo, M.G. Bernardini, C.L. Bianco, L. Caito, B. Patricelli, L.J. Rangel Lemos, R. Ruffini; “GRB 080916C and the high-energy emission in the fireshell scenario”; *International Journal of Modern Physics D*, 20, 1949 (2011).

In this paper we discuss a possible explanation for the high energy emission (up to  $\sim$  GeV) seen in GRB 080916C. We propose that the GeV emission is originated by the collision between relativistic baryons in the fireshell after the transparency and the nucleons located in molecular clouds near the burst site. This collision should give rise pion production, whose immediate decay provides high energy photons, neutrinos and leptons. Using a public code (SYBILL) we simulate these relativistic collisions in their simple form, so that we can draw our preliminar results in this paper. We will present moreover our hypothesis that the delayed onset of this emission identifies in a complete way the P-GRB emission.

22. B. Patricelli, M.G. Bernardini, C.L. Bianco, L. Caito, L. Izzo, R. Ruffini, G. Vereshchagin; “A new spectral energy distribution of photons in the fireshell model of GRBs”; *International Journal of Modern Physics D*, 20, 1983 (2011).

The analysis of various Gamma-Ray Bursts (GRBs) having a low energetics (an isotropic energy  $E_{iso} \lesssim 10^{53}$  ergs) within the fireshell model has shown how the  $N(E)$  spectrum of their prompt emission can be reproduced in a satisfactory way by a convolution of thermal spectra. Nevertheless, from the study of very energetic bursts ( $E_{iso} \lesssim 10^{54}$  ergs) such as, for example, GRB 080319B, some discrepancies between the numerical simulations and the observational data have been observed. We investigate a different spectrum of photons in the comoving frame of the fireshell in order to better reproduce the spectral properties of GRB prompt emission within the fireshell model. We introduce

a phenomenologically modified thermal spectrum: a thermal spectrum characterized by a different asymptotic power-law index in the low energy region. Such an index depends on a free parameter  $\alpha$ , so that the pure thermal spectrum corresponds to the case  $\alpha = 0$ . We test this spectrum by comparing the numerical simulations with the observed prompt emission spectra of various GRBs. From this analysis it has emerged that the observational data can be correctly reproduced by assuming a modified thermal spectrum with  $\alpha = -1.8$ .

23. A.V. Penacchioni, R. Ruffini, L. Izzo, M. Muccino, C.L. Bianco, L. Caito, B. Patricelli, L. Amati; "Evidence for a proto-black hole and a double astrophysical component in GRB 101023"; *Astronomy & Astrophysics*, 538, A58 (2012).

*Context:* It has been recently shown that GRB 090618, observed by AGILE, Coronas Photon, Fermi, Konus, Suzaku and Swift, is composed of two very different components: episode 1, lasting 50 s, shows a thermal plus power-law spectrum with a characteristic temperature evolving in time as a power law; episode 2 (the remaining 100 s) is a canonical long GRB. We have associated episode 1 to the progenitor of a collapsing bare core leading to the formation of a black hole: what was defined as a "proto black hole". *Aims:* In precise analogy with GRB 090618 we aim to analyze the 89s of the emission of GRB 101023, observed by Fermi, Gemini, Konus and Swift, to see if there are two different episodes: the first one presenting a characteristic black-body temperature evolving in time as a broken power law, and the second one consistent with a canonical GRB. *Methods:* To obtain information on the spectra, we analyzed the data provided by the GBM detector onboard the Fermi satellite, and we used the heasoft package XSPEC and RMFIT to obtain their spectral distribution. We also used the numerical code GRBsim to simulate the emission in the context of the fireshell scenario for episode 2. *Results:* We confirm that the first episode can be well fit by a black body plus power-law spectral model. The temperature changes with time following a broken power law, and the photon index of the power-law component presents a soft-to-hard evolution. We estimate that the radius of this source increases with time with a velocity of  $1.5 \times 10^4 km/s$ . The second episode appears to be a canonical GRB. By using the Amati and the Atteia relations, we determined the cosmological redshift,  $z \sim 0.9 \pm 0.084(stat.) \pm 0.2(sys.)$ . The results of GRB 090618 are compared and contrasted with the results of GRB 101023. Particularly striking is the scaling law of the soft X-ray component of the afterglow. *Conclusions:* We identify GRB 090618 and GRB 101023 with a new family of GRBs related to a single core collapse and presenting two astrophysical components: a first one related to the proto-black hole prior to the process of gravitational collapse (episode 1), and a second one, which is the canonical GRB (episode 2) emitted during the formation of the black hole. For the first time we are witnessing the process of a black hole formation from the instants preceding the gravitational collapse up to the GRB emission. This analysis indicates progress towards developing

---

a GRB distance indicator based on understanding the P-GRB and the prompt emission, as well as the soft X-ray behavior of the late afterglow.

24. R. Negreiros, R. Ruffini, C. L. Bianco, J. A. Rueda; “Cooling of young neutron stars in GRB associated to supernovae”; *Astronomy & Astrophysics*, 540, A12 (2012).

*Context:* The traditional study of neutron star cooling has been generally applied to quite old objects such as the Crab Pulsar (957 years) or the central compact object in Cassiopeia A (330 years) with an observed surface temperature  $\sim 10^6$  K. However, recent observations of the late ( $t = 10^8$ – $10^9$  s) emission of the supernovae (SNe) associated to GRBs (GRB-SN) show a distinctive emission in the X-ray regime consistent with temperatures  $\sim 10^7$ – $10^8$  K. Similar features have been also observed in two Type Ic SNe SN 2002ap and SN 1994I that are not associated to GRBs. *Aims:* We advance the possibility that the late X-ray emission observed in GRB-SN and in isolated SN is associated to a hot neutron star just formed in the SN event, here defined as a neo-neutron star. *Methods:* We discuss the thermal evolution of neo-neutron stars in the age regime that spans from  $\sim 1$  minute (just after the proto-neutron star phase) all the way up to ages  $< 10$ – $100$  yr. We examine critically the key factor governing the neo-neutron star cooling with special emphasis on the neutrino emission. We introduce a phenomenological heating source, as well as new boundary conditions, in order to mimic the high temperature of the atmosphere for young neutron stars. In this way we match the neo-neutron star luminosity to the observed late X-ray emission of the GRB-SN events: URCA-1 in GRB980425-SN1998bw, URCA-2 in GRB030329-SN2003dh, and URCA-3 in GRB031203-SN2003lw. *Results:* We identify the major role played by the neutrino emissivity in the thermal evolution of neo-neutron stars. By calibrating our additional heating source at early times to  $\sim 10^{12}$ – $10^{15}$  erg/g/s, we find a striking agreement of the luminosity obtained from the cooling of a neo-neutron stars with the prolonged ( $t = 10^8$ – $10^9$  s) X-ray emission observed in GRB associated with SN. It is therefore appropriate a revision of the boundary conditions usually used in the thermal cooling theory of neutron stars, to match the proper conditions of the atmosphere at young ages. The traditional thermal processes taking place in the crust might be enhanced by the extreme high-temperature conditions of a neo-neutron star. Additional heating processes that are still not studied within this context, such as  $e^+e^-$  pair creation by overcritical fields, nuclear fusion, and fission energy release, might also take place under such conditions and deserve further analysis. *Conclusions:* Observation of GRB-SN has shown the possibility of witnessing the thermal evolution of neo-neutron stars. A new campaign of dedicated observations is recommended both of GRB-SN and of isolated Type Ic SN.

25. L. Izzo, R. Ruffini, A.V. Penacchioni, C.L. Bianco, L. Caito, S.K. Chakrabarti, J.A. Rueda, A. Nandi, B. Patricelli; “A double component in GRB 090618:

a proto-black hole and a genuinely long gamma-ray burst”; *Astronomy & Astrophysics*, 543, A10 (2012).

*Context:* The joint X-ray and gamma-ray observations of GRB 090618 by very many satellites offer an unprecedented possibility of testing crucial aspects of theoretical models. In particular, they allow us to test (a) in the process of gravitational collapse, the formation of an optically thick  $e^+e^-$ -baryon plasma self-accelerating to Lorentz factors in the range  $200 < \Gamma < 3000$ ; (b) its transparency condition with the emission of a component of  $10^{53-54}$  baryons in the TeV region and (c) the collision of these baryons with the circumburst medium (CBM) clouds, characterized by dimensions of  $10^{15-16}$  cm. In addition, these observations offer the possibility of testing a new understanding of the thermal and power-law components in the early phase of this GRB. *Aims:* We test the fireshell model of GRBs in one of the closest ( $z = 0.54$ ) and most energetic ( $E_{iso} = 2.90 \times 10^{53}$  erg) GRBs, namely GRB 090618. It was observed at ideal conditions by several satellites, namely *Fermi*, *Swift*, Konus-WIND, AGILE, RT-2, and Suzaku, as well as from on-ground optical observatories. *Methods:* We analyzed the emission from GRB 090618 using several spectral models, with special attention to the thermal and power-law components. We determined the fundamental parameters of a canonical GRB within the context of the fireshell model, including the identification of the total energy of the  $e^+e^-$  plasma,  $E_{tot}^{e^+e^-}$ , the proper GRB (P-GRB), the baryon load, the density and structure of the CBM. *Results:* We find evidence of the existence of two different episodes in GRB 090618. The first episode lasts 50 s and is characterized by a spectrum consisting of a thermal component, which evolves between  $kT = 54$  keV and  $kT = 12$  keV, and a power law with an average index  $\gamma = 1.75 \pm 0.04$ . The second episode, which lasts for  $\sim 100$  s, behaves as a canonical long GRB with a Lorentz gamma factor at transparency of  $\Gamma = 495$ , a temperature at transparency of 29.22 keV and with a characteristic size of the surrounding clouds of  $R_{cl} \sim 10^{15-16}$  cm and masses of  $\sim 10^{22-24}$  g. *Conclusions:* We support the recently proposed two-component nature of GRB 090618, namely, episode 1 and episode 2, with a specific theoretical analysis. We furthermore illustrate that episode 1 cannot be considered to be either a GRB or a part of a GRB event, but it appears to be related to the progenitor of the collapsing bare core, leading to the formation of the black hole, which we call a “proto-black hole”. Thus, for the first time, we are witnessing the process of formation of a black hole from the phases just preceding the gravitational collapse all the way up to the GRB emission.

26. B. Patricelli, M.G. Bernardini, C.L. Bianco, L. Caito, G. De Barros, L. Izzo, R. Ruffini, G.V. Vereshchagin; “Analysis of GRB 080319B and GRB 050904 within the Fireshell Model: Evidence for a Broader Spectral Energy Distribution”; *The Astrophysical Journal*, 756, 16 (2012).

The observation of GRB 080319B, with an isotropic energy  $E_{iso} = 1.32 \times 10^{54}$

erg, and GRB 050904, with  $E_{iso} = 1.04 \times 10^{54}$  erg, offers the possibility of studying the spectral properties of the prompt radiation of two of the most energetic Gamma Ray Bursts (GRBs). This allows us to probe the validity of the fireshell model for GRBs beyond  $10^{54}$  erg, well outside the energy range where it has been successfully tested up to now ( $10^{49}$ – $10^{53}$  erg). We find that in the low energy region, the prompt emission spectra observed by *Swift* BAT reveals more power than theoretically predicted. The opportunities offered by these observations to improve the fireshell model are outlined in this paper. One of the distinguishing features of the fireshell model is that it relates the observed GRB spectra to the spectrum in the comoving frame of the fireshell. Originally, a fully radiative condition and a comoving thermal spectrum were adopted. An additional power-law in the comoving thermal spectrum is required due to the discrepancy of the theoretical and observed light curves and spectra in the fireshell model for GRBs 080319B and 050904. A new phenomenological parameter  $\alpha$  is correspondingly introduced in the model. We perform numerical simulations of the prompt emission in the *Swift* BAT bandpass by assuming different values of  $\alpha$  within the fireshell model. We compare them with the GRB 080319B and GRB 050904 observed time-resolved spectra, as well as with their time-integrated spectra and light curves. Although GRB 080319B and GRB 050904 are at very different redshifts ( $z=0.937$  and  $z=6.29$  respectively), a value of  $\alpha = -1.8$  leads for both of them to a good agreement between the numerical simulations and the observed BAT light curves, time-resolved and time-integrated spectra. Such a modified spectrum is also consistent with the observations of previously analyzed less energetic GRBs and reasons for this additional agreement are given. Perspectives for future low energy missions are outlined.

27. M. Muccino, R. Ruffini, C.L. Bianco, L. Izzo, A.V. Penacchioni; “GRB 090227B: The missing link between the genuine short and long GRBs”; *The Astrophysical Journal*, 763, 125 (2013).

The time-resolved spectral analysis of GRB 090227B, made possible by the *Fermi*-GBM data, allows to identify in this source the missing link between the genuine short and long GRBs. Within the Fireshell model of the Gamma-Ray Bursts (GRBs) we predict genuine short GRBs: bursts with the same inner engine of the long bursts but endowed with a severely low value of the Baryon load,  $B \lesssim 5 \times 10^{-5}$ . A first energetically predominant emission occurs at the transparency of the  $e^+e^-$  plasma, the Proper-GRB (P-GRB), followed by a softer emission, the extended afterglow. The typical separation between the two emissions is expected to be of the order of  $10^{-3} - 10^{-2}$  s. We identify the P-GRB of GRB 090227B in the first 96 ms of emission, where a thermal component with the temperature  $kT = (517 \pm 28)$  keV and a flux comparable with the non thermal part of the spectrum is observed. This non thermal component as well as the subsequent emission, where there is no evidence for a thermal spectrum, is identified with the extended afterglow. We deduce a the-

oretical cosmological redshift  $z = 1.61 \pm 0.14$ . We then derive the total energy  $E_{e^+e^-}^{tot} = (2.83 \pm 0.15) \times 10^{53}$  ergs, the Baryon load  $B = (4.13 \pm 0.05) \times 10^{-5}$ , the Lorentz  $\Gamma$  factor at transparency  $\Gamma_{tr} = (1.44 \pm 0.01) \times 10^4$ , and the intrinsic duration  $\Delta t' \sim 0.35$  s. We also determine the average density of the CircumBurst Medium (CBM),  $\langle n_{CBM} \rangle = (1.90 \pm 0.20) \times 10^{-5}$  particles/cm<sup>3</sup>. There is no evidence of beaming in the system. In view of the energetics and of the Baryon load of the source, as well as of the low interstellar medium and of the intrinsic time scale of the signal, we identify the GRB progenitor as a binary neutron star. From the recent progress in the theory of neutron stars, we obtain masses of the stars  $m_1 = m_2 = 1.34M_{\odot}$  and their corresponding radii  $R_1 = R_2 = 12.24$  km and thickness of their crusts  $\sim 0.47$  km, consistent with the above values of the Baryon load, of the energetics and of the time duration of the event.

28. A.V. Penacchioni, R. Ruffini, C.L. Bianco, L. Izzo, M. Muccino, G.B. Pisani, J.A. Rueda; “GRB 110709B in the induced gravitational collapse paradigm”; *Astronomy & Astrophysics*, 551, A133 (2013).

*Context:* GRB 110709B is the first source for which *Swift* BAT triggered twice, with a time separation of  $\sim 10$  minutes. The first emission (called here Episode 1) goes from 40 s before the first trigger up to 60 s after it. The second emission (hereafter Episode 2) goes from 35 s before the second trigger to 100 s after it. These features reproduce the ones of GRB 090618, which has been recently interpreted within the Induced Gravitational Collapse paradigm (IGC). In line with this paradigm we assume the progenitor to be a close binary system composed of a core of an evolved star and a Neutron Star (NS). The evolved star explodes as a Supernova (SN) and ejects material that is partially accreted by the NS. We identify this process with Episode 1. The accretion process brings the NS over its critical mass, thus gravitationally collapsing to a BH. This process leads to the GRB emission, Episode 2. The double trigger has given for the first time the possibility to have a coverage of the X-ray emission observed by XRT both prior to and during the prompt phase of GRB 110709B. *Aims:* We analyze the spectra and time variability of Episode 1 and 2 and compute the relevant parameters of the binary progenitor, as well as the astrophysical parameters both in the SN and the GRB phase in the IGC paradigm. *Methods:* We perform a time-resolved spectral analysis of Episode 1 by fitting the spectrum with a blackbody (BB) plus a power-law (PL) spectral model. From the BB fluxes and temperatures of Episode 1 and the luminosity distance  $d_L$ , we evaluate the evolution with time of the radius of the BB emitter, associated here to the evolution of the SN ejecta. We analyze Episode 2 within the Fireshell model, identifying the Proper-GRB (P-GRB) and simulating the light curve and spectrum. We establish the redshift to be  $z = 0.75$ , following the phenomenological methods by Amati, by Yonetoku and by Grupe, and our analysis of the late X-ray afterglow. It is most remarkable that the determination of the cosmological redshift on the ground of the scaling of the late X-ray afterglow, already verified in GRB 090618 and GRB 101023, is again verified

by this analysis. *Results:* We find for Episode 1 a temperature of the BB component that evolves with time following a broken PL, with the slope of the PL at early times  $\alpha = 0$  (constant function) and the slope of the PL at late times  $\beta = -4 \pm 2$ . The break occurs at  $t = 41.21$  s. The total energy of Episode 1 is  $E_{iso}^{(1)} = 1.42 \times 10^{53}$  erg. The total energy of Episode 2 is  $E_{iso}^{(2)} = 2.43 \times 10^{52}$  erg. We find at transparency a Lorentz factor  $\Gamma \sim 1.73 \times 10^2$ , laboratory radius of  $6.04 \times 10^{13}$  cm, P-GRB observed temperature  $kT_{P-GRB} = 12.36$  keV, baryon load  $B = 5.7 \times 10^{-3}$  and P-GRB energy of  $E_{P-GRB} = 3.44 \times 10^{50}$  erg. We find a remarkable coincidence of the cosmological redshift by the scaling of the XRT data and with three other phenomenological methods. *Conclusions:* We interpret GRB 110709B as a member of the IGC sources, together with GRB 970828, GRB 090618 and GRB 101023. The existence of the XRT data during the prompt phase of the emission of GRB 110709B (Episode 2) offers an unprecedented tool for improving the diagnostic of GRBs emission.

29. G.B. Pisani, L. Izzo, R. Ruffini, C.L. Bianco, M. Muccino, A.V. Penacchioni, J.A. Rueda, Y. Wang; “Novel distance indicator for gamma-ray bursts associated with supernovae”; *Astronomy & Astrophysics*, 552, L5 (2013).

*Context:* In recent years it has been proposed that the temporal coincidence of a Gamma Ray Burst (GRB) and a type Ib/c supernova (SN) can be explained by the concept of Induced Gravitational Collapse (IGC) of a Neutron Star (NS) to a Black Hole (BH) by accretion of matter ejected by a SN Ib/c. This scenario reveals a possible common behavior in the late time X-ray emission of this subclass of GRBs. *Aims:* We want to test if such a common behavior can actually be present in the sources belonging to this GRB sub-class and if this may lead to a redshift estimator for these sources. *Methods:* We build a sample of GRBs belonging to this sub-class, and we rescale the X-ray light curves of all of them both in time and in flux to a common cosmological redshift. *Results:* We found that the X-ray light curves of all the GRBs of the sample with a measured redshift present a common late time behavior when rescaled to a common redshift  $z = 1$ . We then use this result to estimate the redshift of the GRBs of the sample with no measured redshift. *Conclusions:* The common behavior in the late decay of the X-ray light curves of the GRBs of the sample points to a common physical mechanism in this particular phase of the GRB emission, possibly related to the SN process. This scenario may represent an invaluable tool to estimate the redshift of GRBs belonging to this sub-class of events. More GRBs are therefore needed in order to enlarge the subclass and to make more stringent constraints on the redshift estimates performed with this method for GRBs pertaining to this class.

30. C.L. Bianco, M. G. Bernardini, L. Caito, G. De Barros, L. Izzo, M. Muccino, B. Patricelli, A.V. Penacchioni, G.B. Pisani, R. Ruffini; “The canonical GRB scenario”; *Il Nuovo Cimento C*, 36 s01, 21 (2013).

The canonical GRB scenario implied by the fireshell model is briefly summarized.

31. A.V. Penacchioni, R. Ruffini, L. Izzo, M. Muccino, C.L. Bianco, L. Caito, B. Patricelli; “Evidences for a double component in the emission of GRB 101023”; *Il Nuovo Cimento C*, 36 s01, 117 (2013).

In this work we present the results of the analysis of GRB 101023 in the fireshell scenario. Its redshift is not known, so we attempted to infer it from the Amati Relation, obtaining  $z = 0.9$ . Its light curve presents a double emission, which makes it very similar to the already studied GRB 090618. We called each part Episode 1 and Episode 2. We performed a time-resolved spectral analysis with RMFIT using different spectral models, and fitted the light curve with a numerical code integrating the fireshell equations of motion. We used Fermi GBM data to build the light curve, in particular the second NaI detector, in the range (8.5–1000 keV). We considered different hypotheses regarding which part of the light curve could be the GRB and performed the analysis of all of them. We noticed a great variation of the temperature with time in the first episode, as well as almost no variation of the progenitor radius. We found that the first emission does not match the requirements for a GRB, while the second part perfectly agrees with being a canonical GRB, with a P-GRB lasting 4 s.

32. M. Muccino, R. Ruffini, C.L. Bianco, L. Izzo, A.V. Penacchioni, G.B. Pisani; “GRB 090510: A Disguised Short Gamma-Ray Burst with the Highest Lorentz Factor and Circumburst Medium”; *The Astrophysical Journal*, 772, 62 (2013).

GRB 090510, observed both by Fermi and AGILE satellites, is the first bright short-hard Gamma-Ray Burst (GRB) with an emission from the keV up to the GeV energy range. Within the Fireshell model, we interpret the faint precursor in the light curve as the emission at the transparency of the expanding  $e^+e^-$  plasma: the Proper-GRB (P-GRB). From the observed isotropic energy we assume a total plasma energy  $E_{e^+e^-}^{tot} = (1.10 \pm 0.06) \times 10^{53}$  erg and derive a Baryon load  $B = (1.45 \pm 0.28) \times 10^{-3}$  and a Lorentz factor at transparency  $\Gamma_{tr} = (6.7 \pm 1.6) \times 10^2$ . The main emission  $\sim 0.4$ s after the initial spike is interpreted as the extended afterglow, due to the interaction of the ultrarelativistic baryons with the CircumBurst Medium (CBM). Using the condition of fully radiative regime, we infer a CBM average spherically symmetric density of  $\langle n_{CBM} \rangle = (1.85 \pm 0.14) \times 10^3$  particles/cm<sup>3</sup>, one of the highest found in the Fireshell model. The value of the filling factor,  $1.5 \times 10^{-10} \leq \mathcal{R} \leq 3.8 \times 10^{-8}$ , leads to the estimate of filaments with densities  $n_{fil} = n_{CBM}/\mathcal{R} \approx (10^6 - 10^{14})$  particles/cm<sup>3</sup>. The sub-MeV and the MeV emissions are well reproduced. When compared to the canonical GRBs with  $\langle n_{CBM} \rangle \approx 1$  particles/cm<sup>3</sup> and to the disguised short GRBs with  $\langle n_{CBM} \rangle \approx 10^{-3}$  particles/cm<sup>3</sup>, the case of GRB 090510 leads to the existence of a new family of bursts exploding in an

over-dense galactic region with  $\langle n_{CBM} \rangle \approx 10^3$  particles/cm<sup>3</sup>. The joint effect of the high  $\Gamma_{tr}$  and the high density compresses in time and “inflates” in intensity the extended afterglow, making it appear as a short burst, which we here define as “disguised short GRB by excess”. The determination of the above parameters values may represent an important step towards the explanation of the GeV emission.

33. R. Ruffini, M. Muccino, C.L. Bianco, M. Enderli, L. Izzo, M. Kovacevic, A.V. Penacchioni, G.B. Pisani, J.A. Rueda, Y. Wang; “On Binary Driven Hypernovae and their nested late X-ray emission”; *Astronomy & Astrophysics*, 565, L10 (2014).

*Context:* The induced gravitational collapse (IGC) paradigm addresses the very energetic ( $10^{52}$ – $10^{54}$  erg) long gamma-ray bursts (GRBs) associated to supernovae (SNe). Unlike the traditional “collapsar” model, an evolved FeCO core with a companion neutron star (NS) in a tight binary system is considered as the progenitor. This special class of sources, here named “binary driven hypernovae” (BdHNe), presents a composite sequence composed of four different episodes with precise spectral and luminosity features.

*Aims:* We first compare and contrast the steep decay, the plateau, and the power-law decay of the X-ray luminosities of three selected BdHNe (GRB 060729, GRB 061121, and GRB 130427A). Second, to explain the different sizes and Lorentz factors of the emitting regions of the four episodes, for definiteness, we use the most complete set of data of GRB 090618. Finally, we show the possible role of r-process, which originates in the binary system of the progenitor.

*Methods:* We compare and contrast the late X-ray luminosity of the above three BdHNe. We examine correlations between the time at the starting point of the constant late power-law decay  $t_a^*$ , the average prompt luminosity  $\langle L_{iso} \rangle$ , and the luminosity at the end of the plateau  $L_a$ . We analyze a thermal emission ( $\sim 0.97$ – $0.29$  keV), observed during the X-ray steep decay phase of GRB 090618.

*Results:* The late X-ray luminosities of the three BdHNe, in the rest-frame energy band 0.3–10 keV, show a precisely constrained “nested” structure. In a space-time diagram, we illustrate the different sizes and Lorentz factors of the emitting regions of the three episodes. For GRB 090618, we infer an initial dimension of the thermal emitter of  $\sim 7 \times 10^{12}$  cm, expanding at  $\Gamma \approx 2$ . We find tighter correlations than the Dainotti-Willingale ones.

*Conclusions:* We confirm a constant slope power-law behavior for the late X-ray luminosity in the source rest frame, which may lead to a new distance indicator for BdHNe. These results, as well as the emitter size and Lorentz factor, appear to be inconsistent with the traditional afterglow model based on synchrotron emission from an ultra-relativistic ( $\Gamma \sim 10^2$ – $10^3$ ) collimated jet outflow. We argue, instead, for the possible role of r-process, originating in the binary system, to power the mildly relativistic X-ray source.

34. R. Ruffini, L. Izzo, M. Muccino, G.B. Pisani, J.A. Rueda, Y. Wang, C. Barbarino, C.L. Bianco, M. Enderli, M. Kovacevic; “Induced gravitational collapse at extreme cosmological distances: the case of GRB 090423”; *Astronomy & Astrophysics*, 569, A39 (2014).

*Context:* The induced gravitational collapse (IGC) scenario has been introduced in order to explain the most energetic gamma ray bursts (GRBs),  $E_{iso} = 10^{52} - 10^{54}$  erg, associated with type Ib/c supernovae (SNe). It has led to the concept of binary-driven hypernovae (BdHNe) originating in a tight binary system composed by a FeCO core on the verge of a SN explosion and a companion neutron star (NS). Their evolution is characterized by a rapid sequence of events: 1) The SN explodes, giving birth to a new NS ( $\nu$ NS). The accretion of SN ejecta onto the companion NS increases its mass up to the critical value; 2) The consequent gravitational collapse is triggered, leading to the formation of a black hole (BH) with GRB emission; 3) A novel feature responsible for the emission in the GeV, X-ray, and optical energy range occurs and is characterized by specific power-law behavior in their luminosity evolution and total spectrum; 4) The optical observations of the SN then occurs.

*Aims:* We investigate whether GRB 090423, one of the farthest observed GRB at  $z = 8.2$ , is a member of the BdHN family.

*Methods:* We compare and contrast the spectra, the luminosity evolution, and the detectability in the observations by *Swift* of GRB 090423 with the corresponding ones of the best known BdHN case, GRB 090618.

*Results:* Identification of constant slope power-law behavior in the late X-ray emission of GRB 090423 and its overlapping with the corresponding one in GRB 090618, measured in a common rest frame, represents the main result of this article. This result represents a very significant step on the way to using the scaling law properties, proven in Episode 3 of this BdHN family, as a cosmological standard candle.

*Conclusions:* Having identified GRB 090423 as a member of the BdHN family, we can conclude that SN events, leading to NS formation, can already occur already at  $z = 8.2$ , namely at 650 Myr after the Big Bang. It is then possible that these BdHNe originate stem from 40-60  $M_{\odot}$  binaries. They are probing the Population II stars after the completion and possible disappearance of Population III stars.

35. M. Muccino, C.L. Bianco, L. Izzo, Y. Wang, M. Enderli, M. Kovacevic, G.B. Pisani, A.V. Penacchioni, R. Ruffini; “The Genuine Short GRB 090227B and the Disguised by Excess GRB 090510”; *Gravitation and Cosmology*, 20, 197 (2014).

GRB 090227B and GRB 090510, traditionally classified as short gamma-ray Bursts (GRBs), indeed originate from different systems. For GRB 090227B we inferred a total energy of the  $e^+e^-$  plasma  $E_{e^+e^-}^{tot} = (2.83 \pm 0.15) \times 10^{53}$  erg, a baryon load of  $B = (4.1 \pm 0.05) \times 10^{-5}$ , and a CircumBurst Medium (CBM)

average density  $\langle n_{CBM} \rangle = (1.90 \pm 0.20) \times 10^{-5} \text{ cm}^{-3}$ . From these results we have assumed the progenitor of this burst to be a symmetric neutron stars (NSs) merger with masses  $m = 1.34M_{\odot}$ , radii  $R = 12.24 \text{ km}$ . GRB 090510, instead, has  $E_{e^+e^-}^{tot} = (1.10 \pm 0.06) \times 10^{53} \text{ erg}$ ,  $B = (1.45 \pm 0.28) \times 10^{-3}$ , implying a Lorentz factor at transparency of  $\Gamma = (6.7 \pm 1.7) \times 10^2$ , which are characteristic of the long GRB class, and a very high CBM density,  $\langle n_{CBM} \rangle = (1.85 \pm 0.14) \times 10^3 \text{ cm}^{-3}$ . The joint effect of the high values of  $\Gamma$  and of  $\langle n_{CBM} \rangle$  compresses in time and “inflates” in intensity in an extended afterglow, making appear GRB 090510 as a short burst, which we here define as “disguised short GRB by excess” occurring an overdense region with  $10^3 \text{ cm}^{-3}$ .

36. M. Muccino, C.L. Bianco, L. Izzo, Y. Wang, M. Enderli, G.B. Pisani, A.V. Penacchioni, R. Ruffini; “Two short bursts originating from different astrophysical systems: The genuine short GRB 090227B and the disguised short GRB 090510 by excess”; *Journal of the Korean Physical Society*, 65, 865 (2014).

GRB 090227B and GRB 090510 are two gamma-ray bursts (GRBs) traditionally classified as short bursts. The major outcome of our analysis is that they indeed originate from different systems. In the case of GRB 090227B, from the inferred values of the total energy of the  $e^+e^-$  plasma,  $E_{e^+e^-}^{tot} = (2.83 \pm 0.15) \times 10^{53} \text{ erg}$ , the engulfed baryonic mass  $M_B$ , expressed as  $B = M_B c^2 / E_{e^+e^-}^{tot} = (4.1 \pm 0.05) \times 10^{-5}$ , and the circumburst medium (CBM) average density,  $\langle n_{CBM} \rangle = (1.90 \pm 0.20) \times 10^{-5} \text{ cm}^{-3}$ , we have assumed the progenitor of this burst to be a symmetric neutron star (NS) merger with masses  $m = 1.34M_{\odot}$ , radii  $R = 12.24 \text{ km}$ , and crustal thicknesses of  $\sim 0.47 \text{ km}$ . In the case of GRB 090510, we have derived the total plasma energy,  $E_{e^+e^-}^{tot} = (1.10 \pm 0.06) \times 10^{53} \text{ erg}$ , the Baryon load,  $B = (1.45 \pm 0.28) \times 10^{-3}$ , and the Lorentz factor at transparency,  $\Gamma = (6.7 \pm 1.7) \times 10^2$ , which are characteristic of the long GRB class, as well as a very high CBM density,  $\langle n_{CBM} \rangle = (1.85 \pm 0.14) \times 10^3 \text{ cm}^{-3}$ . The joint effect of the high values of  $\Gamma$  and  $\langle n_{CBM} \rangle$  compresses in time and “inflates” in intensity the extended afterglow, making GRB 090510 appear to be a short burst, which we here define as a “disguised short GRB by excess”, occurring in an overdense region with  $10^3 \text{ cm}^{-3}$ .

37. R. Ruffini, J.A. Rueda, C. Barbarino, C. L. Bianco, H. Dereli, M. Enderli, L. Izzo, M. Muccino, A.V. Penacchioni, G.B. Pisani, Y. Wang; “Induced Gravitational Collapse in the BATSE era: the case of GRB 970828”; *Astronomy Reports*, in press (2014).

Following the recently established “Binary-driven HyperNova” (BdHN) paradigm, we here interpret GRB 970828 in terms of the four episodes typical of such a model. The “Episode 1”, up to 40 s after the trigger time  $t_0$ , with a time varying thermal emission and a total energy of  $E_{iso,1st} = 2.60 \times 10^{53} \text{ erg}$ , is interpreted as due to the onset of an hyper-critical accretion process onto a companion neutron star, triggered by the companion star, an FeCO core approaching a SN

explosion. The “Episode 2”, observed up  $t_0+90$  s, is interpreted as a canonical gamma ray burst, with an energy of  $E_{tot}^{e^+e^-} = 1.60 \times 10^{53}$  erg, a baryon load of  $B = 7 \times 10^{-3}$  and a bulk Lorentz factor at transparency of  $\Gamma = 142.5$ . From this Episode 2, we infer that the GRB exploded in an environment with a large average particle density  $\langle n \rangle \approx 10^3$  particles/cm<sup>3</sup> and dense clouds characterized by typical dimensions of  $(4 \div 8) \times 10^{14}$  cm and  $\delta n/n \sim 10$ . The “Episode 3” is identified from  $t_0+90$  s all the way up to  $10^{5-6}$  s: despite the paucity of the early X-ray data, typical in the BATSE, pre-Swift era, we find extremely significant data points in the late X-ray afterglow emission of GRB 970828, which corresponds to the ones observed in all BdHNe sources. The “Episode 4”, related to the Supernova emission, does not appear to be observable in this source, due to the presence of darkening from the large density of the GRB environment, also inferred from the analysis of the Episode 2.

38. R. Ruffini, Y. Wang, M. Kovacevic, C.L. Bianco, M. Enderli, M. Muccino, A.V. Penacchioni, G.B. Pisani, J. Rueda; “GRB 130427A and SN 2013cq: A Multi-wavelength Analysis of An Induced Gravitational Collapse Event”; *The Astrophysical Journal*, in press (2014).

We have performed our data analysis of the observations by *Swift*, *NuStar* and *Fermi* satellites in order to probe the induced gravitational collapse (IGC) paradigm for GRBs associated with supernovae (SNe), in the “terra incognita” of GRB 130427A. We compare and contrast our data analysis with those in the literature. We have verified that the GRB 130427A conforms to the IGC paradigm by examining the power law behavior of the luminosity in the early  $10^4$  s of the XRT observations. This has led to the identification of the four different episodes of the “binary driven hypernovae” (BdHNe) and to the prediction, on May 2, 2013, of the occurrence of SN 2013cq, duly observed in the optical band on May 13, 2013. The exceptional quality of the data has allowed the identification of novel features in *Episode 3* including: a) the confirmation and the extension of the existence of the recently discovered “nested structure” in the late X-ray luminosity in GRB 130427A, as well as the identification of a spiky structure at  $10^2$  s in the cosmological rest-frame of the source; b) a power law emission of the GeV luminosity light curve and its onset at the end of *Episode 2*; c) different Lorentz  $\Gamma$  factors for the emitting regions of the X-ray and GeV emissions in this *Episode 3*. These results make it possible to test the details of the physical and astrophysical regimes at work in the BdHNe: 1) a newly born neutron star and the supernova ejecta, originating in *Episode 1, 2*) a newly formed black hole originating in *Episode 2*, and 3) the possible interaction among these components, observable in the standard features of *Episode 3*.

## 5.2 Conference proceedings

1. R. Ruffini, M.G. Bernardini, C.L. Bianco, P. Chardonnet, F. Fraschetti, V. Gurzadyan, L. Vitagliano, S.-S. Xue; “The Blackholic energy: long and short Gamma-Ray Bursts (New perspectives in physics and astrophysics from the theoretical understanding of Gamma-Ray Bursts, II)”; in Proceedings of the XIth Brazilian School on Cosmology and Gravitation, Mangaratiba, Rio de Janeiro (Brazil), July August 2004, M. Novello, S.E. Perez Bergliaffa, Editors; AIP Conference Proceedings, 782, 42 (2005).

We outline the confluence of three novel theoretical fields in our modeling of Gamma-Ray Bursts (GRBs): 1) the ultrarelativistic regime of a shock front expanding with a Lorentz gamma factor  $\sim 300$ ; 2) the quantum vacuum polarization process leading to an electron-positron plasma originating the shock front; and 3) the general relativistic process of energy extraction from a black hole originating the vacuum polarization process. There are two different classes of GRBs: the long GRBs and the short GRBs. We here address the issue of the long GRBs. The theoretical understanding of the long GRBs has led to the detailed description of their luminosities in fixed energy bands, of their spectral features and made also possible to probe the astrophysical scenario in which they originate. We are specially interested, in this report, to a subclass of long GRBs which appear to be accompanied by a supernova explosion. We are considering two specific examples: GRB980425/SN1998bw and GRB030329/SN2003dh. While these supernovae appear to have a standard energetics of  $10^{49}$  ergs, the GRBs are highly variable and can have energetics  $10^4 - 10^5$  times larger than the ones of the supernovae. Moreover, many long GRBs occurs without the presence of a supernova. It is concluded that in no way a GRB can originate from a supernova. The precise theoretical understanding of the GRB luminosity we present evidence, in both these systems, the existence of an independent component in the X-ray emission, usually interpreted in the current literature as part of the GRB afterglow. This component has been observed by Chandra and XMM to have a strong decay on scale of months. We have named here these two sources respectively URCA-1 and URCA-2, in honor of the work that George Gamow and Mario Shoenberg did in 1939 in this town of Urca identifying the basic mechanism, the Urca processes, leading to the process of gravitational collapse and the formation of a neutron star and a supernova. The further hypothesis is considered to relate this X-ray source to a neutron star, newly born in the Supernova. This hypothesis should be submitted to further theoretical and observational investigation. Some theoretical developments to clarify the astrophysical origin of this new scenario are outlined. We turn then to the theoretical developments in the short GRBs: we first report some progress in the understanding the dynamical phase of collapse, the mass-energy formula and the extraction

of blackholc energy which have been motivated by the analysis of the short GRBs. In this context progress has also been accomplished on establishing an absolute lower limit to the irreducible mass of the black hole as well as on some critical considerations about the relations of general relativity and the second law of thermodynamics. We recall how this last issue has been one of the most debated in theoretical physics in the past thirty years due to the work of Bekenstein and Hawking. Following these conceptual progresses we analyze the vacuum polarization process around an overcritical collapsing shell. We evidence the existence of a separatrix and a dyadosphere trapping surface in the dynamics of the electron-positron plasma generated during the process of gravitational collapse. We then analyze, using recent progress in the solution of the Vlasov-Boltzmann-Maxwell system, the oscillation regime in the created electron-positron plasma and their rapid convergence to a thermalized spectrum. We conclude by making precise predictions for the spectra, the energy fluxes and characteristic time-scales of the radiation for short-bursts. If the precise luminosity variation and spectral hardening of the radiation we have predicted will be confirmed by observations of short-bursts, these systems will play a major role as standard candles in cosmology. These considerations will also be relevant for the analysis of the long-bursts when the baryonic matter contribution will be taken into account.

2. R. Ruffini, M.G. Bernardini, C.L. Bianco, P. Chardonnet, F. Fraschetti, V. Gurzadyan, L. Vitagliano, S.-S. Xue; "Black hole physics and astrophysics: The GRB-Supernova connection and URCA-1 URCA-2"; in Proceedings of the Tenth Marcel Grossmann Meeting on General Relativity, Rio de Janeiro, Brazil, July 2003, M. Novello, S.E. Perez-Bergliaffa, Editors; p. 369; World Scientific, (Singapore, 2006).

We outline the confluence of three novel theoretical fields in our modeling of Gamma-Ray Bursts (GRBs): 1) the ultrarelativistic regime of a shock front expanding with a Lorentz gamma factor  $\sim 300$ ; 2) the quantum vacuum polarization process leading to an electron-positron plasma originating the shock front; and 3) the general relativistic process of energy extraction from a black hole originating the vacuum polarization process. There are two different classes of GRBs: the long GRBs and the short GRBs. We here address the issue of the long GRBs. The theoretical understanding of the long GRBs has led to the detailed description of their luminosities in fixed energy bands, of their spectral features and made also possible to probe the astrophysical scenario in which they originate. We are specially interested, in this report, to a subclass of long GRBs which appear to be accompanied by a supernova explosion. We are considering two specific examples: GRB980425/SN1998bw and GRB030329/SN2003dh. While these supernovae appear to have a standard energetics of  $10^{49}$  ergs, the GRBs are highly variable and can have energetics  $10^4 - 10^5$  times larger than the ones of the supernovae. Moreover, many long GRBs occurs without the presence of a supernova. It is concluded that in no way a

GRB can originate from a supernova. The precise theoretical understanding of the GRB luminosity we present evidence, in both these systems, the existence of an independent component in the X-ray emission, usually interpreted in the current literature as part of the GRB afterglow. This component has been observed by Chandra and XMM to have a strong decay on scale of months. We have named here these two sources respectively URCA-1 and URCA-2, in honor of the work that George Gamow and Mario Shoenberg did in 1939 in this town of Urca identifying the basic mechanism, the Urca processes, leading to the process of gravitational collapse and the formation of a neutron star and a supernova. The further hypothesis is considered to relate this X-ray source to a neutron star, newly born in the Supernova. This hypothesis should be submitted to further theoretical and observational investigation. Some theoretical developments to clarify the astrophysical origin of this new scenario are outlined.

3. M.G. Bernardini, C.L. Bianco, P. Chardonnet, F. Fraschetti, R. Ruffini, S.-S. Xue; "General features of GRB 030329 in the EMBH model"; in Proceedings of the Tenth Marcel Grossmann Meeting on General Relativity, Rio de Janeiro, Brazil, July 2003, M. Novello, S.E. Perez-Bergliaffa, Editors; p. 2459; World Scientific, (Singapore, 2006).

GRB 030329 is considered within the EMBH model. We determine the three free parameters and deduce its luminosity in given energy bands comparing it with the observations. The observed substructures are compared with the predictions of the model: by applying the result that substructures observed in the extended afterglow peak emission (E-APE) do indeed originate in the collision of the accelerated baryonic matter (ABM) pulse with the inhomogeneities in the interstellar medium around the black-hole, masks of density inhomogeneities are considered in order to reproduce the observed temporal substructures. The induced supernova concept is applied to this system and the general consequences that we are witnessing are the formation of a cosmological thriptych of a black hole originating the GRB 030329, the supernova SN2003dh and a young neutron star. Analogies to the system GRB 980425–SN1998bw are outlined.

4. R. Ruffini, M.G. Bernardini, C.L. Bianco, P. Chardonnet, A. Corsi, F. Fraschetti, S.-S. Xue; "GRB 970228 and its associated Supernova in the EMBH model"; in Proceedings of the Tenth Marcel Grossmann Meeting on General Relativity, Rio de Janeiro, Brazil, July 2003, M. Novello, S.E. Perez-Bergliaffa, Editors; p. 2465; World Scientific, (Singapore, 2006).

The  $\gamma$ -ray burst of 1997 February 28 is analyzed within the Electromagnetic Black Hole model. We first estimate the value of the total energy deposited in the dyadosphere,  $E_{dya}$ , and the amount of baryonic matter left over by the EMBH progenitor star,  $B = M_B c^2 / E_{dya}$ . We then consider the role of the interstellar medium number density  $n_{ISM}$  and of the ratio  $R$  between the effective

emitting area and the total surface area of the  $\gamma$ -ray burst source, in reproducing the prompt emission and the X-ray afterglow of this burst. Some considerations are also done concerning the possibility of explaining, within the theory, the observed evidence for a supernova in the optical afterglow.

5. F. Frascchetti, M.G. Bernardini, C.L. Bianco, P. Chardonnet, R. Ruffini, S.-S. Xue; "Inferences on the ISM structure around GRB980425 and GRB980425-SN1998bw association in the EMBH Model"; in Proceedings of the Tenth Marcel Grossmann Meeting on General Relativity, Rio de Janeiro, Brazil, July 2003, M. Novello, S.E. Perez-Bergliaffa, Editors; p. 2451; World Scientific, (Singapore, 2006).

We determine the four free parameters within the EMBH model for GRB 980425 and deduce its luminosity in given energy bands, its spectra and its time variability in the prompt radiation. We compute the basic kinematical parameters of GRB 980425. In the extended afterglow peak emission the Lorentz  $\gamma$  factor is lower than the critical value 150 which has been found in Ruffini et al. (2002) to be necessary in order to perform the tomography of the ISM surrounding the GRB as suggested by Dermer & Mitman (1999). The detailed structure of the density inhomogeneities as well as the effects of radial apparent superluminal effects are evaluated within the EMBH model. Under the assumption that the energy distribution of emitted radiation is thermal in the comoving frame, time integrated spectra of EMBH model for prompt emission are computed. The induced supernova concept is applied to this system and general consequences on the astrophysical and cosmological scenario are derived.

6. R. Ruffini, M.G. Bernardini, C.L. Bianco, P. Chardonnet, F. Frascchetti, R. Guida, S.-S. Xue; "GRB 050315: A step in the proof of the uniqueness of the overall GRB structure"; in "GAMMA-RAY BURSTS IN THE SWIFT ERA: Sixteenth Maryland Astrophysics Conference", Washington, DC, USA, November 29th - December 2nd 2005, Stephen S. Holt, Neil Gehrels, John A. Nousek, Editors; AIP Conference Proceedings, 836, 103 (2006).

Using the Swift data of GRB 050315, we progress in proving the uniqueness of our theoretically predicted Gamma-Ray Burst (GRB) structure as composed by a proper-GRB, emitted at the transparency of an electron-positron plasma with suitable baryon loading, and an afterglow comprising the "prompt radiation" as due to external shocks. Detailed light curves for selected energy bands are theoretically fitted in the entire temporal region of the Swift observations ranging over  $10^6$  seconds.

7. R. Ruffini, M.G. Bernardini, C.L. Bianco, P. Chardonnet, F. Frascchetti, S.-S. Xue; "Theoretical Interpretation of GRB 031203 and URCA-3"; in "Relativistic Astrophysics and Cosmology - Einsteins Legacy", B. As-

chenbach, V. Burwitz, G. Hasinger, B. Leibundgut, Editors; Springer-Verlag (2007).

8. R. Ruffini, M.G. Bernardini, C.L. Bianco, L. Caito, P. Chardonnet, M.G. Dainotti, F. Fraschetti, R. Guida, M. Rotondo, G. Vereshchagin, L. Vitagliano, S.-S. Xue; "The Blackholic energy and the canonical Gamma-Ray Burst"; in Proceedings of the XIIth Brazilian School on Cosmology and Gravitation, Mangaratiba, Rio de Janeiro (Brazil), September 2006, M. Novello, S.E. Perez Bergliaffa, Editors; AIP Conference Proceedings, 910, 55 (2007).

Gamma-Ray Bursts (GRBs) represent very likely "the" most extensive computational, theoretical and observational effort ever carried out successfully in physics and astrophysics. The extensive campaign of observation from space based X-ray and  $\gamma$ -ray observatory, such as the *Vela*, CGRO, BeppoSAX, HETE-II, INTEGRAL, *Swift*, R-XTE, *Chandra*, XMM satellites, have been matched by complementary observations in the radio wavelength (e.g. by the VLA) and in the optical band (e.g. by VLT, Keck, ROSAT). The net result is unprecedented accuracy in the received data allowing the determination of the energetics, the time variability and the spectral properties of these GRB sources. The very fortunate situation occurs that these data can be confronted with a mature theoretical development. Theoretical interpretation of the above data allows progress in three different frontiers of knowledge: **a)** the ultrarelativistic regimes of a macroscopic source moving at Lorentz gamma factors up to  $\sim 400$ ; **b)** the occurrence of vacuum polarization process verifying some of the yet untested regimes of ultrarelativistic quantum field theories; and **c)** the first evidence for extracting, during the process of gravitational collapse leading to the formation of a black hole, amounts of energies up to  $10^{55}$  ergs of blackholic energy — a new form of energy in physics and astrophysics. We outline how this progress leads to the confirmation of three interpretation paradigms for GRBs proposed in July 2001. Thanks mainly to the observations by *Swift* and the optical observations by VLT, the outcome of this analysis points to the existence of a "canonical" GRB, originating from a variety of different initial astrophysical scenarios. The communality of these GRBs appears to be that they all are emitted in the process of formation of a black hole with a negligible value of its angular momentum. The following sequence of events appears to be canonical: the vacuum polarization process in the dyadosphere with the creation of the optically thick self accelerating electron-positron plasma; the engulfment of baryonic mass during the plasma expansion; adiabatic expansion of the optically thick "fireshell" of electron-positron-baryon plasma up to the transparency; the interaction of the accelerated baryonic matter with the interstellar medium (ISM). This leads to the canonical GRB composed of a proper GRB (P-GRB), emitted at the moment of transparency, followed by an extended afterglow. The sole parameters in this scenario are the total energy of the dyadosphere  $E_{dya}$ , the fireshell baryon loading  $M_B$  defined by the di-

dimensionless parameter  $B \equiv M_{BC}^2 / E_{dya}$ , and the ISM filamentary distribution around the source. In the limit  $B \rightarrow 0$  the total energy is radiated in the P-GRB with a vanishing contribution in the afterglow. In this limit, the canonical GRBs explain as well the short GRBs. In these lecture notes we systematically outline the main results of our model comparing and contrasting them with the ones in the current literature. In both cases, we have limited ourselves to review already published results in refereed publications. We emphasize as well the role of GRBs in testing yet unexplored grounds in the foundations of general relativity and relativistic field theories.

9. R. Ruffini, M.G. Bernardini, C.L. Bianco, L. Caito, P. Chardonnet, M.G. Dainotti, F. Fraschetti, R. Guida, G. Vereshchagin, S.-S. Xue; "The role of GRB 031203 in clarifying the astrophysical GRB scenario"; in Proceedings of the 6<sup>th</sup> Integral Workshop - The Obscured Universe, Moscow, (Russia), July 2006, S. Grebenev, R. Sunyaev, C. Winkler, A. Parmar, L. Ouwehand, Editors; ESA Special Publication, SP-622, 561 (2007).

The luminosity and the spectral distribution of the afterglow of GRB 031203 have been presented within our theoretical framework, which envisages the GRB structure as composed by a proper-GRB, emitted at the transparency of an electron-positron plasma with suitable baryon loading, and an afterglow comprising the "prompt emission" as due to external shocks. In addition to the GRB emission, there appears to be a prolonged soft X-Ray emission lasting for  $10^6$ – $10^7$  seconds followed by an exponential decay. This additional source has been called by us URCA-3. It is urgent to establish if this component is related to the GRB or to the Supernova (SN). In this second case, there are two possibilities: either the interaction of the SN ejecta with the interstellar medium or, possibly, the cooling of a young neutron star formed in the SN 2003lw process. The analogies and the differences between this triptych GRB 031203 / SN 2003lw / URCA-3 and the corresponding ones GRB 980425 / SN 1998bw / URCA-1 and GRB 030329 / SN 2003dh / URCA-2, as well as GRB 060218 / SN 2006aj are discussed.

10. M.G. Bernardini, C.L. Bianco, L. Caito, M.G. Dainotti, R. Guida, R. Ruffini; "GRB970228 and the class of GRBs with an initial spikelike emission: do they follow the Amati relation?"; in Relativistic Astrophysics Proceedings of the 4<sup>th</sup> Italian-Sino Workshop, Pescara (Italy), July 2007, C.L. Bianco, S.-S. Xue, Editors; AIP Conference Proceedings, 966, 7 (2008).

On the basis of the recent understanding of GRB050315 and GRB060218, we return to GRB970228, the first Gamma-Ray Burst (GRB) with detected afterglow. We proposed it as the prototype for a new class of GRBs with "an occasional softer extended emission lasting tenths of seconds after an initial spikelike emission". Detailed theoretical computation of the GRB970228 light curves in selected energy bands for the prompt emission are presented and compared with observational *BeppoSAX* data. From our analysis we conclude

that GRB970228 and likely the ones of the above mentioned new class of GRBs are “canonical GRBs” have only one peculiarity: they exploded in a galactic environment, possibly the halo, with a very low value of CBM density. Here we investigate how GRB970228 unveils another peculiarity of this class of GRBs: they do not fulfill the “Amati relation”. We provide a theoretical explanation within the fireshell model for the apparent absence of such correlation for the GRBs belonging to this new class.

11. C.L. Bianco, M.G. Bernardini, L. Caito, M.G. Dainotti, R. Guida, R. Ruffini; “The “Fireshell” Model and the “Canonical” GRB Scenario; in Relativistic Astrophysics Proceedings of the 4<sup>th</sup> Italian-Sino Workshop, Pescara (Italy), July 2007, C.L. Bianco, S.-S. Xue, Editors; AIP Conference Proceedings, 966, 12 (2008).

In the “fireshell” model we define a “canonical GRB” light curve with two sharply different components: the Proper-GRB (P-GRB), emitted when the optically thick fireshell of electron-positron plasma originating the phenomenon reaches transparency, and the afterglow, emitted due to the collision between the remaining optically thin fireshell and the CircumBurst Medium (CBM). We outline our “canonical GRB” scenario, originating from the gravitational collapse to a black hole, with a special emphasis on the discrimination between “genuine” and “fake” short GRBs.

12. L. Caito, M.G. Bernardini, C.L. Bianco, M.G. Dainotti, R. Guida, R. Ruffini; “GRB 060614: A Progress Report”; in Relativistic Astrophysics Proceedings of the 4<sup>th</sup> Italian-Sino Workshop, Pescara (Italy), July 2007, C.L. Bianco, S.-S. Xue, Editors; AIP Conference Proceedings, 966, 16 (2008).

The explosion of GRB 060614, detected by the Swift satellite, produced a deep break in the GRB scenario opening new horizons of investigation, because it can’t be traced back to any traditional scheme of classification. In fact, it manifests peculiarities both of long bursts and of short bursts. Above all, it is the first case of long duration near GRB without any bright Ib/c associated Supernova. We will show that, in our canonical GRB scenario, this “anomalous” situation finds a natural interpretation and allows us to discuss a possible variation to the traditional classification scheme, introducing the distinction between “genuine” and “fake” short bursts.

13. M.G. Dainotti, M.G. Bernardini, C.L. Bianco, L. Caito, R. Guida, R. Ruffini; “GRB 060218 and the Binaries as Progenitors of GRB-SN Systems”; in Relativistic Astrophysics Proceedings of the 4<sup>th</sup> Italian-Sino Workshop, Pescara (Italy), July 2007, C.L. Bianco, S.-S. Xue, Editors; AIP Conference Proceedings, 966, 25 (2008).

We study the Gamma-Ray Burst (GRB) 060218: a particularly close source at  $z = 0.033$  with an extremely long duration, namely  $T_{90} \sim 2000$  s, related to SN 2006aj. This source appears to be a very soft burst, with a peak in the spectrum

at 4.9 keV, therefore interpreted as an X-Ray Flash (XRF). It fulfills the Amati relation. I present the fitting procedure, which is time consuming. In order to show its sensitivity I also present two examples of fits with the same value of  $B$  and different value of  $E_{e^\pm}^{tot}$ . We fit the X- and  $\gamma$ -ray observations by *Swift* of GRB 060218 in the 0.1–150 keV energy band during the entire time of observations from 0 all the way to  $10^6$  s within a unified theoretical model. The free parameters of our theory are only three, namely the total energy  $E_{e^\pm}^{tot}$  of the  $e^\pm$  plasma, its baryon loading  $B \equiv M_B c^2 / E_{e^\pm}^{tot}$ , as well as the CircumBurst Medium (CBM) distribution. We justify the extremely long duration of this GRB by a total energy  $E_{e^\pm}^{tot} = 2.32 \times 10^{50}$  erg, a very high value of the baryon loading  $B = 1.0 \times 10^{-2}$  and the effective CircumBurst Medium (CBM) density which shows a radial dependence  $n_{cbm} \propto r^{-\alpha}$  with  $1.0 \leq \alpha \leq 1.7$  and monotonically decreases from 1 to  $10^{-6}$  particles/cm<sup>3</sup>. We recall that this value of the  $B$  parameter is the highest among the sources we have analyzed and it is very close to its absolute upper limit expected. By our fit we show that there is no basic differences between XRFs and more general GRBs. They all originate from the collapse process to a black hole and their difference is due to the variability of the three basic parameters within the range of full applicability of the theory. We also think that the smallest possible black hole, formed by the gravitational collapse of a neutron star in a binary system, is consistent with the especially low energetics of the class of GRBs associated with SNe Ib/c.

14. R. Guida, M.G. Bernardini, C.L. Bianco, L. Caito, M.G. Dainotti, R. Ruffini; “The Amati Relation within the Fireshell Model”; in Relativistic Astrophysics Proceedings of the 4<sup>th</sup> Italian-Sino Workshop, Pescara (Italy), July 2007, C.L. Bianco, S.-S. Xue, Editors; AIP Conference Proceedings, 966, 46 (2008).

In this work we show the existence of a spectral-energy correlation within our “fireshell” model for GRBs. The free parameters of the model are the total energy  $E_{tot}^{e^\pm}$  of the  $e^\pm$  plasma and its baryon loading  $B \equiv M_B c^2 / E_{tot}^{e^\pm}$ , characterizing the source, and the parameters describing the effective CircumBurst medium (CBM) distribution, namely its particle number density  $\rho$  and its effective emitting area  $R$ . We build a sample of pseudo-GRBs, i.e. a set of theoretically simulated light curves, varying the total energy of the electron-positron plasma  $E_{tot}^{e^\pm}$  and keeping the same baryon loading; the parametrization used to describe the distribution of the CircumBurst medium is the same as well for all the pseudo-GRBs. The values of these parameters ( $B$ ,  $\rho$  and  $R$ ) used in this work are equal to the ones assumed to fit GRB050315, a *Swift* burst representing a good example of what in the literature has been addressed as “canonical light curve”. For each GRB of the sample we calculate the  $\nu F_\nu$  spectrum integrating the theoretically computed light curve over the total time, namely from our  $T_0$ , the end of the Proper-GRB (P-GRB), up to the end of our afterglow phase, when the fireshell Lorentz gamma factor is close to unity; we exclude the P-GRB from this spectral computation because, following our “canonical”

GRB scenario, this component of the GRB emission is physically different from the other component, that is our afterglow component, so one should take care in no mixing them. We find that the maximum of this spectrum, that is the observed peak energy  $E_{p,tot}$ , correlates with the initial electron-positron plasma energy  $E_{tot}^{e\pm}$  in a way very similar to the Amati one:  $E_{p,tot} \propto (E_{tot}^{e\pm})^{0.5}$ .

15. R. Guida, M.G. Bernardini, C.L. Bianco, L. Caito, M.G. Dainotti, R. Ruffini; “Theoretical interpretation of the Amati relation within the fireshell model”; in GAMMA-RAY BURSTS 2007: Proceedings of the Santa Fe Conference, Santa Fe (NM, USA), November 2007, M. Galassi, D. Palmer, E. Fenimore, Editors; AIP Conference Proceedings, 1000, 60 (2008).

We discuss within our theoretical “fireshell” model for Gamma-Ray Bursts (GRBs) the theoretical interpretation of the phenomenological correlation between the isotropic-equivalent radiated energy of the prompt emission  $E_{iso}$  and the cosmological rest-frame  $\nu F_\nu$  spectrum peak energy  $E_p$  observed by Amati and collaborators. Possible reasons for some of the outliers of this relation are given.

16. L. Caito, M.G. Bernardini, C.L. Bianco, M.G. Dainotti, R. Guida, R. Ruffini; “GRB 060614: a Fake Short Gamma-Ray Burst”; in GAMMA-RAY BURSTS 2007: Proceedings of the Santa Fe Conference, Santa Fe (NM, USA), November 2007, M. Galassi, D. Palmer, E. Fenimore, Editors; AIP Conference Proceedings, 1000, 301 (2008).

The explosion of GRB 060614 produced a deep break in the GRB scenario and opened new horizons of investigation because it can’t be traced back to any traditional scheme of classification. In fact, it manifests peculiarities both of long bursts and of short bursts and, above all, it is the first case of long duration near GRB without any bright Ib/c associated Supernova. We will show that, in our canonical GRB scenario, this “anomalous” situation finds a natural interpretation and allows us to discuss a possible variation to the traditional classification scheme, introducing the distinction between “genuine” and “fake” short bursts.

17. C.L. Bianco, M.G. Bernardini, L. Caito, M.G. Dainotti, R. Guida, R. Ruffini; “Short and canonical GRBs”; in GAMMA-RAY BURSTS 2007: Proceedings of the Santa Fe Conference, Santa Fe (NM, USA), November 2007, M. Galassi, D. Palmer, E. Fenimore, Editors; AIP Conference Proceedings, 1000, 305 (2008).

Within the “fireshell” model for the Gamma-Ray Bursts (GRBs) we define a “canonical GRB” light curve with two sharply different components: the Proper-GRB (P-GRB), emitted when the optically thick fireshell of electron-positron plasma originating the phenomenon reaches transparency, and the afterglow, emitted due to the collision between the remaining optically thin fireshell and the CircumBurst Medium (CBM). We outline our “canonical GRB”

scenario, with a special emphasis on the discrimination between “genuine” and “fake” short GRBs.

18. C.L. Bianco, M.G. Bernardini, L. Caito, M.G. Dainotti, R. Guida, R. Ruffini, G. Vereshchagin, S.-S. Xue; “The Equations of motion of the “fireshell””; in OBSERVATIONAL EVIDENCE FOR BLACK HOLES IN THE UNIVERSE: Proceedings of the 2<sup>nd</sup> Kolkata Conference, Kolkata (India), February 2008, S.K. Chakrabarti, A.S. Majumdar, Editors; AIP Conference Proceedings, 1053, 259 (2008).

The Fireshell originating a Gamma-Ray Burst (GRB) encompasses an optically thick regime followed by an optically thin one. In the first one the fireshell self-accelerates from a Lorentz gamma factor equal to 1 all the way to 200-300. The physics of this system is based on the continuous annihilation of electron-positron pairs in an optically thick  $e^+e^-$  plasma with a small baryon loading. In the following regime, the optically thin fireshell, composed by the baryons left over after the transparency point, ballistically expands into the CircumBurst Medium (CBM). The dynamics of the fireshell during both regimes will be analyzed. In particular we will re-examine the validity of the constant-index power-law relation between the fireshell Lorentz gamma factor and its radial coordinate, usually adopted in the current literature on the grounds of an “ultrarelativistic” approximation. Such expressions are found to be mathematically correct but only approximately valid in a very limited range of the physical and astrophysical parameters and in an asymptotic regime which is reached only for a very short time, if any.

19. M.G. Bernardini, C.L. Bianco, L. Caito, M.G. Dainotti, R. Guida, R. Ruffini; “The “Canonical” GRBs within the fireshell model”; in OBSERVATIONAL EVIDENCE FOR BLACK HOLES IN THE UNIVERSE: Proceedings of the 2<sup>nd</sup> Kolkata Conference, Kolkata (India), February 2008, S.K. Chakrabarti, A.S. Majumdar, Editors; AIP Conference Proceedings, 1053, 267 (2008).

Within the fireshell model we define a “canonical” GRB light curve with two sharply different components: the Proper-GRB (P-GRB), emitted when the optically thick fireshell of electron-positron plasma originating the phenomenon reaches transparency, and the afterglow, emitted due to the collision between the remaining optically thin fireshell and the CircumBurst Medium (CBM). On the basis of the recent understanding of GRB970228 as the prototype for a new class of GRBs with “an occasional softer extended emission lasting tenths of seconds after an initial spikelike emission” we outline our “canonical” GRB scenario, originating from the gravitational collapse to a black hole, with a special emphasis on the discrimination between short GRBs and the ones appearing as such due to their peculiar astrophysical setting.

20. M.G. Dainotti, M.G. Bernardini, C.L. Bianco, L. Caito, R. Guida, R. Ruffini; “GRB 060218: the density mask and its peculiarity compared to the

other sources"; in OBSERVATIONAL EVIDENCE FOR BLACK HOLES IN THE UNIVERSE: Proceedings of the 2<sup>nd</sup> Kolkata Conference, Kolkata (India), February 2008, S.K. Chakrabarti, A.S. Majumdar, Editors; AIP Conference Proceedings, 1053, 283 (2008).

The Swift satellite has given continuous data in the range 0.3150 keV from 0 s to 106 s for GRB060218 associated with SN2006aj. It has an unusually long duration ( $T_{90} \sim 2100$  s). We plan to fit the complete  $\gamma$ - and X-ray light curves of this long duration GRB, including the prompt emission and we give peculiar attention to the afterglow lightcurve in order to better constrain the density mask. We apply our "fireshell" model based on the formation of a black hole, giving the relevant references. The initial total energy of the electron-positron plasma  $E_{e^\pm}^{tot} = 2.32 \times 10^{50}$  erg has a particularly low value similarly to the other GRBs associated with SNe. For the first time we observe a baryon loading  $B = 10^{-2}$  which coincides with the upper limit for the dynamical stability of the fireshell. The effective CircumBurst Medium (CBM) density shows a radial dependence  $n_{cbm} \propto r^{-a}$  with  $1.0 \leq a \leq 1.7$  and monotonically decreases from 1 to  $10^{-6}$  particles/cm<sup>3</sup>. Such a behavior is interpreted as due to a fragmentation in the fireshell. Such a fragmentation is crucial in explaining both the unusually large  $T_{90}$  and the consequently inferred abnormal low value of the CBM effective density. We present the comparison between the density mask of this source and the ones of a normal GRB 050315 and a fake short, GRB 970228, making some assumptions on the CBM behaviour in the surrounding of the Black hole.

21. L. Caito, M.G. Bernardini, C.L. Bianco, M.G. Dainotti, R. Guida, R. Ruffini; "GRB 060614 in the canonical fireshell model"; in OBSERVATIONAL EVIDENCE FOR BLACK HOLES IN THE UNIVERSE: Proceedings of the 2<sup>nd</sup> Kolkata Conference, Kolkata (India), February 2008, S.K. Chakrabarti, A.S. Majumdar, Editors; AIP Conference Proceedings, 1053, 291 (2008).

Gamma-Ray Burst (GRB) 060614 is the first nearby long duration GRB clearly not associated to any bright Ib/c Supernova. The explosion of this burst undermines one of the fundamental assumptions of the standard scenario and opens new horizons and hints of investigation. GRB 060614, hardly classifiable as a short GRB, is not either a "typical" long GRB since it occurs in a low star forming region. Moreover, it presents deep similarities with GRB 970228, which is the prototype of the "fake" short bursts, or better canonical GRBs disguised as short ones. Within the "fireshell" model, we test if this "anomalous" source can be a disguised short GRB.

22. L.J. Rangel Lemos, S. Casanova, R. Ruffini, S.S. Xue; "Fermis approach to the study of  $pp$  interactions"; in OBSERVATIONAL EVIDENCE FOR BLACK HOLES IN THE UNIVERSE: Proceedings of the 2<sup>nd</sup> Kolkata Conference, Kolkata (India), February 2008, S.K. Chakrabarti, A.S. Majumdar, Editors; AIP Conference Proceedings, 1053, 275 (2008).

The physics of hadronic interactions found much difficulties for explain the experimental data. In this work we study the approach of Fermi (1950) about the multiplicity of pions emitted in  $pp$  interactions and in follow we compare with the modern approach

23. R. Ruffini, A.G. Aksenov, M.G. Bernardini, C.L. Bianco, L. Caito, M.G. Dainotti, G. De Barros, R. Guida, G.V. Vereshchagin, S.-S. Xue; “The canonical Gamma-Ray Bursts and their ‘precursors’”; in 2008 NANJING GAMMA-RAY BURST CONFERENCE, Proceedings of the 2008 Nanjing Gamma-Ray Burst Conference, Nanjing (China), June 2008, Y.-F. Huang, Z.-G. Dai, B. Zhang, Editors; AIP Conference Proceedings, 1065, 219 (2008).

The fireshell model for Gamma-Ray Bursts (GRBs) naturally leads to a canonical GRB composed of a proper-GRB (P-GRB) and an afterglow. P-GRBs, introduced by us in 2001, are sometimes considered “precursors” of the main GRB event in the current literature. We show in this paper how the fireshell model leads to the understanding of the structure of GRBs, with precise estimates of the time sequence and intensities of the P-GRB and the of the afterglow. It leads as well to a natural classification of the canonical GRBs which overcomes the traditional one in short and long GRBs.

24. M.G. Bernardini, C.L. Bianco, L. Caito, M.G. Dainotti, R. Guida, R. Ruffini; “Preliminary analysis of GRB060607A within the fireshell model”; in 2008 NANJING GAMMA-RAY BURST CONFERENCE; Proceedings of the 2008 Nanjing Gamma-Ray Burst Conference, Nanjing (China), June 2008, Y.-F. Huang, Z.-G. Dai, B. Zhang, Editors; AIP Conference Proceedings, 1065, 227 (2008).

GRB060607A is a very distant ( $z = 3.082$ ) and energetic event ( $E_{iso} \sim 10^{53}$  erg). Its main peculiarity is that the peak of the near-infrared afterglow has been observed with the REM robotic telescope, allowing to infer the initial Lorentz gamma factor of the emitting system. We present a preliminary analysis of the spectra and light curves of GRB060607A prompt emission within the fireshell model. We show that the  $N(E)$  spectrum of the prompt emission, whose behavior is usually described as “simple power-law”, can also be fitted in a satisfactory way by a convolution of thermal spectra as predicted by the model we applied. The theoretical time-integrated spectrum of the prompt emission as well as the light curves in the BAT and XRT energy band are in good agreement with the observations, enforcing the plausibility of our approach. Furthermore, the initial value of Lorentz gamma factor we predict is compatible with the one deduced from the REM observations.

25. C.L. Bianco, M.G. Bernardini, L. Caito, M.G. Dainotti, R. Guida, R. Ruffini; “The “fireshell” model and the “canonical GRB” scenario”; in 2008 NANJING GAMMA-RAY BURST CONFERENCE; Proceedings of the 2008

Nanjing Gamma-Ray Burst Conference, Nanjing (China), June 2008, Y.-F. Huang, Z.-G. Dai, B. Zhang, Editors; AIP Conference Proceedings, 1065, 223 (2008).

The Swift observation of GRB 060614, as well as the catalog analysis by Norris & Bonnell (2006), opened the door “on a new Gamma-Ray Bursts (GRBs) classification scheme that straddles both long and short bursts” (Gehrels et al. 2006). Within the “fireshell” model for the Gamma-Ray Bursts (GRBs) we define a “canonical GRB” light curve with two sharply different components: the Proper-GRB (P-GRB), emitted when the optically thick fireshell of electron-positron plasma originating the phenomenon reaches transparency, and the afterglow, emitted due to the collision between the remaining optically thin fireshell and the CircumBurst Medium (CBM). We here outline our “canonical GRB” scenario, which implies three different GRB classes: the “genuine” short GRBs, the “fake” or “disguised” short GRBs and the other (so-called “long”) GRBs. We also outline some implications for the theoretical interpretation of the Amati relation.

26. G. De Barros, M.G. Bernardini, C.L. Bianco, L. Caito, M.G. Dainotti, R. Guida, R. Ruffini; “Is GRB 050509b a genuine short GRB?”; in 2008 NANJING GAMMA-RAY BURST CONFERENCE; Proceedings of the 2008 Nanjing Gamma-Ray Burst Conference, Nanjing (China), June 2008, Y.-F. Huang, Z.-G. Dai, B. Zhang, Editors; AIP Conference Proceedings, 1065, 231 (2008).

Within our “fireshell” model we introduced a “canonical” GRB scenario which differentiates physically the “proper GRB” (P-GRB) emission when photons decouple, and the afterglow emission due to interaction of the accelerated baryons with the CircumBurst Medium (CBM). The ratio between energetics of the two components is ruled by the baryon loading of the fireshell. We here analyse the possibility that GRB050509b is the first case of a “genuine” short GRB the ones with smaller baryon loading. In such a case, the GRB050509b “prompt emission” would be dominated by the “proper GRB” and, moreover, the P-GRB total energy would be greater than the afterglow one. Our fit of the afterglow data and of the P-GRB energetics indicates that this source present the smallest baryon loading we ever encountered so far, being on the order of  $10^{-4}$ .

27. G. De Barros, A.G. Aksenov, C.L. Bianco, R. Ruffini, G.V. Vereshchagin; “Fireshell versus Fireball scenarios”; in 2008 NANJING GAMMA-RAY BURST CONFERENCE; Proceedings of the 2008 Nanjing Gamma-Ray Burst Conference, Nanjing (China), June 2008, Y.-F. Huang, Z.-G. Dai, B. Zhang, Editors; AIP Conference Proceedings, 1065, 234 (2008).

We revisit Cavallo and Rees classification based on the analysis of initial conditions in electron-positron-photon plasma which appears suddenly around

compact astrophysical objects and gives origin to GRBs. These initial conditions were recently studied in [1,2] by numerical integration of relativistic Boltzmann equations with collision integrals, including binary and triple interactions between particles. The main conclusion is that the pair plasma in GRB sources quickly reaches thermal equilibrium well before its expansion starts. In light of this work we comment on each of the four scenarios proposed by Cavallo and Rees and discuss their applicability to describe evolution of GRB sources.

28. M.G. Bernardini, C.L. Bianco, L. Caito, M.G. Dainotti, R. Guida, R. Ruffini; “GRB970228 as a prototype for the class of GRBs with an initial spike-like emission”; in Proceedings of the Eleventh Marcel Grossmann Meeting on General Relativity, Berlin, Germany, July 2006, H. Kleinert, R.T. Jantzen, Editors; World Scientific, (Singapore, 2008).

We interpret GRB970228 prompt emission within our “canonical” GRB scenario, identifying the initial spikelike emission with the Proper-GRB (P-GRB) and the following bumps with the afterglow peak emission. Furthermore, we emphasize the necessity to consider the “canonical” GRB as a whole due to the highly non-linear nature of the model we applied.

29. M.G. Bernardini, C.L. Bianco, L. Caito, M.G. Dainotti, R. Guida, R. Ruffini; “GRB980425 and the puzzling URCA1 emission”; in Proceedings of the Eleventh Marcel Grossmann Meeting on General Relativity, Berlin, Germany, July 2006, H. Kleinert, R.T. Jantzen, Editors; World Scientific, (Singapore, 2008).

We applied our “fireshell” model to GRB980425 observational data, reproducing very satisfactory its prompt emission. We use the results of our analysis to provide a possible interpretation for the X-ray emission of the source S1. The effect on the GRB analysis of the lack of data in the pre-Swift observations is also outlined.

30. C.L. Bianco, M.G. Bernardini, L. Caito, P. Chardonnet, M.G. Dainotti, F. Frascetti, R. Guida, R. Ruffini, S.-S. Xue; “Theoretical interpretation of ‘long’ and ‘short’ GRBs”; in Proceedings of the Eleventh Marcel Grossmann Meeting on General Relativity, Berlin, Germany, July 2006, H. Kleinert, R.T. Jantzen, Editors; World Scientific, (Singapore, 2008).

Within the “fireshell” model we define a “canonical GRB” light curve with two sharply different components: the Proper-GRB (P-GRB), emitted when the optically thick fireshell of electron-positron plasma originating the phenomenon reaches transparency, and the afterglow, emitted due to the collision between the remaining optically thin fireshell and the CircumBurst Medium (CBM). We here present the consequences of such a scenario on the theoretical interpretation of the nature of “long” and “short” GRBs.

31. C.L. Bianco, M.G. Bernardini, P. Chardonnet, F. Fraschetti, R. Ruffini, S.-S. Xue; "Theoretical interpretation of luminosity and spectral properties of GRB 031203"; in Proceedings of the Eleventh Marcel Grossmann Meeting on General Relativity, Berlin, Germany, July 2006, H. Kleinert, R.T. Jantzen, Editors; World Scientific, (Singapore, 2008).

We show how an emission endowed with an instantaneous thermal spectrum in the co-moving frame of the expanding fireshell can reproduce the time-integrated GRB observed non-thermal spectrum. An explicit example in the case of GRB 031203 is presented.

32. C.L. Bianco, R. Ruffini; "The 'Fireshell' model in the Swift era"; in Proceedings of the Eleventh Marcel Grossmann Meeting on General Relativity, Berlin, Germany, July 2006, H. Kleinert, R.T. Jantzen, Editors; World Scientific, (Singapore, 2008).

We here re-examine the validity of the constant-index power-law relation between the fireshell Lorentz gamma factor and its radial coordinate, usually adopted in the current Gamma-Ray Burst (GRB) literature on the grounds of an "ultrarelativistic" approximation. Such expressions are found to be mathematically correct but only approximately valid in a very limited range of the physical and astrophysical parameters and in an asymptotic regime which is reached only for a very short time, if any.

33. L. Caito, M.G. Bernardini, C.L. Bianco, M.G. Dainotti, R. Guida, R. Ruffini; "Theoretical interpretation of GRB011121"; in Proceedings of the Eleventh Marcel Grossmann Meeting on General Relativity, Berlin, Germany, July 2006, H. Kleinert, R.T. Jantzen, Editors; World Scientific, (Singapore, 2008).

GRB 011121, detected by the BeppoSAX satellite, is studied as a prototype to understand the presence of flares observed by Swift in the afterglow of many GRB sources. Detailed theoretical analysis of the GRB 011121 light curves in selected energy bands are presented and compared with observational data. An interpretation of the flare of this source is provided by the introduction of the three-dimensional structure of the CircumBurst Medium(CBM).

34. M.G. Dainotti, M.G. Bernardini, C.L. Bianco, L. Caito, R. Guida, R. Ruffini; "On GRB 060218 and the GRBs related to Supernovae Ib/c"; in Proceedings of the Eleventh Marcel Grossmann Meeting on General Relativity, Berlin, Germany, July 2006, H. Kleinert, R.T. Jantzen, Editors; World Scientific, (Singapore, 2008).

We study the Gamma-Ray Burst (GRB) 060218: a particularly close source at  $z = 0.033$  with an extremely long duration, namely  $T_{90} \sim 2000$  s, related to SN 2006aj. This source appears to be a very soft burst, with a peak in the spectrum at 4.9 keV, therefore interpreted as an X-Ray Flash (XRF) and it obeys to the

Amati relation. We fit the X- and  $\gamma$ -ray observations by Swift of GRB 060218 in the 0.1150 keV energy band during the entire time of observations from 0 all the way to 106 s within a unified theoretical model. The details of our theoretical analysis have been recently published in a series of articles. The free parameters of the theory are only three, namely the total energy  $E_{e^\pm}^{tot}$  of the  $e^\pm$  plasma, its baryon loading  $B = M_B c^2 / E_{e^\pm}^{tot}$ , as well as the CircumBurst Medium (CBM) distribution. We fit the entire light curve, including the prompt emission as an essential part of the afterglow. We recall that this value of the  $B$  parameter is the highest among the sources we have analyzed and it is very close to its absolute upper limit expected. We successfully make definite predictions about the spectral distribution in the early part of the light curve, exactly we derive the instantaneous photon number spectrum  $N(E)$  and we show that although the spectrum in the co-moving frame of the expanding pulse is thermal, the shape of the final spectrum in the laboratory frame is clearly non thermal. In fact each single instantaneous spectrum is the result of an integration of thousands of thermal spectra over the corresponding EQuiTemporal Surfaces (EQTS). By our fit we show that there is no basic differences between XRFs and more general GRBs. They all originate from the collapse process to a black hole and their difference is due to the variability of the three basic parameters within the range of full applicability of the theory.

35. R. Guida, M.G. Bernardini, C.L. Bianco, L. Caito, M.G. Dainotti, R. Ruffini; "Theoretical interpretation of GRB060124"; in Proceedings of the Eleventh Marcel Grossmann Meeting on General Relativity, Berlin, Germany, July 2006, H. Kleinert, R.T. Jantzen, Editors; World Scientific, (Singapore, 2008).

We show the preliminary results of the application of our "fireshell" model to GRB060124. This source is very peculiar because it is the first event for which both the prompt and the afterglow emission were observed simultaneously by the three Swift instruments: BAT (15 - 350 keV), XRT (0,2 - 10 keV) and UVOT (170 - 650 nm), due to the presence of a precursor  $\sim 570$  s before the main burst. We analyze GRB060124 within our "canonical" GRB scenario, identifying the precursor with the P-GRB and the prompt emission with the afterglow peak emission. In this way we reproduce correctly the energetics of both these two components. We reproduce also the observed time delay between the precursor (P-GRB) and the main burst. The effect of such a time delay in our model will be discussed.

36. R. Ruffini, M.G. Bernardini, C.L. Bianco, L. Caito, P. Chardonnet, C. Cherubini, M.G. Dainotti, F. Frascchetti, A. Geralico, R. Guida, B. Patricelli, M. Rotondo, J. Rueda Hernandez, G. Vereshchagin, S.-S. Xue; "Gamma-Ray Bursts"; in Proceedings of the Eleventh Marcel Grossmann Meeting on General Relativity, Berlin, Germany, July 2006, H. Kleinert, R.T. Jantzen, Editors; World Scientific, (Singapore, 2008).

We show by example how the uncoding of Gamma-Ray Bursts (GRBs) offers unprecedented possibilities to foster new knowledge in fundamental physics and in astrophysics. After recalling some of the classic work on vacuum polarization in uniform electric fields by Klein, Sauter, Heisenberg, Euler and Schwinger, we summarize some of the efforts to observe these effects in heavy ions and high energy ion collisions. We then turn to the theory of vacuum polarization around a Kerr-Newman black hole, leading to the extraction of the blackholic energy, to the concept of dyadosphere and dyadotorus, and to the creation of an electron-positron-photon plasma. We then present a new theoretical approach encompassing the physics of neutron stars and heavy nuclei. It is shown that configurations of nuclear matter in bulk with global charge neutrality can exist on macroscopic scales and with electric fields close to the critical value near their surfaces. These configurations may represent an initial condition for the process of gravitational collapse, leading to the creation of an electron-positron-photon plasma: the basic self-accelerating system explaining both the energetics and the high energy Lorentz factor observed in GRBs. We then turn to recall the two basic interpretational paradigms of our GRB model: 1) the Relative Space-Time Transformation (RSTT) paradigm and 2) the Interpretation of the Burst Structure (IBS) paradigm. These paradigms lead to a “canonical” GRB light curve formed from two different components: a Proper-GRB (P-GRB) and an extended afterglow comprising a raising part, a peak, and a decaying tail. When the P-GRB is energetically predominant we have a “genuine” short GRB, while when the afterglow is energetically predominant we have a so-called long GRB or a “fake” short GRB. We compare and contrast the description of the relativistic expansion of the electron-positron plasma within our approach and within the other ones in the current literature. We then turn to the special role of the baryon loading in discriminating between “genuine” short and long or “fake” short GRBs and to the special role of GRB 991216 to illustrate for the first time the “canonical” GRB bolometric light curve. We then propose a spectral analysis of GRBs, and proceed to some applications: GRB 031203, the first spectral analysis, GRB 050315, the first complete light curve fitting, GRB 060218, the first evidence for a critical value of the baryon loading, GRB 970228, the appearance of “fake” short GRBs. We finally turn to the GRB-Supernova Time Sequence (GSTS) paradigm: the concept of induced gravitational collapse. We illustrate this paradigm by the systems GRB 980425 / SN 1998bw, GRB 030329 / SN 2003dh, GRB 031203 / SN 2003lw, GRB 060218 / SN 2006aj, and we present the enigma of the URCA sources. We then present some general conclusions.

37. R. Ruffini, A.G. Aksenov, M.G. Bernardini, C.L. Bianco, L. Caito, M.G. Dainotti, G. De Barros, R. Guida, G. Vereshchagin, S.-S. Xue; “The canonical Gamma-Ray Bursts: long, ‘fake’-‘disguised’ and ‘genuine’ short bursts; in PROBING STELLAR POPULATIONS OUT TO THE DISTANT UNIVERSE: CEFALU 2008, Proceedings of the International Confer-

ence; Cefal (Italy), September 2008, G. Giobbi, A. Tornambe, G. Raimondo, M. Limongi, L. A. Antonelli, N. Menci, E. Brocato, Editors; AIP Conference Proceedings, 1111, 325 (2009).

The Gamma-Ray Bursts (GRBs) offer the unprecedented opportunity to observe for the first time the blackholic energy extracted by the vacuum polarization during the process of gravitational collapse to a black hole leading to the formation of an electron-positron plasma. The uniqueness of the Kerr-Newman black hole implies that very different processes originating from the gravitational collapse a) of a single star in a binary system induced by the companion, or b) of two neutron stars, or c) of a neutron star and a white dwarf, do lead to the same structure for the observed GRB. The recent progress of the numerical integration of the relativistic Boltzmann equations with collision integrals including 2-body and 3-body interactions between the particles offer a powerful conceptual tool in order to differentiate the traditional “fireball” picture, an expanding hot cavity considered by Cavallo and Rees, as opposed to the “fireshell” model, composed of an internally cold shell of relativistically expanding electron-positron-baryon plasma. The analysis of the fireshell naturally leads to a canonical GRB composed of a proper-GRB and an extended afterglow. By recalling the three interpretational paradigms for GRBs we show how the fireshell model leads to an understanding of the GRB structure and to an alternative classification of short and long GRBs.

38. M.G. Bernardini, M.G. Dainotti, C.L. Bianco, L. Caito, R. Guida, R. Ruffini; “Prompt emission and X-ray flares: the case of GRB 060607 A”; in PROBING STELLAR POPULATIONS OUT TO THE DISTANT UNIVERSE: CEFALU 2008, Proceedings of the International Conference; Cefal (Italy), September 2008, G. Giobbi, A. Tornambe, G. Raimondo, M. Limongi, L. A. Antonelli, N. Menci, E. Brocato, Editors; AIP Conference Proceedings, 1111, 383 (2009).

GRB 060607A is a very distant and energetic event. Its main peculiarity is that the peak of the near-infrared (NIR) afterglow has been observed with the REM robotic telescope, allowing to estimate the initial Lorentz gamma factor within the fireball forward shock model. We analyze GRB 060607A within the fireshell model. The initial Lorentz gamma factor of the fireshell can be obtained adopting the exact solutions of its equations of motion, dealing only with the BAT and XRT observations, that are the basic contribution to the afterglow emission, up to a distance from the progenitor  $r \sim 10^{18}$  cm. According to the “canonical GRB” scenario we interpret the whole prompt emission as the peak of the afterglow emission, and we show that the observed temporal variability of the prompt emission can be produced by the interaction of the fireshell with overdense CircumBurst Medium (CBM) clumps. This is indeed the case also of the X-ray flares which are present in the early phases of the afterglow light curve.

39. C.L. Bianco, M.G. Bernardini, L. Caito, M.G. Dainotti, R. Guida, R. Ruffini; "The 'fireshell' model and the 'canonical GRB' scenario. Implications for the Amati relation"; in PROBING STELLAR POPULATIONS OUT TO THE DISTANT UNIVERSE: CEFALU 2008, Proceedings of the International Conference; Cefal (Italy), September 2008, G. Giobbi, A. Tornambe, G. Raimondo, M. Limongi, L. A. Antonelli, N. Menci, E. Brocato, Editors; AIP Conference Proceedings, 1111, 587 (2009).

Within the "fireshell" model for GRBs we define a "canonical GRB" light curve with two sharply different components: the Proper-GRB (P-GRB), emitted when the optically thick fireshell reaches transparency, and the extended afterglow, emitted due to the collision between the remaining optically thin fireshell and the CircumBurst Medium (CBM). We here outline our "canonical GRB" scenario, which implies three different GRB classes: the "genuine" short GRBs, the "fake" or "disguised" short GRBs and the other (so-called "long") GRBs. We will also outline the corresponding implications for the Amati relation, which are opening its use for cosmology.

40. R. Ruffini, A.G. Aksenov, M.G. Bernardini, C.L. Bianco, L. Caito, P. Chardonnet, M.G. Dainotti, G. De Barros, R. Guida, L. Izzo, B. Patricelli, L.J. Rangel Lemos, M. Rotondo, J.A. Rueda Hernandez, G. Vereshchagin, S.-S. Xue; "The Blackholic energy and the canonical Gamma-Ray Burst IV: the 'long', 'genuine short' and 'fake disguised short' GRBs"; in Proceedings of the XIIIth Brazilian School on Cosmology and Gravitation, Mangaratiba, Rio de Janeiro (Brazil), July-August 2008, M. Novello, S.E. Perez Bergliaffa, Editors; AIP Conference Proceedings, 1132, 199 (2009).

We report some recent developments in the understanding of GRBs based on the theoretical framework of the "fireshell" model, already presented in the last three editions of the "Brazilian School of Cosmology and Gravitation". After recalling the basic features of the "fireshell model", we emphasize the following novel results: 1) the interpretation of the X-ray flares in GRB afterglows as due to the interaction of the optically thin fireshell with isolated clouds in the CircumBurst Medium (CBM); 2) an interpretation as "fake - disguised" short GRBs of the GRBs belonging to the class identified by Norris & Bonnell; we present two prototypes, GRB 970228 and GRB 060614; both these cases are consistent with an origin from the final coalescence of a binary system in the halo of their host galaxies with particularly low CBM density  $n_{cbm} \sim 10^{-3}$  particles/cm<sup>3</sup>; 3) the first attempt to study a genuine short GRB with the analysis of GRB 050509B, that reveals indeed still an open question; 4) the interpretation of the GRB-SN association in the case of GRB 060218 via the "induced gravitational collapse" process; 5) a first attempt to understand the nature of the "Amati relation", a phenomenological correlation between the isotropic-equivalent radiated energy of the prompt emission  $E_{iso}$  with the cosmolog-

ical rest-frame  $\nu F_\nu$  spectrum peak energy  $E_{p,i}$ . In addition, recent progress on the thermalization of the electron-positron plasma close to their formation phase, as well as the structure of the electrodynamics of Kerr-Newman Black Holes are presented. An outlook for possible explanation of high-energy phenomena in GRBs to be expected from the AGILE and the Fermi satellites are discussed. As an example of high energy process, the work by Enrico Fermi dealing with ultrarelativistic collisions is examined. It is clear that all the GRB physics points to the existence of overcritical electrodynamic fields. In this sense we present some progresses on a unified approach to heavy nuclei and neutron stars cores, which leads to the existence of overcritical fields under the neutron star crust.

41. A.G. Aksenov, M.G. Bernardini, C.L. Bianco, L. Caito, C. Cherubini, G. De Barros, A. Geralico, L. Izzo, F.A. Massucci, B. Patricelli, M. Rontondo, J.A. Rueda Hernandez, R. Ruffini, G. Vereshchagin, S.-S. Xue; "The fireshell model for Gamma-Ray Bursts"; in *The Shocking Universe*, Proceedings of the conference held in Venice (Italy), September 2009, G. Chincarini, P. D'Avanzo, R. Margutti, R. Salvaterra, Editors; SIF Conference Proceedings, 102, 451 (2010).

The fireshell model for GRBs is briefly outlined, and the currently ongoing developments are summarized.

42. M.G. Bernardini, C.L. Bianco, L. Caito, L. Izzo, B. Patricelli, R. Ruffini; "The end of the prompt emission within the fireshell model"; in *The Shocking Universe*, Proceedings of the conference held in Venice (Italy), September 2009, G. Chincarini, P. D'Avanzo, R. Margutti, R. Salvaterra, Editors; SIF Conference Proceedings, 102, 489 (2010)

The shallow decay emission, revealed by the Swift satellite in the X-ray afterglow of a good sample of bursts, is a puzzle. Within the fireshell model it has been recently proposed an alternative explanation: if we assume that after the prompt phase the system has a range of Lorentz factors, the plateau phase is simply the product of the injection of slower material into the fireshell. This injection produces a modification both in the dynamics of the fireshell and in the spectrum of the emitted radiation. We postulate that this spread in the fireshell Lorentz factor occurs when the fireshell becomes transparent and do not depend on a prolonged activity of the central engine. The aim of this paper is to characterize dynamically the system in order to understand the nature of that material.

43. L. Izzo, M.G. Bernardini, C.L. Bianco, L. Caito, B. Patricelli, R. Ruffini; "GRB 090423 in the fireshell scenario"; in *The Shocking Universe*, Proceedings of the conference held in Venice (Italy), September 2009, G. Chincarini, P. D'Avanzo, R. Margutti, R. Salvaterra, Editors; SIF Conference Proceedings, 102, 537 (2010).

44. B. Patricelli, M.G. Bernardini, C.L. Bianco, L. Caito, L. Izzo, R. Ruffini, G. Vereshchagin; "A new spectral energy distribution of photons in the fireshell model of GRBs"; in *The Shocking Universe, Proceedings of the conference held in Venice (Italy), September 2009*, G. Chincarini, P. Davanzo, R. Margutti, R. Salvaterra, Editors; *SIF Conference Proceedings*, 102, 559 (2010).

The fireshell model of Gamma Ray Bursts (GRBs) postulates that the emission process is thermal in the comoving frame of the fireshell, but this is just a first approximation. We investigate a different spectrum of photons in the comoving frame in order to better reproduce the observed spectral properties of GRB prompt emission. We introduce a modified thermal spectrum whose low energy slope depends on an index  $\alpha$ , left as a free parameter. We test it by comparing the numerical simulations with observed BAT spectra integrated over different intervals of time. We find that the observational data can be correctly reproduced by assuming  $\alpha = -1.8$ .

45. C.L. Bianco, M.G. Bernardini, L. Caito, G. De Barros, L. Izzo, B. Patricelli, R. Ruffini; "Disguised Short Bursts and the Amati Relation"; in *Deciphering the ancient universe with Gamma-Ray Bursts, Proceedings of the conference held in Kyoto (Japan), April 2010*, N. Kawai, S. Nagataki, Editors; *AIP Conference Proceedings*, 1279, 299 (2010).

The class of "Disguised short" GRBs implied by the fireshell scenario is presented, with special emphasis on the implications for the Amati relation.

46. L. Izzo, M.G. Bernardini, C.L. Bianco, L. Caito, B. Patricelli, L.J. Rangel Lemos, R. Ruffini; "On GRB 080916C and GRB 090902B observed by the Fermi satellite"; in *Deciphering the ancient universe with Gamma-Ray Bursts, Proceedings of the conference held in Kyoto (Japan), April 2010*, N. Kawai, S. Nagataki, Editors; *AIP Conference Proceedings*, 1279, 343 (2010).

We propose a possible explanation, in the context of the Fireshell scenario, for the high-energy emission observed in GRB 080916C and GRB 090902B. The physical process underlying this emission consists mainly in the interaction of the baryon in the Fireshell with some high-density region around the burst site. Moreover we associate the observed delay of the onset of the high-energy emission as due to the P-GRB emission.

47. B. Patricelli, M.G. Bernardini, C.L. Bianco, L. Caito, G. De Barros, L. Izzo, R. Ruffini; "Black Holes in Gamma Ray Bursts"; in *Deciphering the ancient universe with Gamma-Ray Bursts, Proceedings of the conference held in Kyoto (Japan), April 2010*, N. Kawai, S. Nagataki, Editors; *AIP Conference Proceedings*, 1279, 406 (2010).

Within the fireshell model, Gamma Ray Bursts (GRBs) originate from an optically thick  $e^\pm$  plasma created by vacuum polarization process during the for-

mation of a Black Hole (BH). Here we briefly recall the basic features of this model, then we show how it is possible to interpret GRB observational properties within it. In particular we present, as a specific example, the analysis of GRB 050904 observations of the prompt emission light curve and spectrum in the Swift BAT energy band (15-150 keV).

48. M.G. Bernardini, C.L. Bianco, L. Caito, M.G. Dainotti, R. Guida, R. Ruffini; "The GRB classification within the "fireshell" model: short, long and "fake" short GRBs"; in Proceedings of the 3rd Stueckelberg Workshop on Relativistic Field Theories, Pescara, Italy, July 2008, N. Carlevaro, R. Ruffini, G.V. Vereshchagin, Editors; Cambridge Scientific Publishers, (UK, 2011).
49. C.L. Bianco, M.G. Bernardini, L. Caito, M.G. Dainotti, R. Guida, R. Ruffini, G.V. Vereshchagin, S.-S. Xue; "Equations of motion of the "fireshell""; in Proceedings of the 3rd Stueckelberg Workshop on Relativistic Field Theories, Pescara, Italy, July 2008, N. Carlevaro, R. Ruffini, G.V. Vereshchagin, Editors; Cambridge Scientific Publishers, (UK, 2011).
50. L. Caito, M.G. Bernardini, C.L. Bianco, M.G. Dainotti, R. Guida, R. Ruffini; "GRB 060614: another example of "fake" short burst from a merging binary system"; in Proceedings of the 3rd Stueckelberg Workshop on Relativistic Field Theories, Pescara, Italy, July 2008, N. Carlevaro, R. Ruffini, G.V. Vereshchagin, Editors; Cambridge Scientific Publishers, (UK, 2011).
51. G. De Barros, M.G. Bernardini, C.L. Bianco, L. Caito, R. Guida, R. Ruffini; "Analysis of GRB 050509b"; in Proceedings of the 3rd Stueckelberg Workshop on Relativistic Field Theories, Pescara, Italy, July 2008, N. Carlevaro, R. Ruffini, G.V. Vereshchagin, Editors; Cambridge Scientific Publishers, (UK, 2011).
52. R. Ruffini, L. Izzo, A.V. Penacchioni, C.L. Bianco, L. Caito, S.K. Chakrabarti, A. Nandi; "GRB 090618: a possible case of multiple GRB?"; in Proceedings of the 25th Texas Symposium on Relativistic Astrophysics, held in Heidelberg (Germany), December 2010, F.M. Rieger, C. van Eldik, W. Hofmann, Editors; PoS(Texas2010), 101.
53. L.J. Rangel Lemos, C.L. Bianco, H.J. Mosquera Cuesta, J.A. Rueda, R. Ruffini; "Luminosity function of BATSE GRBs dominated by extended afterglow"; in Proceedings of the 25th Texas Symposium on Relativistic Astrophysics, held in Heidelberg (Germany), December 2010, F.M. Rieger, C. van Eldik, W. Hofmann, Editors; PoS(Texas2010), 204.
54. R. Ruffini, A.G. Aksenov, M.G. Bernardini, C.L. Bianco, L. Caito, P. Chardonnet, M.G. Dainotti, G. De Barros, R. Guida, L. Izzo, B. Patricelli,

- L.J. Rangel Lemos, M. Rotondo, J.A. Rueda Hernandez, G. Vereshchagin, She-Sheng Xue; "Black Holes Energetics and GRBs"; in *The Sun, the Stars, the Universe and General Relativity: Proceedings of Sobral 2009*; S.E. Perez Bergliaffa, M. Novello, R. Ruffini, Editors; Cambridge Scientific Publishers (UK, 2011).
55. C.L. Bianco, L. Amati, M.G. Bernardini, L. Caito, G. De Barros, L. Izzo, B. Patricelli, R. Ruffini; "The class of 'disguised' short GRBs and its implications for the Amati relation"; in *GRBs as probes - from the progenitors environment to the high redshift Universe*, Proceedings of the conference held in Como (Italy), May 2011, S. Campana, P. D'Avanzo, A. Melandri, Editors; *Mem. S.A.It. Suppl.*, 21, 139 (2012).
56. A.V. Penacchioni, R. Ruffini, L. Izzo, M. Muccino, C.L. Bianco, L. Caito, B. Patricelli; "Evidences for a double component in the emission of GRB 101023"; in *GRBs as probes - from the progenitors environment to the high redshift Universe*, Proceedings of the conference held in Como (Italy), May 2011, S. Campana, P. D'Avanzo, A. Melandri, Editors; *Mem. S.A.It. Suppl.*, 21, 230 (2012).
57. M.G. Bernardini, C.L. Bianco, L. Caito, L. Izzo, B. Patricelli, R. Ruffini; "The X-Ray Flares of GRB 060607A within the Fireshell Model"; in *Proceedings of the Twelfth Marcel Grossmann Meeting on General Relativity*, Paris, France, July 2009, T. Damour, R.T. Jantzen, R. Ruffini, Editors; World Scientific, (Singapore, 2012).
58. L. Izzo, M.G. Bernardini, C.L. Bianco, L. Caito, B. Patricelli, R. Ruffini; "GRB 090423 in the Fireshell Scenario: A Canonical GRB at Redshift 8.2"; in *Proceedings of the Twelfth Marcel Grossmann Meeting on General Relativity*, Paris, France, July 2009, T. Damour, R.T. Jantzen, R. Ruffini, Editors; World Scientific, (Singapore, 2012).
59. B. Patricelli, M.G. Bernardini, C.L. Bianco, L. Caito, L. Izzo, R. Ruffini, G.V. Vereshchagin; "A New Spectral Energy Distribution of Photons in the Fireshell Model of GRBs"; in *Proceedings of the Twelfth Marcel Grossmann Meeting on General Relativity*, Paris, France, July 2009, T. Damour, R.T. Jantzen, R. Ruffini, Editors; World Scientific, (Singapore, 2012).
60. C.L. Bianco, M.G. Bernardini, L. Caito, G. De Barros, L. Izzo, M. Muccino, B. Patricelli, A.V. Penacchioni, G.B. Pisani, R. Ruffini; "Needs for a new GRB classification following the fireshell model: genuine short, disguised short and long GRBs"; in *Proceedings of the Gamma-Ray Bursts 2012 Conference*, held in Munich (Germany), May 2012, A. Rau, J. Greiner, Editors; *PoS(GRB 2012)*, 043.

61. A.V. Penacchioni, G.B. Pisani, R. Ruffini, C.L. Bianco, L. Izzo, M. Muccino; “The proto-black hole concept in GRB 101023 and its possible extension to GRB 110709B”; in Proceedings of the Gamma-Ray Bursts 2012 Conference, held in Munich (Germany), May 2012, A. Rau, J. Greiner, Editors; PoS(GRB 2012), 042.
62. B. Patricelli, M.G. Bernardini, C.L. Bianco, L. Caito, L. Izzo, R. Ruffini; “GRB 050904: The study of a high redshift GRB within the Fireshell Model”; in Proceedings of the Twelfth Marcel Grossmann Meeting on General Relativity, Paris, France, July 2009, T. Damour, R.T. Jantzen, R. Ruffini, Editors; World Scientific, (Singapore, 2012).
63. L. Izzo, G.B. Pisani, M. Muccino, J.A. Rueda, Y.Wang, C.L. Bianco, A.V. Penacchioni, R. Ruffini; “A common behavior in the late X-ray afterglow of energetic GRB-SN systems”; EAS Publications Series, Volume 61, 595-597 (2013).
64. R. Ruffini; “Black Holes, Supernovae and Gamma Ray Bursts”; in Proceedings of the Thirteenth Marcel Grossmann Meeting on General Relativity, Stockholm, Sweden, July 2012, R.T. Jantzen, K. Rosquist, R. Ruffini, Editors; World Scientific, (Singapore, 2014).



L E

# On binary-driven hypernovae and their nested late X-ray emission

R. Ruffini<sup>1,2,3,4</sup>, M. Muccino<sup>1,2</sup>, C. L. Bianco<sup>1,2</sup>, M. Enderli<sup>1,3</sup>, L. Izzo<sup>1,2</sup>, M. Kovacevic<sup>1,3</sup>, A. V. Penacchioni<sup>4</sup>,  
G. B. Pisani<sup>1,3</sup>, J. A. Rueda<sup>1,2,4</sup>, and Y. Wang<sup>1,2</sup>

<sup>1</sup> Dip. di Fisica and ICRA, Sapienza Università di Roma, piazzale Aldo Moro 5, 00185 Rome, Italy  
e-mail: marco.muccino@icra.it

<sup>2</sup> ICRANet, piazza della Repubblica 10, 65122 Pescara, Italy

<sup>3</sup> Université de Nice Sophia Antipolis, CEDEX 2, Grand Château Parc Valrose, BP 2135, 06103 Nice, France

<sup>4</sup> ICRANet-Rio, Centro Brasileiro de Pesquisas Físicas, rua Dr. Xavier Sigaud 150, 22290-180 Rio de Janeiro, Brazil

Received 14 March 2014 / Accepted 28 April 2014

## ABSTRACT

**Context.** The induced gravitational collapse (IGC) paradigm addresses the very energetic ( $10^{52}$ – $10^{54}$  erg) long gamma-ray bursts (GRBs) associated to supernovae (SNe). Unlike the traditional “collapsar” model, an evolved FeCO core with a companion neutron star (NS) in a tight binary system is considered as the progenitor. This special class of sources, here named “binary-driven hypernovae” (BdHNe), presents a composite sequence composed of four different episodes with precise spectral and luminosity features.

**Aims.** We first compare and contrast the steep decay, the plateau, and the power-law decay of the X-ray luminosities of three selected BdHNe (GRB 060729, GRB 061121, and GRB 130427A). Second, to explain the different sizes and Lorentz factors of the emitting regions of the four episodes, for definiteness, we use the most complete set of data of GRB 090618. Finally, we show the possible role of r-process, which originates in the binary system of the progenitor.

**Methods.** We compare and contrast the late X-ray luminosity of the above three BdHNe. We examine correlations between the time at the starting point of the constant late power-law decay  $t_a^*$ , the average prompt luminosity ( $L_{\text{iso}}$ ), and the luminosity at the end of the plateau  $L_a$ . We analyze a thermal emission ( $\sim 0.97$ – $0.29$  keV), observed during the X-ray steep decay phase of GRB 090618.

**Results.** The late X-ray luminosities of the three BdHNe, in the rest-frame energy band 0.3–10 keV, show a precisely constrained “nested” structure. In a space–time diagram, we illustrate the different sizes and Lorentz factors of the emitting regions of the three episodes. For GRB 090618, we infer an initial dimension of the thermal emitter of  $\sim 7 \times 10^{12}$  cm, expanding at  $\Gamma \approx 2$ . We find tighter correlations than the Dainotti–Willingale ones.

**Conclusions.** We confirm a constant slope power-law behavior for the late X-ray luminosity in the source rest frame, which may lead to a new distance indicator for BdHNe. These results, as well as the emitter size and Lorentz factor, appear to be inconsistent with the traditional afterglow model based on synchrotron emission from an ultra-relativistic ( $\Gamma \sim 10^2$ – $10^3$ ) collimated jet outflow. We argue, instead, for the possible role of r-process, originating in the binary system, to power the mildly relativistic X-ray source.

**Key words.** supernovae: general – binaries: general – gamma-ray burst: general – black hole physics – stars: neutron – nuclear reactions, nucleosynthesis, abundances

## 1. Introduction

The induced gravitational collapse (IGC) paradigm has been widely illustrated (Ruffini et al. 2006, 2007, 2008; Rueda & Ruffini 2012; Izzo et al. 2012a). It assumes that long, energetic ( $10^{52}$ – $10^{54}$  erg) gamma-ray bursts (GRBs) associated to supernovae (SNe) originate in a close binary system composed of an evolved massive star (likely a FeCO core) in the latest phases of its thermonuclear evolution and a neutron star (NS) companion. From an observational point of view, the complete time sequence of the IGC paradigm binary system has been identified in GRB 090618 (Izzo et al. 2012b), GRB 101023 (Penacchioni et al. 2012), GRB 110907B (Penacchioni et al. 2013), and GRB 970828 (Ruffini et al. 2013). We name these especially energetic systems, here, fulfilling the IGC paradigm, “binary-driven hypernovae” (BdHNe), to differentiate them from the traditional less energetic hypernovae.

In this Letter we introduce the IGC paradigm space-time diagram for the four distinct emission episodes (see Fig. 1):

*Episode 1* corresponds to the onset of the FeCO core SN explosion, creating a new-NS ( $\nu$ -NS, see A). Part of the SN ejecta triggers an accretion process onto the NS companion (see Rueda & Ruffini 2012; Izzo et al. 2012a, and B in Fig. 1), and a prolonged

interaction between the  $\nu$ -NS and the NS binary companion occurs (C). This leads to a spectrum with an expanding thermal component plus an extra power law (see Fig. 16 in Izzo et al. 2012b, and Fig. 4 in Ruffini et al. 2013).

*Episode 2* occurs when the companion NS reaches its critical mass and collapses to a black hole (BH), emitting the GRB (D) with Lorentz factors  $\Gamma \approx 10^2$ – $10^3$  (for details, see e.g. Ruffini et al. 2010; Izzo et al. 2012b; Ruffini et al. 2013).

*Episode 3*, observed in the X-rays, shows very precise behavior consisting of a steep decay, starting at the end point of the prompt emission (see E), and then a plateau phase, followed by a late constant power-law decay (see, e.g., Izzo et al. 2012b; Penacchioni et al. 2012; Ruffini et al. 2013).

*Episode 4*, not shown in Fig. 1, corresponds to the optical SN emission due to the  $^{56}\text{Ni}$  decay (see Arnett 1996) occurring after  $\sim 10$ – $15$  days in the cosmological rest frame. In all BdHNe, the SN appears to have the same luminosity as in the case of SN 1998bw (Amati et al. 2007). Although the presence of the SN is implicit in all the sources fulfilling the IGC paradigm, it is only detectable for GRBs at  $z \lesssim 1$ , in view of the limitations of the current optical telescopes.

We are going to see in this Letter that Episodes 1 and 2 can differ greatly in luminosity and timescale from source to source,

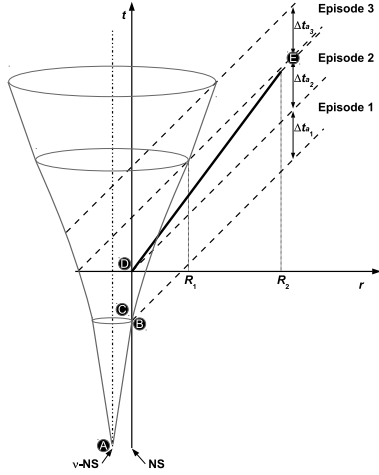


**Fig. 1.** IGC space–time diagram (not in scale) illustrates the relativistic motion of Episode 2 ( $\Gamma \approx 500$ , thick line) and the non-relativistic Episode 1 ( $\Gamma \approx 1$ ) and Episode 3 ( $\Gamma \approx 2$ ). Emissions from different radii,  $R_1$  ( $\sim 10^{13}$  cm) and  $R_2$  ( $\sim 10^{16}$ – $10^{17}$  cm), contribute to the transition point (E). Clearly, the X-ray luminosity originates in the SN remnant or in the newly-born BH, but not in the GRB.

while we confirm that in Episode 3, the late X-ray luminosities overlap: they follow a common power-law behavior with a constant slope in the source rest frame (Pisani et al. 2013). We point out here that the starting point of this power-law component is a function of the GRB isotropic energy  $E_{\text{iso}}$ .

The main goals of this Letter consist in a) comparing and contrasting the steep decay, the plateau, and the power-law decay of the X-ray luminosities as functions of  $E_{\text{iso}}$  by considering three selected GRBs (060729, 061121, and 130427A); b) pointing out the difference in the size and the Lorentz factors of the emitting regions of Episodes 1, 2, and 3 (for definiteness we use as prototype the source with the most complete dataset, GRB 090618); c) drawing attention to the possible role of the r-process, originating in the binary system of the progenitor, to power the mildly relativistic X-ray emission in the late phases of Episode 3.

## 2. The case of GRB 090618

We illustrate the difference in the emitting region sizes in the three episodes and their corresponding Lorentz factors:

*Episode 1* has a thermal component expanding from  $\sim 10^9$  cm to  $\sim 10^{10}$  cm on a rest-frame timescale of  $\sim 30$  s with an average velocity of  $\sim 4 \times 10^8$  cm s $^{-1}$  (see Izzo et al. 2012b). The total energy is  $4.1 \times 10^{52}$  erg, well above the traditional kinetic energy expected in the early phases of a SN, and it originates in the accretion of the material of the SN ejecta on the companion NS in the binary system (Rueda & Ruffini 2012; Ruffini et al. 2013).

*Episode 2* has been shown to be the ultra-relativistic prompt emission episode (e.g., the actual GRB) stemming from the collapse of the NS to a BH. Its isotropic energy is  $2.5 \times 10^{53}$  erg. The characteristic Lorentz factor at the transparency of the fireshell has been found to be  $\Gamma = 490$  for GRB 090618. The characteristic spatial extension goes all the way up to  $\sim 10^{16}$ – $10^{17}$  cm, reached at the end of Episode 2 (see Fig. 10 in Izzo et al. 2012b).

*Episode 3* has an isotropic energy of  $\approx 6 \times 10^{51}$  erg. A striking feature occurs during its steep decay phase: in the early observed 150 s, Page et al. (2011) have found a thermal component with a decreasing temperature from  $\sim 0.97$  keV to  $\sim 0.29$  keV (see also Starling et al. 2012). The surface radius

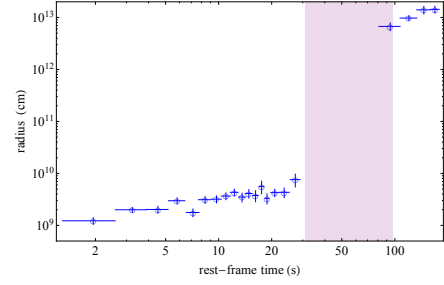


**Fig. 2.** Radii (open blue circles) of the emitting regions, measured in the cosmological rest frame. Episode 1 radius ranges from  $\sim 10^9$  cm to  $\sim 10^{10}$  and expands at  $\Gamma \approx 1$  (Izzo et al. 2012b). The Episode 3 radius, in the early phases of the steep decay, starts from a value of  $\sim 7 \times 10^{12}$  cm and expands at  $\Gamma \approx 2$ . The Episode 2 rest-frame duration is indicated by the shaded purple region. The expansion velocity at late times is expected to approach the asymptotic value of  $0.1c$  observed in the optical spectra (Della Valle 2011), in the absence of any further acceleration process.

of the emitter can be inferred from the observed temperature  $T_0$  and flux  $F_{BB}$  of the thermal component. We have, in fact (Izzo et al. 2012b),

$$r \approx \Gamma d_l (1+z)^{-2} \sqrt{F_{BB} / (\sigma T_0^4)}, \quad (1)$$

where  $d_l$  is the luminosity distance in the  $\Lambda$ CDM cosmological model and  $\sigma$  the Stefan-Boltzmann constant. As usual,  $\Gamma = 1/\sqrt{1-\beta^2}$ , where  $\beta = v/c$  is the expansion velocity in units of the speed of light  $c$ .

In parallel, the relation between the detector arrival time  $t_a^d$ , the cosmological rest-frame arrival time  $t_a$  and the laboratory time  $t$ , is given by  $t_a^d \equiv t_a(1+z) = t(1-\beta \cos \theta)(1+z)$ , where  $\theta$  is the displacement angle of the considered photon emission point from the line of sight (see, e.g., Bianco et al. 2001). We can then deduce the expansion velocity  $\beta$ , assumed to be constant, from the ratio between the variation of the emitter radius  $\Delta r$  and the emission duration in laboratory frame  $\Delta t$ , i.e.  $\beta = \Delta r / (c \Delta t)$ . Using the condition  $\beta \leq \cos \theta \leq 1$  (Bianco et al. 2001), we obtain  $0.75 \leq \beta \leq 0.89$  and, correspondingly,  $1.50 \leq \Gamma \leq 2.19$  and radii  $r \sim 10^{13}$  cm (see Fig. 2).

As is clear from Fig. 1, a sharp transition occurs between the end of Episode 2, where the characteristic dimensions reached by the GRB are  $\sim 10^{16}$ – $10^{17}$  cm, and the emission at the beginning of X-ray luminosity, with an initial size of  $\sim 7 \times 10^{12}$  cm. This leads to the conclusion that the X-ray emission of Episode 3 originates in the SN ejecta or in the accretion on the newly born BH and, anyway, not from the GRB.

## 3. The “nested” structure of Episode 3

We now turn to show the “nested” structure of the late X-ray luminosity. Pisani et al. (2013) have shown that the X-ray rest-frame 0.3–10 keV luminosity light curves present a constant decreasing power-law behavior, at  $t_a \gtrsim 10^4$  s, with typical slopes of  $-1.7 \lesssim \alpha_X \lesssim -1.3$ . This has been proven in a sample of six BdHNe: GRBs 060729, 061007, 080319B, 090618, 091127, and 111228, hereafter *golden sample* (GS, see, e.g., Izzo et al. 2013; Pisani et al. 2013). That the late X-ray emission could play a fundamental role as a distance indicator has been explored inferring the redshifts of GRBs 101023 and 110709B (Penacchioni et al. 2012, 2013). The IGC paradigm also allowed predicting  $\sim 10$ – $15$  days in the cosmological rest frame before its discovery, the occurrence of the SN associated to GRB 130427A, the most luminous source ever observed in  $\gamma$  rays with  $E_{\text{iso}} \approx 10^{54}$  erg

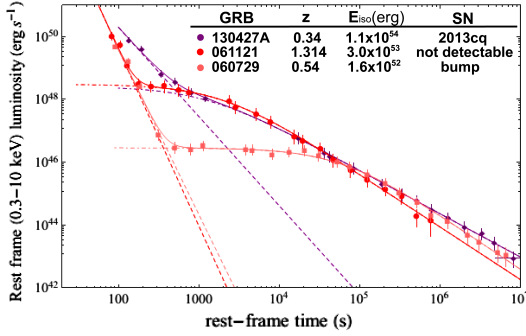


**Fig. 3.** Rest-frame 0.3–10 keV re-binned luminosity light curves of GRB 130427A (purple), GRB 061121 (red, shifted by 50 s in rest frame), and GRB 060729 (pink). The light curves are fitted by using a power-law for the steep decay phase (dashed lines) and the function in Eq. (2) for the plateau and the late decay phases (dot-dashed curves).

and  $z = 0.34$  (Xu et al. 2013b; Flores et al. 2013). This was later confirmed by the observations (de Ugarte Postigo et al. 2013; Levan et al. 2013; Watson et al. 2013; Xu et al. 2013a).

We compare and contrast GRB 130427A X-ray data with GRB 060729, a member of the GS, and GRB 061121, which shows the general behavior of BdHNe. GRB 060729, at  $z = 0.54$ , has  $E_{\text{iso}} = 1.6 \times 10^{52}$  erg (Grupe et al. 2007) and a SN bump in its optical afterglow (Cano et al. 2011). GRB 061121, at  $z = 1.314$  (Bloom et al. 2006), has  $E_{\text{iso}} = 3.0 \times 10^{53}$  erg, and its Episode 4 is clearly missing in view of the high cosmological redshift.

In Fig. 3 we have plotted the rebinned rest-frame 0.3–10 keV luminosity light curves of GRBs 130427A, 060729, and 061121. Their steep decay is modeled by a power-law function, i.e.  $L_p(t_a/100)^{-\alpha_p}$ , where  $L_p$  and  $\alpha_p$  are the power-law parameters. The plateau and the late power-law decay are instead modeled by using the following phenomenological function

$$L(t_a) = L_X (1 + t_a/\tau)^{\alpha_X}, \quad (2)$$

where  $L_X$ ,  $\alpha_X$ , and  $\tau$ , respectively, are the plateau luminosity, the late power-law decay index, and the characteristic timescale of the end of the plateau. From Eq. (2), we have defined the end of the plateau at the rest-frame time  $t_a^* = \tau[(1/2)^{1/\alpha_X} - 1]$ , when the luminosity of the plateau is half of the initial one,  $L_a(t_a^*) = L_X/2$ .

From this fitting procedure, we can conclude that the three BdHNe systems considered here share the following properties:

- the power-law decay for the more energetic sources starts directly from the steep decay, well before the  $t_a \approx 2 \times 10^4$  s, as indicated in Pisani et al. (2013); consequently, the plateau shrinks as a function of the increasing  $E_{\text{iso}}$  (see Fig. 3);
- the luminosities in the power-law decay are uniquely functions of the cosmological rest-frame arrival time  $t_a$  independently on the  $E_{\text{iso}}$  of each source (see Fig. 3);
- most remarkably, the overlapping of the X-ray light curves reveals a “nested” structure of BdHNe Episodes 3.

In our sample of BdHNe, we verify the applicability of the Dainotti-Willingale relations  $\langle L_{\text{iso}} \rangle - t_a^*$  and  $L_a - t_a^*$  (Dainotti et al. 2008, 2011b; Willingale et al. 2007), where  $\langle L_{\text{iso}} \rangle = E_{\text{iso}}/t_{a,90}$  is the averaged luminosity of the prompt and  $t_{a,90}$  is the rest-frame  $t_{90}$  duration of the burst. The resulting correlations,  $\log_{10} Y_i = m_i \log_{10} X_i + q_i$ , are shown in Fig. 4. The parameters of each BdHNe and the best fit parameters,  $m_i$  and  $q_i$  (where  $i = 1, 2$ ), are summarized in Table 1. As is clear from the extra scatter values  $\sigma_i$ , our total BdHNe sample provides tighter correlations. The extra scatter of the  $L_a - t_a^*$ ,  $\sigma = 0.26$ , is less than the Dainotti et al. (2011a) ones, i.e.,  $\sigma = 0.76$  for the whole sample of 62 bursts and

$\sigma = 0.40$  for the best subsample of eight bursts (*U0095*). The Dainotti-Willingale correlations consider X-ray afterglows characterized by a steep decay, a plateau phase, and a late power-law decay (Nousek et al. 2006; Zhang et al. 2006), independently of their energetics. In our BdHNe sample we limit the attention to a) the most energetic sources,  $10^{52}$ – $10^{54}$  erg, b) the presence of four emission episodes (neglecting Episode 4 for  $z > 1$ ), and c) sources with determined redshift and complete data at  $t_a = 10^4$ – $10^6$  s. All these conditions appear to be necessary to fulfill the nested structure in Fig. 3 and the tighter correlations between the astrophysical parameters  $\langle L_{\text{iso}} \rangle$ ,  $L_a$ , and  $t_a^*$  in Fig. 4.

To explain the above nested power-law decay and constrained correlations, we consider the decay of heavy elements produced in the r-process as a viable energy source (Burbidge et al. 1957), originating in binary NS mergers (see, e.g., Li & Paczyński 1998; Janka et al. 1999; Rosswog et al. 2004; Oechslin et al. 2007; Goriely et al. 2011; Piran et al. 2014).

Li & Paczyński (1998) have shown that the emission from the surface of an optically thick expanding ejecta in an adiabatic regime provides a flat light curve (see also Arnett 1982). This can explain, in principle, the observed steep decay and plateau phase of Episode 3 (see Fig. 3). After the ejecta becomes transparent, the heating source term due to the nuclear decays of the heavy nuclei, generated via r-process, becomes directly observable and dominates. The avalanche of decays with different lifetimes then provides the total energy release per unit mass per time that follows a power-law distribution, whose decay index has been estimated to be  $-1.4 \lesssim \alpha \lesssim -1.1$  (Metzger et al. 2010). These values are strikingly similar to the ones we have found in the late X-ray luminosity.

This power-law behavior is different from the exponential decay observed in the optical light curves of traditional SN, powered by the decay of a single element ( $^{56}\text{Ni} \rightarrow ^{56}\text{Co} \rightarrow ^{56}\text{Fe}$ ), which is not produced in the avalanche of many decays as in the r-process.

## 4. Conclusions

To summarize, short GRBs have been shown to come from binary NS mergers (see, e.g., Goodman 1986; Paczynski 1986; Eichler et al. 1989; Meszaros & Rees 1997; Rosswog et al. 2003; Lee et al. 2004; and more recently Muccino et al. 2013). Our subclass of long, extremely energetic ( $10^{52}$ – $10^{54}$  erg) sources is also initially driven by a tight binary system, formed by a  $\nu$ -NS and a companion NS, surrounded by the SN ejecta (see Fig. 1). Then we denoted these most energetic GRBs by “BdHNe”. This is clearly different from the gravitational collapse of a single massive progenitor star described by the collapsar model (Woosley 1993; MacFadyen & Woosley 1999; Woosley & Bloom 2006).

We compared and contrasted the late X-ray luminosities of three BdHNe with different  $E_{\text{iso}}$ , finding a nested structure. We showed tight correlations between  $\langle L_{\text{iso}} \rangle$ ,  $L_a$  and  $t_a^*$  (see Fig. 4 and Table 1) in agreement with the Dainotti-Willingale ones.

The above scaling laws, the nesting, and the initial dimension of  $\sim 7 \times 10^{12}$  cm and Lorentz factor of  $\Gamma \approx 2$  obtained from the steep decay of the X-ray luminosity put stringent limits on alternative theoretical models. They do not appear to be explainable within the traditional fireball jetted model, originating in the synchrotron radiation emitted by a decelerating relativistic shell with  $\Gamma \sim 10^2$  and colliding with the circumburst medium at distances  $\sim 10^{16}$  cm (see, e.g., Sari et al. 1998; Piran 2005; Meszaros 2006; Gehrels et al. 2009, and reference therein). In this Letter we alternatively proposed that the late X-ray luminosity comes from the wide angle emission of the SN ejecta or

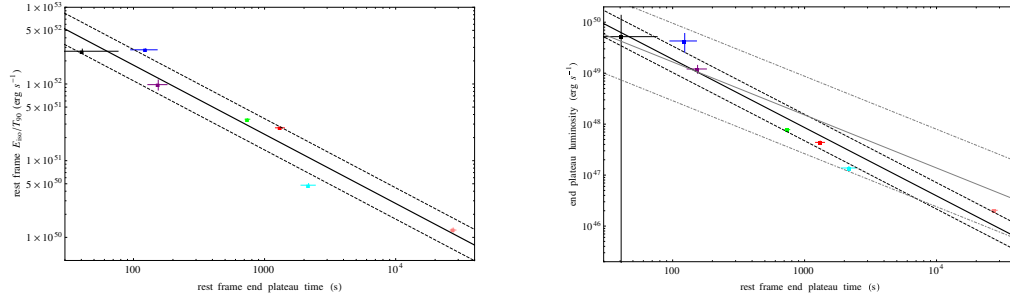


**Fig. 4.** The  $\langle L_{\text{iso}} \rangle - t_{\text{a}}^*$  (left) and the  $L_{\text{a}} - t_{\text{a}}^*$  (right) correlations (solid black lines) and the corresponding  $1\sigma$  confidence levels (dashed black lines). The sources considered are GRB 060729 (pink), GRB 061007 (black), GRB 080319B (blue), GRB 090618 (green), GRB 091127 (red), GRB 111228A (cyan), and GRB 130427A (purple). The tighter BdHNe  $L_{\text{a}} - t_{\text{a}}^*$  correlation is compared to the one in Dainotti et al. (2011a), corresponding to  $m = -1.04$  and  $q = 51.30$  (solid gray line) and  $\sigma = 0.76$  (dot-dashed gray lines).

**Table 1.** List of the quantities of the sources considered and best fit parameters of the correlations in Fig. 4.

GRB	$\langle L_{\text{iso}} \rangle$ ( $10^{50}$ erg/s)	$t_{\text{a}}^*$ (ks)	$L_{\text{a}}$ ( $10^{47}$ erg/s)
060729	$1.25 \pm 0.08$	$27.4 \pm 1.4$	$0.20 \pm 0.01$
061007	$267 \pm 18$	$0.041 \pm 0.036$	$521 \pm \text{unc}$
080319B	$279 \pm 7$	$0.12 \pm 0.03$	$430 \pm 170$
090618	$34.7 \pm 0.3$	$0.74 \pm 0.03$	$7.81 \pm 0.17$
091127	$26.8 \pm 0.3$	$1.31 \pm 0.10$	$4.39 \pm 0.26$
111228A	$4.79 \pm 0.24$	$2.17 \pm 0.27$	$1.38 \pm 0.10$
130427A	$98 \pm 15$	$0.16 \pm 0.03$	$121 \pm 21$
Correlation	$m_i$	$q_i$	$\sigma_i$
$\langle L_{\text{iso}} \rangle - t_{\text{a}}^*$	$-(0.90 \pm 0.09)$	$54.0 \pm 0.3$	$0.20 \pm 0.05$
$L_{\text{a}} - t_{\text{a}}^*$	$-(1.34 \pm 0.14)$	$52.0 \pm 0.4$	$0.26 \pm 0.08$

in the accretion on the newly born BH. We call the attention on the role of the energy release in the SN ejecta from the decay of very heavy nuclei generated by r-process in binary NSs (Li & Paczyński 1998). This heavy nuclei avalanche decay (see, e.g., Metzger et al. 2010) may well explain the late X-ray luminosity of Episode 3. This emission follows the steep decay and plateau phase of the adiabatic optically thick expansion, prior to reaching transparency (see Fig. 3).

In the case of binary systems with longer periods and/or a lower accretion rate, which do not allow the NS companion to reach its critical mass and to form a BH, Episode 2 is missing. The presence of the companion NS will nevertheless strip the H and He envelopes of the core progenitor star. These sources have low energetic bursts ( $E_{\text{iso}} < 10^{52}$  erg), such as GRB 060218 and GRB 980425, and their X-ray luminosity light curves do not overlap with the ones of our more energetic sample of BdHNe. These systems do not conform to the IGC paradigm and are traditional hypernovae<sup>1</sup>.

**Acknowledgements.** This work made use of data supplied by the UK Swift Science Data Center at the University of Leicester. M.E., M.K., and G.B.P. are supported by the Erasmus Mundus Joint Doctorate Program by grant Nos. 2012-1710, 2013-1471, and 2011-1640, respectively, from the EACEA of the European Commission. We warmly thank the anonymous referee for very constructive suggestions that improved the presentation of this Letter.

## References

Amati, L., Della Valle, M., Frontera, F., et al. 2007, A&A, 463, 913  
 Arnett, D. 1996, Space Sci. Rev., 78, 559  
 Arnett, W. D. 1982, ApJ, 253, 785  
 Bianco, C. L., Ruffini, R., & Xue, S.-S. 2001, A&A, 368, 377  
 Bloom, J. S., Perley, D. A., & Chen, H. W. 2006, GCN Circ., 5826  
 Burbidge, E. M., Burbidge, G. R., Fowler, W. A., & Hoyle, F. 1957, Rev. Mod. Phys., 29, 547  
 Cano, Z., Bersier, D., Guidorzi, C., et al. 2011, MNRAS, 413, 669  
 Dainotti, M. G., Cardone, V. F., & Capozziello, S. 2008, MNRAS, 391, L79

<sup>1</sup> <http://nsm.utdallas.edu/texas2013/proceedings/3/1/Ruffini.pdf>

Dainotti, M. G., Fabrizio Cardone, V., Capozziello, S., Ostrowski, M., & Willingale, R. 2011a, ApJ, 730, 135  
 Dainotti, M. G., Ostrowski, M., & Willingale, R. 2011b, MNRAS, 418, 2202  
 de Ugarte Postigo, A., Xu, D., Leloudas, G., et al. 2013, GCN Circ., 14646, 1  
 Della Valle, M. 2011, International Journal of Modern Physics D, 20, 1745  
 Eichler, D., Livio, M., Piran, T., & Schramm, D. N. 1989, Nature, 340, 126  
 Flores, H., Covino, S., Xu, D., et al. 2013, GRB Coordinates Network, Circular Service, 14491, 1  
 Gehrels, N., Ramirez-Ruiz, E., & Fox, D. B. 2009, ARA&A, 47, 567  
 Goodman, J. 1986, ApJ, 308, L47  
 Goriely, S., Bauswein, A., & Janka, H.-T. 2011, ApJ, 738, L32  
 Grupe, D., Gronwall, C., Wang, X.-Y., et al. 2007, ApJ, 662, 443  
 Izzo, L., Rueda, J. A., & Ruffini, R. 2012a, A&A, 548, L5  
 Izzo, L., Ruffini, R., Penacchioni, A. V., et al. 2012b, A&A, 543, A10  
 Izzo, L., Pisani, G. B., Muccino, M., et al. 2013, EAS Pub. Ser., 61, 595  
 Janka, H.-T., Eberl, T., Ruffert, M., & Fryer, C. L. 1999, ApJ, 527, L39  
 Lee, W. H., Ramirez-Ruiz, E., & Page, D. 2004, ApJ, 608, L5  
 Levan, A. J., Fruchter, A. S., Graham, J., et al. 2013, GRB Coordinates Network, Circular Service, 14686, 1  
 Li, L.-X., & Paczyński, B. 1998, ApJ, 507, L59  
 MacFadyen, A. I., & Woosley, S. E. 1999, ApJ, 524, 262  
 Meszaros, P. 2006, Rep. Prog. Phys., 69, 2259  
 Meszaros, P., & Rees, M. J. 1997, ApJ, 482, L29  
 Metzger, B. D., Martínez-Pinedo, G., Darbha, S., et al. 2010, MNRAS, 406, 2650  
 Muccino, M., Ruffini, R., Bianco, C. L., Izzo, L., & Penacchioni, A. V. 2013, ApJ, 763, 125  
 Nousek, J. A., Kouveliotou, C., Grupe, D., et al. 2006, ApJ, 642, 389  
 Oechslin, R., Janka, H.-T., & Marek, A. 2007, A&A, 467, 395  
 Paczyński, B. 1986, ApJ, 308, L43  
 Page, K. L., Starling, R. L. C., Fitzpatrick, G., et al. 2011, MNRAS, 416, 2078  
 Penacchioni, A. V., Ruffini, R., Izzo, L., et al. 2012, A&A, 538, A58  
 Penacchioni, A. V., Ruffini, R., Bianco, C. L., et al. 2013, A&A, 551, A133  
 Piran, T. 2005, Rev. Mod. Phys., 76, 1143  
 Piran, T., Korobkin, O., & Rosswog, S. 2014 [arXiv:1401.2166]  
 Pisani, G. B., Izzo, L., Ruffini, R., et al. 2013, A&A, 552, L5  
 Rosswog, S., Ramirez-Ruiz, E., & Davies, M. B. 2003, MNRAS, 345, 1077  
 Rosswog, S., Speith, R., & Wynn, G. A. 2004, MNRAS, 351, 1121  
 Rueda, J. A., & Ruffini, R. 2012, ApJ, 758, L7  
 Ruffini, R., Bernardini, M. G., Bianco, C. L., et al. 2008, in The Eleventh Marcel Grossmann Meeting, eds. H. Kleinert, R. T. Jantzen, & R. Ruffini (Singapore: World Scientific), 368  
 Ruffini, R., Bernardini, M. G., Bianco, C. L., et al. 2006, in The Tenth Marcel Grossmann Meeting., eds. M. Novello, S. Perez Bergliaffa, & R. Ruffini (Singapore: World Scientific), 369  
 Ruffini, R., Bernardini, M. G., Bianco, C. L., et al. 2007, ESA SP, 622, 561  
 Ruffini, R., Vereshchagin, G., & Xue, S.-S. 2010, Phys. Rep., 487, 1  
 Ruffini, R., Izzo, L., Muccino, M., et al. 2013, A&A, submitted [arXiv:1311.7432]  
 Sari, R., Piran, T., & Narayan, R. 1998, ApJ, 497, L17  
 Starling, R. L. C., Page, K. L., Pe'Er, A., Beardmore, A. P., & Osborne, J. P. 2012, MNRAS, 427, 2950  
 Watson, A. M., Butler, N., Kutuyev, A., et al. 2013, GCN Circ., 14666, 1  
 Willingale, R., O'Brien, P. T., Osborne, J. P., et al. 2007, ApJ, 662, 1093  
 Woosley, S. E. 1993, ApJ, 405, 273  
 Woosley, S. E., & Bloom, J. S. 2006, ARA&A, 44, 507  
 Xu, D., de Ugarte Postigo, A., Kruehler, T., et al. 2013a, GCN Circ., 14597, 1  
 Xu, D., de Ugarte Postigo, A., Schulze, S., et al. 2013b, GCN Circ., 14478, 1  
 Zhang, B., Fan, Y. Z., Dyks, J., et al. 2006, ApJ, 642, 354



# Induced gravitational collapse at extreme cosmological distances: the case of GRB 090423

R. Ruffini<sup>1,2,3,4</sup>, L. Izzo<sup>1,2</sup>, M. Muccino<sup>1</sup>, G. B. Pisani<sup>1,3</sup>, J. A. Rueda<sup>1,2,4</sup>, Y. Wang<sup>1</sup>, C. Barbarino<sup>1,5</sup>, C. L. Bianco<sup>1,2</sup>,  
M. Enderli<sup>1,3</sup>, and M. Kovacevic<sup>1,3</sup>

<sup>1</sup> Dip. di Fisica and ICRA, Sapienza Università di Roma, P.le Aldo Moro 5, 00185 Rome, Italy  
e-mail: Ruffini@icra.it

<sup>2</sup> ICRA-Net, Piazza della Repubblica 10, 65122 Pescara, Italy

<sup>3</sup> Université de Nice-Sophia Antipolis, Cedex 2, Grand Château Parc Valrose, Nice, France

<sup>4</sup> ICRA-Net-Rio, Centro Brasileiro de Pesquisas Físicas, Rua Dr. Xavier Sigaud 150, 22290-180 Rio de Janeiro, RJ, Brazil

<sup>5</sup> INAF-Napoli, Osservatorio Astronomico di Capodimonte, Salita Moiariello 16, 80131 Napoli, Italy

Received 17 January 2014 / Accepted 25 May 2014

## ABSTRACT

**Context.** The induced gravitational collapse (IGC) scenario has been introduced in order to explain the most energetic gamma ray bursts (GRBs),  $E_{\text{iso}} = 10^{52} - 10^{54}$  erg, associated with type Ib/c supernovae (SNe). It has led to the concept of binary-driven hypernovae (BdHNe) originating in a tight binary system composed by a FeCO core on the verge of a SN explosion and a companion neutron star (NS). Their evolution is characterized by a rapid sequence of events: 1) the SN explodes, giving birth to a new NS ( $\nu$ NS). The accretion of SN ejecta onto the companion NS increases its mass up to the critical value; 2) the consequent gravitational collapse is triggered, leading to the formation of a black hole (BH) with GRB emission; 3) a novel feature responsible for the emission in the GeV, X-ray, and optical energy range occurs and is characterized by specific power-law behavior in their luminosity evolution and total spectrum; 4) the optical observations of the SN then occurs.

**Aims.** We investigate whether GRB 090423, one of the farthest observed GRB at  $z = 8.2$ , is a member of the BdHN family.

**Methods.** We compare and contrast the spectra, the luminosity evolution, and the detectability in the observations by *Swift* of GRB 090423 with the corresponding ones of the best known BdHN case, GRB 090618.

**Results.** Identification of constant slope power-law behavior in the late X-ray emission of GRB 090423 and its overlapping with the corresponding one in GRB 090618, measured in a common rest frame, represents the main result of this article. This result represents a very significant step on the way to using the scaling law properties, proven in Episode 3 of this BdHN family, as a cosmological standard candle.

**Conclusions.** Having identified GRB 090423 as a member of the BdHN family, we can conclude that SN events, leading to NS formation, can already occur, namely at 650 Myr after the Big Bang. It is then possible that these BdHNe stem from 40–60  $M_{\odot}$  binaries. They are probing the Population II stars after the completion and possible disappearance of Population III stars.

**Key words.** gamma-ray burst: general – gamma-ray burst: individual: GRB 090423 – black hole physics

## 1. Introduction

The induced gravitational collapse (IGC) paradigm (Ruffini 2011; Rueda & Ruffini 2012; Izzo et al. 2012b) has been proposed to explain a class of very energetic ( $E_{\text{iso}} \sim 10^{52} - 10^{54}$  erg) long gamma ray bursts (GRBs) associated with supernovae (SNe). A new class of systems, with progenitor a tight binary composed by a FeCO core and a companion neutron star (NS), has been considered. These systems evolve in a very rapid sequence lasting a few hundred seconds in their rest frame: 1) the SN explodes giving birth to a new NS ( $\nu$ NS); 2) the accretion of the SN ejecta onto the companion NS increases its mass, reaching the critical value; 3) the gravitational collapse is triggered, leading to the formation of a black hole (BH) with GRB emission. Such systems have been called binary-driven hypernovae (BdHN Ruffini et al. 2014a).

Observationally, this authentic cosmic matrix is characterized by four distinct episodes, with the “in” state represented

by a FeCO core and a NS and the “out” state by a  $\nu$ NS and a BH. Each episode contains specific signatures in its spectrum and luminosity evolution. Up to now, the IGC paradigm has been verified in a dozen GRBs, all with redshift up to  $z \sim 1$  (Izzo et al. 2012a; Penacchioni et al. 2012, 2013; Pisani et al. 2013; Ruffini et al. 2013).

Various approaches have been followed to reach an understanding of long GRBs. One of these has been the use of statistical tools to obtain general results that examine the most complete source catalog (see, e.g., Nousek et al. 2006; Kann et al. 2011; Salvaterra et al. 2012; Margutti et al. 2013, and references therein).

We follow a different approach here. We first identified the specific class of BdHNe of GRBs related to SNe, as mentioned above, widely tested at  $z \approx 1$ . We furthermore explore the members of this class by extending our analysis to higher values of the cosmological redshifts. We do that by taking the scaling laws for the cosmological transformations into account, as well as the

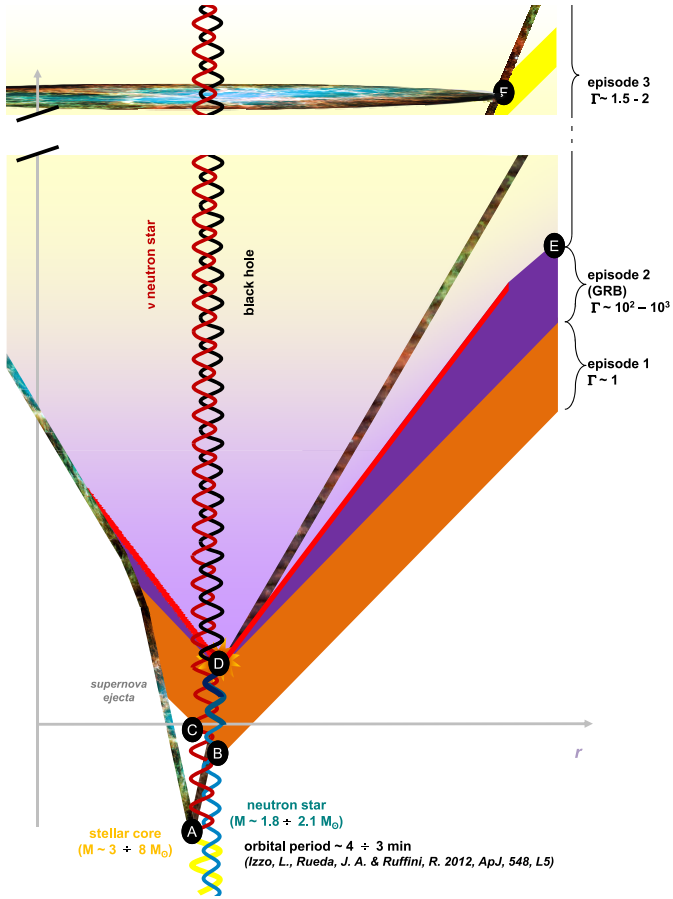


**Fig. 1.** Space-time diagram of the induced gravitational collapse applied to GRB 090618 (Enderli 2013; Ruffini 2013). The sequence is summarized as follows: A) the explosion as a SN of the evolved FeCO core which creates a  $\nu$ -NS and its remnant; B) the beginning of the accretion of the SN ejecta onto the companion NS, emitting Episode 1; C) a prolonged interaction between the  $\nu$ -NS and the NS binary companion; D) the companion NS reaches its critical mass by accretion, and a BH is formed with the consequent emission of a GRB; E) the arrival time at the separatrix between Episodes 2 and 3; F) the optical emission of the SN due to the decay of  $^{56}\text{Ni}$  after  $t_a^d \sim 10(1+z)$  days in the observer frame (Episode 4).

specific sensitivities of the GRB detectors (in this case *Swift*, Gehrels et al. 2005; and *Fermi*, Meegan et al. 2009).

Our aim is to verify that such BdHNe, originating in a SN and a companion NS, did form in the earliest phases of the universe. If this is confirmed, we go on to examine the possibility that all GRBs with  $E_{\text{iso}} \sim 10^{52} - 10^{54}$  erg are indeed associated to SN and belong to the BdHN family independently of their space and time location.

## 2. The four episodes of BdHNe sources

In order to achieve this goal, we recall the four above-mentioned episodes, present in the most general BdHN (see Fig. 1):

*Episode 1* has the imprint of the onset of a SN in the tight binary system with the companion neutron star (NS; see Fig. 2). It stemmed from the hyper-critical accretion of the SN matter ejecta ( $\sim 10^{-2} M_{\odot} \text{ s}^{-1}$ ) (Rueda & Ruffini 2012). Decades of conceptual progress have passed from the original work of Bondi & Hoyle (1944) and Bondi (1952) to the problem of a “hypercritical” accretion rate. This problem has acquired growing scientific interest as it moved from the classical astronomical field to the

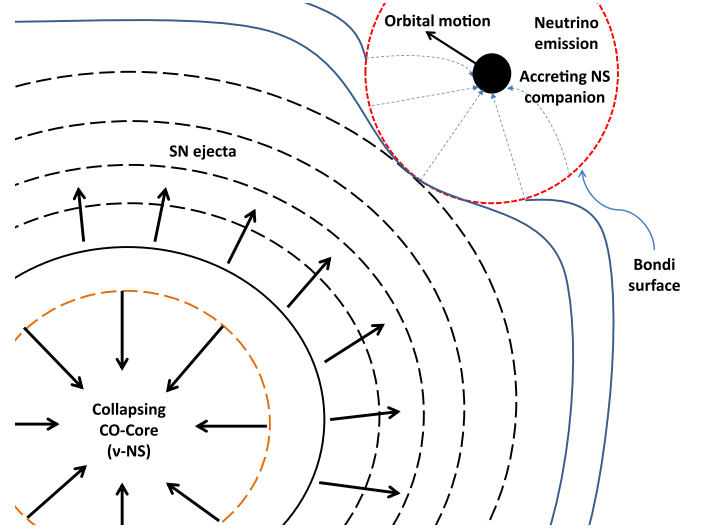


**Fig. 2.** Sketch (not in scale) of the accretion induced gravitational collapse (IGC) scenario.

domain of the relativistic astrophysics. The crucial role of neutrino cooling, earlier considered by Zel’dovich et al. (1972) and later on by Bisnovaty-Kogan & Lamzin (1984) in SN fallback, has been recognized to play a crucial role in describing binary common envelope systems by Chevalier (1989, 1993). In the work by Fryer et al. (1996), and more recently in Fryer (2009), it was clearly shown that an accretion rate  $\dot{M} \sim 10^{-2} M_{\odot} \text{ s}^{-1}$  onto a neutron star (NS) could lead in a few seconds to the formation of a black hole (BH), when neutrino physics in the description of the accreting NS is taken into due account. The data acquired in Episode 1 of GRB 090618 (Izzo et al. 2012a), as well as the one in GRB 101023 (Penacchioni et al. 2012), GRB 110709B (Penacchioni et al. 2013), and GRB 970828 (Ruffini et al. 2013), give for the first time the possibility to probe the Bondi-Hoyle hypercritical accretion and possibly the associated neutrino emission, which was theoretically considered by Zel’dovich et al. (1972); Chevalier (1993); Fryer et al. (1996), and Fryer (2009).

*Episode 2* is the canonical GRB emission, which originated in the collapse of the companion NS, which reached its critical mass by accretion of the SN ejecta and then collapsed to a black hole (BH), indeed emitting the GRB.

*Episode 3* observed in X-rays by *Swift*-XRT, shows very precise behavior consisting of steep decay, starting at the end point of the prompt emission, and then a plateau phase followed by a late power-law decay (see Pisani et al. 2013 and also Fig. 3). The late X-ray luminosities of BdHNe, in their rest-frame energy band 0.3–10 keV, show a common power-law behavior with a constant decay index clustering around  $\alpha = -1.5 \pm 0.2$ . The occurrence of such a constant afterglow decay has been observed in all the BdHN sources examined. For example, see in Fig. 4 the data for GRB 130427A, GRB 061121, GRB 060729, respectively. It appears an authentic nested structure, in the late X-ray emission of GRBs associated to SNe, and it has indeed to be indicated as the qualifying feature for a GRB to be a member of the BdHNe family (Ruffini et al. 2014a). It is clear that such a phenomenon offers a strong challenge for explaining by any GRB model.

In addition to these X-ray features, the observations of GRB 130427A by the *Swift*, *Fermi*, and *Konus-WIND* satellites and a large number of optical telescopes have led to the evidence of such power laws at very high energies, in  $\gamma$ -rays and

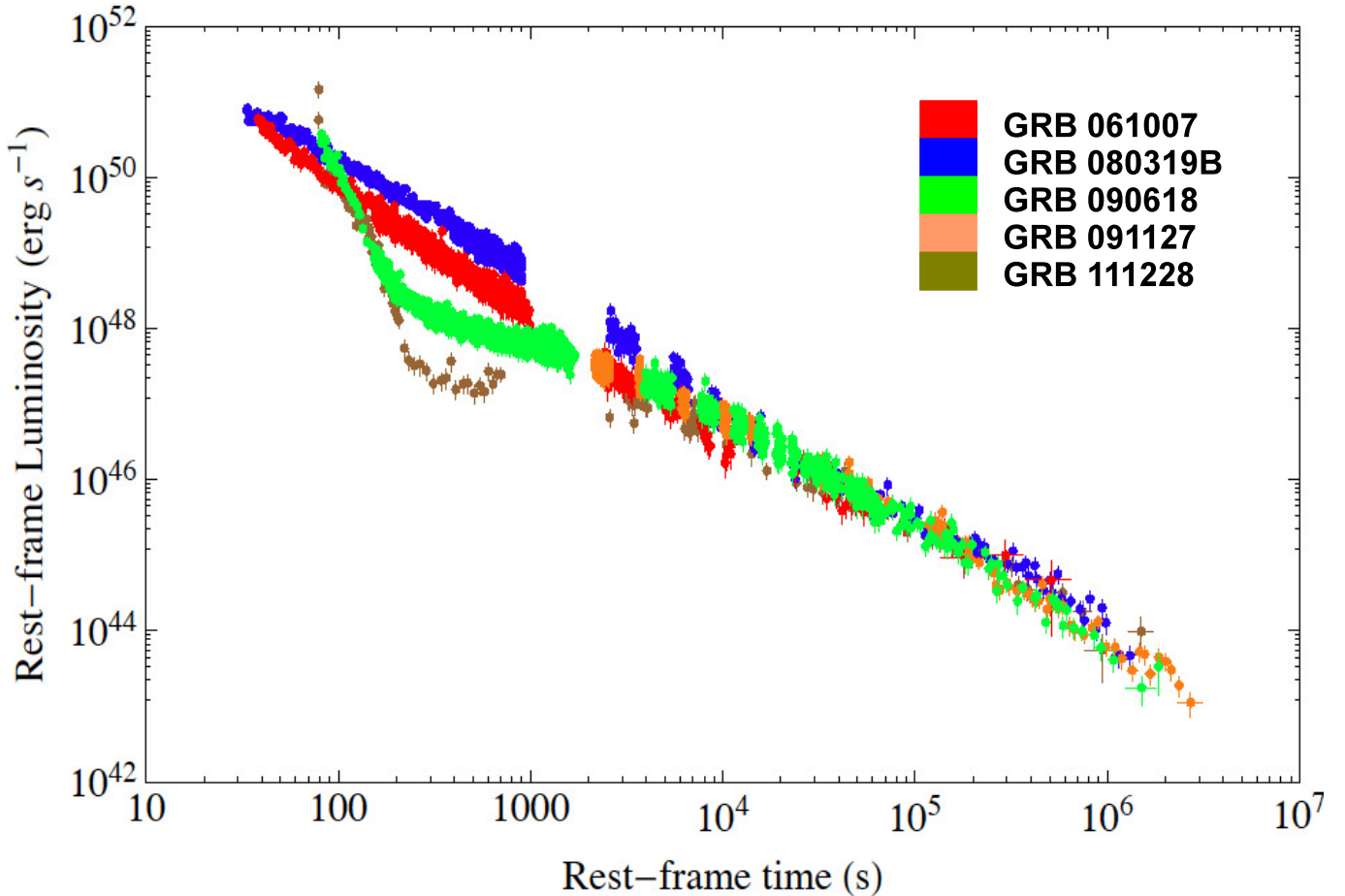


**Fig. 3.** Rest-frame, X-ray afterglow, luminosity light curves of some IGC GRBs-SNe belonging to the “golden sample” described in Pisani et al. (2013). The overlapping after  $10^4$  s is clearly evident, confirming the presence of an Episode 3 in this GRB.

at the optical wavelengths (Fermi-LAT collaboration & Fermi-GBM collaboration 2014; Melandri et al. 2014; see also Ruffini et al. 2014b).

*Episode 4* is characterized by the emergence of the SN emission after about 10–15 days from the occurrence of the GRB in the rest frame of the source, which has been observed for almost all the sources fulfilling the IGC paradigm with  $z \sim 1$ .

### 3. GRB 090423 compared and contrasted with GRB 090618

We first consider the data of GRB 090423, one of the farthest GRB ever observed at  $z = 8.2$  (Salvaterra et al. 2009; Tanvir et al. 2009), with the prototypical member of the BdHNe class, namely GRB 090618, and its associated SN (Izzo et al. 2012a). In other words we proceed with a specific ansatz: we verify that GRB 090423, at  $z = 8.2$ , presents analogous intrinsic features to GRB 090618, which was observed at  $z = 0.54$ .

We proceed by examining (see Sect. 4) each one of the above episodes for both sources, by a detailed spectral analysis and simulations. We first verify that Episode 1 of GRB 090618 transposed at redshift  $z = 8.2$  should not have triggered the *Swift*-BAT detector. Indeed, no precursor in the light curve of GRB 090423 was detected. Consequently, we do not address any theoretical considerations of the hypercritical accretion in Episode 1 of GRB 090423, since it is not observable in this source (see Sect. 5). We also notice that the distance of

GRB 090423 prevents any possible detection of a SN associated with this GRB, and therefore Episode 4 cannot be observed in GRB 090423.

For Episode 2, we have found that indeed the transposed emission of GRB 090618 should provide a positive trigger: we show in Sect. 6 that the duration, the observed luminosity and the spectral emission of Episode 2 in GRB 090423 present analogous intrinsic features to the transposed ones of GRB 090618 and differ only in the spectral energy distribution due to different circumburst medium properties.

For Episode 3, the crucial result, probing the validity of the above ansatz, is that the late X-ray emission in GRB 090423, computed in the rest frame of the burst at  $z = 8.2$ , precisely coincides (overlaps) with the corresponding late X-ray emission in GRB 090618, as evaluated in the rest frame of the source at  $z = 0.54$ , see Sect. 7. The occurrence of this extraordinary coincidence in Episode 3 proves that GRB 090423 is indeed a member of the BdHN family. This in particular opens the possibility of elaborating a role for the late X-ray emission in BdHNe as a standard candle.

### 4. The data

GRB 090423 was discovered on 23 April 2009, 07:55:19 UT,  $T_0$  from here, by the *Swift* Burst Alert Telescope (BAT; Krimm et al. 2009), at coordinates RA =  $09^{\text{h}} 55^{\text{m}} 35^{\text{s}}$ , Dec =  $+18^{\circ} 09' 37''$  (J2000.0;  $3'$  at 90% containment radius). The

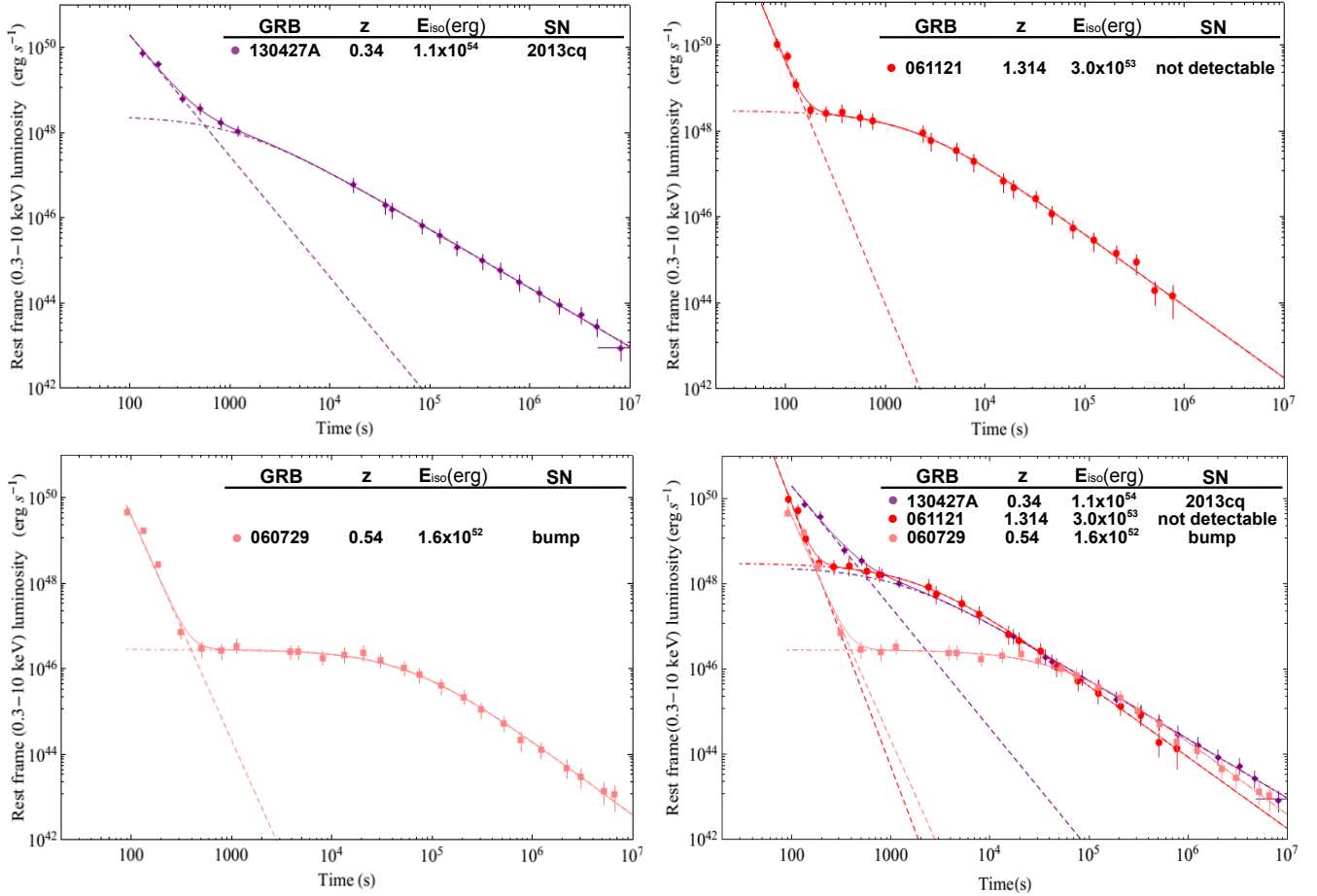


**Fig. 4.** Rest-frame, (0.3–10) keV, and re-binned luminosity light curves of GRB 130427A (*upper left*), GRB 061121 (*upper right*), GRB 060729 (*lower left*) and a combined picture (*lower right*). The fits to their emission is done using a power-law function for the early steep decay and a phenomenological function for the following emission, which is described well in [Ruffini et al. \(2014a\)](#).

*Swift*-BAT light curve showed a double-peaked structure with a duration of about 20 s. The X-ray Telescope (XRT; [Burrows et al. 2005](#)) on board the same spacecraft started to observe GRB 090423 72.5 s after the initial trigger, finding a fading source and providing enhanced coordinates for the follow-up by on-ground telescopes that have allowed the discovery of its redshift ( $z = 8.2$ , [Salvaterra et al. 2009](#); [Tanvir et al. 2009](#)). The light curve is characterized by an intense and long flare peaking at about  $T_0 + 180$ , followed by a power-law decay, observed from the second orbit of *Swift* ([Stratta & Perri 2009](#)). The prompt emission from GRB 090423 was also detected by the *Fermi* Gamma-Ray Burst Monitor (GBM, trigger 262166127/090423330; [von Kienlin 2009a](#)), whose on-ground location was consistent with the *Swift* position. The Large Area Telescope (LAT) on-board the *Fermi* satellite did not detect any signal from GRB 090423. The GBM light curve showed a single-structured peak with a duration of about 12 s, whose spectral energy distribution was best fit with a power law with an exponential cut-off energy, parameterized as  $E_{\text{peak}} = (82 \pm 15)$  keV. The observed fluence was computed from *Fermi* data to be  $S_\gamma = 1.1 \times 10^{-6}$  ergs/cm<sup>2</sup> that, considering the standard  $\Lambda$ CDM cosmological model, corresponds to an isotropic energy emitted of  $E_{\text{iso}} = 1.1 \times 10^{53}$  ergs for the spectroscopic redshift  $z = 8.2$  ([von Kienlin 2009b](#)). With these values for  $E_{\text{peak}}$  and  $E_{\text{iso}}$ , GRB 090423 satisfies the Amati relation, which is only valid for long GRBs ([Amati et al. 2002](#)).

## 5. The impossibility of detecting Episode 1

It has become natural to ask if observations of Episodes 1 and 2 in the hard X-ray energy range could be addressed for the case of GRB 090423. We have first analyzed a possible signature of Episode 1 in GRB 090423. Since the *Swift*-BAT, (15–150) keV, light curve is a single-structured peak with duration of  $\sim 19$  s, as detected by *Swift*-BAT, with no thermal emission in its spectrum and no detection of any emission from a precursor in the *Swift* and *Fermi* data, we have considered the definite possibility that Episode 1 was not observed at all. In this light, the best way to check this possibility consists in verifying that the Episode 1 emission is below the threshold of the *Swift*-BAT detector, consequently, it could have not triggered the *Swift*-BAT. We have considered the prototype of Episode 1 as the one observed in GRB 090618 ([Izzo et al. 2012b](#)), which is at redshift  $z = 0.54$ , and then we transposed it at redshift  $z = 8.2$ , simulating the observed emission of GRB 090618 as if it had been observed at this large distance. Then, we performed a time-resolved spectral analysis of Episode 1 in GRB 090618, using a Band function as spectral model, and finally we translated the specific photon spectra obtained from the analysis at the redshift of GRB 090423. This last operation consists in two transformations, concerning the peak energy  $E_{\text{peak}}$  of the Band function and the normalization value  $K_{\text{Band}}$ . The new value of the peak energy is simply given by  $E_{\text{peak},8} = E_{\text{peak}} (1 + 0.54)/(1 + 8.2)$ , while the

normalization, which corresponds to the specific photon flux at 1 keV, requires knowledge of the luminosity distances of the two bursts,  $d_l(z)$  :

$$K_{\text{Band},8} = K_{\text{Band}} \left( \frac{1 + 8.2}{1 + 0.54} \right)^2 \left( \frac{d_l(0.54)}{d_l(8.2)} \right)^2. \quad (1)$$

Another transformation concerns the observational time of Episode 1 of GRB 090618 at redshift  $z = 8.2$ . At large distances, any astrophysical event will be dilated in time by the cosmological redshift effect, which in the current case modifies the time interval by a quantity  $(1 + 8.2)/(1 + 0.54) = 5.97$ . The knowledge of this time interval is fundamental since it represents the exposure of a simulated spectrum translated at  $z = 8.2$ . We considered Fermi GBM data for analyzing the time-resolved spectra of GRB 090618, as described by Izzo et al. (2012b). The wide energy range of Fermi GBM NaI detectors, (8–1000) keV, allows a more accurate determination of the Band parameters, which are used as input values for the simulated spectra. We also rebinned the Fermi data considering a signal-to-noise ratio (SNR) = 10, and finally performed our spectral analysis. The next step consisted in transforming the peak energy of the Band function and of the normalization of all these time-resolved photon spectra  $N(E)$ , as described above.

Following the work of Band (2003), the sensitivity of an instrument to detect a burst depends on its burst trigger algorithm. The *Swift*-BAT trigger algorithm, in particular, looks for excesses in the detector count rate above expected background and constant sources. There are several criteria for determining the correct BAT threshold significance  $\sigma_0$  for a single GRB (Barthelmy et al. 2005), but in this work we have considered the treatment given in Band (2003). Recently, the threshold of *Swift*-BAT has been modified to allow detecting of subthreshold events, but since GRB 090423 was detected before, the Band (2003) analysis is still valid for our purposes. The preset threshold significance for *Swift*-BAT can be expressed by the following formula:

$$\sigma_0 = \frac{A_{\text{eff}} f_{\text{det}} f_{\text{mask}} \Delta t \int_{15}^{150} \epsilon(E) N(E) dE}{\sqrt{A_{\text{eff}} f_{\text{det}} \Delta t \int_{15}^{150} B(E) dE}}, \quad (2)$$

where  $A_{\text{eff}}$  is the effective area of the detector,  $f_{\text{det}}$  the fraction of the detector plane that is active,  $f_{\text{mask}}$  the fraction of the coded mask that is open,  $\Delta t$  the exposure of the photon spectrum  $N(E)$ ,  $\epsilon(E)$  the efficiency of the detector, and  $B(E)$  the background. We considered the values for these parameters as the ones given in the Band work (with the exception of the detecting area, assumed to be  $A_{\text{eff}} = 5200 \text{ cm}^2$ ), while the efficiency and the background were obtained from the *Swift*-BAT integrated spectrum of GRB 090423 using the XSPEC fitting package. Then we considered as input photon spectra  $N(E)$  the ones obtained from the Fermi GBM analysis of Episode 1 of GRB 090618 and translated for the redshift  $z = 8.2$ . It is appropriate to note that the transformations of spectra presented above are the correct ones: since the sensitivity of *Swift*-BAT strongly depends on the peak energy of the photon flux of the single spectra of the GRB (for the *Swift*-BAT case, see e.g. Fig. 7 of Band 2003), we find that at  $z = 8.2$  the observed peak energies of any spectrum will be lowered by a factor  $(1 + 0.54)/(1 + 8.2)$ . Our procedure also takes this further effect of the cosmological redshift into account.

Since the threshold significance of *Swift*-BAT is variable from a minimum value of  $\sigma_0 = 5.5$  up to a maximum value of 11<sup>1</sup>, with an average value of  $\sigma_0 = 6.7$ , the results of this

<sup>1</sup> [http://swift.gsfc.nasa.gov/about\\_swift/bat\\_desc.html](http://swift.gsfc.nasa.gov/about_swift/bat_desc.html)

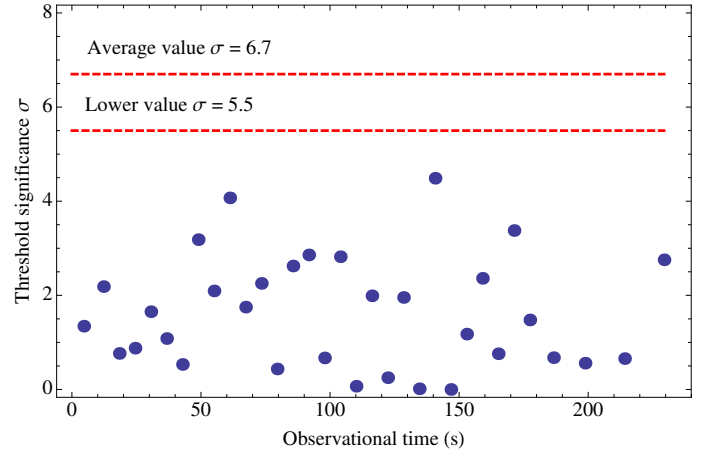


**Fig. 5.** Threshold significance  $\sigma_0$  computed using the treatment of Band (2003) for any single time-resolved spectra of the first emission episode in GRB 090618, as if they were emitted at redshift 8.2. The dashed lines correspond to the values for the threshold significance of  $\sigma_0 = 5.5$  and  $\sigma_0 = 6.7$ .

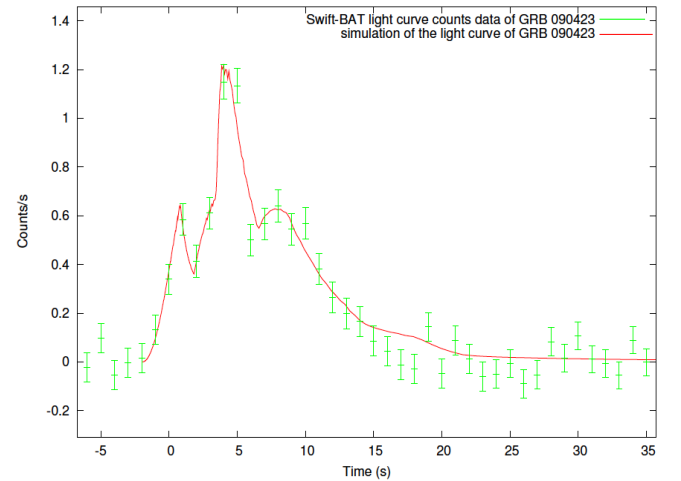


**Fig. 6.** *Swift*-BAT (15–150 keV) light curve emission of GRB 090423. The red line corresponds to the simulation of the GRB emission in the fireshell scenario (Izzo et al. 2010).

first analysis suggest that an Episode 1 similar to the one of GRB 090618 would not have been detected in GRB 090423 (see Fig. 5).

## 6. Detection of Episode 2 and its analysis

Episode 2 emission of GRB 090423, detected by *Swift*-BAT, was examined in the context of the fireshell scenario (Izzo et al. 2010; Ruffini 2011). A Lorentz Gamma factor of  $\Gamma \sim 1100$  and a baryon load  $B = 8 \times 10^{-4}$  were obtained. The simulations of the observed spikes in the observed time interval (0–440) s lead to homogeneous circumburst medium ( $\mathcal{R} = 10^{-8}$ , see Bianco & Ruffini 2005 for a complete description), and an average density of  $10^{-1}$  particles  $\text{cm}^{-3}$ . The simulation of the GRB 090423 emission is shown in Fig. 6.

We can now compare and contrast the emission observed in GRB 090423, expressed at  $z = 8.2$  (see Fig. 6, Izzo et al. 2010), and the portion of the emission of GRB 090618 if observed at  $z = 8.2$ , (see Fig. 7, Izzo et al. 2012a). In view of the *Swift*-BAT threshold, only the dashed region in Fig. 8, lasting 6 s, would be

**Table 1.** Results of the spectral fits of the  $T_{90}$  duration of GRB 090423 and of the  $\Delta t_{A,obs}$  time interval for GRB 090618.

	$\alpha$	$\beta$ (keV)	$E_{p,i}$ (keV)	norm. (ph/cm <sup>2</sup> /s/keV)	$\chi^2$	$\Delta t_{obs}$ (s)
090618	$-0.66 \pm 0.57$	$-1.99 \pm 0.05$	$284.57 \pm 172.10$	$0.3566 \pm 0.16$	0.924	6.1
090423	$-0.78 \pm 0.34$	$-3.5 \pm 0.5$	$433.6 \pm 133.5$	$0.015 \pm 0.010$	0.856	10.4

**Notes.** The latter is computed in a time interval corresponding to the one expected to be observed if GRB 090618 is transposed at the redshift  $z = 8.2$ , and in the observed energy range (89.6–896) keV.

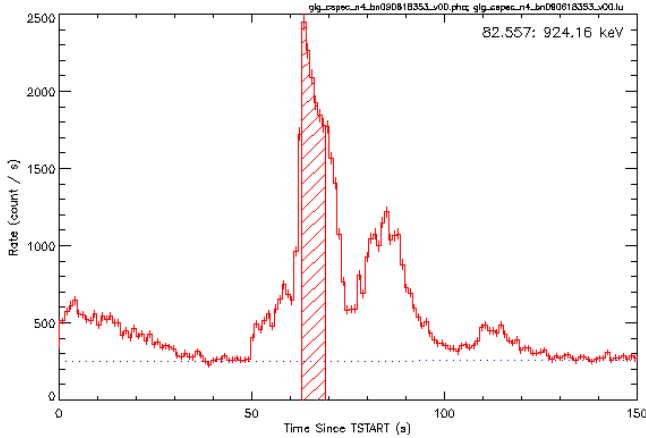


**Fig. 7.** Light curve of Episode 2 in GRB 090618, ranging from 50 to 150 s. The dashed region represents the portion which would have triggered the *Swift*-BAT if this GRB had been at the redshift  $z = 8.2$ . The observed duration of that interval is approximately  $\Delta t \approx 6$  s. The results obtained in Fig. 6, when scaled to  $z = 0.54$ , provide  $\Delta T \approx 3$  s.

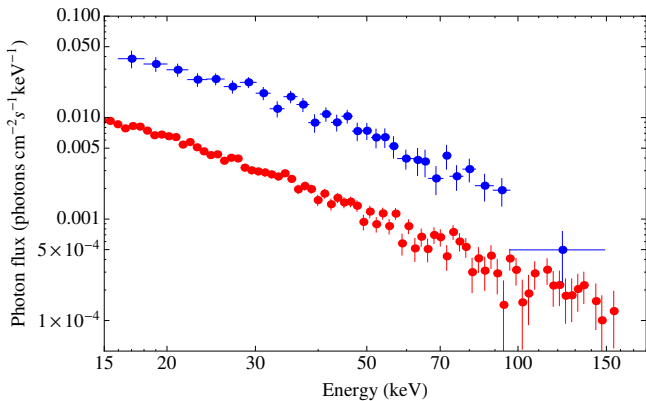


**Fig. 8.** Spectra of GRB 090423 (blue data) and of the spectrum of the emission of GRB 090618 (red data) considered as possible Episode 2 if GRB 090618 had been observed at  $z = 8.2$ . The low-energy photon index is  $\approx -0.8$ , which corresponds to the expectations from the Fireshell scenario (Ruffini 2011; Patricelli et al. 2012).

detectable. The observed flux in Fig. 6 and the one of the dashed region in Fig. 8 will be similar when compared in a common frame.

For the above considerations, the analysis presented in the previous section can be applied to Episode 2 of GRB 090618. Assuming a detector threshold for *Swift*-BAT of  $\sigma_0 = 6.7$ , see Eq. (2), only the dashed region in Fig. 7 is detectable when transposing GRB 090618 at  $z = 8.2$ . In the observer frame, this emission corresponds to the time interval ( $T_{0,G} + 63.0$ ,  $T_{0,G} + 69.1$ ) s, with  $T_{0,G}$  the trigger time of Fermi GBM data

of GRB 090618. This time interval, at  $z = 8.2$ , has a duration  $\Delta t_{A,obs} = \Delta t_{obs} \times 5.97 = 36.4$  s, owing to the time dilation by the cosmological redshift  $z$  (see Fig. 6). The remaining emission of GRB 090618 is unobservable, since below the threshold of the *Swift*-BAT detector. We note that  $\Delta t_{A,obs}$  is quite comparable to the observed duration of GRB 090423 (see Fig. 6).

We turn now to comparing and contrasting the spectral energy distributions in the rest frame of the two GRBs. We consider the spectrum of GRB 090618 in the energy range (89.6–896) keV, which corresponds to the *Swift*-BAT band (15–150) keV in the rest frame of GRB 090423. As for the time interval in GRB 090423, we consider the observational time interval (63.0–69.1) s, determined from applying Eq. (2) to the entire Episode 2 of GRB 090618 (see the dashed region in Fig. 7). We fitted the spectral emission observed in GRB 090423 with a Band function (Band et al. 1993), and the results provide an intrinsic peak energy  $E_{p,i} = (284.57 \pm 172.10)$  keV (see Table 1). The same model provides for the spectral emission of GRB 090423, in the  $T_{90}$  time duration, an intrinsic peak energy of  $E_{p,i} = (433.6 \pm 133.5)$  keV. However, the break in GRB 090423 is steeper, while in GRB 090618 it is more shallow. This is clear in Fig. 8, where we show the spectra of both GRBs that are transformed to a common frame, which is the one at redshift  $z = 8.2$ . Very likely, the difference in the steepening at high energies is related to the structure of the circumburst medium (CBM): the more fragmented the CBM, the larger the cutoff energy of the fireshell spectrum (Bianco & Ruffini 2005). Another important result is that the low energy index  $\alpha$  is quite similar in both GRBs. This agrees with the expectation from the fireshell scenario, where a photon index of  $\approx -0.8$  is expected in the early emission of a GRB (Patricelli et al. 2012).

The isotropic energy emitted in the time interval delineated by the dashed region in Fig. 7 has been computed to be  $E_{iso} = 3.49 \times 10^{52}$  erg, which is very similar to the one computed for the  $T_{90}$  duration, in the same energy range, for GRB 090423,  $E_{iso} = 4.99 \times 10^{52}$  erg.

## 7. Striking observations of Episode 3

That in long GRBs the X-ray emission, observed by *Swift*-XRT in energy range 0.3–10 keV, presents a typical structure composed of a steep decay, a plateau phase and a late power-law decay, was clearly expressed by Nousek, Zhang and their collaborators (Nousek et al. 2006; Zhang et al. 2006). This structure acquires a special meaning when examined in the most energetic sources,  $E_{iso} = 10^{52}$ – $10^{54}$  erg, and leads to the fundamental proof that GRB 090423 is a BdHN source.

It has only been after applying the IGC paradigm to the most energetic long GRBs associated to SNe that we noticed the most unique characterizing property of the BdHN sources: while the steep decay and the plateau phase can be very different from source to source, the late X-ray power-law component overlaps,

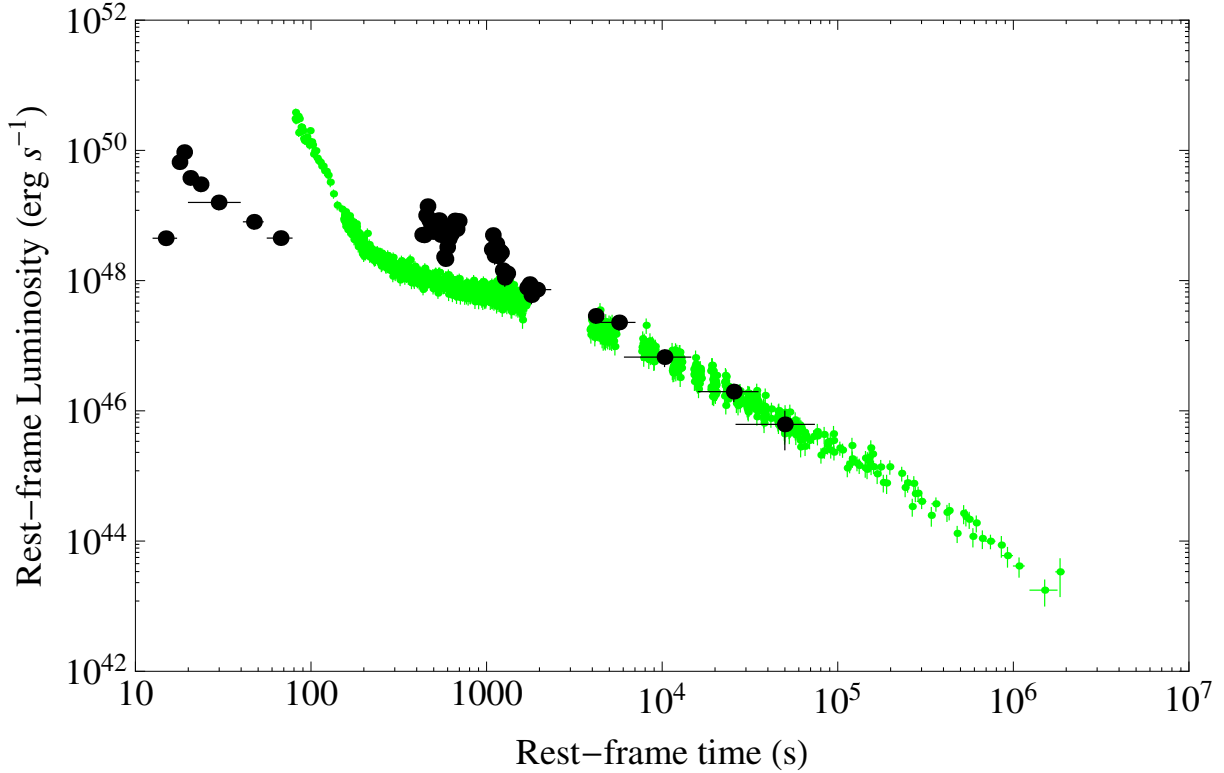


**Fig. 9.** Behavior of the Episode 3 luminosity of GRB 090423 (black dots) compared with the prototype case of GRB 090618 (green data).

when computed in the cosmological rest-frame (see [Pisani et al. 2013](#) and [Fig. 3](#)). This has become the crucial criterion for asserting membership of a GRB in the BdHN family. Indeed, when we report the late X-ray emission of Episode 3 in GRB 090423 at  $z = 8.2$ , and GRB 090618 at  $z = 0.54$ , we observe a complete overlapping at times longer than  $10^4$  s, see [Fig. 9](#).

### 7.1. Recent progress in understanding the nature of Episode 3

We recall:

- that the X-ray luminosity of Episode 3 in all BdHN sources presents precise scaling laws (see, e.g., [Fig. 3](#));
- that the very high energy emission all the way, up to 100 GeV, in GRB 130427A, as well as the optical one, follows a power-law behavior similar to the one in the X-ray emission described above. The corresponding spectral energy distribution is also described by a power-law function ([Kouveliotou et al. 2013](#); [Ruffini et al. 2014b](#)). These results clearly require a common origin for this emission process in Episode 3;
- that an X-ray thermal component has been observed in the early phases of Episode 3 of GRB 060202, 060218, 060418, 060729, 061007, 061121, 081007, 090424, 100316D, 100418A, 100621A, 101219B, and 120422A ([Page et al. 2011](#); [Starling et al. 2012](#); [Friis & Watson 2013](#)). In particular, this feature has been clearly observed in GRB 090618 and GRB 130427A ([Ruffini et al. 2014b](#)). This implies an emission region size of  $10^{12-13}$  cm in these early phases of Episode 3, with an expansion velocity of  $0.1 < v/c < 0.9$ , with a bulk Lorentz  $\Gamma$  factor  $\lesssim 2$  ([Ruffini et al. 2014a](#)).

The simultaneous occurrence of these three features imposes very stringent constraints on any possible theoretical models. In

particular, the traditional synchrotron ultra-relativistic scenario of the Collapsar jet model ([Woosley 1993](#); [Meszaros & Rees 2000](#)) does not appear suitable for explaining these observational facts.

In [Ruffini et al. \(2014a\)](#), we have recently pointed out the possibility of using the nuclear decay of ultra-heavy nuclei originally produced in the close binary phase of Episode 1 by r-process as an energy source of Episode 3. There is the remarkable coincidence that this set of processes leads to the value of the power-law emission with decay index  $\alpha$ , similar to the one observed and reported in [Metzger et al. \(2010\)](#). The total energy emitted in the decay of these ultra-heavy elements agrees with the observations in Episode 3 of BdHN sources ([Ruffini et al. 2014a](#)). An additional possibility of process-generating a scale-invariant power law in the luminosity evolution and spectrum are the ones expected from type-I and type-II Fermi acceleration mechanisms ([Fermi 1949](#)). The application of these acceleration mechanisms to the BdHN remnant has two clear advantages: 1) for us, to fulfill the above-mentioned power laws, both for the luminosity and the spectrum; and 2) for Fermi, to solve the long-standing problem, formulated by Fermi in his classic paper, of identifying the injection source to make his acceleration mechanism operational on an astrophysical level.

## 8. Conclusions

The ansatz that GRB 090423 is the transposed of GRB 090618 at  $z = 8.2$  has passed scrutiny. It is viable with respect to Episodes 1 and 4 and has obtained important positive results from the analysis of Episodes 2 and 3:

- Episodes 1 and 4 have not been detected in GRB 090423. This is consistent with the fact that the flux of Episodes 1 and 4 of GRB 090618 should not be observed by the

*Swift*-BAT detector or by the optical telescopes, owing to the very high redshift of the source and the current sensitivities of X-ray and optical detectors;

- Episode 2 of GRB 090423 has definitely been observed by *Swift*-BAT: its observed emission is comparable 1) to energy emitted ( $3.49 \times 10^{52}$  erg for GRB 090618 and  $4.99 \times 10^{52}$  erg for GRB 090423); 2) to the observed time duration (34 s for the observable part of GRB 090618 when transposed to  $z = 8.2$  and 19 s for GRB 090423); and 3) to the spectral energy distribution: the low energy part of the spectra of both GRBs is consistent with the expectation of the fireshell model (Patricelli et al. 2012). There is a significant difference only in the high energy part of the spectrum of GRB 090423, where a cutoff is observed at lower energy than the one in GRB 090618. This can be explained, in the fireshell scenario, by the existence of a dense and homogeneous CBM (Bianco & Ruffini 2005), which is expected for bursts at high redshifts;
- Episode 3 shows the striking feature of the overlapping of the late X-ray luminosities of Episode 3 in GRB 090618 and GRB 090423, when compared in their cosmological rest frames (see Fig. 9). This result confirms the extension of the relation presented in Pisani et al. (2013) for  $z \leq 1$ , all the way up to  $z = 8.2$ .

From an astrophysical point of view, all the above results clearly indicate that

- a) GRB 090423 is fully consistent with being a member of the BdHN family, and the associated SN did occur already at  $z = 8.2$ : the possibility of having an evolved binary system about 650 Myr after the Big Bang is not surprising, since the lifetime of massive stars with a mass up to  $30 M_{\odot}$  is  $\sim 10$  Myr (Woosley et al. 2002), which is similar to expectations from normal Population II binary stars also at  $z = 8.2$ , as pointed out by Belczynski et al. (2010);
- b) the FeCO core and the NS companion occurring at  $z = 8.2$  also implies the existence, as the progenitor, of a massive binary  $\sim 40\text{--}60 M_{\odot}$ . Such massive binaries have recently been identified in  $\eta$  Carinae (Damineli et al. 2000). The very rapid evolution of such very massive stars will lead first to a binary X-ray source, like Cen-X3 (see, e.g., Gursky & Ruffini 1975) and Giacconi & Ruffini (1978), which will further evolve in the FeCO with the binary NS companion. A similar evolution starting from a progenitor of two very massive stars was considered by Fryer et al. (1999) and by Bethe & Brown (1998), leading to the formation of binary NSs or postulating the occurrence of GRBs. They significantly differ from the IGC model and also differ in their final outcomes;
- c) the results presented in this article open the way to considering the late X-ray power-law behavior in Episode 3 as a distance indicator and represents a significant step toward formulating a cosmological standard candle based on Episode 3 of these BdHN sources.

We turn now to fundamental issues in physics.

- 1) The traditional fireball jet model (Meszaros 2006) describes GRBs as a single phenomenon, originating in a collapsar (Woosley 1993) and characterized by jet emission moving at Lorentz  $\Gamma$  factor in the range  $\approx 200\text{--}2000$ . This contrasts with the BdHN model where the GRB is actually composed

of three different episodes that are conceptually very different among each other (see Fig. 1): Episode 1 is non-relativistic, and Episode 2 is ultra-relativistic with Lorentz  $\Gamma$  factor  $\approx 200\text{--}2000$ , Episode 3 is mildly relativistic, with  $\Gamma \approx 2$ .

- 2) The description of Episode 1, see Fig. 2, proposes the crucial role of the Bondi-Hoyle hypercritical accretion process of the SN ejecta onto the NS companion. This requires an urgent analysis of the neutrino emission pioneered in the classic papers of Zel'dovich et al. (1972); Chevalier (1993); Fryer et al. (1996), and (Fryer 2009).
- 3) The binary nature of the progenitors in the BdHN model and the presence of the specific scaling power laws in the luminosity in Episode 3 of GRB 090423, as well as in all the other sources of the “golden sample” (see Fig. 3; Pisani et al. 2013), has led us to consider the decay of heavy nuclear material originating in  $r$ -processes (Ruffini et al. 2014a), as well as type-I and type-II Fermi acceleration mechanism as possible energy sources of the mildly relativistic Episode 3 (Ruffini et al. 2014b).

*Acknowledgements.* We are very grateful to the referee for the very thoughtful considerations and advices which greatly improved the presentation of our manuscript. We thank David W. Arnett for fruitful discussions and support. We are also grateful to Elena Zaninoni and Gennaro De Tommaso for their comments on the manuscript. This work made use of data supplied by the UK *Swift* Science Data Centre at the University of Leicester. G.B.P., M.E., and M.K. are supported by the Erasmus Mundus Joint Doctorate Program by grant Nos. 2011-1640, 2012-1710, and 2013-1471, respectively, from the EACEA of the European Commission.

## References

- Amati, L., Frontera, F., Tavani, M., et al. 2002, A&A, 390, 81  
 Band, D. L. 2003, ApJ, 588, 945  
 Band, D., Matteson, J., Ford, L., et al. 1993, ApJ, 413, 281  
 Barthelmy, S. D., Barbier, L. M., Cummings, J. R., et al. 2005, Space Sci. Rev., 120, 143  
 Belczynski, K., Holz, D. E., Fryer, C. L., et al. 2010, ApJ, 708, 117  
 Bethe, H. A., & Brown, G. E. 1998, ApJ, 506, 780  
 Bianco, C. L., & Ruffini, R. 2005, ApJ, 620, L23  
 Bisnovatyi-Kogan, G. S., & Lamzin, S. A. 1984, Sov. Astron., 28, 187  
 Bondi, H. 1952, MNRAS, 112, 195  
 Bondi, H., & Hoyle, F. 1944, MNRAS, 104, 273  
 Burrows, D., Hill, J., Nousek, J., et al. 2005, Space Sci. Rev., 120, 165  
 Chevalier, R. A. 1989, ApJ, 346, 847  
 Chevalier, R. A. 1993, ApJ, 411, L33  
 Damineli, A., Kaufer, A., Wolf, B., et al. 2000, ApJ, 528, L101  
 Enderli, M. 2013, 27th Texas Symp. on Relativistic Astrophysics, Dallas, TX (USA), December 8–13  
 Fermi, E. 1949, Phys. Rev., 75, 1169  
 Fermi-LAT collaboration, & Fermi-GBM collaboration. 2014, Science, 343, 42  
 Friis, M., & Watson, D. 2013, ApJ, 771, 15  
 Fryer, C. L. 2009, ApJ, 699, 409  
 Fryer, C. L., Benz, W., & Herant, M. 1996, ApJ, 460, 801  
 Fryer, C. L., Woosley, S. E., & Hartmann, D. H. 1999, ApJ, 526, 152  
 Gehrels, N., Sarazin, C. L., O’Brien, P. T., et al. 2005, Nature, 437, 851  
 Giacconi, R., & Ruffini, R. 1978, Physics and astrophysics of neutron stars and black holes (Amsterdam: North Holland Publishing)  
 Gursky, H., & Ruffini, R. 1975, Neutron stars, black holes and binary X-ray sources; Proceedings of the Annual Meeting, San Francisco, Calif., February 28, 1974, (Dordrecht: D. Reidel Publishing), Astrophys. Space Sci. Lib. 48  
 Izzo, L., Bernardini, M. G., Bianco, C. L., et al. 2010, JKPS, 57-3, 551  
 Izzo, L., Rueda, J. A., & Ruffini, R. 2012a, A&A, 548, L5  
 Izzo, L., Ruffini, R., Penacchioni, A. V., et al. 2012b, A&A, 543, A10  
 Kann, D. A., Klose, S., Zhang, B., et al. 2011, ApJ, 734, 96  
 Kouveliotou, C., Granot, J., Racusin, J. L., et al. 2013, ApJ, 779, L1  
 Krimm, H. A., Beardmore, A. P., Evans, P. A., et al. 2009, GRB Coordinates Network, 9198, 1  
 Margutti, R., Zaninoni, E., Bernardini, M. G., et al. 2013, MNRAS, 428, 729

<sup>2</sup> <http://nsm.utdallas.edu/texas2013/proceedings/3/1/Ruffini.pdf>

- Meegan, C., Lichti, G., Bhat, P. N., et al. 2009, *ApJ*, 702, 791
- Melandri, A., Pian, E., D'Elia, V., et al. 2014, *A&A*, 567, A29
- Meszáros, P. 2006, *Rep. Prog. Phys.*, 69, 2259
- Meszáros, P., & Rees, M. J. 2000, *ApJ*, 530, 292
- Metzger, B. D., Martínez-Pinedo, G., Darbha, S., et al. 2010, *MNRAS*, 406, 2650
- Nousek, J. A., Kouveliotou, C., Grupe, D., et al. 2006, *ApJ*, 642, 389
- Page, K. L., Starling, R. L. C., Fitzpatrick, G., et al. 2011, *MNRAS*, 416, 2078
- Patricelli, B., Bernardini, M. G., Bianco, C. L., et al. 2012, *ApJ*, 756, 16
- Penacchioni, A. V., Ruffini, R., Izzo, L., et al. 2012, *A&A*, 538, A58
- Penacchioni, A. V., Ruffini, R., Bianco, C. L., et al. 2013, *A&A*, 551, A133
- Pisani, G. B., Izzo, L., Ruffini, R., et al. 2013, *A&A*, 552, L5
- Rueda, J. A., & Ruffini, R. 2012, *ApJ*, 758, L7
- Ruffini, R. 2011, *Int. J. Mod. Phys. D*, 20, 1797
- Ruffini, R. 2013, 27th Texas Symposium on Relativistic Astrophysics, Dallas, TX (USA), December 8–13
- Ruffini, R., Izzo, L., Muccino, M., et al. 2013, [[arXiv:1311.7432](https://arxiv.org/abs/1311.7432)]
- Ruffini, R., Muccino, M., Bianco, C. L., et al. 2014a, *A&A*, 565, L10
- Ruffini, R., Wang, Y., Kovacevic, M., et al. 2014b, *ApJ*, submitted [[arXiv:1405.5723](https://arxiv.org/abs/1405.5723)]
- Salvaterra, R., Della Valle, M., Campana, S., et al. 2009, *Nature*, 461, 1258
- Salvaterra, R., Campana, S., Vergani, S. D., et al. 2012, *ApJ*, 749, 68
- Starling, R. L. C., Page, K. L., Pe'Er, A., Beardmore, A. P., & Osborne, J. P. 2012, *MNRAS*, 427, 2950
- Stratta, G., & Perri, M. 2009, *GRB Coordinates Network*, 9212, 1
- Tanvir, N. R., Fox, D. B., Levan, A. J., et al. 2009, *Nature*, 461, 1254
- von Kienlin, A. 2009a, *GRB Coordinates Network*, 9229, 1
- von Kienlin, A. 2009b, *GRB Coordinates Network*, 9251, 1
- Woosley, S. E. 1993, *ApJ*, 405, 273
- Woosley, S. E., Heger, A., & Weaver, T. A. 2002, *Rev. Mod. Phys.*, 74, 1015
- Zel'dovich, Y. B., Ivanova, L. N., & Nadezhin, D. K. 1972, *Sov. Astron.*, 16, 209
- Zhang, B., Fan, Y. Z., Dyks, J., et al. 2006, *ApJ*, 642, 354



# The Genuine Short GRB 090227B and the Disguised by Excess GRB 090510<sup>‡</sup>

Marco Muccino<sup>1,2\*</sup>, Carlo Luciano Bianco<sup>1,2</sup>, Luca Izzo<sup>1,2</sup>,  
Yu Wang<sup>1,2</sup>, Maxime Enderli<sup>1,3</sup>, Milos Kovacevic<sup>1,3</sup>,  
Giovanni Battista Pisani<sup>1,3</sup>, Ana Virginia Penacchioni<sup>4</sup>, and Remo Ruffini<sup>1,2,3,4</sup>

<sup>1</sup>*Dipartimento di Fisica and ICRA, Sapienza Università di Roma, Piazzale Aldo Moro 5, I-00185 Rome, Italy*

<sup>2</sup>*ICRANet, Piazza della Repubblica 10, I-65122 Pescara, Italy*

<sup>3</sup>*Université de Nice Sophia Antipolis, Nice, CEDEX 2, Grand Château Parc Valrose, Nice, France*

<sup>4</sup>*ICRANet-Rio, CBPF, Rua Dr. Xavier Sigaud 150, Rio de Janeiro, RJ, 22290-180, Brazil*

Received April 15, 2014

**Abstract**—GRB 090227B and GRB 090510, traditionally classified as short gamma-ray Bursts (GRBs), indeed originate from different systems. For GRB 090227B we inferred a total energy of the  $e^+e^-$  plasma  $E_{e^+e^-}^{\text{tot}} = (2.83 \pm 0.15) \times 10^{53}$  erg, a baryon load of  $B = (4.1 \pm 0.05) \times 10^{-5}$ , and a CircumBurst Medium (CBM) average density  $\langle n_{\text{CBM}} \rangle = (1.90 \pm 0.20) \times 10^{-5} \text{ cm}^{-3}$ . From these results we have assumed the progenitor of this burst to be a symmetric neutron stars (NSs) merger with masses  $m = 1.34 M_{\odot}$ , radii  $R = 12.24$  km. GRB 090510, instead, has  $E_{e^+e^-}^{\text{tot}} = (1.10 \pm 0.06) \times 10^{53}$  erg,  $B = (1.45 \pm 0.28) \times 10^{-3}$ , implying a Lorentz factor at transparency of  $\Gamma = (6.7 \pm 1.7) \times 10^2$ , which are characteristic of the long GRB class, and a very high CBM density,  $\langle n_{\text{CBM}} \rangle = (1.85 \pm 0.14) \times 10^3 \text{ cm}^{-3}$ . The joint effect of the high values of  $\Gamma$  and of  $\langle n_{\text{CBM}} \rangle$  compresses in time and “inflates” in intensity in an extended afterglow, making appear GRB 090510 as a short burst, which we here define as “disguised short GRB by excess” occurring an overdense region with  $10^3 \text{ cm}^{-3}$ .

**DOI:** 10.1134/S0202289314030116

## 1. INTRODUCTION

After the initial BATSE classification of Gamma-Ray Bursts (GRBs) into “long” and “short” ones [1–4], in the recent years, owing to the observations by the *Swift* satellite [5], a third class of bursts with hybrid properties between short and long ones has been discovered: “short GRBs with extended emission” [6].

In the Fireshell model [7, 9], GRBs originate from an optically thick  $e^+e^-$  plasma in thermal equilibrium [10], formed around a Kerr-Newman black hole. This shell of plasma expands and engulfs a baryonic remnant, keeping its thermal equilibrium [11]. The engulfed baryonic mass  $M_B$  is described by the Baryon load  $B = M_B c^2 / E_{e^{\pm}}^{\text{tot}}$ , where  $E_{e^{\pm}}^{\text{tot}}$  is the total plasma energy. The canonical GRB is composed of

emission at the transparency, the Proper-GRB (P-GRB), and an extended afterglow, due to collisions of accelerated baryons with the CircumBurst Medium (CBM) with density  $n_{\text{CBM}}$ . In this scenario the “short GRBs with extended emission” [6] have been successfully interpreted as “disguised short bursts” [12–14]: canonical long bursts with  $3 \times 10^{-4} \leq B \leq 10^{-2}$ , exploding in halos of their host galaxies, with  $\langle n_{\text{CBM}} \rangle \approx 10^{-3} \text{ cm}^{-3}$ . “Genuine short” GRBs [8, 15], instead, are characterized by smaller baryon loads,  $B \lesssim 10^{-5}$  (see Fig. 1, right plot), therefore the energy emitted in their P-GRB is predominant, and an additional nonthermal component originating from the extended afterglow is expected.

We present our results on two short bursts: GRB 090227B, the first genuine short GRB, originating from a symmetric binary NSs merger [16], and GRB 090510, a *disguised short GRBs by excess* occurring in a medium with  $\langle n_{\text{CBM}} \rangle \approx 10^3 \text{ cm}^{-3}$  [17].

## 2. THE GENUINE SHORT GRB 090227B

GRB 090227B has been detected by the *Fermi*-GBM [18] and the *Konus*-Wind [19] detectors. Due

\*E-mail: marco.muccino@cra.it

<sup>‡</sup>Based on a plenary talk given at the 11th International Conference on Gravitation, Astrophysics and Cosmology of Asia-Pacific Countries (ICGAC-11), October 1–5, 2013, Almaty, Kazakhstan.

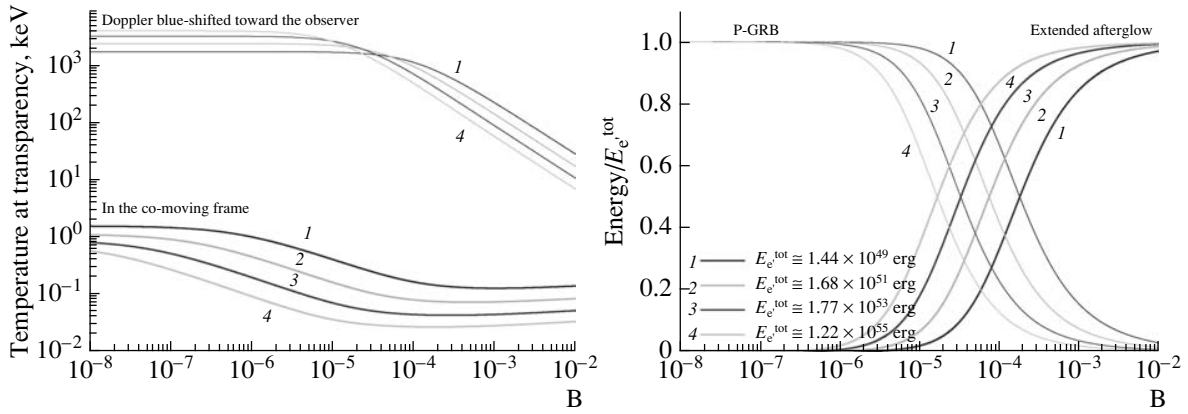


**Fig. 1.** The comoving and blueshifted temperatures of a plasma at the transparency, and the fraction of energy radiated in the P-GRB and in the extended afterglow as functions of  $B$  for selected values of  $E_{e^+e^-}^{\text{tot}}$ .

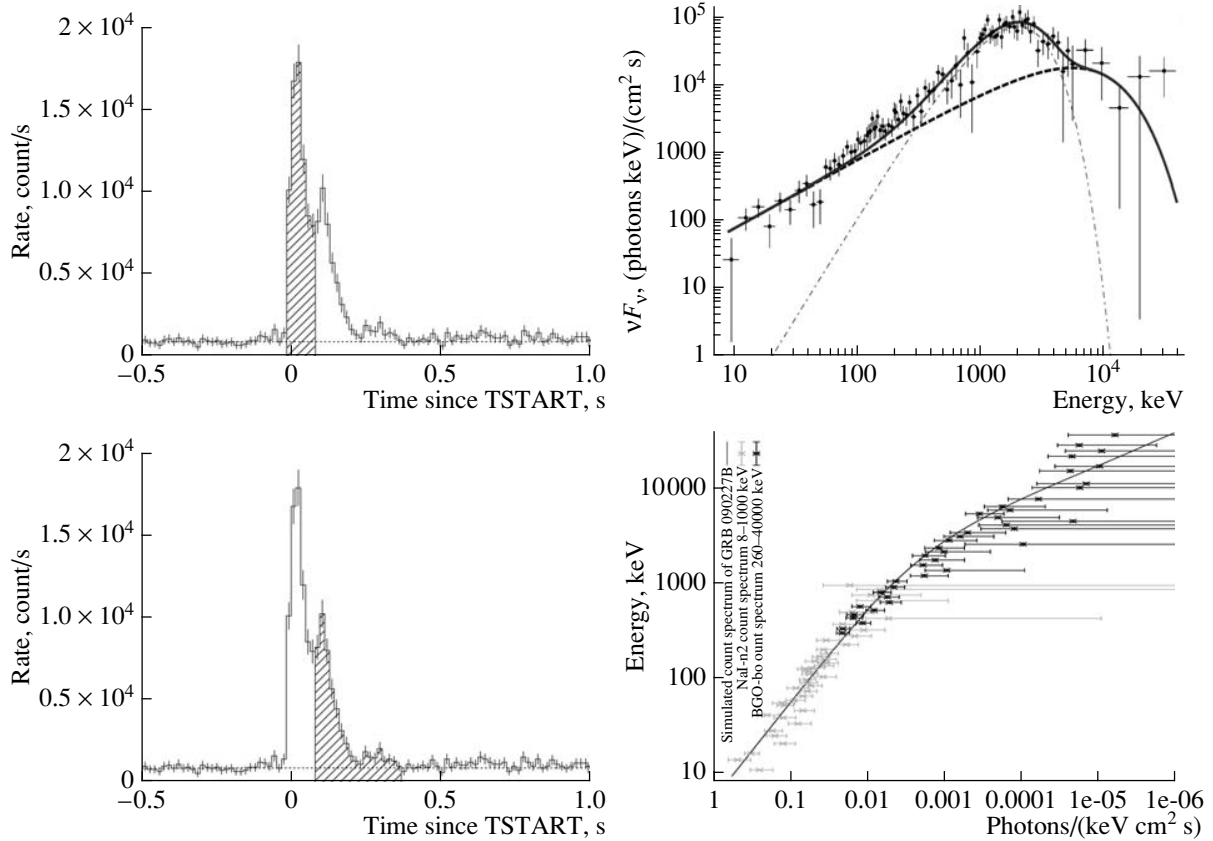


**Fig. 2.** Left: the NaI-n2 light curves of the P-GRB (upper panel) and the extended afterglow (lower panel). Right: the simulated  $\nu F_\nu$  spectrum of a P-GRB (upper panel, solid red curve) as a sum of the onset of the extended afterglow (8 keV–40 MeV, dashed blue line) and of the BB emission of the P-GRB (dashed-dotted green line), compared to the observed data; (lower panel) the simulated photon spectrum of the extended-afterglow (8 keV–40 MeV) compared to the NaI-n2 (green) and the BGO-b0 (blue) data in the time interval from  $T_0 + 0.015$  s to  $T_0 + 0.385$  s.

to the lack of X-rays and optical follow-up, its redshift is unknown.

We have analyzed the *Fermi*-GBM data from the

NaI-n2 (8–900 keV) and the BGO-b0 (250 keV–40 MeV) detectors. The NaI-n2 light curve (see Fig. 2, left panels) shows two spike-like structures.

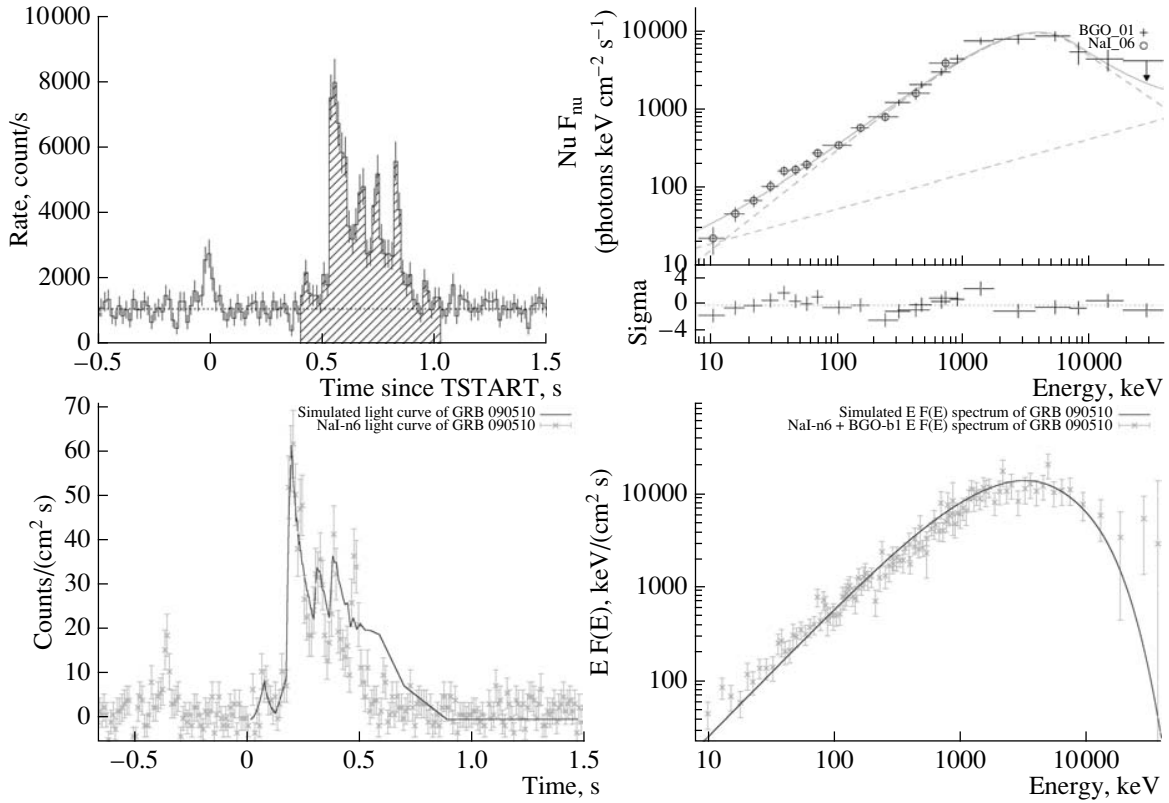


**Fig. 3.** Upper panels: the NaI-n6 light curve (left) and the NaI+BGO  $\nu F_\nu$  spectrum in the  $\Delta T_2$  time interval. Lower panels: (left) the simulated light curve and spectrum (8 keV–40 MeV) of the early  $\sim 0.4$  s of the extended afterglow (right).

We indicate the trigger time by  $T_0$ . The spectrum of the first spike (from  $T_0 - 0.016$  s to  $T_0 + 0.080$  s) is best fitted by black body (BB) plus Band [20] model (see Table 1). The best fit of the second spike (from  $T_0 + 0.080$  s to  $T_0 + 0.368$  s) is a Band model (see Table 1). Consequently, we have interpreted the first spike, where a thermal spectrum is present, as a P-GRB and the second one as an extended afterglow.

Having identified the P-GRB, the correct value of  $B$  is determined when the theoretical energy and temperature of the P-GRB match the observed ones of thermal emission, namely,  $E_{\text{BB}}$  and  $kT_{\text{obs}}$ . Since the redshift  $z$  of GRB 090227B is unknown, we have estimated the ratio  $E_{\text{P-GRB}}/E_{e^+e^-}^{\text{tot}}$  from the ratio of the observed fluences  $S_{\text{BB}}/S_{\text{tot}}$ . The fluence of the BB component of the P-GRB (see Table 1, first interval) is  $S_{\text{BB}} = (1.54 \pm 0.45) \times 10^{-5}$  erg/cm<sup>2</sup>. The total fluence of the burst is  $S_{\text{tot}} = (3.79 \pm 0.20) \times 10^{-5}$  erg/cm<sup>2</sup> and has been evaluated in the time interval from  $T_0 - 0.016$  s to  $T_0 + 0.896$  s. Therefore we have  $E_{\text{P-GRB}}/E_{e^+e^-}^{\text{tot}} = (40.67 \pm 0.12)\%$ . From the right plot in Fig. 1, for each energy ratio we have a possible range for  $B$  and  $E_{e^+e^-}^{\text{tot}}$ . In turn, for each couple of  $B$  and  $E_{e^+e^-}^{\text{tot}}$  we can determine the blueshifted

temperature  $kT_{\text{blue}}$  (Fig. 1, left plot) and, correspondingly, the redshift by the ratio  $kT_{\text{blue}}/kT_{\text{obs}} = 1 + z$ . We have computed the isotropic energy  $E_{\text{iso}}$  for each value of  $z$ , searching for the correct value fulfilling the condition  $E_{\text{iso}} \equiv E_{e^+e^-}^{\text{tot}}$ . We have found the equality at  $z = 1.61 \pm 0.14$  for  $B = (4.13 \pm 0.05) \times 10^{-5}$  and  $E_{e^+e^-}^{\text{tot}} = (2.83 \pm 0.15) \times 10^{53}$  erg. The corresponding Lorentz factor at the transparency is  $\Gamma_{\text{tr}} = (1.44 \pm 0.01) \times 10^4$ . From a simulation of the extended afterglow light curve and spectrum [29, 30], we have derived the average CBM density  $\langle n_{\text{CBM}} \rangle = (1.90 \pm 0.20) \times 10^{-5}$  cm<sup>-3</sup>, typical of the galactic halos environment. In Fig. 2, lower right panel, we have plotted the simulated spectrum of early  $\sim 0.4$  s of emission. In the upper right panel, we have reproduced the total observed spectrum of the first spike (8–40000 keV) as a sum of the thermal spectrum of the P-GRB and of the early extended afterglow onset (from  $T_0 + 0.015$  s to  $T_0 + 0.080$  s).

### 3. THE DISGUISED SHORT BY EXCESS GRB 090510

GRB 090510 has been detected by the *Fermi*-GBM [21], *Fermi*-LAT [22], *Swift*-BAT [23], *AGILE* [24], *Konus*-Wind [25], and *Suzaku*-WAM [26]

**Table 1.** Results of spectral analysis of the P-GRB (best fit BB + Band model) and of the extended afterglow (EA, best fit Band model) in the energy range 8 keV–40 MeV

	$kT$ (keV)	$\alpha$	$\beta$	$E_p$ (keV) ( $\text{erg cm}^{-2} \text{s}^{-1}$ )	$F_{\text{tot}}/10^{-5}$ ( $\text{erg cm}^{-2} \text{s}^{-1}$ )	$F_{BB}/10^{-5}$	C-STAT/DOF
P-GRB	$517 \pm 28$	$-0.80 \pm 0.05$	$-2.14 \pm 0.17$	$952 \pm 251$	$31.3 \pm 1.3$	$16.1 \pm 4.7$	263.51/239
EA		$-0.79 \pm 0.06$	$-2.01 \pm 0.10$	$1048 \pm 178$	$2.66 \pm 0.26$		276.50/241

**Table 2.** The  $\Delta T_1$  time interval: parameters of BB + PL and Compt models in the energy range 8–7000 keV. The  $\Delta T_2$  time interval: parameters of the best fits (Band + PL) in the energy ranges 8 keV–30 GeV (GBM + LAT)

Int	Model	$kT-E_p$ (keV)	$\alpha$	$\beta$	$\gamma$	$F_{\text{tot}}/10^{-6}$ ( $\text{erg cm}^{-2} \text{s}^{-1}$ )	C-STAT/DOF
$\Delta T_1$	BB + PL	$34.2 \pm 7.5$	...	...	$-1.10 \pm 0.14$	$7.6 \pm 1.3$	188.60/193
	Compt	$990 \pm 554$	$-0.81 \pm 0.22$	...	...	$4.4 \pm 1.6$	189.97/194
$\Delta T_2$	Band + PL	$3941 \pm 346$	$-0.71 \pm 0.07$	$-2.97 \pm 0.26$	$-1.62 \pm 0.05$	$83.3 \pm 6.8$	199.20/256

detectors. Optical observations by VLT/FORS2 located its host galaxy at redshift  $z = 0.903 \pm 0.003$  [27].

We have analyzed the *Fermi*-GBM data from NaI-n6 (8–900 keV) and BGO-b1 (260 keV–40 MeV) detectors and the LAT data in the energy range 100 MeV–30 GeV. The light curve of GRB 090510 is composed of two episodes, 0.5 s apart (see Fig. 3, upper left plot). From the analysis of the first episode, from  $T_0 - 0.064$  s to  $T_0 + 0.016$  s (in the following  $\Delta T_1$ ), we have found that BB+PL and Compt are the viable best fits (see Table 2). From our theoretical interpretation, the BB+PL, being equally probable as the Compt model, is adopted for its physical meaning. Therefore, the interval  $\Delta T_1$  has

been identified as the P-GRB. The total energy of the first episode is  $E_1 = (2.28 \pm 0.39) \times 10^{51}$  erg.

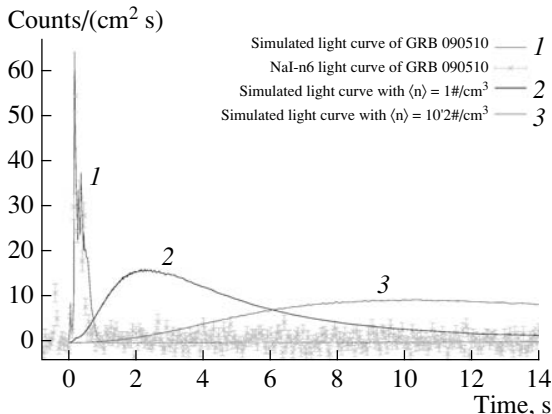
The second episode, from  $T_0 + 0.400$  s to  $T_0 + 1.024$  s (in the following  $\Delta T_2$ ), is interpreted as the extended afterglow. Combining the GBM (8 keV–40 MeV) and the LAT data up to 30 GeV [28], the best fit of this episode is Band+PL, and its total energy is  $E_2 = (1.08 \pm 0.06) \times 10^{53}$  erg. The results are shown in Fig. 3 and Table 2.

We have started a simulation using as input parameters  $E_{e^+e^-}^{\text{tot}}$ , constrained to the isotropic energy of the burst,  $E_{\text{iso}} = (1.10 \pm 0.06) \times 10^{53}$  erg, and the Baryon load  $B = (1.45 \pm 0.28) \times 10^{-3}$ , determined as illustrated in Section 2. This implies a Lorentz factor at transparency  $\Gamma_{\text{tr}} = (6.7 \pm 1.6) \times 10^2$ . From simulation of the extended afterglow light curve (see Fig. 3, lower left panel) and of the corresponding spectrum (8 keV–40 MeV) of the early  $\sim 0.4$  s of the emission (lower right panel), we have inferred a very high CBM average density,  $\langle n_{\text{CBM}} \rangle = (1.85 \pm 0.14) \times 10^3 \text{ cm}^{-3}$ .

#### 4. CONCLUSIONS

Although their intrinsic duration is  $T_{90} < 2$  s, a detailed time-resolved spectral analysis has allowed for shedding light on the astrophysical origin of GRB 090227B and GRB 090510, proving that the GRBs classification is indeed much more complex.

GRB 090227B represents a real genuine short burst with  $B = (4.13 \pm 0.05) \times 10^{-5}$ . This implies that the P-GRB energy is comparable to the one of the extended afterglow. Within the Fireshell scenario, we have determined its cosmological redshift,  $z =$

**Fig. 4.** The NaI-n6 light curve (crosses) and the extended afterglow simulations corresponding to  $\langle n_{\text{CBM}} \rangle \approx 10^3 \text{ cm}^{-3}$  (1),  $1 \text{ cm}^{-3}$  (2), and  $10^{-2} \text{ cm}^{-3}$  (3).

$1.61 \pm 0.14$ , as well as the energy,  $E_{e^+e^-}^{\text{tot}} = (2.83 \pm 0.15) \times 10^{53}$  erg, and the Lorentz factor at the transparency,  $\Gamma_{\text{tr}} = (1.44 \pm 0.01) \times 10^4$ . From the average density of the CBM,  $\sim 10^{-5} \text{ cm}^{-3}$ , typical of the galactic halo of host galaxies [12–14], we infer that the progenitor of GRB 090227B is a merger of two NSs. In fact, the inferred baryon load is consistent with the mass of the crusts of a symmetric binary system of two neutron stars (NSs), with masses  $m = 1.34 M_{\odot}$  and radii  $R = 12.24$  km, as described by the new model of NS fulfilling the global charge neutrality condition [31]. In this picture, assuming the NL3 nuclear model parameters, the NS critical mass is  $M_{\text{cr}} = 2.67 M_{\odot}$ . From the above characteristics of the binary NSs, we inferred an absolute upper limit on the energy emitted via gravitational waves,  $\sim 9.6 \times 10^{52}$  ergs [32]. More details are given in the published paper [16].

In the case of GRB 090510, we point out that the inferred baryon of  $B = 1.45 \times 10^{-3}$ , is typical of long GRBs, and not consistent with the values inferred for genuine short bursts, see, e.g., GRB 090227B. Also the CBM density of  $\sim 10^3 \text{ cm}^{-3}$ , typical of dense clouds in the inner galactic regions, points at a different origin than the merger scenario for real short GRBs, see, e.g., [16, 33, 34]. The short nature of GRB 090510 is a by-product of the relativistic motion of the burst,  $\Gamma_{\text{tr}} = (6.7 \pm 1.6) \times 10^2$ , and of the high-density environment. Therefore its extended afterglow emission is compressed in time and “inflated” in intensity with respect to the canonical one (see Fig. 4), making it apparently closer to the genuine short class of GRBs [16]. More details are given in the published paper [17].

Within the Fireshell model, three different possible structures of the canonical GRB, supported by observational evidences, are derived.

(1) Long GRBs have  $3.0 \times 10^{-4} \lesssim B \leq 10^{-2}$  and explode in environments with densities of  $\langle n_{\text{CBM}} \rangle \approx 1 \text{ cm}^{-3}$ , which are typical of the inner galactic regions and in agreement with the observational evidence of their occurrence close to star-forming regions.

(2) Disguised short GRBs have the same Baryon load as the long ones, but they occur in different environments. (a) *Disguised short GRBs by excess* occur in overdense media, e.g.,  $\langle n_{\text{CBM}} \rangle \approx 10^3 \text{ cm}^{-3}$ , as in the present case of GRB 090510 [17], therefore the bulk of  $\gamma$ -ray emission occurs at short time-scale as for the genuine short GRBs. (b) *Disguised short GRBs by defect* occur in a CBM with  $\langle n_{\text{CBM}} \rangle \approx 10^{-3} \text{ cm}^{-3}$ , typical of galactic halos [12–14] as confirmed by the observed offset from the center of their

host galaxies [35, 36]. Therefore, their  $\gamma$ -ray emission is deflated in intensity and characterized by an extended emission, see, e.g., [6, 12–14].

(3) Genuine short GRBs occur for  $B \lesssim 10^{-5}$  and  $\langle n_{\text{CBM}} \rangle \approx 10^{-5} \text{ cm}^{-3}$ , typical again of galactic halos. In these bursts the P-GRB emission is large as the extended afterglow one, and no X-ray emission and, consequently, no redshift determination are expected, as in the case GRB 090227B. Their progenitors are NSs mergers [16].

## REFERENCES

1. R. W. Klebesadel, in *Gamma-Ray Bursts—Observations, Analyses and Theories*, ed. C. Ho, R. I. Epstein, and E. E. Fenimore (Cambridge University Press, 1992), p. 161–168.
2. J.-P. Dezalay et al., in *American Institute of Physics Conference Series*, ed. W. S. Paciesas and G. J. Fishman, **265**, 304 (1992).
3. C. Kouveliotou et al., *ApJ Lett.* **413**, L101 (1993).
4. M. Tavani, *ApJ Lett.* **497**, L21 (1998), astro-ph/9802192.
5. N. Gehrels et al., *Nature (London)* **437**, 851 (2005), astro-ph/0505630.
6. J. P. Norris and J. T. Bonnell, *ApJ* **643**, 266 (2006), astro-ph/0601190.
7. R. Ruffini et al., *ApJ Lett.* **555**, L117 (2001), astro-ph/0106534.
8. R. Ruffini et al., *ApJ Lett.* **555**, L113 (2001), astro-ph/0106532.
9. R. Ruffini et al., *ApJ Lett.* **555**, L107 (2001), astro-ph/0106531.
10. A. G. Aksenov, R. Ruffini, and G. V. Vereshchagin, *Phys. Rev. Lett.* **99**, 125003 (2007), arXiv: 0707.3250.
11. R. Ruffini, J. D. Salmonson, J. R. Wilson, and S. Xue, *A&A* **359**, 855 (2000), astro-ph/0004257.
12. M. G. Bernardini et al., *A&A* **474**, L13 (2007).
13. L. Caito et al., *A&A* **521**, A80+ (2010), arXiv: 1006.4842.
14. G. de Barros et al., *A&A* **529**, A130 (2011), arXiv: 1101.5612.
15. R. Ruffini et al., *ApJ Lett.* **581**, L19 (2002), astro-ph/0210648.
16. M. Muccino et al., *ApJ* **763**, 125 (2013), arXiv: 1205.6600.
17. M. Muccino et al., *ApJ* **772**, 62 (2013), arXiv: 1306.3467.
18. S. Guiriec, *GCN* **8921**, 1 (2009).
19. S. Golenetskii et al., *GCN* **8926**, 1 (2009).
20. D. Band et al., *ApJ* **413**, 281 (1993).
21. S. Guiriec, V. Connaughton, and M. Briggs, *GCN* **9336**, 1 (2009).
22. M. Ohno and V. Pelassa, *GCN* **9334**, 1 (2009).
23. E. A. Hoversten et al., *GCN* **9331**, 1 (2009).
24. F. Longo et al., *GCN* **9343**, 1 (2009).
25. S. Golenetskii et al., *GCN* **9344**, 1 (2009).
26. N. Ohmori et al., *GCN* **9355**, 1 (2009).

27. A. Rau, S. McBreen, and T. Kruehler, GCN **9353**, 1 (2009).
28. M. Ackermann et al., ApJ **716**, 1178 (2010), arXiv: 1005.2141.
29. C. L. Bianco and R. Ruffini, ApJ Lett. **605**, L1 (2004), astro-ph/0403379.
30. B. Patricelli et al., ApJ **756**, 16 (2012), arXiv: 1206.5605.
31. R. Belvedere et al., Nucl. Phys. A **883**, 1 (2012); <http://www.sciencedirect.com/science/article/pii/S0375947412001029>.
32. J. A. Rueda and R. Ruffini, arXiv: 1205.6915.
33. S. I. Blinnikov, I. D. Novikov, T. V. Perevodchikova, and A. G. Polnarev, Sov. Astron. Lett. **10**, 177 (1984).
34. B. Paczynski, ApJ Lett. **494**, L45 (1998), astro-ph/9710086.
35. W. Fong, E. Berger, and D. B. Fox, ApJ **708**, 9 (2010), arXiv: 0909.1804.
36. E. Berger, New Astron. Rev. **55**, 1 (2011), arXiv: 1005.1068.



# Two Short Bursts Originating from Different Astrophysical Systems: the Genuine Short GRB 090227B and the Disguised Short GRB 090510 by Excess

Marco MUCCINO,\* Carlo Luciano BIANCO, Luca IZZO and Yu WANG

*Dip. di Fisica and International Center of Relativistic Astrophysics,  
Sapienza Università di Roma, Piazzale Aldo Moro 5, I-00185 Rome, Italy  
and ICRANet, Piazza della Repubblica 10, I-65122 Pescara, Italy*

Maxime ENDERLI and Giovanni Battista PISANI

*Dip. di Fisica and International Center of Relativistic Astrophysics,  
Sapienza Università di Roma, Piazzale Aldo Moro 5, I-00185 Rome, Italy and  
Université de Nice Sophia Antipolis, Nice, CEDEX 2, Grand Château Parc Valrose*

Ana Virginia PENACCHIONI

*ICRANet-Rio, Centro Brasileiro de Pesquisas Fisicas,  
Rua Dr. Xavier Sigaud 150, Rio de Janeiro, RJ, 22290-180, Brazil*

Remo RUFFINI

*Dip. di Fisica and International Center of Relativistic Astrophysics,  
Sapienza Università di Roma, Piazzale Aldo Moro 5, I-00185 Rome, Italy  
ICRANet, Piazza della Repubblica 10, I-65122 Pescara, Italy  
Université de Nice Sophia Antipolis, Nice, CEDEX 2, Grand Château Parc Valrose and  
ICRANet-Rio, Centro Brasileiro de Pesquisas Fisicas,  
Rua Dr. Xavier Sigaud 150, Rio de Janeiro, RJ, 22290-180, Brazil.*

(Received 30 November 2014, in final form 12 March 2014)

GRB 090227B and GRB 090510 are two gamma-ray bursts (GRBs) traditionally classified as short bursts. The major outcome of our analysis is that they indeed originate from different systems. In the case of GRB 090227B, from the inferred values of the total energy of the  $e^+e^-$  plasma,  $E_{e^+e^-}^{tot} = (2.83 \pm 0.15) \times 10^{53}$  erg, the engulfed baryonic mass  $M_B$ , expressed as  $B = M_B c^2 / E_{e^+e^-}^{tot} = (4.1 \pm 0.05) \times 10^{-5}$ , and the circumburst medium (CBM) average density,  $\langle n_{CBM} \rangle = (1.90 \pm 0.20) \times 10^{-5} \text{ cm}^{-3}$ , we have assumed the progenitor of this burst to be a symmetric neutron star (NS) merger with masses  $m = 1.34 M_\odot$ , radii  $R = 12.24$  km, and crustal thicknesses of  $\sim 0.47$  km. In the case of GRB 090510, we have derived the total plasma energy,  $E_{e^+e^-}^{tot} = (1.10 \pm 0.06) \times 10^{53}$  erg, the Baryon load,  $B = (1.45 \pm 0.28) \times 10^{-3}$ , and the Lorentz factor at transparency,  $\Gamma = (6.7 \pm 1.7) \times 10^2$ , which are characteristic of the long GRB class, as well as a very high CBM density,  $\langle n_{CBM} \rangle = (1.85 \pm 0.14) \times 10^3 \text{ cm}^{-3}$ . The joint effect of the high values of  $\Gamma$  and  $\langle n_{CBM} \rangle$  compresses in time and “inflates” in intensity the extended afterglow, making GRB 090510 appear to be a short burst, which we here define as a “disguised short GRB by excess”, occurring in an overdense region with  $10^3 \text{ cm}^{-3}$ .

PACS numbers: 98.70.Rz, 97.60.Jd

Keywords: Gamma-ray burst: general — Gamma-ray burst: GRB 090227B, GRB 090510

DOI: 10.3938/jkps.65.0

## I. INTRODUCTION

The initial BATSE classification of GRBs into “long” and “short” [1–4] was clearly premature both from an observational and a theoretical point of view. This fact

became clear after the discovery by the *Swift* satellite [5] of a third class of bursts with hybrid properties between the short and the long ones: the “short GRBs with an extended emission” [6].

In the Fireshell model [7–9], GRBs originate from an optically-thick  $e^+e^-$  plasma in thermal equilibrium [10] formed around a Kerr-Newman black hole. This plasma is confined in an expanding shell and engulfs

\*E-mail: marco.muccino@cra.it

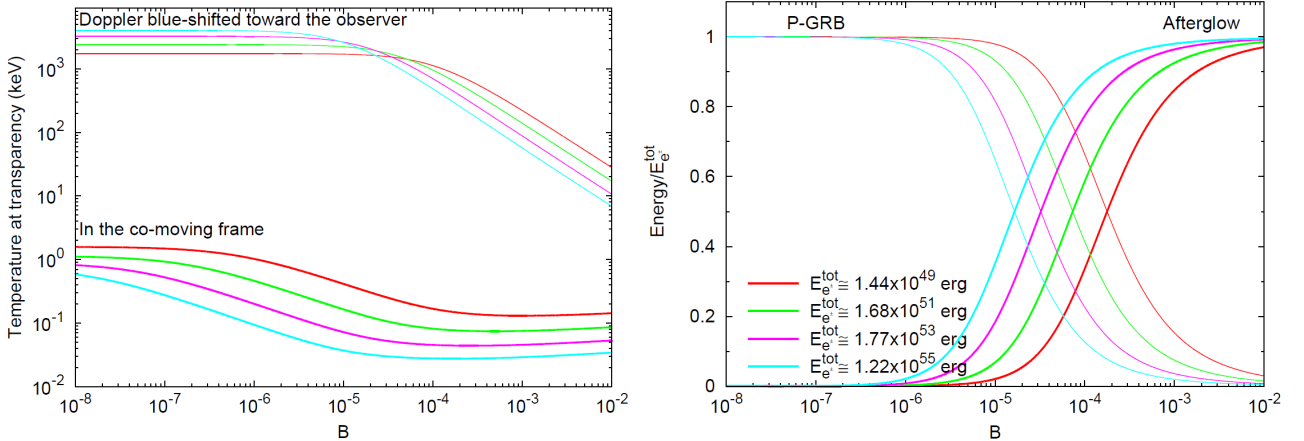


Fig. 1. (Color online) Co-moving and blue-shifted temperatures of the plasma at transparency, and the fraction of energy radiated in the P-GRB and in the extended afterglow as functions of  $B$  for selected values of  $E_{e^+e^-}^{tot}$ .

the baryonic remnant, which thermalizes with the pairs [11]. The engulfed baryonic mass  $M_B$  is described by the Baryon load  $B = M_B c^2 / E_{e^\pm}^{tot}$ , where  $E_{e^\pm}^{tot}$  is the total plasma energy. The canonical GRB is composed of emissions at the transparency, the Proper-GRB (P-GRB), and the extended afterglow due to collisions of accelerated baryons with the CircumBurst Medium (CBM) with density  $n_{CBM}$ . In this scenario the “short GRBs with an extended emission” [6] have been successfully interpreted as “disguised short bursts” [12–14]: canonical long bursts with  $3 \times 10^{-4} \leq B \leq 10^{-2}$ , exploding in halos of their host galaxies, with  $\langle n_{CBM} \rangle \approx 10^{-3} \text{ cm}^{-3}$ . The “genuine short” GRBs [8,15], instead, are characterized by smaller Baryon loads,  $B \lesssim 10^{-5}$  (see Fig. 1, right plot); therefore, the energy emitted in their P-GRB is predominant and an additional non-thermal component originating from the extended afterglow is expected.

We here show our results on two bursts classified as short GRBs: GRB 090227B the first genuine short GRB originating from a symmetric binary NS merger [16], and GRB 090510, a member of a yet different subclass of disguised short bursts occurring in a medium with  $\langle n_{CBM} \rangle \approx 10^3 \text{ cm}^{-3}$ , *i.e.*, *disguised short GRBs by excess* [17].

## II. THE GENUINE SHORT GRB 090227B.

GRB 090227B has been detected by the *Fermi*-GBM [18] and the *Konus*-Wind [19] detectors. No X rays and optical observations were reported; thus, the redshift of the source is unknown. We have analyzed the *Fermi*-GBM data from the NaI-n2 (8 – 900 keV) and the BGO-b0 (250 keV – 40 MeV) detectors. The NaI-n2 light curve (see Fig. 2, left panels) shows two spike-like structures. We indicate the trigger time by  $T_0$ . The spectrum of the first spike (from  $T_0 - 0.016 \text{ s}$  to  $T_0 + 0.080 \text{ s}$ ) is best fitted by using a black body (BB) plus Band [20] model (see

Tab. 1). The best fit of the second spike (from  $T_0 + 0.080 \text{ s}$  to  $T_0 + 0.368 \text{ s}$ ) is best fitted by using a Band model (see Tab. 1). Consequently, we have interpreted the first spike, where a thermal spectrum is present, as the P-GRB, and the second one as the extended afterglow.

Having identified the P-GRB, we can determine the correct value of  $B$  when the theoretical energy and temperature of the P-GRB match the ones observed in the thermal emission, namely,  $E_{BB}$  and  $kT_{obs}$ . Because the redshift  $z$  of GRB 090227B is unknown, we have estimated the ratio  $E_{PGRB} / E_{e^+e^-}^{tot}$  from the ratio of the observed fluences  $S_{BB} / S_{tot}$ . The fluence of the BB component of the P-GRB (see Tab 1, first interval) is  $S_{BB} = (1.54 \pm 0.45) \times 10^{-5} \text{ erg/cm}^2$ . The total fluence of the burst is  $S_{tot} = (3.79 \pm 0.20) \times 10^{-5} \text{ erg/cm}^2$  and has been evaluated in the time interval from  $T_0 - 0.016 \text{ s}$  to  $T_0 + 0.896 \text{ s}$ . Therefore, we have  $E_{P-GRB} / E_{e^+e^-}^{tot} = (40.67 \pm 0.12)\%$ . From the energy diagram in Fig. 1, for each energy ratio, we have a possible range for  $B$  and  $E_{e^+e^-}^{tot}$ . In turn, for each couple of  $B$  and  $E_{e^+e^-}^{tot}$ , we can determine the blue-shifted temperature  $kT_{blue}$  (temperatures diagram in Fig. 1) and, correspondingly, the redshift by the ratio  $kT_{blue} / kT_{obs} = 1 + z$ . We have computed the isotropic energy  $E_{iso}$  for each value of  $z$ , searching for the correct value fulfilling the condition  $E_{iso} \equiv E_{e^+e^-}^{tot}$ . We have found the equality at  $z = 1.61 \pm 0.14$  for  $B = (4.13 \pm 0.05) \times 10^{-5}$  and  $E_{e^+e^-}^{tot} = (2.83 \pm 0.15) \times 10^{53} \text{ erg}$ . The corresponding Lorentz factor at transparency is  $\Gamma_{tr} = (1.44 \pm 0.01) \times 10^4$ .

From the simulation of the extended afterglow light curve and spectrum, we have derived the average CBM density  $\langle n_{CBM} \rangle = (1.90 \pm 0.20) \times 10^{-5} \text{ cm}^{-3}$ , typical of the galactic halos environment. In Fig. 2, lower right panel, we have plotted the simulated spectrum of the early  $\sim 0.4 \text{ s}$  of emission. In the upper right panel, we have reproduced the total observed spectrum of the first spike (8–40000 keV) as the sum of the thermal spectrum

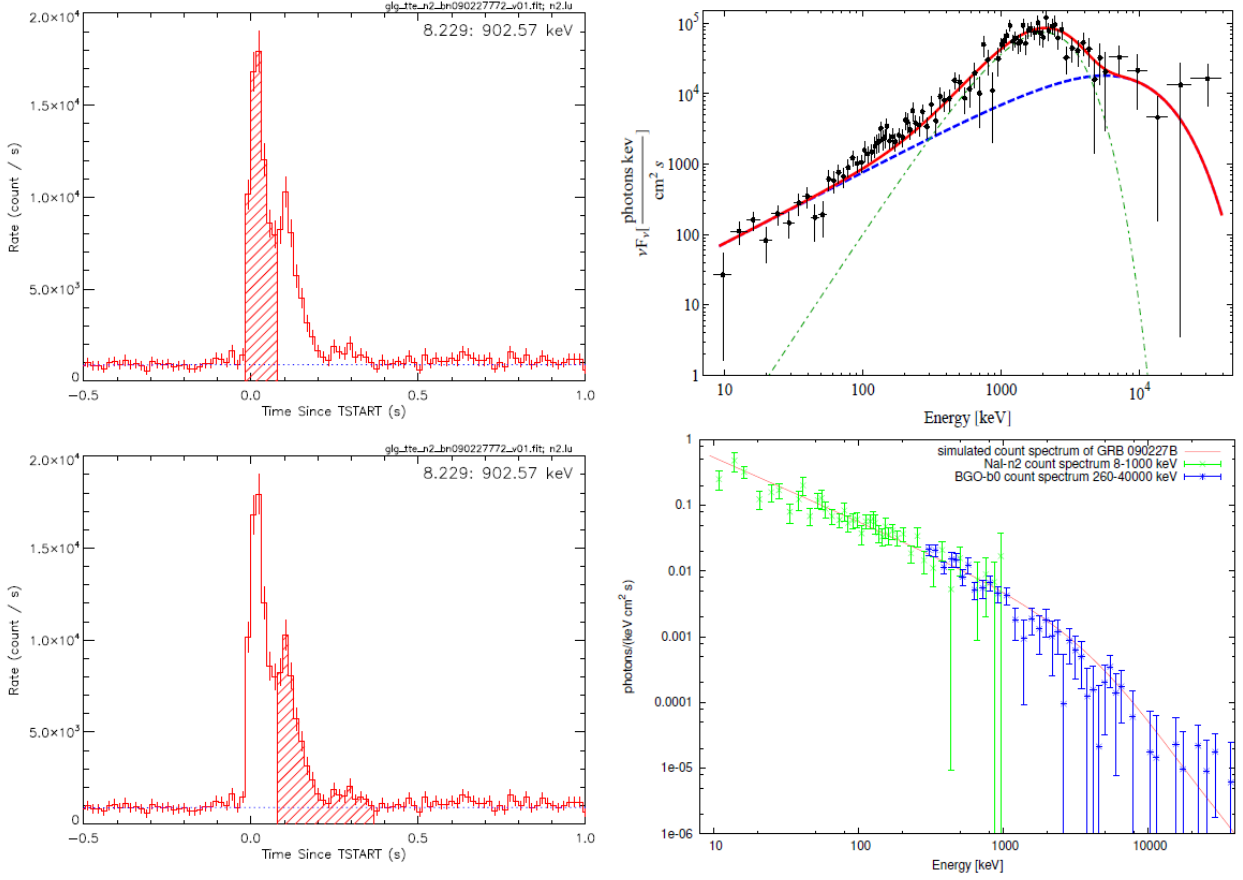


Fig. 2. (Color online) Left: the NaI-n2 light curves of the P-GRB (upper panel) and the extended afterglow (lower panel). Right: (upper panel) the simulated  $\nu F_\nu$  spectrum of the P-GRB (solid red curve) as the sum of the on-set of the extended afterglow (8 keV–40 MeV, dashed blue line) and of the BB emission of the P-GRB (dashed-dotted green line), compared to the observed data; (lower panel) the simulated photon spectrum of the extended-afterglow (8 keV–40 MeV) compared to the NaI-n2 (green) and the BGO-b0 (blue) data in the time interval from  $T_0 + 0.015$  s to  $T_0 + 0.385$  s.

Table 1. Results of the spectral analysis of the P-GRB (best fit BB+Band model) and of the extended afterglow (EA, best fit Band model) in the energy range 8 keV – 40 MeV.

Component	$kT$ [keV]	$\alpha$	$\beta$	$E_p$ [keV]	$F_{tot}/10^{-5}$ [erg/(cm <sup>2</sup> s)]	$F_{BB}/10^{-5}$ [erg/(cm <sup>2</sup> s)]	C-STAT/DOF
<b>P-GRB</b>	$517 \pm 28$	$-0.80 \pm 0.05$	$-2.14 \pm 0.17$	$952 \pm 251$	$31.3 \pm 1.3$	$16.1 \pm 4.7$	263.51/239
<b>EA</b>		$-0.79 \pm 0.06$	$-2.01 \pm 0.10$	$1048 \pm 178$	$2.66 \pm 0.26$		276.50/241

of the P-GRB and of the fireshell simulation (from  $T_0 + 0.015$  s to  $T_0 + 0.080$  s) due to the early on-set of the extended afterglow.

In conclusion, GRB 090227B represents a real genuine short burst with  $B \lesssim 10^{-5}$ . This implies that the energy emitted at the transparency condition of the fireshell is comparable to that emitted at the extended afterglow. The inferred baryon load is consistent with the mass of the crusts of a binary neutron star (NS), as described by the new model of NS fulfilling the global charge neutrality condition [21]. Therefore, from the above theoretical

results and from the average density of the CBM, which is typical of the halo of the host galaxy, we infer that the progenitor of GRB 090227B is a merger of two NSs. More details are given in the conclusions and in a published paper [16].

### III. THE DISGUISED SHORT GRB 090510 BY EXCESS

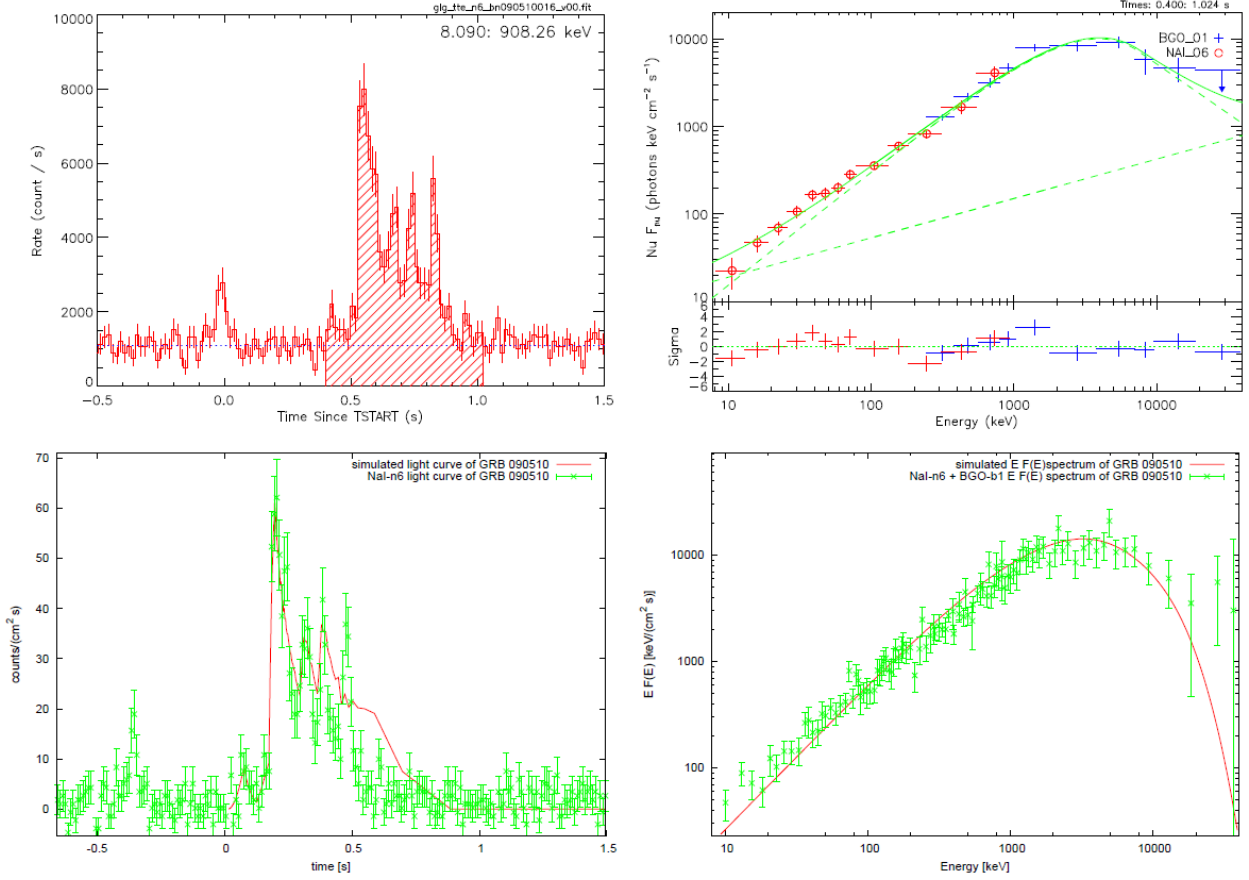


Fig. 3. (Color online) Upper panels: the NaI-n6 light curve (left) and the NaI+BGO  $\nu F_\nu$  spectrum in the  $\Delta T_2$  time interval. Lower panels: (left) the simulated light curve (8–1000 keV) and (right) the corresponding spectrum of the early  $\sim 0.4$  s of the extended afterglow in the energy range 8 keV – 40 MeV.

Table 2.  $\Delta T_1$  time interval: parameters of BB+PL and Compt models in the energy range 8–7000 keV.  $\Delta T_2$  time interval: parameters of the best fits (Band+PL) in the energy ranges (a) 8–40000 keV (GBM) and (b) 8 keV – 30 GeV (GBM+LAT).

Int	Model	$kT/E_p$ (keV)	$\alpha$	$\beta$	$\gamma$	$F_{tot}/10^{-6}$ (erg cm $^{-2}$ s $^{-1}$ )	C-STAT DOF
$\Delta T_1$	<b>BB+PL</b>	$34.2 \pm 7.5$	...	...	$-1.10 \pm 0.14$	$7.6 \pm 1.3$	188.60/193
	<b>Compt</b>	$990 \pm 554$	$-0.81 \pm 0.22$	...	...	$4.4 \pm 1.6$	189.97/194
$\Delta T_2^{(a)}$	<b>Band+PL</b>	$3941 \pm 346$	$-0.70 \pm 0.10$	$-3.13 \pm 0.97$	$-1.55 \pm 0.54$	$43.6 \pm 1.9$	207.78/236
$\Delta T_2^{(b)}$	<b>Band+PL</b>	$3941 \pm 346$	$-0.71 \pm 0.07$	$-2.97 \pm 0.26$	$-1.62 \pm 0.05$	$83.3 \pm 6.8$	199.20/256

GRB 090510 has been detected by the *Fermi*-GBM [22] and *Fermi*-LAT [23], *Swift*-BAT [24], AGILE [25], *Konus*-Wind [26], and *Suzaku*-WAM [27] detectors. Optical observations by VLT/FORS2 located its host galaxy at a redshift  $z = 0.903 \pm 0.003$  [28].

We have analyzed the *Fermi*-GBM data from the NaI-n6 (8–900 keV) and the BGO-b1 (260 keV–40 MeV) detectors and the LAT data in the energy range 100 MeV–30 GeV. The light curve of GRB 090510 is composed of two different episodes, 0.5 s apart (see Fig. 3, upper left plot). From the analysis of the first episode

from  $T_0 - 0.064$  s to  $T_0 + 0.016$  s (in the following  $\Delta T_1$ ), we have found that BB+PL and Compt are the viable best fits (see Tab. 2). From our theoretical interpretation, the BB+PL model, being equally probable as the Compt model, is adopted for its physical meaning. Therefore, the interval  $\Delta T_1$  has been identified as the P-GRB. The total energy of the first episode is  $E_1 = (2.28 \pm 0.39) \times 10^{51}$  erg.

The second episode from  $T_0 + 0.400$  s to  $T_0 + 1.024$  s (in the following  $\Delta T_2$ ) is interpreted as the extended afterglow. The best fit of this episode is obtained with

the Band+PL model, both considering the GBM data only (8 keV – 40 MeV) and including the LAT data up to 30 GeV [29]; its total energy is  $E_2 = (1.08 \pm 0.06) \times 10^{53}$  erg. The results are shown in Fig. 3 and in Tab. 2.

We started the simulation by using as input parameters  $E_{e^+e^-}^{tot}$ , constrained to the isotropic energy of the burst,  $E_{iso} = (1.10 \pm 0.06) \times 10^{53}$  erg, and the Baryon load  $B = (1.45 \pm 0.28) \times 10^{-3}$ , determined by matching the theoretically-simulated energy  $E_{tr}$  and temperature  $kT_{th} = kT_{blue}/(1+z)$  of the P-GRB with the ones observed in the faint pulse,  $E_1$  and  $kT_{obs}$ . The results of our simulation are  $\Gamma_{tr} = (6.7 \pm 1.6) \times 10^2$ ,  $r_{tr} = (6.51 \pm 0.92) \times 10^{13}$  cm,  $E_{tr} = (2.94 \pm 0.50)\% E_{e^+e^-}^{tot}$ , and  $kT_{th} = (34.2 \pm 7.5)$  keV. The theoretically-predicted P-GRB energy slightly differs from the observed  $E_1 = (2.28 \pm 0.39) \times 10^{51}$  erg =  $(2.08 \pm 0.35)\% E_{iso}$  because emission below the threshold is expected between the small precursor and the main emission (see light curves in Fig. 3); thus, the value of  $E_1$  is certainly underestimated.

Using the above values of  $E_{e^+e^-}^{tot}$  and  $B$ , we have simulated the light curve of the extended afterglow light curve of the NaI-n6 detector (see Fig. 3, lower left panel) and the corresponding spectrum of the early  $\sim 0.4$  s of the emission (lower right panel) in the energy range 8 keV – 40 MeV by using the spectral model described in Refs. [30] and [31]. The inferred CBM average value is, indeed, very high,  $\langle n_{CBM} \rangle = (1.85 \pm 0.14) \times 10^3$  cm $^{-3}$ .

We point out that the inferred baryon load of GRB 090510,  $B = 1.45 \times 10^{-3}$ , is typical of long GRBs and is not consistent with the values inferred for genuine short bursts (see, *e.g.*, GRB 090227B). Also the CBM density of  $\sim 10^3$  cm $^{-3}$ , typical of dense clouds in the inner galactic regions, points to a different origin than the merger scenario for real short GRBs (see, *e.g.*, Refs. [16], [32], and [33]). The short nature of GRB 090510 is the by-product of the relativistic motion of the burst ( $\Gamma \approx 700$ ) and of its high-density environment. More details are given in the conclusions and in a published paper [17].

#### IV. CONCLUSIONS

Thanks to detailed time-resolved spectral analyses on time scales as short as 16 ms, we have identified the P-GRB of both the considered sources. For GRB 090227B, we have also determined the cosmological redshift,  $z = 1.61 \pm 0.14$ , as well as the energy,  $E_{e^+e^-}^{tot} = (2.83 \pm 0.15) \times 10^{53}$  erg, the Lorentz factor at the transparency,  $\Gamma_{tr} = (1.44 \pm 0.01) \times 10^4$ , and the Baryon load,  $B = (4.13 \pm 0.05) \times 10^{-5}$ , characteristic of the class of genuine short GRBs. We conclude that GRB 090227B originates from a symmetric NS merger [34] because of (1) the CBM average density  $\sim 10^{-5}$  cm $^{-3}$ , typical of a galactic halo environment [12–14]; (2) the high energy  $E_{e^+e^-}^{tot}$  (assuming no beaming) released in a short time interval of  $\sim 0.4$  s; (3) the Baryon load  $B$ , which is consis-

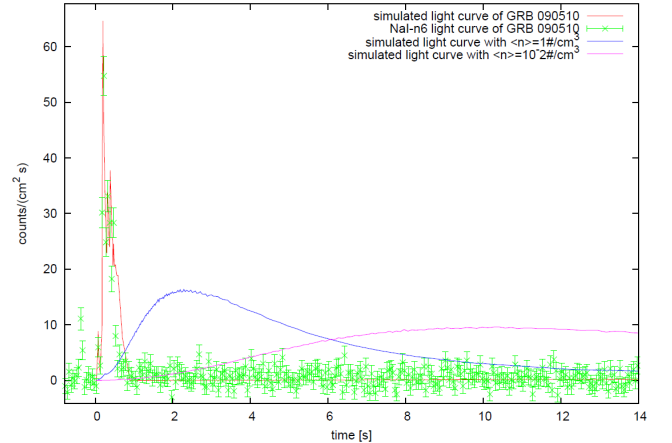


Fig. 4. (Color online) The 50 ms NaI-n6 light curve (green data) and the extended afterglow simulations corresponding to CBM average densities of a “disguised short GRB by excess” ( $\langle n_{CBM} \rangle \approx 10^3$  cm $^{-3}$ , red curve), of a canonical long GRB ( $\langle n_{CBM} \rangle = 1$  cm $^{-3}$ , blue curve), and of a “disguised short GRB by defect” ( $\langle n_{CBM} \rangle = 10^{-2}$  cm $^{-3}$ , purple curve). For larger densities the extended afterglow compresses in time and “inflates” in intensity.

tent with two NSs having masses  $m = 1.34M_{\odot}$  and radii  $R = 12.24$  km, assuming the NL3 nuclear model parameters for which the critical mass for a NS is  $M_{cr} = 2.67M_{\odot}$  [21]. From the above characteristics of the binary NS, we inferred an absolute upper limit on the energy emitted via gravitational waves,  $\sim 9.6 \times 10^{52}$  ergs [34].

In the case of GRB 090510, the P-GRB has been identified with the first episode (see Fig. 3). The inferred Baryon load,  $B = (1.45 \pm 0.28) \times 10^{-3}$ , is typical of long GRBs. From the simulations of the extended afterglow (see Fig. 3), we have found that GRB 090510 occurs in an over-dense medium with  $\langle n_{CBM} \rangle \approx 10^3$  cm $^{-3}$ . The joint effect of the high value of the Lorentz factor,  $\Gamma_{tr} = (6.7 \pm 1.6) \times 10^2$ , and the high density compresses in time the emission of the extended afterglow. Therefore, its light curve is shortened in time and “inflated” in intensity with respect to the canonical one for disguised short bursts (see Fig. 4), making it apparently closer to the genuine short class of GRBs [16].

Although their intrinsic durations are  $T_{90} < 2$  s, GRB 090227B and GRB 090510 have been shown to originate from different astrophysical systems, proving that the GRBs classification is, indeed, much more complex. Within the Fireshell model, we can generally conclude that three different possible structures of the canonical GRB exist, which is supported by observational evidences:

(1) Long GRBs have  $3.0 \times 10^{-4} \lesssim B \leq 10^{-2}$  and explode in environments with densities of  $\langle n_{CBM} \rangle \approx 1$  cm $^{-3}$ , which are typical of the inner galactic regions and are in agreement with the observational evidences for their occurrence close to star-forming regions [33].

(2) Disguised short GRBs have the same Baryon load

as the long ones, but they occur in different environments. (a) *Disguised short GRBs by excess* occur in over-dense media, e.g.,  $\langle n_{CBM} \rangle \approx 10^3 \text{ cm}^{-3}$ , as in the present case of GRB 090510 [17]; therefore, the bulk of  $\gamma$ -ray emission occurs on a short time-scale as for genuine short GRBs. (b) *Disguised short GRBs by defect* occur in a CBM with  $\langle n_{CBM} \rangle \approx 10^{-3} \text{ cm}^{-3}$ ; therefore, their  $\gamma$ -ray emission is deflated in intensity and characterized by an extended emission (see, e.g., Ref. [6]). The CBM density of these sources is typical of galactic halos [12–14], as was recently confirmed by the observed off-set from the center of their host galaxies [35,36].

(3) Genuine short GRBs occur for  $B \lesssim 10^{-5}$  in a CBM with  $\langle n_{CBM} \rangle \approx 10^{-5} \text{ cm}^{-3}$ , typical again of galactic halos. Unlike the disguised short GRBs by defect, in the genuine short bursts, the P-GRB emission is large as it is for the extended afterglow one; therefore, no X-ray afterglow and, consequently, no redshift determination is expected, as in the case GRB 090227B. Their progenitors are NS mergers [16].

## ACKNOWLEDGMENTS

We acknowledge the hospitality at the Asia Pacific Center for Theoretical Physics (APCTP) where part of this work was done.

## REFERENCES

- [1] R. W. Klebesadel, *Gamma-Ray Bursts - Observations, Analyses and Theories* (Cambridge University Press, 1992), p. 161.
- [2] J. P. Dezalay, C. Barat, R. Talon, R. Syunyaev, O. Terekhov and A. Kuznetsov, *American Institute of Physics Conference Series* **265**, (AIPC Series, 1992), p. 304.
- [3] C. Kouveliotou, C. A. Meegan, G. J. Fishman, N. P. Bhat, M. S. Briggs, T. M. Koshut, W. S. Paciesas and G. N. Pendleton, *Astrophys. J.* **413**, L101 (1993).
- [4] M. Tavani, *Astrophys. J.*, **497**, L21 (1998).
- [5] N. Gehrels *et al.*, *Nature* **437**, 851 (2005).
- [6] J. P. Norris and J. T. Bonnell, *Astrophys. J.* **643**, 266 (2006).
- [7] R. Ruffini, C. L. Bianco, F. Frascchetti, S. S. Xue and P. Chardonnet, *Astrophys. J.* **555**, L117 (2001).
- [8] R. Ruffini, C. L. Bianco, F. Frascchetti, S. S. Xue and P. Chardonnet, *Astrophys. J.* **555**, L113 (2001).
- [9] R. Ruffini, C. L. Bianco, F. Frascchetti, S. S. Xue and P. Chardonnet, *Astrophys. J.* **555**, L107 (2001).
- [10] A. G. Aksenov, R. Ruffini and G. V. Vereshchagin, *Physical Review Letters* **99**, 125003 (2007).
- [11] R. Ruffini, J. D. Salmonson, J. R. Wilson and S. S. Xue., *Astronomy & Astrophysics* **359**, 855 (2000).
- [12] M. G. Bernardini, C. L. Bianco, L. Caito, M. G. Dainotti, R. Guida and R. Ruffini, *Astronomy & Astrophysics* **474**, L13 (2007).
- [13] L. Caito, L. Amati, M. G. Bernardini, C. L. Bianco, G. de Barros, L. Izzo, B. Patricelli and R. Ruffini, *Astronomy & Astrophysics* **521**, A80 (2010).
- [14] G. de Barros, L. Amati, M. G. Bernardini, C. L. Bianco, L. Caito, L. Izzo, B. Patricelli and R. Ruffini, *Astronomy & Astrophysics* **529**, A130 (2011).
- [15] R. Ruffini, C. L. Bianco, P. Chardonnet, F. Frascchetti and S. S. Xue, *Astrophys. J.* **581**, L19 (2002).
- [16] M. Muccino, R. Ruffini, C. L. Bianco, L. Izzo and A. V. Penacchioni, *Astrophys. J.* **763**, 125 (2013).
- [17] M. Muccino, R. Ruffini, C. L. Bianco, L. Izzo, A. V. Penacchioni and G. B. Pisani, *Astrophys. J.* **772**, 62 (2013).
- [18] S. Guiriec, *GCN Circ.* 8921 (2009).
- [19] S. Golenetskii, R. Aptekar, E. Mazets, V. Pal'Shin, D. Frederiks, P. Oleynik, M. Ulanov, D. Svinkin and T. Cline, *GCN Circ.* 8926 (2009).
- [20] D. Band *et al.*, *Astrophys. J.* **413**, 281 (1993).
- [21] R. Belvedere, D. Pugliese, J. A. Rueda, R. Ruffini and S. S. Xue, *Nuclear Physics A* **883**, 1 (2012).
- [22] S. Guiriec, V. Connaughton and M. Briggs, *GCN Circ.* 9336 (2009).
- [23] M. Ohno and V. Pelassa, *GCN Circ.* 9334 (2009).
- [24] E. A. Hoversten, S. D. Barthelmy, D. N. Burrows, M. M. Chester, D. Grupe, J. A. Kennea, H. A. Krimm, N. P. M. Kuin, D. M. Palmer and T. N. Ukwatta, *GCN Circ.* 9331 (2009).
- [25] F. Longo *et al.*, *GCN Circ.* 9343 (2009).
- [26] S. Golenetskii, R. Aptekar, E. Mazets, V. Pal'Shin, D. Frederiks, P. Oleynik, M. Ulanov, D. Svinkin and T. Cline, *GCN Circ.* 9344 (2009).
- [27] N. Ohmori *et al.*, *GCN Circ.* 9355 (2009).
- [28] A. Rau, S. McBreen and T. Kruehler, *et al.*, *GCN*, 9353 (2009).
- [29] M. Ackermann *et al.*, *Astrophys. J.* **716**, 1178 (2010).
- [30] C. L. Bianco and R. Ruffini, *Astrophys. J.* **605** L1 (2004).
- [31] B. Patricelli, M. G. Bernardini, C. L. Bianco, L. Caito, G. de Barros, L. Izzo, R. Ruffini and G. V. Vereshchagin, *Astrophys. J.* **756** 16 (2012).
- [32] S. I. Blinnikov, I. D. Novikov, T. V. Perevodchikova and A. G. Polnarev *et al.* *Soviet Astronomy Letters* **10**, 177 (1984).
- [33] B. Paczynski, *Astrophys. J. Letters* **494**, 45 (1998).
- [34] J. A. Rueda and R. Ruffini, *Astrophys. J. Letters* **758**, L7 (2012).
- [35] W. Fong, E. Berger and D. B. Fox, *Astrophys. J.* **708**, 9 (2010).
- [36] E. Berger, *New Astron. Rev.* **55**, 1 (2011).



# Induced Gravitational Collapse in the BATSE era: the case of GRB 970828

R. Ruffini<sup>1,2,3,5</sup>

Jorge A. Rueda<sup>1,2</sup>, C. Barbarino<sup>1</sup>, C. L. Bianco<sup>1,2</sup>

, H. Dereli<sup>3,4</sup>, M. Enderli<sup>1,3</sup>, L. Izzo<sup>1,2</sup>,

M. Muccino<sup>1</sup>, A. V. Penacchioni<sup>5</sup>, G. B. Pisani<sup>1,3</sup>, Y. Wang<sup>1</sup>

<sup>1</sup>*Dip. di Fisica and ICRA, Sapienza Università di Roma, Piazzale Aldo Moro 5, I-00185 Rome, Italy.*

<sup>2</sup>*ICRANet, Piazza della Repubblica 10, I-65122 Pescara, Italy.*

<sup>3</sup>*Universite de Nice Sophia Antipolis, CEDEX 2, Grand Chateau Parc Valrose, Nice, France.*

<sup>4</sup>*Observatoire de la Côte d'Azur, F-06304 Nice, France.*

<sup>5</sup>*ICRANet-Rio, Rua Dr. Xavier Sigaud 150, Rio de Janeiro, RJ, 22290-180, Brazil.*

November 18, 2014

## Abstract

Following the recently established “Binary-driven HyperNova” (BdHN) paradigm, we here interpret GRB 970828 in terms of the four episodes typical of such a model. The “Episode 1”, up to 40 s after the trigger time  $t_0$ , with a time varying thermal emission and a total energy of  $E_{iso,1st} = 2.60 \times 10^{53}$  erg, is interpreted as due to the onset of an hyper-critical accretion process onto a companion neutron star, triggered by the companion star, an FeCO core approaching a SN explosion. The “Episode 2”, observed up  $t_0+90$  s, is interpreted as a canonical gamma ray burst, with an energy of  $E_{tot}^{e^+e^-} = 1.60 \times 10^{53}$  erg, a baryon load of  $B = 7 \times 10^{-3}$  and a bulk Lorentz factor at transparency of  $\Gamma = 142.5$ . From this Episode 2, we infer that the GRB exploded in an environment with a large average particle density  $\langle n \rangle \approx 10^3$  particles/cm<sup>3</sup> and dense clouds characterized by typical dimensions of  $(4 \div 8) \times 10^{14}$  cm and  $\delta n/n \sim 10$ . The “Episode 3” is identified from  $t_0+90$  s all the way up to  $10^{5-6}$  s: despite the paucity of the early X-ray data, typical in the

BATSE, pre-Swift era, we find extremely significant data points in the late X-ray afterglow emission of GRB 970828, which corresponds to the ones observed in all BdHNe sources. The “Episode 4”, related to the Supernova emission, does not appear to be observable in this source, due to the presence of darkening from the large density of the GRB environment, also inferred from the analysis of the Episode 2.

## 1 Introduction

The Gamma Ray Burst (GRB) 970828 is one of the first GRBs with an observed X-ray and radio afterglow and a determined redshift of  $z=0.9578$  from the identification of its host galaxy [1]. It was detected by the All Sky Monitor (ASM) detector on board the Rossi X-ray Timing Explorer (RXTE) spacecraft [2], and then observed also by the Burst And Transient Source Experiment (BATSE) on board the Compton Gamma-Ray Observatory [3]. The crucial data on the afterglow of GRB 970828 were collected by the Advanced Satellite for Cosmology and Astrophysics (ASCA) in the (2 - 10) keV energy range, one day after the RXTE detection [4], and by ROSAT [5] in the (0.1 - 2.4) keV, one week later. Observations on optical wavelengths failed to detect the optical afterglow [6, 7]. The fluence measured by BATSE implies an isotropic energy for the total emission of  $E_{iso} = 4.2 \times 10^{53}$  erg. This source is still presenting today, after 15 years from its discovery, an extremely rich problematic in the identification of its astrophysical nature.

The recent joint GRB observations made by satellites as Swift [8], Fermi [9], AGILE [10], Konus-WIND [11] in hard X-rays energy range, as well as the follow-up of their afterglow emission in the (0.3 - 10) keV range by the X-Ray Telescope (XRT) [12] on-board Swift, and the corresponding follow-up observations in the optical and radio wavelengths have made possible a new understanding of the entire GRB process. In this paper we start a procedure of revisiting previous GRBs in the BATSE, pre-Swift era, including the new understanding mentioned above. In particular, we apply to GRB 970828 the new BdHN scenario, in which GRBs associated with Supernovae (SNe) [13, 14], are composed of four different episodes [15, 16, 30, 31].

- The “Episode 1” corresponds to the emission from an hyper-critical accretion onto the a neutron star (NS) due to the onset of a Supernova

(SN) companion in a close binary system. The hyper-critical accretion induces allows the NS to reach the critical mass [32] finally collapsing to a black hole (BH). In the specific case of GRB 970828, this episode is clearly identified, see Fig. 1. The observed hard X-ray emission is composed of a thermal spectrum plus a power-law component, both evolving in time. The presence of an evolving thermal component allows the determination of the time decay of the blackbody temperature  $kT$  (from 80 to 25 keV), in the rest-frame time of 20 s, leading to the estimate of the emitter radius between 5000 and 25000 km.

- The “Episode 2”, corresponding to the observations of the GRB, is related to the collapse of the NS into a BH. The characteristic parameters of the GRB 970828 are the Lorentz Gamma factor of  $\Gamma \approx 150$ , the baryon load  $B = 7 \times 10^{-3}$  and a large circumburst density of the order of  $10^3$  particles/cm<sup>3</sup>.
- The “Episode 3”, in soft X-rays, occurs when the prompt emission from the GRB fades away and an additional component, discovered by Swift XRT [33, 34] emerges. It has been shown [31] that this component, in energetic ( $E_{iso} \geq 10^{52}$  erg) BdHNe, when referred to the rest-frame of the source, follows a standard behavior of the light curve evolution. This emission encompasses the SN shock break out and the expanding SN ejecta ( $v/c \approx 0.1$ ). In the case of GRB 970828, the X-ray emission observed by ASCA and ROSAT perfectly overlap with the common trend observed in BdHN systems and exemplified in Fig. 5.
- The “Episode 4” is represented by the observations of the optical emission of the SN, which has been observed in some BdHN sources, with  $z \leq 0.9$ , [GRB 090618, GRB 060729, GRB 091127, GRB 111228, GRB 080319B, see e.g. 31]. It is generally hard to detect a SN at  $z=0.9578$  and in the case of GRB 970828 is even more difficult due to the very large presence of circumburst material, which has also hampered the observations of the optical afterglow, making this source a ‘dark’ GRB.

The presence of an evolving thermal component in the first 20 s of the emission of GRB 970828, using BATSE data, has been indicated by [35], where they have considered the emission in the first 20 s of Episode 1. They then have fitted the evolution of the temperature  $kT$  and the ratio  $\mathcal{R} = (Flux_{BB}/\sigma T_{obs}^4)^{1/2}$ ,

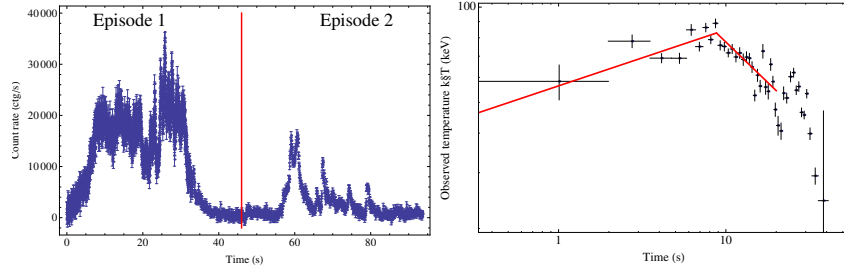


Figure 1: *Left panel:* BATSE-LAD light curve of GRB 970828 in the 25-1900 keV energy range. *Right panel:* The behavior of the observed temperature in GRB 970828 and the best fit with a broken power-law function of the first 20 s as presented in [35].

where  $Flux_{BB}$  is the observed flux of the instantaneous blackbody,  $\sigma$  the Stefan constant and  $T_{obs}$  the observed temperature, whose evolution in time is fitted with a broken power-law function, see Fig. 1. In their theoretical interpretation, this thermal emission was associated to the photospheric GRB emission of a relativistic expanding fireball [36], and they inferred a bulk Lorentz Gamma factor of the expanding plasma,  $\Gamma \approx (305 \pm 28)Y_0^{1/4}$ , with  $Y_0 \geq 1$  the ratio between the entire fireball energy and the energy emitted in  $\gamma$ -rays [36]. Since the fireball photospheric radius is given by  $r_{ph} = (\mathcal{R} D \Gamma)/(1.06(1+z)^2)$ , with  $D$  the luminosity distance of the GRB, they obtain for  $r_{ph}$  the value of  $2.7 \times 10^{11} Y_0^{1/4}$ . In [35], the authors have also attributed the remaining GRB emission to an unspecified engine activity and neglected all data after 20 s. In their own words, “we neglect here late-time episodes of engine activity that occur after  $\sim 25$  and  $\sim 60$  s in this burst”. As we will show in the following of this article, we notice the presence of a thermal component in the first 40s, and we attribute it to a non-relativistic initial expansion with radius evolving from  $2 \times 10^9$  to  $3 \times 10^{10}$  cm, see Fig. 2. In addition, we identify the GRB emission between  $t_0+50$  s and  $t_0+90$  s and the third episode between  $10^4$ - $10^6$  s.

In Section 2 we give a summary of the observations of GRB 970828 and describe our data analysis. We proceed in Section 3 to the description of Episode 1, with the details of the expanding black body emitter, the analysis of the non-thermal component and its interpretation in the BdHN paradigm. In Section 4 we describe Episode 2, the authentic GRB emission. It is well explained in

the context of the fireshell scenario, see e.g. [13] for a complete review of the model. In Section 5 we describe Episode 3, pointing out the clear overlapping of the observed late X-ray data within the theoretical expectation of a BdHN member. In Section 6 we discuss about the theoretically expected SN emission, not observed due to the large circumburst medium. Conclusions are given in the last Section.

## 2 Data Analysis

GRB 970828 was discovered with the All-Sky Monitor (ASM) on board the Rossi X-Ray Timing Explorer (RXTE) on 1997 August 28th [3]. Within 3.6 hr the RXTE/PCA scanned the region of the sky around the error box of the ASM burst and detected a weak X-ray source [4, 37]. GRB 970828 was also observed by the Burst and Transient Source Experiment (BATSE) and the GRB experiment on Ulysses [3]. The BATSE-LAD light curve is characterized by two main emission phenomena, see Fig. 1: the first lasts about 40 s and is well described by two main pulses, the second one is more irregular, being composed by several sharp pulses, lasting other 40 s.

The X-ray afterglow was discovered by the ASCA satellite 1.17 days after the GRB trigger [38]. The X-ray afterglow observations continued up to 7-10 days from the burst detection. The optical observations, which started about 4 hr after the burst, did not report any possible optical afterglow for GRB 970828 up to  $R=23.8$  [7]. However, the observations at radio wavelengths of the burst position, 3.5 hrs after the initial burst, succeeded in identifying a source at a good significance level of  $4.5 \sigma$  [1] inside the ROSAT error circle ( $10''$ ). The following deep searches for a possible optical counterpart of this radio source led to the identification of an interacting system of faint galaxies, successively recognized as the host galaxy of GRB 970828. The spectroscopic observations of the brightest of this system of galaxies led to the identification of their redshift, being  $z=0.9578$ . The lack of an optical transient associated with the afterglow of GRB 970828 can be explained as due to the presence of strong absorption, due to dusty clouds in the burst site environment, whose presence does not affect the X-ray and the radio observations of the GRB afterglow. The absence of an optical afterglow [7], together with the large intrinsic absorption column detected in the ASCA X-ray data [39] and the contemporary detection

in radio-wavelengths of the GRB afterglow, imply a very large value for the circum-burst medium (CBM); the variable absorption might be an indication of a strong inhomogeneous CBM distribution.

To analyze in detail this GRB, we have considered the observations of the BATSE-LAD detector, which observed GRB 970828 in the 25-1900 keV energy range, and then we have reduced the data by using the RMFIT software package. For the spectral analysis we have considered the High Energy Resolution Burst (HERB) data, which consist of 128 separate high energy resolution spectra stored during the burst emission. The light curve, shown in Fig. 1, was obtained by using the Medium Energy Resolution (MER) data, which consist of 4.096 16-channel spectra summed from triggered detectors.

### 3 The Episode 1

#### 3.1 The onset of the Supernova and the hyper-critical accretion

In analogy to the cases of GRB 090618 [15], we analyze here the first emission episode in GRB 970828 to seek for a thermal signature. We have rebinned the light curve assuming a signal-to-noise ratio for each time bin of 20. This large value of counts per bin allows us to consider a gaussian distribution for the photons in each bin, so in the following we will use a  $\chi^2$  statistic.

As often done in GRB analysis, we first perform a time-integrated spectral analysis of the first 40 s of emission, which corresponds to the Episode 1, to identify the best-fit model and the possible presence of thermal features. We make use of different spectral models, see Table 1, to determine the best-fit function. We also check if nested models really improve the best-fit, as in the case of models with an extra power-law component. We find that the best-fit corresponds to a double blackbody model with an extra power-law component. The check between the Band and the double black body plus power law is minimal ( $P_{val} = 9\%$ ) but with this last model we note an improvement of the best fit at high energies.

It has already been emphasized that the integrated spectral analysis often misses the nature of the physical components and also the nature of the underlying physical mechanisms. We perform therefore a time-resolved spectral

Table 1: Spectral analysis (25 keV - 1.94 MeV) of the first 40 s of emission in GRB 970828. The following symbols represent: \* temperature (keV) of the second black body; † normalization of the power law component in units of  $\text{ph cm}^{-2} \text{s}^{-1} \text{keV}^{-1}$ .

Spectral model	$\alpha$ ( $\gamma$ )	$\beta$	$\gamma_{ext}$	$E_{peak}$ (keV)	$kT$ (keV)	$\chi^2/DOF$
Power Law	$-1.38 \pm 0.01$	-	-	-	-	6228.1/115
Cut-off PL	$-0.77 \pm 0.02$	-	-	$465.4 \pm 10.6$	-	203.83/114
Band	$-0.60 \pm 0.03$	$-2.15 \pm 0.05$	-	$360.5 \pm 12.5$	-	106.48/113
Band+PL	$-0.41 \pm 0.15$	$-2.41 \pm 0.33$	$-1.47 \pm 0.17$	$335.8 \pm 17.6$	-	104.12/111
cutoff + PL	$-0.47 \pm 0.17$	-	$-1.28 \pm 0.16$	$338.7 \pm 17.9$	-	104.28/112
BB + po	-	-	$-1.50 \pm 0.01$	-	$63.71 \pm 0.92$	228.09/113
BB + BB + po	$-1.53 \pm 0.17$	-	$0.010 \pm 0.001$ †	$40.01 \pm 2.05$ *	$106.8 \pm 6.3$	101.78/111

analysis to determine the existence and the evolution of a thermal component. We find that the double blackbody model observed in the time-integrated spectrum can be explained by the presence of an instantaneous single blackbody with a temperature  $kT$  varying in intensity and time, showing a double decay trend. We note that the timing of these trends corresponds to the two main spikes in the observed light curve of this first episode, see Fig. 2. We have then analyzed this characteristic evolution of the blackbody in both time intervals, corresponding each one to an observed decay trend of the temperature. From the observed flux of the blackbody component  $\phi_{BB,obs}$  for each interval, we obtain the evolution of the emitter radius in the rest-frame:

$$r_{em} = \left( \frac{\phi_{BB,obs}}{\sigma T_{obs}^4} \right)^{1/2} \frac{D}{(1+z)^2} \quad (1)$$

whose evolution is shown in Fig. 2. It is very interesting that the radius monotonically increases, without showing an analog double trend which is observed for the temperature, see Fig. 2. The global evolution of the emitter radius is well-described with a power-law function  $r = \alpha t^\delta$  and a best fit of the data provides for the  $\delta = 0.41 \pm 0.04$  and  $\alpha = (5.38 \pm 0.52) 10^8 \text{ cm}$ , with an  $R^2$  statistic value of 0.98, see Fig. 2.

It is appropriate to discuss the power law component observed in the time resolved spectra. In BdHNe, the tight geometry of the binary system implies that as the external layers of the SN core starts to expand, an hyper-critical accretion phenomenon is induced onto the NS companion.

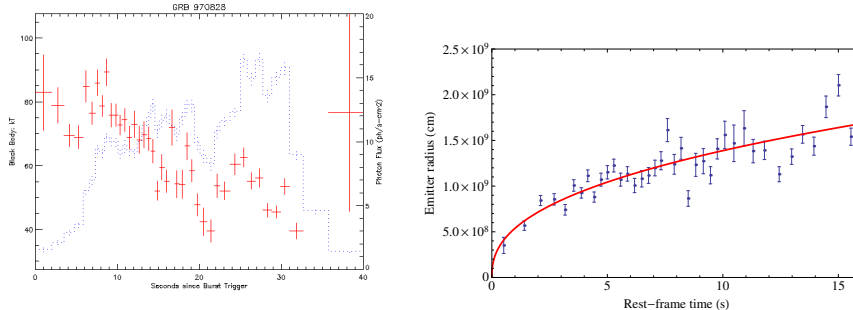


Figure 2: (*Left panel*) The evolution of the temperature  $kT$  (red crosses) as obtained from a time-resolved spectral analysis of the first 40 s of emission of GRB 970828. The light curve of the first episode (blue dots) is shown in background. (*Right panel*) Evolution of the rest-frame radius of the first episode of GRB 970828. The solid line corresponds to the best fit of this dataset with a power-law function  $r \propto t^\delta$ , with  $\delta = 0.41 \pm 0.04$ .

### 3.2 Binary progenitor and binary-driven hypercritical accretion

The first estimates of the IGC process [14, 15] were based on a simplified model of the binary parameters and the Bondi-Hoyle-Lyttleton accretion formalism [17–19]. The following discussion is based on the more recent and accurate results presented in [20], in which the collapsing CO cores leading to SN Ic are simulated to calculate realistic profiles for the density and ejection velocity of the SN outer layers. The hydrodynamic evolution of the accreting material falling into the Bondi-Hoyle accretion region is also computed from numerical simulations all the way up to its incorporation onto the NS surface.

The hypercritical accretion onto the NS from the SN ejecta can be estimated from the Bondi-Hoyle-Lyttleton formula

$$\dot{M}_{\text{BHL}} = 4\pi r_{\text{BHL}}^2 \rho (v^2 + c_s^2)^{1/2}, \quad (2)$$

where  $\rho$  is the SN ejecta density,  $v$  is the ejecta velocity in the rest-frame of the NS, which includes a component from the ejecta velocity,  $v_{\text{ej}}$ , and another component from the orbital velocity of the NS,  $v_{\text{orb}}$ ;  $c_s$  is the SN ejecta sound

speed, and  $r_{\text{BHL}}$  is the Bondi radius

$$r_{\text{BHL}} = \frac{GM_{\text{NS}}}{v^2 + c_s^2}, \quad (3)$$

being  $G$  the gravitational constant and  $M_{\text{NS}}$  is the NS mass. The conditions of the binary system are such that both the velocity components,  $v_{\text{orb}}, v_{\text{ej}}$ , are typically much higher than the sound speed. The ejecta velocity as a function of time is determined by the explosion energy and the nature of the SN explosion. The orbital velocity depends upon the orbital separation, which in turn depends upon the radius of the CO core and the binary interactions prior to the explosion of the CO core. The effect of the NS magnetic field is negligible in this process [14, 21]: for a neutron star with surface magnetic field  $B = 10^{12}$  G, mass  $M_{\text{NS}} = 1.4 M_{\odot}$ , and radius  $r_{\text{NS}} = 10^6$  cm, one has that for accretion rates  $\dot{M} > 2.6 \times 10^{-8} M_{\odot} \text{ s}^{-1} = 0.8 M_{\odot} \text{ yr}^{-1}$ , the Alfvén magnetospheric radius satisfies  $R_A = [B^2 R^6 / (\dot{M} \sqrt{2GM_{\text{NS}}})]^{2/7} < r_{\text{NS}}$ .

The evolution of the SN ejecta density near the NS companion depends on the SN explosion and the structure of the progenitor just prior to collapse. The compactness of the CO core is such that there is no Roche lobe overflow prior to the SN explosion. The Roche lobe radius can be computed from [22],  $R_{\text{L,CO}}/a \approx 0.49q^{2/3}/[0.6q^{2/3} + \ln(1 + q^{1/3})]$ , where  $q = M_{\text{CO}}/M_{\text{NS}}$ . For a CO core progenitor  $M_{\text{CO}} \approx 5 M_{\odot}$ ,  $R_{\text{CO}} \approx 3 \times 10^9$  cm, no Roche lobe overflow occurs for binary periods  $P \geq 2$  min, or binary separations  $a \geq 6 \times 10^9$  cm, assuming a NS companion mass  $M_{\text{NS}} \geq 1.4 M_{\odot}$ .

In order to derive the accretion onto the NS, the explosion has to be modeled. We have recently performed the numerical simulations following two different approaches [20]: the first assuming a homologous outflow with a set explosion energy and a second approach following the collapse, bounce, and explosion of a  $20M_{\odot}$  (zero-age main sequence mass) progenitor. The calculation uses a 1D core-collapse code [23] to follow the collapse and bounce and then injects energy just above the proto-NS to drive different SN explosions mimicking the convective-engine paradigm. With this progenitor and explosion, we produce the density and velocity evolution history at the position of the Bondi-Hoyle surface of the NS companion.

Under the above conditions, we have found from our numerical simulations in [20] that hypercritical accretion rates of up to  $10^{-2} M_{\odot}/\text{s}$  occur in these systems. This infall rate is well above the critical Eddington rate. The Eddington

accretion limit, or critical accretion rate makes a series of assumptions: 1) the potential energy gained by the accreting material is released in the form of photons which exert pressure finally reducing the accretion rate, 2) the inflowing material and outflowing radiation is spherically symmetric, 3) the photons are not trapped in the flow and can deposit momentum to the inflowing material, and 4) the opacity is dominated by electron scattering. However, many of these assumptions break down in the IGC scenario, allowing hypercritical accretion rates.

It can be shown that the photons for the hypercritical accretion rates in the IGC are trapped in the flow. Chevalier [24] derived the trapping radius where photons emitted diffuse outward at a slower velocity than infalling material flows inward:

$$r_{\text{trapping}} = \min[(\dot{M}_{\text{BHL}}\kappa)/(4\pi c), r_{\text{BHL}}] \quad (4)$$

where  $\kappa$  is the opacity (in  $\text{cm}^2 \text{g}^{-1}$ ) and  $c$  is the speed of light. If the trapping radius is near or equal to the Bondi radius, the photons are trapped in the flow and the Eddington limit does not apply. We estimate for our CO core a Rosseland mean opacity roughly  $5 \times 10^3 \text{ cm}^2 \text{g}^{-1}$ , a factor  $\sim 10^4$  higher than electron scattering. Combined with our high accretion rates, it is clear that the Eddington limit does not apply in this scenario and hypercritical accretion must occur.

The inflowing material shocks as it piles up onto the NS producing an atmosphere on top of the NS which, by compression, becomes sufficiently hot to emit neutrinos [21, 24–26]. The neutrinos have become then crucial in cooling the infalling material, allowing its incorporation into the NS [21, 27, 28]. We compute the neutrino emission following [21, 28]. We thus take into account  $e^-$  and  $e^+$  capture by free protons and neutrons, and pair and plasma  $\nu\bar{\nu}$  creation;  $\nu$  absorption processes include  $\nu_e$  capture by free neutrons,  $\bar{\nu}_e$  by free protons, and  $\nu\bar{\nu}$  annihilation.  $\nu$  scattering includes  $e^-$  and  $e^+$  scattering off  $\nu$  and neutral current opacities by nuclei. The three species  $\nu_{e,\mu,\tau}$  are tracked separately by the transport algorithm.

As material piles up, the accretion shock moves outward. The accretion shock weakens as it moves out and the entropy jump becomes smaller, producing an unstable atmosphere with respect to Rayleigh-Taylor convection. Previous simulations [28, 29] of such instabilities accretion process have shown that they can accelerate above the escape velocity driving outflows from the accreting NS

with final velocities approaching the speed of light, causing the ejection of up to 25% of the accreting material. The entropy of the material at the base of our atmosphere,  $S_{\text{bubble}}$ , is given by [21]:

$$S_{\text{bubble}} = 38.7 \left( \frac{M_{\text{NS}}}{2M_{\odot}} \right)^{7/8} \left( \frac{\dot{M}_{\text{BHL}}}{0.1 M_{\odot} \text{s}^{-1}} \right)^{-1/4} \left( \frac{r_{\text{NS}}}{10^6 \text{ cm}} \right)^{-3/8} \quad (5)$$

$k_B$  per nucleon, where  $r_{\text{NS}}$  is the radius of the NS. The corresponding temperature of the bubble,  $T_{\text{bubble}}$ , is:

$$T_{\text{bubble}} = 195 S_{\text{bubble}}^{-1} \left( \frac{r_{\text{NS}}}{10^6 \text{ cm}} \right)^{-1}. \quad (6)$$

Under the hypercritical accretion of the IGC, the temperature of the bubble when it begins to rise is  $T_{\text{bubble}} \sim 5$  MeV. If it rises adiabatically, expanding in all dimensions, it drops to 5 keV at a radius of  $10^9$  cm, far too cool to observe. However, if it is ejected in a jet, as simulated in Fryer [28], it expands laterally but not radially, so we have roughly  $\rho \propto r^2$  and  $T \propto r^{-2/3}$ . In that simplified bubble evolution, the outflow would have a temperature  $T_{\text{bubble}} \sim 50$  keV at  $10^9$  cm and  $T_{\text{bubble}} \sim 15$  keV at  $6 \times 10^9$  cm. This could explain the temperature and size evolution of the blackbody observed in the Episode 1 of BdHNe. For example, the blackbody observed in Episode 1 of GRB 090618 [15] evolves as  $T \propto r^{-m}$  with  $m = 0.75 \pm 0.09$ , in agreement with this simplified theoretical estimate. For the present case of GRB 970828, the fully lateral bubble evolution do not match perfectly, implying that the above simplified picture needs further refinement and/or the presence of other mechanisms. We are currently deepening our analysis of the possible explanation of the thermal emission observed in Episode 1 of BdHNe as based on convective instabilities in the hypercritical accretion process, and the results will be presented elsewhere.

Concerning the power-law component observed in the luminosity of Episode 1 in addition to the blackbody one, we advance the possibility that such a high-energy emission could come from the angular momentum of the binary system as follows.

The angular momentum per unit mass accreting by the NS can be estimated as

$$j_{\text{acc}} \approx \frac{1}{2} \omega_{\text{orb}} r_B^2, \quad (7)$$

where  $\omega_{\text{orb}} = v_{\text{orb}}/a$  is the orbital angular velocity,  $v_{\text{orb}} = (GM_T/a)^{1/2}$  is the orbital velocity,  $a$  the separation distance of the binary components,  $M_T =$

$M_{\text{CO}} + M_{\text{NS}}$  is the total mass of the binary.  $r_B$  is the Bondi capture radius. From our numerical simulations, we know that when the neutron star reaches the critical mass, the inequality  $v_{\text{ej}} \ll v_{\text{orb}}$  is satisfied, so we can approximate Eq. (3) as

$$r_{\text{BHL}} \approx \frac{2GM_{\text{NS}}}{v_{\text{orb}}^2} \rightarrow \frac{2GM_{\text{crit}}}{v_{\text{orb}}^2} = \frac{2GM_{\text{BH}}}{v_{\text{orb}}^2}, \quad (8)$$

where  $M_{\text{BH}} = M_{\text{crit}}$ , is the mass of the newly-formed black hole, so it equals  $M_{\text{crit}}$ , the critical mass of the NS.

The black hole can gain angular momentum up to it reaches the maximal value allowed by the Kerr solution

$$j_{\text{maxBH}} = \frac{GM_{\text{BH}}}{c}. \quad (9)$$

Therefore we have (see Fig. 3)

$$\frac{j_{\text{maxBH}}}{j_{\text{acc}}} = \frac{1}{2} \frac{M_T}{M_{\text{BH}}} \sqrt{\frac{GM_T}{c^2 a}} = \frac{1}{2} \left(1 + \frac{M_{\text{CO}}}{M_{\text{BH}}}\right) \sqrt{\frac{G(M_{\text{CO}} + M_{\text{BH}})}{c^2 a}}. \quad (10)$$

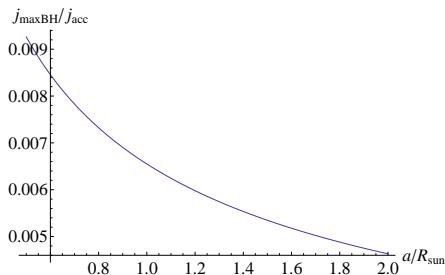


Figure 3: Maximal black hole to accretion angular momentum ratio,  $j_{\text{maxBH}}/j_{\text{acc}}$ , as a function of the binary separation in units of solar radius. Here for simplicity we have used  $M_{\text{CO}} \approx 6 M_{\odot}$  and  $M_{\text{BH}} \approx 3 M_{\odot}$ .

It becomes then clear from the above first simplified estimate that the angular momentum carried out by the accreted material highly exceed the maximal angular momentum that the newly-born black hole can support, and therefore angular momentum dissipation, very likely in form of collimated emission, is likely to occur. We are currently performing numerical simulations of this process in order to assess the validity and accuracy of these first order of magnitude estimates.

### 3.3 A possible explanation for the non-thermal component and the compactness problem

It is well known [see 41] that most of GRBs emit a large fraction of observed high-energy photons ( $E \gg 1$  MeV) which can interact with low-energy photons to produce electron-positron pairs via  $\gamma\gamma \rightarrow e^+e^-$  in a compact region with radius  $R$  that, with a naive estimate, can be considered  $< c\delta t$ . This would imply an optical depth  $\tau \gg 1$ , but we know that GRB spectra are non-thermal, so we are in presence of a paradox. This issue can be solved assuming a relativistic expansion of the emitting source, with Lorentz factor  $\Gamma \gg 1$  [41, 42]. In this case, in fact, we would have  $R < 2\gamma^2 c\delta t$  and consequently a decrease of the estimated optical depth [43–45].

The observed high-energy photon spectrum is often modeled by a single power-law  $KE^{-\gamma}$ , with  $E_{min} < E < E_{max}$  and power-law index  $\gamma$ . The energy  $E_{max}$  is the highest observed photon energy. In the frame of the emitting material, where the photons are assumed to be isotropic, a photon with energy  $E'$  can annihilate a second photon with energy  $E'_{th}$ , yielding an electron-positron pair. The threshold for this process is described by

$$E'E'_{th} \geq (m_e c^2)^2, \quad (11)$$

where  $m_e$  is the electron mass. If the source is moving toward the observer with a Lorentz factor  $\Gamma$ , then the photons previously analyzed have detected energy of  $E = \Gamma E'/(1+z)$  and  $E_{th} \geq \Gamma E'_{th}/(1+z)$ , respectively. Therefore in the observer frame photons with energy  $E_{max}$  annihilate only with other photons having energy  $E_{max,th} = [\Gamma m_e c^2/(1+z)]^2 E_{max}^{-1}$ .

Although the observed high-energy photon spectrum is a power-law up to 4 MeV in the rest frame of the burst, there is no observational evidence for the presence of a cut-off due to the  $e^+e^-$ -pair creation. Therefore we can estimate the minimum Lorentz factor of the non-thermal component allowed by the observations from the maximum energy observed in the first episode  $E_{max} \sim 2MeV$ . From this assumption, it is straightforward to impose that the threshold energy  $E_{max,th}$  for the pair creation process has to be  $E_{max,th} < E_{max}$  [see e.g. case (III) in 46]. It follows then a lower limit on the Lorentz factor from the observed energy  $E_{max}$

$$\Gamma_{min} \geq \frac{E_{max}}{m_e c^2} (1+z). \quad (12)$$

We can identify  $E_{max}$  with the cut-off energy of the spectrum  $E_c$ , but for the moment we treat them as different energies. Following the considerations in [46], we have calculated the averaged number of photons interacting with  $E_{max}$  from  $E_{max,th}$  to  $E_c \geq E_{max}$  on the cross-section of the process integrated over all the angles  $\theta$

$$\langle \sigma N_{max,th} \rangle = 4\pi d_z^2 \Delta t \int_{E_{max,th}}^{+\infty} K E^{-\gamma} dE \int_1^{\frac{E_{max} E}{(m_e c^2)^2}} \frac{3}{16} \sigma_T s ds = \frac{2E_{max,th}^{1-\gamma}}{\xi} \quad (13)$$

and we have correspondingly evaluated the optical depth

$$\tau_{\gamma\gamma} = \frac{\langle \sigma N_{max,th} \rangle}{4\pi(\Gamma^2 c \Delta t)^2}, \quad (14)$$

by defining the following quantities

$$d_z = \frac{D}{1+z}, \quad s = \frac{E_{max} E (1 - \cos \theta)}{2(m_e c^2)^2}, \quad \xi \equiv \left[ \frac{3\pi\sigma_T d_z^2 K \Delta t}{4(\gamma^2 - 1)} \right]^{-1},$$

and using the Thomson cross-section  $\sigma_T$ . The condition  $\tau_{\gamma\gamma} < 1$  yields to a lower limit on the Lorentz  $\Gamma$  factor. We have applied these considerations to non-thermal spectrum of the first episode of GRB 970828, and considered for  $\Delta t$  in Eq. 14 the whole duration of the first episode in GRB 970828. Therefore we have calculated an averaged lower limit on the Lorentz factor, i.e.  $\Gamma_{min} = 77$  for the whole first episode.

Therefore, a relativistic outflow of the accretion process of the SN onto the companion NS, can explain the origin of the power-law high energy component observed in Episode 1.

## 4 The Episode 2 : the GRB emission

Turning now to the second emission episode, we have computed the isotropic energies emitted in this episode, by considering a Band model as the best fit for the observed integrated spectra:  $E_{iso,2nd} = 1.6 \times 10^{53}$  erg. In what follows we explain this second emission episode of GRB 970828 as a single canonical GRB emission in the context of the Fireshell scenario.

In this model [47, 48], a GRB originates from an optically thick  $e^+e^-$ -plasma created in the process of vacuum polarization, during the process of gravitational collapse leading to a Kerr-Newman black hole [49, 50]. The dynamics of this expanding plasma is described by its total energy  $E_{tot}^{e^+e^-}$ , the baryon load  $B =$

$M_B c^2 / E_{tot}^{e^+e^-}$  and the circumburst medium (CBM) distribution around the burst site. The GRB light curve emission is characterized by a first brief emission, named the proper GRB or P-GRB, originating in the process of the transparency emission of the  $e^+e^-$ -plasma, followed by a multi-wavelength emission due to the collisions of the residual accelerated baryons and leptons with the CBM. This latter emission is assumed in a fully radiative regime. Such a condition is introduced for mathematical simplicity and in order to obtain a lower limit on the CBM density. This condition establishes a necessary link between the CBM inhomogeneities and filamentary distribution [51] with the observed structures in the  $\gamma$  and X-ray light curves in the prompt and early afterglow phase. In the spherically symmetric approximation the interaction of the accelerated plasma with the CBM can be described by the matter density distribution  $n_{CBM}$  around the burst site and the fireshell surface filling factor  $\mathcal{R} = A_{eff}/A_{vis}$ , which is the ratio between the effective emitting area and the total one [52]. The spectral energy distribution in the comoving frame of the shell is well-described by a “modified” thermal emission model [53], which differs from a classical blackbody model by the presence of a tail in the low-energy range.

In this context, to simulate the second episode of GRB 970828, which is the actual GRB emission, we need to identify the P-GRB signature in the early second episode light curve. From the identification of the P-GRB thermal signature, and the consequent determination of the energy emitted at transparency, we can obtain the value of the baryon load  $B$  assuming that the total energy of the  $e^+e^-$ -plasma is given by the isotropic energy  $E_{iso}$  observed for the second episode of GRB 970828, as it was done for the second episode in GRB 090618, see e.g. [15]. We have then started to seek for a possible thermal signature attributable to the P-GRB emission in the early emission of the second episode. As it is shown in Fig. 4, the early emission of the second episode is characterized by an intense spike, anticipated by a weak emission of 9 s. Our search for the P-GRB emission is concentrated in this time interval, since from the fireshell theory the expected energy of the P-GRB emission, in case of long GRBs for which the baryon load is in between  $10^{-3} - 10^{-2}$ , is of the order of  $10^{-2}$  of the prompt emission. The observed fluence (10-1000 keV) in the P-GRB emission, computed from the fit with the power-law function is  $S_{obs} = (1.54 \pm 0.10) \times 10^{-6}$  erg/cm<sup>2</sup>, which corresponds to an isotropic energy of the P-GRB of  $E_{iso,PGRB} = 1.46 \times 10^{51}$  erg, which is quantitatively in agreement

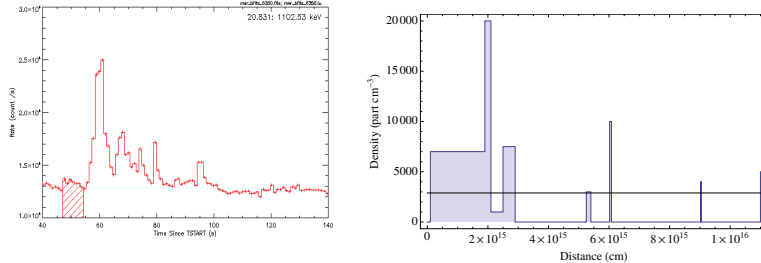


Figure 4: *Left panel:* Light curve of the second episode in GRB 970828. The dashed region represents the P-GRB emission. *Right panel:* The radial CBM density distribution for GRB 970828. The characteristic masses of each cloud are on the order of  $\sim 10^{22}$  g and  $10^{15}$  cm in radii. The black line corresponds to the average value for the particle density.

Table 2: Spectral analysis (25 keV - 1.94 MeV) of the P-GRB emission in the second episode of GRB 970828.

Spectral model	$\gamma$	$\beta$	$E_{cutoff}(keV)$	$kT(keV)$	$\chi^2/DOF$
power-law	$-1.18 \pm 0.04$				91.495/115
cutoff PL	$-1.15 \pm 0.08$		$2251 \pm 1800$		91.157/114
BB + PL	$-1.16 \pm 0.06$			$69.6 \pm 40.0$	90.228/113
Band	$-0.96 \pm 0.44$	$-1.23 \pm 0.08$	$958.8 \pm 800.0$		90.439/113

with the energetic of the P-GRB for this GRB (it is  $\approx 0.01$  % the total energy of the second episode, the GRB). However, due to the paucity of photons in this time interval, we are not able to put tight constraints, e.g. about a possible observed temperature of the P-GRB.

With these results, we can estimate the value of the baryon load from the numerical solutions of the fireshell equations of motion. These solutions for four different values of the total  $e^+e^-$ -plasma energy are shown in the Fig. 4 of [15]. We find that the baryon load is  $B = 7 \times 10^{-3}$ , which corresponds to a Lorentz gamma factor at transparency  $\Gamma = 142.5$ . The GRB emission was simulated with very good approximation by using a density mask characterized by an irregular behavior: all the spikes correspond to spherical clouds with a large particle density  $\langle n \rangle \sim 10^3$  part/cm<sup>3</sup>, and with radius of the order of  $(4 - 8) \times 10^{14}$  cm, see Fig. 4. Considering all the clouds found in our analysis, the average density of the CBM medium is  $\langle n \rangle = 3.4 \times 10^3$  particles/cm<sup>3</sup>. The

Table 3: Final results of the simulation of GRB 970828 in the fireshell scenario

Parameter	Value
$E_{tot}^{e^+e^-}$	$(1.60 \pm 0.03) \times 10^{53}$ erg
$B$	$(7.00 \pm 0.55) \times 10^{-3}$
$\Gamma_0$	$142.5 \pm 57$
$kT_{th}$	$(7.4 \pm 1.3)$ keV
$E_{P-GRB,th}$	$(1.46 \pm 0.43) \times 10^{51}$ erg
$\langle n \rangle$	$3.4 \times 10^3$ part/cm <sup>3</sup>
$\delta n/n$	$10$ part/cm <sup>3</sup>

corresponding masses of the blobs are of the order of  $10^{24}$  g, in agreement with the clumps found in GRB 090618.

## 5 The Episode 3 : the late X-ray afterglow

The most remarkable confirmation of the BdHN paradigm applied to GRB 970828, comes from the late X-ray afterglow emission. As shown in [31], from the knowledge of the redshift of the source, we can compute the X-ray luminosity light curve in the common rest frame energy range 0.3–10 keV after  $\approx 10^4$  s from the initial GRB emission. However, while in [31] the analysis is based on the available X-ray data (0.3–10 keV) from the *Swift*-XRT detector, GRB 970828 occurred in the pre-*Swift* era. Its observational X-ray data are available in the energy range 2–10 keV, since the data were collected by three different satellites: *RXTE*, *ASCA* and *ROSAT*. To further confirm the progenitor mechanism for GRB 970828, we verify the overlapping of the late X-ray data with the ones of the 'Golden Sample' (GS) sources presented in [31]. To this aim, we have computed its luminosity light curve  $L_{rf}$  in a common rest-frame energy range 0.3–10 keV. Since the observed energy band is different (2–10 keV), the expression for the flux light curve  $f_{rf}$  in the 0.3–10 keV rest-frame energy range is not as expressed in Eq. 2 of [31], but it becomes

$$f_{rf} = f_{obs} \frac{\left(\frac{10}{1+z}\right)^{2-\gamma} - \left(\frac{0.3}{1+z}\right)^{2-\gamma}}{10^{2-\gamma} - 2^{2-\gamma}}, \quad (15)$$

where  $\gamma$  is the photon index of the power-law spectral energy distribution of the X-ray data. All the other data transformations, reported in [31], remain unchanged.

We made use in particular of the *RXTE*-PCA observations and *ASCA* data presented in [39]; the averaged photon indexes are taken from the text, for

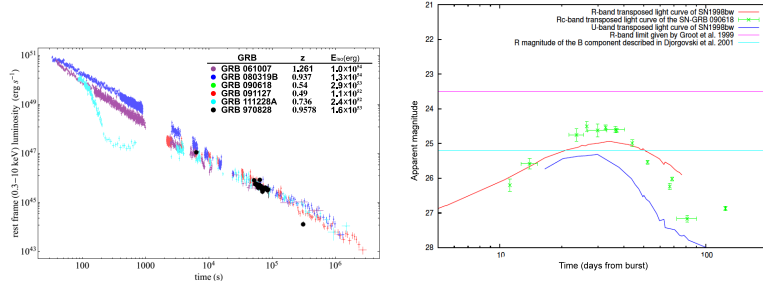


Figure 5: *Left panel:* The late X-ray (0.3 - 10 keV) light curves of some GRBs presented in [31] and of GRB 970828 (black open circles). The overlap of the light curve of GRB 970828 with the members of the BdHN class is clearly evident, confirming that an Induced Gravitational Collapse (IGC) mechanism is operating also in GRB 970828. *Right panel:* The light curve of the SN associated with GRB 090618 (green data), the  $U$ - (blue line) and  $R$ -band (red line) light curve of SN 1998bw transposed at the redshift of GRB 970828,  $z = 0.9578$ , and not corrected for the intrinsic host-galaxy absorption. The purple and cyan line represents the limit given in the deep images by [1] and [7] respectively.

$RXTE$ -PCA ( $\gamma \sim 2$ ), and from Tab. 1, for the  $ASCA$  data, of the same paper. The last data-point by  $ROSAT$  is taken from Fig. 7 in [1], with a corresponding photon index  $\sim 2$ ; the error on the observed flux is the 25% as indicated for the count rate [5]. We show in Fig. 5 the late X-ray (0.3 - 10 keV) light curve of GRB 970828 and we compare it with some GRBs of the “Golden Sample” presented in [31]: GRB 061007, GRB 080319B, GRB 090618, GRB 091127 and GRB 111228A. The perfect overlap with the late X-ray light curves of BdHN sources confirms the presence of a BdHN mechanism operating also in GRB 970828.

## 6 Limits on the Episode 4 : SN-related observations

The analysis of GRB 090618 [15] and GRB 101023 [16] represents an authentic “Rosetta Stone” for the understanding of the GRB-SN phenomenon.

The presence of a supernova emission, observed ten days after the burst in the cosmological rest-frame of GRB 090618, was found to have the same luminosity of SN 1998bw [54], the SN related to GRB 980425 and which is the prototype of SNe connected with GRBs [55]. We have transposed the data of the “bump” Rc-band light curve observed in the optical afterglow of GRB 090618, associated to the presence of an underlying supernova [54], to the redshift of GRB 970828. This simple operation concerns only the transformation of the observed flux, under the assumption that the SN has the same intrinsic luminosity. Moreover, we have also transposed the  $U$  and  $R$ -band light curves of SN 1998bw [56], which is the prototype of a supernova associated to a GRB. From the  $K$ -correction transformation formula, the  $U$ -band light curve, transposed at  $z=0.9578$ , corresponds approximately to the observed  $R$ -band light curve, so in principle we should consider the  $U = 365$  nm transposed light curve as the actual one observed with the  $Rc = 647$  nm optical filter. These transposed light curves are shown in Fig. 5. We conclude that the Supernova emission could have been seen between 20 and 40 days after the GRB trigger, neglecting any possible intrinsic extinction. The optical observations were made up to 7 days from the GRB trigger, reaching a limit of  $R \sim 23.8$  [7], and subsequent deeper images after  $\sim 60$  days [1]. So there are no observations in this time interval. It is appropriate to notice that the  $R$ -band extinction value should be large since the observed column density from the X-ray observations of the GRB afterglow is large as well [39]: the computed light curve for the possible SN of GRB 970828 should be lowered by more than 1 magnitude, leading to a SN bump below the  $R = 25.2$  limit, see Fig. 5. The presence of very dense clouds of matter near the burst site might have darkened both the supernova emission and the GRB optical afterglow. Indeed we find the presence of clouds in our simulation at the average distances of  $\sim 10^{15-16}$  cm from the GRB progenitor, with average density of  $\langle n \rangle \approx 10^3$  part/cm<sup>3</sup> and typical dimensions of  $(4 - 8) \times 10^{14}$  cm, see Fig. 4.

## 7 Conclusions

In conclusion, the recent progress in the observations of X and  $\gamma$ -ray emission, with satellites such as Swift, Fermi, AGILE, Suzaku, Coronas-PHOTON, the possibility of observing GRB afterglows with the new generation of optical

and radio telescopes, developed since 1997, and the theoretical understanding of the BdHN paradigm, have allowed to revisit the data of GRB 970828 and give a new conceptual understanding of the underlying astrophysical scenario.

We verify in this paper that GRB 970828 is a member of the BdHN family. This new understanding leads to a wealth of information on the different emission episodes which are observed during an IGC process. In Episode 1, we determine the evolution of the thermal component and of the radius of the blackbody emitter, given by Eq. (1), see Figs. 1, 2. The onset of the SN is here observed for the first time in an unprecedented circumstance: a SN exploding in a close binary system with a companion NS. The energetics are correspondingly much larger than the one to be expected in an isolated SN, and presents an high energy component likely associated to an outflow process in the binary accreting system. In Episode 2, the GRB, we give the details of the CBM structure, see Fig. 4, of the simulation of the light curve and the spectrum of the real GRB emission. We have also shown in Table 2 the final results of the GRB simulation, the total energy of the  $e^+e^-$  plasma, the baryon load  $B$ , the temperature of the P-GRB  $kT_{th}$  and the Lorentz Gamma factor at transparency  $\Gamma$ , as well the average value of the CBM density  $\langle n_{CBM} \rangle$  and the density ratio of the clouds  $\delta n/n$ . In Episode 3, we have shown that the late afterglow emission observed by ASCA and ROSAT, although limited to few data points, when considered in the cosmological rest-frame of the emitter, presents a successful overlap with the standard luminosity behavior of other members of the BdHN family [31], which is the most striking confirmation that in GRB 970828 an IGC process is working. Finally, from this latter analogy with the late X-ray afterglow decay of the “Golden Sample” [31], and with the optical bump observed in GRB 090618, see Fig. 5, associated to a SN emission [54], we have given reasons why a SN associated to GRB 970828 was not observable due to the large interstellar local absorption, in agreement with the large column density observed in the ASCA X-ray data [39] and with the large value we have inferred for the CBM density distribution,  $\langle n_{CBM} \rangle \approx 10^3$  particles/cm<sup>3</sup>.

The possibility to observe the energy distribution from a GRB in a very wide energy range, thanks to the new dedicated space missions, has allowed to definitely confirm the presence of two separate emission episodes in GRBs associated to SNe. Future planned missions, as the proposed Wide Field Monitor detector on board the LOFT mission [57], will allow to observe the thermal

decay from these objects down to  $kT = 0.5 - 1$  keV. It is important to note the possibility that the Large Area Detector, designed for the LOFT mission, will be also able to observe the afterglow emission from times larger than  $10^4$  s in the rest-frame, allowing to check possible new BdHNe by using the overlapping method described in [31, 58] and consequently estimate the distance, wherever an observed determination of the redshift is missing.

## References

- [1] S. G. Djorgovski, D. A. Frail, S. R. Kulkarni, et al., *ApJ*, 562:654–663, December 2001.
- [2] R. Remillard, A. Wood, D. Smith, and A. Levine. *IAU Circ.*, 6726:1, August 1997.
- [3] D. Smith, A. Levine, R. Remillard, et al., *IAU Circ.*, 6728:1, August 1997.
- [4] A. V. Filippenko, D. Stern, R. R. Treffers, et al., *IAU Circ.*, 6729:1, August 1997.
- [5] J. Greiner, R. Schwarz, J. Englhauser, et al., *IAU Circ.*, 6757:1, October 1997.
- [6] S. C. Odewahn, S. G. Djorgovski, S. R. Kulkarni, et al., *IAU Circ.*, 6735:1, September 1997.
- [7] P. J. Groot, T. J. Galama, J. van Paradijs, et al., *ApJ*, 493:L27, January 1998.
- [8] N. Gehrels, G. Chincarini, P. Giommi, et al., *ApJ*, 611:1005–1020, August 2004.
- [9] C. Meegan, G. Lichti, P. N. Bhat, et al., *ApJ*, 702:791, September 2009.
- [10] M. Tavani, G. Barbiellini, A. Argan, et al., *A&A*, 502:995–1013, August 2009.
- [11] R. L. Aptekar, D. D. Frederiks, S. V. Golenetskii, et al., *Space Sci. Rev.*, 71:265–272, February 1995.
- [12] D. Burrows, J. Hill, J. Nousek, et al., *Space Science Reviews*, 120:165, 2005. 10.1007/s11214-005-5097-2.
- [13] R. Ruffini, M. G. Bernardini, C. L. Bianco, et al., In *ESA Special Publication*, volume 622 of *ESA Special Publication*, page 561, 2007.
- [14] J. A. Rueda and R. Ruffini. *ApJ*, 758:L7, October 2012.
- [15] L. Izzo, R. Ruffini, A. V. Penacchioni, et al., *A&A*, 543:A10, July 2012.

- [16] A. V. Penacchioni, R. Ruffini, L. Izzo, et al., *A&A*, 538:A58, February 2012.
- [17] Hoyle, F., & Lyttleton, R. A. 1939, Proceedings of the Cambridge Philosophical Society, 35, 405.
- [18] Bondi, H., & Hoyle, F. 1944, MNRAS, 104, 273.
- [19] Bondi, H. 1952, MNRAS, 112, 195.
- [20] C.L. Fryer, J.A. Rueda, R. Ruffini, et al., *ApJ*, 793:L36, September 2014.
- [21] Fryer, C. L., Benz, W., & Herant, M. 1996, ApJ, 460, 801.
- [22] Eggleton, P. P. 1983, ApJ, 268, 368.
- [23] Fryer, C. L., Benz, W., Herant, M., & Colgate, S. A. 1999, ApJ, 516, 892.
- [24] Chevalier, R. A. 1989, ApJ, 346, 847.
- [25] Zel'dovich, Y. B., Ivanova, L. N., & Nadezhin, D. K. 1972, Soviet Astronomy, 16, 209.
- [26] Houck, J. C., & Chevalier, R. A. 1991, ApJ, 376, 234.
- [27] Ruffini, R., & Wilson, J. 1973, Physical Review Letters, 31, 1362.
- [28] Fryer, C. L. 2009, ApJ, 699, 409.
- [29] Fryer, C. L., Herwig, F., Hungerford, A., & Timmes, F. X. 2006, ApJ, 646, L131.
- [30] A. V. Penacchioni, R. Ruffini, C. L. Bianco, et al., *A&A*, 551:A133, March 2013.
- [31] G. B. Pisani, L. Izzo, R. Ruffini, et al., *A&A*, 552:L5, April 2013.
- [32] R. Belvedere, D. Pugliese, J. A. Rueda, et al., *Nuclear Physics A*, 883:1–24, June 2012.
- [33] B. Zhang, Y. Z. Fan, J. Dyks, et al., *ApJ*, 642:354, May 2006.
- [34] J. A. Nousek, C. Kouveliotou, D. Grupe, et al., *ApJ*, 642:389, May 2006.
- [35] A. Pe'er, F. Ryde, R. A. M. J. Wijers, et al., *ApJ*, 664:L1, July 2007.

- [36] P. Mészáros. *ARA&A*, 40:137, 2002.
- [37] F. E. Marshall, J. K. Cannizzo, and R. H. D. Corbet. *IAU Circ.*, 6727:1, August 1997.
- [38] T. Murakami, Y. Ueda, A. Yoshida, et al., *IAU Circ.*, 6732:1, September 1997.
- [39] A. Yoshida, M. Namiki, D. Yonetoku, et al., *ApJ*, 557:L27–L30, August 2001.
- [40] L. Izzo, J. A. Rueda, and R. Ruffini. *A&A*, 548:L5, December 2012.
- [41] T. Piran. *Phys. Rep.*, 314:575, 1999.
- [42] M. Ruderman. In P. G. Bergman, E. J. Fenyves, and L. Motz, editors, *Seventh Texas Symposium on Relativistic Astrophysics*, volume 262 of *Annals of the New York Academy of Sciences*, pages 164–180, October 1975.
- [43] E. Woods and A. Loeb. *ApJ*, 453:583, November 1995.
- [44] Y. Lithwick and R. Sari. *ApJ*, 555:540, July 2001.
- [45] B. Zhang and A. Pe’er. *ApJ*, 700:L65–L68, August 2009.
- [46] N. Gupta and B. Zhang. *MNRAS*, 384:L11–L15, February 2008.
- [47] R. Ruffini, C. L. Bianco, F. Fraschetti, et al., *ApJ*, 555:L107–L111, July 2001.
- [48] R. Ruffini, C. L. Bianco, F. Fraschetti, et al., *ApJ*, 555:L117, July 2001.
- [49] D. Christodoulou and R. Ruffini. *Phys. Rev. D*, 4:3552, December 1971.
- [50] T. Damour and R. Ruffini. *Physical Review Letters*, 35:463, August 1975.
- [51] R. Ruffini, C. L. Bianco, S.-S. Xue, et al., *International Journal of Modern Physics D*, 14:97–105, 2005.
- [52] R. Ruffini, M. G. Bernardini, C. L. Bianco, et al., In M. Novello & S. E. Perez Bergliaffa, editor, *XIth Brazilian School of Cosmology and Gravitation*, volume 782 of *American Institute of Physics Conference Series*, page 42, August 2005.

- [53] B. Patricelli, M. G. Bernardini, C. L. Bianco, et al., *ApJ*, 756:16, September 2012.
- [54] Z. Cano, D. Bersier, C. Guidorzi, et al., *MNRAS*, 413:669–685, May 2011.
- [55] M. Della Valle. Supernovae and Gamma-Ray Bursts: A Decade of Observations. *International Journal of Modern Physics D*, 20:1745–1754, 2011.
- [56] T. J. Galama, P. M. Vreeswijk, J. van Paradijs, et al., *Nature*, 395:670, October 1998.
- [57] M. Feroci, J. W. den Herder, E. Bozzo, et al., In *Society of Photo-Optical Instrumentation Engineers (SPIE) Conference Series*, volume 8443 of *Society of Photo-Optical Instrumentation Engineers (SPIE) Conference Series*, September 2012.
- [58] L. Izzo, G. B. Pisani, M. Muccino, et al., In A. J. Castro-Tirado, J. Gorosabel, and I. H. Park, editors, *EAS Publications Series*, volume 61 of *EAS Publications Series*, pages 595–597, July 2013.



## GRB 130427A AND SN 2013CQ: A MULTI-WAVELENGTH ANALYSIS OF AN INDUCED GRAVITATIONAL COLLAPSE EVENT

R. RUFFINI<sup>1,2,3,4</sup>, Y. WANG<sup>1,2</sup>, M. ENDERLI<sup>1,3</sup>, M. MUCCINO<sup>1,2</sup>, M. KOVACEVIC<sup>1,3</sup>, C.L. BIANCO<sup>1,2</sup>, A.V. PENACCHIONI<sup>4</sup>, G.B. PISANI<sup>1,3</sup>, J.A. RUEDA<sup>1,2,4</sup>

*Draft version October 23, 2014*

### ABSTRACT

We have performed our data analysis of the observations by *Swift*, *NuStar* and *Fermi* satellites in order to probe the induced gravitational collapse (IGC) paradigm for GRBs associated with supernovae (SNe), in the “terra incognita” of GRB 130427A. We compare and contrast our data analysis with those in the literature. We have verified that the GRB 130427A conforms to the IGC paradigm by examining the power law behavior of the luminosity in the early  $10^4$  s of the XRT observations. This has led to the identification of the four different episodes of the “binary driven hypernovae” (BdHNe) and to the prediction, on May 2, 2013, of the occurrence of SN 2013cq, duly observed in the optical band on May 13, 2013. The exceptional quality of the data has allowed the identification of novel features in *Episode 3* including: a) the confirmation and the extension of the existence of the recently discovered “nested structure” in the late X-ray luminosity in GRB 130427A, as well as the identification of a spiky structure at  $10^2$  s in the cosmological rest-frame of the source; b) a power law emission of the GeV luminosity light curve and its onset at the end of *Episode 2*; c) different Lorentz  $\Gamma$  factors for the emitting regions of the X-ray and GeV emissions in this *Episode 3*. These results make it possible to test the details of the physical and astrophysical regimes at work in the BdHNe: 1) a newly born neutron star and the supernova ejecta, originating in *Episode 1*, 2) a newly formed black hole originating in *Episode 2*, and 3) the possible interaction among these components, observable in the standard features of *Episode 3*.

**Keywords:** black hole physics — gamma-ray burst: general — nuclear reactions, nucleosynthesis, abundances — stars: neutron — supernovae: general

### 1. INTRODUCTION AND SUMMARY OF PREVIOUS RESULTS

That some long gamma-ray bursts (GRBs) and supernovae (SNe) can occur almost simultaneously has been known for a long time, since the early observations of GRB 980425/SN 1998bw (Galama et al. 1998; Pian et al. 2000). This association of a GRB and a SN occurs most commonly in a family of less energetic long GRBs with the following characteristics: 1) isotropic energies  $E_{iso}$  in the range of  $10^{49}$ – $10^{52}$  erg (Guetta & Della Valle 2007); 2) a soft spectrum with rest-frame peak energy  $E_{p,i} < 100$  keV, although the instruments are sensitive up to GeV; 3) supernova emissions are observable up to a cosmological distance  $z < 1$ . We shall refer to this family in the following as *family 1*. This result has been well recognized in the literature, see e.g. (Maselli et al. 2013).

There is an alternative family of high energetic long GRBs possibly associated with SNe which have a much more complex structure. Their characteristics are: 1)  $E_{iso}$  is in the range  $10^{52}$ – $10^{54}$  erg; 2) they present multiple components in their spectra and in their overall luminosity distribution, ranging from X-ray,  $\gamma$ -ray all the way to GeV emission. They have peak energies from 100 keV to some MeV; 3) in view of their large energetics, their observation extends to the entire universe all the way up to  $z = 8.2$  (Ruffini et al. 2014). We shall refer to this family in the following as *family 2*.

yu.wang@icranet.org

<sup>1</sup> Dip. di Fisica and ICRA, Sapienza Università di Roma, Piazzale Aldo Moro 5, I-00185 Rome, Italy.

<sup>2</sup> ICRANet, Piazza della Repubblica 10, I-65122 Pescara, Italy.

<sup>3</sup> Université de Nice Sophia Antipolis, CEDEX 2, Grand Château Parc Valrose, Nice, France.

<sup>4</sup> ICRANet-Rio, Centro Brasileiro de Pesquisas Físicas, Rua Dr. Xavier Sigaud 150, Rio de Janeiro, RJ, 22290-180, Brazil.

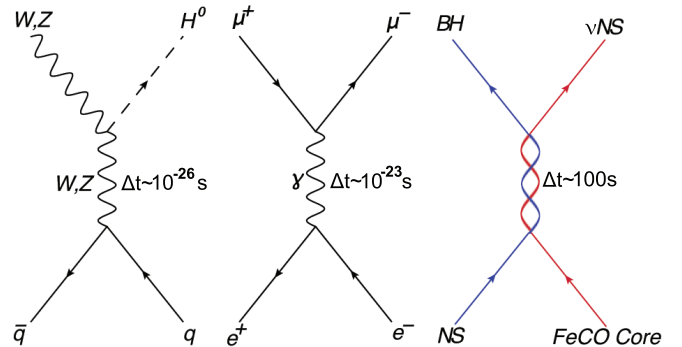


**Figure 1.** Three different matrices in fundamental physics. The first is the quark matrix leading to a Higgs boson. In the middle is the classical electron-positron pair matrix, generating a muon and anti-muon pair. The third matrix is the most recent one, which is considered in the present work.  $\Delta t$  is the duration of intermediate state.

Doubts were advanced that SNe may be associated with very bright long GRBs: naive energetic arguments considered that there can hardly be a SN in a powerful GRB within the single star collapse model (see e.g. Maselli et al. 2013).

The issue of the coincidence of very energetic GRBs with SN has represented for some years an authentic “terra incognita”. The crucial point is to clarify whether this association of GRBs and SNe is only accidental or necessary, independent of their energetics. Up to June 2014, out of 104 long GRBs with known redshift  $z < 1$ , 19 GRBs associated with SNe belonging to the *family 2* have been observed (Kovacevic et al. 2014), and GRB 130427A with isotropic energy  $E_{iso} \simeq 10^{54}$  erg is the most energetic one so far.

In (Ruffini et al. 2001, 2008), we have introduced the paradigm of induced gravitational collapse (IGC) in order to explain the astrophysical reasons for the association of

GRBs with supernovae. This paradigm indicates that all long GRBs, by norm, have to be associated with SNe. The IGC paradigm differs from the traditional collapsar-fireball paradigm (see, e.g., Piran 2005, and references therein). In the collapsar-fireball model the GRB process is described by a single episode: 1) it is assumed to originate in a “collapsar” (Woosley 1993); 2) the spectral and luminosity analysis is typically time integrated over the entire  $T_{90}$  (see e.g. Tavani 1998); 3) the description of the afterglow is dominated by a single ultra-relativistic jetted emission (see, e.g., in Rhoads 1999; van Eerten et al. 2010; van Eerten & MacFadyen 2012; Nava et al. 2013). In contrast, the IGC paradigm considers a multi-component system, similar to the ones described by  $S$ -matrix in particle physics as shown in Figure 1: 1) the “in-states” are represented by a binary system formed by a FeCO core, very close to the onset of a SN event, and a tightly bound companion neutron star (NS) (Ruffini et al. 2008; Rueda & Ruffini 2012; Izzo et al. 2012). The “out-states” are the creation of a new NS ( $\nu$ -NS) and a black hole (BH). In the case of particle physics the  $S$ -matrix describes virtual phenomena occurring on time scales of  $10^{-26}$  s (Aad et al. 2012,  $q\bar{q} \rightarrow WZH^0$ ) and  $10^{-23}$  s (Bernardini 2004,  $e^+e^- \rightarrow \mu^+\mu^-$ ). In the astrophysical case, here considered, the cosmic matrix ( $C$ -matrix) describes real event occurring on timescale  $\sim 200$  s, still a very short time when compared to traditional astrophysical time scales. Following the accretion of the SN ejecta onto the companion NS binary, a BH is expected to be created, giving origin to the GRB; 2) special attention is given to the analysis of the instantaneous spectra in optical, X-ray,  $\gamma$ -ray and GeV energy range (as exemplified in this article); 3) four different episodes are identifiable in the overall emission, each with marked differences in the values of their Lorentz  $\Gamma$  factors (Ruffini et al. 2014b). Actually the possible relevance of a binary system in the explanation of GRBs was already mentioned in a pioneering work of Fryer et al. (1999) and in Broderick (2005), but the binaries in their case were a trigger to the traditional collapsar model.

The opportunity to probe the IGC paradigm (Izzo et al. 2012) has come from the prototypical source GRB 090618, a member of *family 2*. This source, has an extremely high energetics, i.e.,  $E_{iso} = 2.7 \times 10^{53}$  erg, is at a relatively close distance, i.e.,  $z = 0.54$ , and has a coverage by all the existing  $\gamma$ , X-ray and optical observatories.

A wealth of results have been obtained:

1) *Episode 1* corresponding to the onset of the SN and the accretion process onto the companion NS was soon identified in the early 50 s, with a thermal plus power law component in the spectra (see Izzo et al. 2012, Fig. 16), as well as a temporal evolution of the radius of the emitting region expanding from  $10^9$  cm to  $7 \times 10^9$  cm (see Izzo et al. 2012, Fig. 18), leading to a precise determination of its overall energetics of  $4 \times 10^{52}$  erg.

2) *Episode 2* with the GRB emission, following the onset of gravitational collapse and the BH formation, was also clearly identified with the characteristic parameters: an isotropic energy  $E_{iso} = 2.49 \times 10^{53}$ , baryon loading  $B = 1.98 \times 10^{-3}$ , Lorentz factor  $\Gamma = 495$  (see Izzo et al. 2012, Fig. 4), and peak energy  $E_{p,i} = 193$  keV. The average number density of the circumburst medium (CBM) is  $\langle n_{CBM} \rangle = 0.6 \text{ cm}^{-3}$ . The characteristic masses of each CBM cloud have been found to be of the order of  $\sim 10^{22} - 10^{24}$  g, at  $10^{16}$  cm in radii (see Izzo et al. 2012, Fig. 10).

3) *Episode 3* of GRB 090618, detected by *Swift*-XRT, starts

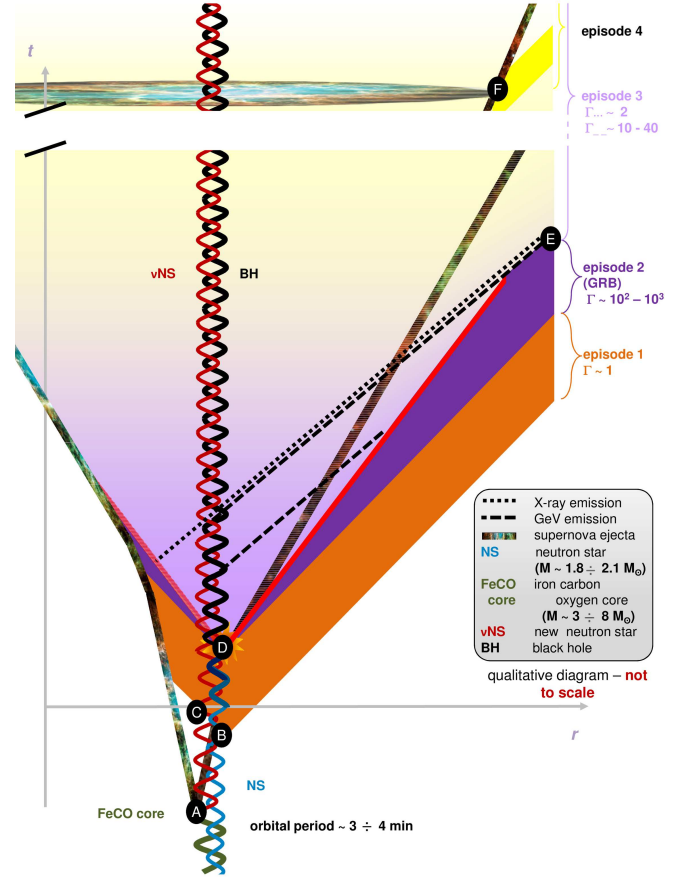


**Figure 2.** IGC space-time diagram (not in scale) illustrates 4 episodes of IGC paradigm: the non-relativistic *Episode 1* ( $\Gamma \simeq 1$ ), the relativistic motion of *Episode 2* ( $\Gamma \simeq 10^2 \sim 10^3$ ), the mildly relativistic *Episode 3* ( $\Gamma \simeq 2$ ), and non-relativistic *Episode 4* ( $\Gamma \simeq 1$ ). Initially there is a binary system composed by a massive star (yellow thick line) and a neutron star (blue line). The massive star evolves and explodes as a SN at point A, forms a  $\nu$ NS (red line). The companion NS accretes the supernova ejecta starting from point B, interacts with the  $\nu$ NS starting from point C, and collapses into a black hole (black line) at point D, this period from point B to point D we define as *Episode 1*. Point D is the starting of *Episode 2*, due to the collision of GRB outflow and interstellar filaments. At point E, *Episode 2* ends and *Episode 3* starts, *Episode 3* lasts till the optical signal of supernova emerges at point F, where the *Episode 4* starts. (Credit to M.Enderli on drawing this visualized space-time diagram.)

at 150 s after the burst trigger and continues all the way up to  $10^6$  s. It consists of three different parts (Nousek et al. 2006): a) a first very steep decay; b) a shallower decay, the plateau and c) a final steeper decay with a fixed power law index. It soon became clear that this *Episode 3*, which had been interpreted in the traditional approach as part of the GRB afterglow (Piran 2005; Rhoads 1999; van Eerten et al. 2010; van Eerten & MacFadyen 2012; Nava et al. 2013), appeared to be the seat of a set of novel independent process occurring after the end of the GRB emission and preceding the optical observation of the SN, which we indicated as *Episode 4*.

Recently, progress has been made in the analysis of *Episode 1*. It is characterized by the explosion of the FeCO core, followed by the hypercritical accretion onto the NS which leads to the reaching of the critical mass of the NS and consequently to its induced gravitational collapse to a BH. The hypercritical accretion of the SN ejecta onto the NS has been estimated using the Bondi-Hoyle-Lyttleton formalism to be

$10^{-2} M_{\odot} s^{-1}$ , here  $M_{\odot}$  is the solar mass (Bondi & Hoyle 1944; Bondi 1952), see e.g., in (Rueda & Ruffini 2012). The inflowing material shocks as it piles up onto the NS, producing a compressed layer on top of the NS (see e.g., Fryer et al. 1996). As this compressed layer becomes sufficiently hot, it triggers the emission of neutrinos which cool the in-falling material, allowing it to be accreted into the NS (Zel'dovich et al. 1972; Ruffini & Wilson 1975; Ruffini et al. 1999, 2000; Fryer et al. 1996, 1999). Recently Fryer et al. (2014) have presented a significant progress in understanding the underlying physical phenomena in the aforementioned hypercritical accretion process of the supernova ejecta into the binary companion neutron star (Ruffini et al. 2008; Rueda & Ruffini 2012). The new treatment, based on the two-dimensional cylindrical geometry smooth particle hydrodynamics code, has simulated numerically the process of hypercritical accretion, the classical Bondi-Hoyle regimes, in the specific case of the IGC paradigm and leading to the first astrophysical application of the neutrino production process considered in Zel'dovich et al. (1972) and in Ruffini & Wilson (1975), see e.g., in R. Ruffini et al. presentation in Zeldovich-100 meeting<sup>5</sup>. Indeed the fundamental role of neutrinos emission allows the accretion rate process to increase the mass of the binary companion star to its critical value and lead to the black hole formation giving origin to the GRB in *Episode 2*. This results confirm and quantifies the general considerations presented in (Rueda & Ruffini 2012).

On *Episode 2* all technical, numerical and basic physical processes have been tested in the literature, and the fireshell model is now routinely applied to all GRBs, see e.g., GRB 101023 in Penacchioni et al. (2012) and GRB 110709B in Penacchioni et al. (2013).

The main aim of this article is dedicated to a deeper understanding of the physical and astrophysical process present in *Episode 3*:

1) to evidence the universality properties of *Episode 3*, observed in additional sources belonging to *family 2*, as compared and contrasted to the very high variability of *Episode 1* and *Episode 2* components;

2) to present observations of GRB130427A leading to identify new physical regimes encountered in *Episode 3* and their interpretation within the IGC paradigm;

3) to evidence the predictive power of the observations of *Episode 3* and outline the underlying physical process leading to the characterization of the two above mentioned families of GRBs.

To start we will summarize in the next paragraph some qualifying new features generally observed in *Episode 3* of selected GRBs of the *Family 2* and proceed in the following paragraphs to the specific new informations acquired *Episode 3* from GRB 130427A. We will then proceed to the general conclusions.

## 2. THE QUALIFYING FEATURES OF EPISODE 3

As observations of additional sources fulfilling the IGC paradigm were performed, some precise qualifying features for characterizing *Episode 3* have been found:

a) In some GRBs with known redshift belonging to this *family 2* the late X-ray luminosities at times larger than  $10^4$  s appeared to overlap, when duly scaled in the proper rest frame of the GRB source (Penacchioni et al. 2012). This was soon

<sup>5</sup> [http://www.icranet.org/index.php?option=com\\_content&task=view&id=747&Itemid=880](http://www.icranet.org/index.php?option=com_content&task=view&id=747&Itemid=880)

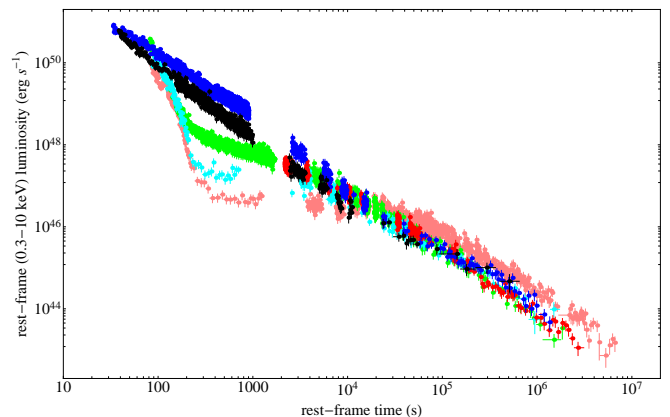


**Figure 3.** The golden sample scaling law (Pisani et al. 2013). X-ray luminosity light curves of the six GRBs with measured redshift in the 0.310 keV rest-frame energy range: in pink GRB 060729,  $z = 0.54$ ; black GRB 061007,  $z = 1.261$ ; blue GRB 080319B,  $z = 0.937$ ; green GRB 090618,  $z = 0.54$ , red GRB 091127,  $z = 0.49$ , and in cyan GRB 111228,  $z = 0.713$ .

confirmed for a sample of 6 GRBs, i.e. GRB 060729, GRB 061007, GRB 080319B, GRB090618, GRB 091127, GRB 111228, which we have called the “golden sample” (GS) (Pisani et al. 2013), see Figure 3. This unexpected result has led to adopt this universal luminosity versus time relation in the late X-ray emission of *Episode 3* as a distance indicator. For some GRBs without a known cosmological redshift and exhibiting the general features of the four episodes, we imposed the overlapping of the late power law X-ray emission in their *Episode 3* with the ones of the GS and we have consequently inferred the value of the cosmological redshift of the source. This in turn has led to inferring the overall energetics of the source and to proceed to a consistent description of each episode following our theoretical model. This has been the case with GRB 101023, having inferred redshift  $z = 0.9$  and  $E_{iso} = 4.03 \times 10^{53}$  erg (Penacchioni et al. 2012), and GRB 110709B, with inferred redshift  $z = 0.75$  and  $E_{iso} = 2.43 \times 10^{52}$  erg (Penacchioni et al. 2013).

The above analysis has initially addressed sources with  $z < 1$ , where the associated SNe are observable. There is no reason to doubt that the IGC paradigm applies as well to sources for  $z > 1$ . In this case clearly the SN is not observable with the current optical telescopes but the existence of all the above episodes, with the exception of *Episode 4* related to the optical observation of the SN, in principle can be verified, if they are above the observational threshold, and the members of the GS are correspondingly further increased. Indeed, significant results have been reached by observing the fulfillment of the above scaling laws in *Episode 3* of GRB 090423, at  $z = 8.2$  (Ruffini et al. 2014). The occurrence of this overlapping in the late X-ray emission observed by XRT has been considered as the necessary and sufficient condition to assert that a GRB fulfills the IGC paradigm.

b) The identification of a thermal emission occurring in the initial very steep decay of *Swift-XRT* data of *Episode 3* in GRB 090618 (Ruffini et al. 2014b). We are currently examining other GRBs showing this feature, e.g., 060729, 061007, 061121 (Page et al. 2011; Starling et al. 2012; Friis & Watson 2013). From these thermal emissions it is possible to infer the dimensions of the X-ray emitting regions as well as their Lorentz  $\Gamma$  factors in this earliest part of *Episode 3* (Ruffini et al. 2014b). A typical mildly relativistic expansion regime with  $\Gamma \lesssim 2$  and characteristic radii  $R \sim 10^{13}$  cm has been iden-

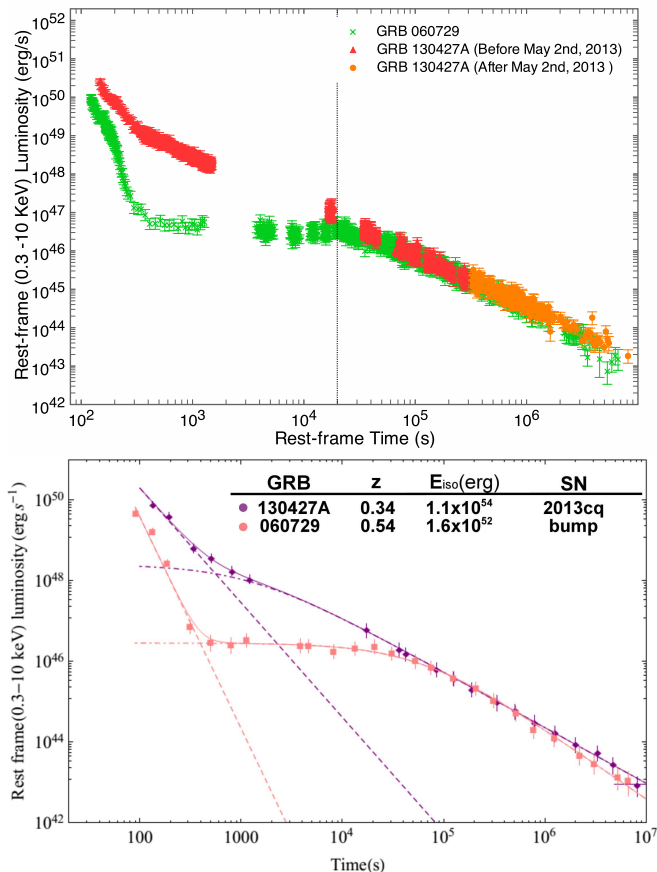


**Figure 4.** **Top:** Overlapping of GRB 130427A and GRB 060729. Green cross is the light curve of GRB 060729. Red triangle and orange dots represent the light curve of GRB 130427A respectively before and after May 2, 2013. The vertical line marks the time of  $2 \times 10^4$  s which is the lower limit for the domain of validity of the Pisani relation prior to GRB 130427A. **Bottom:** This figure shows GRB 060729 and 130427A have different magnitudes of the isotropic energy, but exhibit a common scaling law after  $2 \times 10^4$  s. It also shows that the low isotropic energy GRB 060729 has a longer plateau, while the high isotropic energy GRB 130427A doesn't display an obvious plateau.

tified (Ruffini et al. 2014b). These observational facts lead to a novel approach to the theoretical understanding of the X-ray emission process of *Episode 3*, profoundly different from the ultra-relativistic one in the traditional jet afterglow collapsar paradigm model (Piran 2005; Mészáros 2006). We have concluded that this emission is not only mildly-relativistic, but also linked to a wide angle emission from the SN ejecta, in the absence of any sign of collimation (Ruffini et al. 2014b).

c) From the direct comparison of the late X-ray emission of the *GS* sources, we have recently identified the appearance of a “nested structure”, which we illustrate in Figure 4, comparing and contrasting the corresponding behavior of GRB 130427A with one the *GS* GRB 060729 (Ruffini et al. 2014b). The occurrence of these nested structures shows, among others, that in the case of the most intense sources, the common power law observed for the X-ray luminosities for time larger than  $10^4$  s do extend to earlier times, see Figure 4. Indeed, for the most intense sources the common power law behavior is attained at an earlier time and at higher X-ray luminosities than the characteristic time scale indicated in (Pisani et al. 2013), see Figure 3. As we are going to show, in the present highly energetic GRB 130427A, this behavior starts at much earlier times around 400 s.

Some of the above results were presented by one of the authors in the 2013 Texas Symposium on Relativistic Astrophysics<sup>6</sup>. There, referring to these sources originating in a tight binary system composed of a FeCO core at the onset of a SN event and a companion NS were named “binary driven hypernovae” (BdHNe, Ruffini et al. 2014b), in order to distinguish them from the traditional hypernovae (HN).

The occurrence of the three features of *Episode 3* listed above as obtained by our data analysis are becoming crucial to the theoretical understanding of the GRB-SN phenomena. They have never been envisaged to exist nor predicted in the traditional collapsar-fireball paradigm (Nava et al. 2013; van Eerten & MacFadyen 2012; van Eerten et al. 2010). The IGC paradigm motivated an attentive data analysis of *Episode 3* and the discovery of its universality has been a by-product.

### 3. EPISODE 3 IN THE CASE OF GRB 130427A

We are going to show in this paper, in what follows, how GRB 130427A, associated with SN 2013cq and being the most luminous GRB ever observed in the past 40 years, offers the longest multi-wavelength observations of *Episode 3* so far. It confirms and extends all the above understanding and the corresponding scaling laws already observed in X-ray to lower and higher energies. It allows the exploration of the occurrence of similar constant power law emission in the high energy emission (GeV) and in the optical domain. We proceed with our data analysis of the ultra high GeV energy observations (*Fermi*-LAT), those in soft and hard X-rays (*Swift*-XRT and *NuStar*, respectively) as well as of optical observations (*Swift*-UVOT and ground based satellites). Our results are compared to and contrasted with the current ones in the literature. These observational facts set very specific limits: a) on the Lorentz  $\Gamma$  factor of each component; b) on the corresponding mechanism of emission; c) on the clear independence of any prolongation of the GRB emission of *Episode 2* to the emission process of *Episode 3*.

The observation of the scaling law in the first  $2 \times 10^4$  s alone has allowed us to verify the BdHN nature of this source which necessarily implies the presence of a SN. Consequently, we recall in Sec. 3.1 that we made the successful prediction of the occurrence of a supernova which was observed in the optical band, as predicted on May 2, 2013.

In Sec. 3.2, we summarize our own data reduction of the *Fermi* and *Swift* satellites, we compare and contrast them with the ones in the current literature.

In Sec. 3.3, we discuss the finding of a thermal component in the early part of X-ray emission of *Episode 3*: this is crucial for identifying the existence of X-ray emission of a regime with low Lorentz factor and small radius, typical for supernova ejecta.

In Sec. 3.4 we compare and contrast the broad band (optical, X-ray,  $\gamma$ -rays all the way up to GeV) light curves and spectra of *Episode 3*

In Sec. 3.5 we point out the crucial difference between the X-,  $\gamma$ -ray and GeV emission in *Episode-3*.

In Sec. 3.6 we proceed to a few general considerations on ongoing theoretical activities.

Secs. 4 is the summary and conclusions.

#### 3.1. Identification and prediction

With the appearance of GRB 130427A, we decided, as recalled above, to explore the applicability of the IGC paradigm

<sup>6</sup> <http://nsm.utdallas.edu/texas2013/proceedings/3/1/Ruffini.pdf>

in the “terra incognita” of GRB energies up to  $\sim 10^{54}$  erg. In fact, prior to GRB 130427A, the only known case of an equally energetic source, GRB 080319B, gave some evidence of an optical bump (Bloom et al. 2009; Tanvir et al. 2010), but in no way a detailed knowledge of the SN spectrum or type. We soon noticed in GRB 130427A the characteristic overlapping of the late X-ray decay in the cosmological rest frame of the source with that of GRB 060729, a member of the golden sample (in red in Fig. 4), and from the overlapping we deduced a redshift which was consistent with the observational value  $z = 0.34$  (Levan et al. 2013).

Therefore from the observations of the first  $2 \times 10^4$  s, GRB 130427A has been confirmed to fulfill the IGC paradigm, and we conclude, solely on this ground, that a SN should necessarily be observed under these circumstances. We sent the GCN circular 14526<sup>7</sup> (Ruffini et al. 2013b) on May 2, 2013 predicting that the optical R-band of a SN will reach its peak magnitude in about 10 days in the cosmological rest-frame on the basis of the IGC paradigm, and we encouraged observations. Indeed, starting from May 13, 2013, the telescopes GTC, Skynet and HST discovered the signals from the type Ic supernova SN 2013cq (de Ugarte Postigo et al. 2013; Trotter et al. 2013; Levan et al. 2013a,b; Xu et al. 2013). We kept updating the X-ray *Swift* data for weeks and we confirmed the complete overlapping of the late X-ray luminosities, in the respective cosmological rest frames, of GRB 130427A and GRB 060729 (in orange in Fig. 4). From these data it soon became clear that the power law behavior of the late time X-ray luminosity with index  $\alpha \sim 1.3$  indicated in (Pisani et al. 2013), leading to the new concept of the “nesting of the light curves”, started in this very energetic source already at  $\sim 10^2$  s following an initial phase of steeper decay (Ruffini et al. 2014b).

Contrary to the traditional approach which generally considers a GRB to be composed of the prompt emission followed by the afterglow, both of which vary from source to source, the IGC paradigm for this *family 2* has introduced the *Episode 3* which shows regularities and standard late time light curves, largely independent of the GRB energy. It soon became clear that, with *Episode 3*, we were starting to test the details of the physics and astrophysics of as yet unexplored regimes implied by the IGC paradigm: 1) a  $\nu$ -NS and the SN ejecta, originating in *Episode 1*, 2) a newly formed BH originating in *Episode 2*, and 3) the possible interaction among these components observable in the standard features of *Episode 3*.

The joint observations of the *Swift*, *NuStar* and *Fermi* satellites have offered the unprecedented possibility of clarifying these new regimes with the addition of crucial observations in the optical, X-ray and high energy radiation for *Episode 3* of GRB 130427A, leading to equally unexpected results. The remainder of this article is dedicated to the understanding of *Episode 3* of this remarkable event.

### 3.2. Data Analysis of Episode 3 in GRB 130427A

<sup>7</sup> GCN 14526: The late X-ray observations of GRB 130427A by *Swift*-XRT clearly evidence a pattern typical of a family of GRBs associated to supernova (SN) following the Induce Gravitational Collapse (IGC) paradigm (Rueda & Ruffini 2012; Pisani et al. 2013). We assume that the luminosity of the possible SN associated to GRB 130427A would be the one of 1998bw, as found in the IGC sample described in Pisani et al. 2013. Assuming the intergalactic absorption in the I-band (which corresponds to the R-band rest-frame) and the intrinsic one, assuming a Milky Way type for the host galaxy, we obtain a magnitude expected for the peak of the SN of  $I = 22 - 23$  occurring 13-15 days after the GRB trigger, namely between the 10th and the 12th of May 2013. Further optical and radio observations are encouraged.

GRB 130427A was first observed by the *Fermi*-GBM at 07:47:06.42 UT on April 27 2013 (von Kienlin 2013), which we set as the starting time  $t_0$  throughout the entire analysis. After 51.1 s, the Burst Alert Telescope (BAT) onboard *Swift* was triggered. The *Swift* Ultra Violet Optical Telescope (UVOT) and the *Swift* X-ray Telescope (XRT) began observing at 181 s and 195 s after the GBM trigger respectively (Maselli et al. 2013). Since this was an extremely bright burst, successively more telescopes pointed at the source: the Gemini North telescope at Hawaii (Levan et al. 2013), the Nordic Optical Telescope (NOT) (Xu et al. 2013) and the VLT/X-shooter (Flores et al. 2013) which confirmed the redshift  $z = 0.34$ .

GRB 130427A is one of the few GRBs with an observed adequate fluence in the optical, X-ray and GeV bands simultaneously for hundreds of seconds. In particular it remained continuously in the LAT field of view until 750 s after the trigger of *Fermi*-GBM (Ackermann et al. 2013), which gives us the best opportunity so far to compare the light curves and spectra in different energy bands, and to verify our IGC paradigm. We did the data reduction of *Fermi* and *Swift* satellites by the following methods.

*Fermi*: Data were obtained from the Fermi Science Support Center<sup>8</sup>, and were analyzed using an unbinned likelihood method with Fermi Science Tools v9r27p1<sup>9</sup>. Event selections *P7SOURCE\_V6* and *P7CLEAN\_V6* were used, depending on which one gave more stable results. Recommended data cuts were used (e.g.,  $z_{max} = 100$  degree). The background is composed of the galactic diffuse emission template and the isotropic emission template as well as about 60 point sources which are within the 15 degree radius of the GRB (however, their contribution was found to be negligible). The parameters for the background templates were held fixed during the fit. Luminosity light curve in Figure 5 corresponds to the energy range of 100 MeV to 100 GeV, circle radius of 15 degrees, with a power law spectra assumption. Since the data points up to the last two give a photon index of  $\sim 2.1$  with small errors, we set the photon index for the last two points to the value 2.1 during the fitting procedure in order to obtain more stable results. The light curve can be obtained with great temporal detail before 750 s. However, since we are interested in the general behavior of *Episode 3*, for simplicity we neglected such a fine temporal structure and we rebinned the light curve. Therefore there are only 3 data points up to 750 s. The spectrum is plotted in Figure 6.

*Swift*: XRT data were retrieved from UKSSDC<sup>10</sup> and were analyzed by the standard Swift analysis software included in the NASA’s Heasoft 6.14 with relevant calibration files<sup>11</sup>. In the first 750 s only Windows Timing (WT) data exists and the average count rate exceeds 300 counts/s: the highest count rate even reaches up to 1000 counts/s, far beyond the value of 150 counts/s which is suggested for the WT mode as a threshold of considering pile-up effects (Evans et al. 2007). Pile-up effects cause the detector to misrecognize two or more low energy photons as a single high energy photon, which softens the spectrum. We adopted the method proposed by Romano et al. (2006), fitting dozens of spectra from different inner sizes of box annulus selections in order to determine the extent of the distorted region. Taking the time interval 461 s

<sup>8</sup> <http://Fermi.gsfc.nasa.gov>

<sup>9</sup> <http://Fermi.gsfc.nasa.gov/ssc/data/analysis/software/>

<sup>10</sup> <http://www.Swift.ac.uk>

<sup>11</sup> <http://heasarc.gsfc.nasa.gov/lheasoft/>

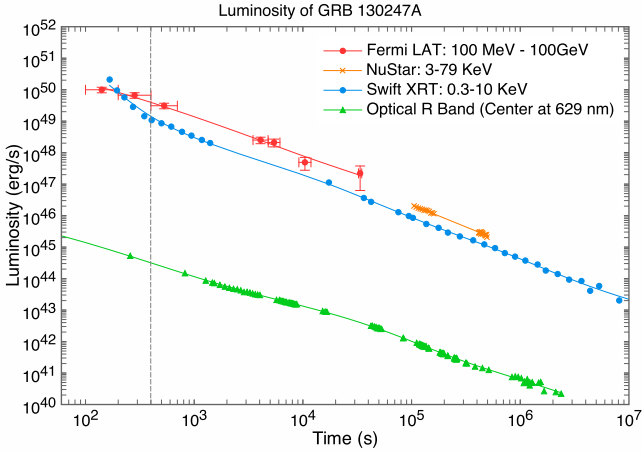


**Figure 5.** The multi-wavelength light curve of GRB 130427A. The high energy (100 MeV–100 GeV) emission detected by *Fermi*-LAT marked with red and soft X-ray (0.3–10 keV) data from *Swift*-XRT marked with blue are deduced from the original data. *NuStar* data (3–79 keV) marked with orange comes from (Kouveliotou et al. 2013). The optical (R band, center at 629 nm) data marked with green comes from ground based satellites (Perley et al. 2013). The error bars are too small with respect to the data points except for *Fermi*-LAT data. The horizontal error bars of *Fermi*-LAT represent the time bin in which the flux is calculated and vertical bars are statistical  $1-\sigma$  errors on the flux (the systematic error of 10% is ignored). The details in the first tens of seconds are ignored as we are interested in the behavior of the high energy light curve on a longer time scale. The vertical gray dashed line at ( $\sim 400$ s) indicates when the constant decaying slope starts. It is clear that all the energy bands have almost the same slope after 400 s in *Episode 3*.

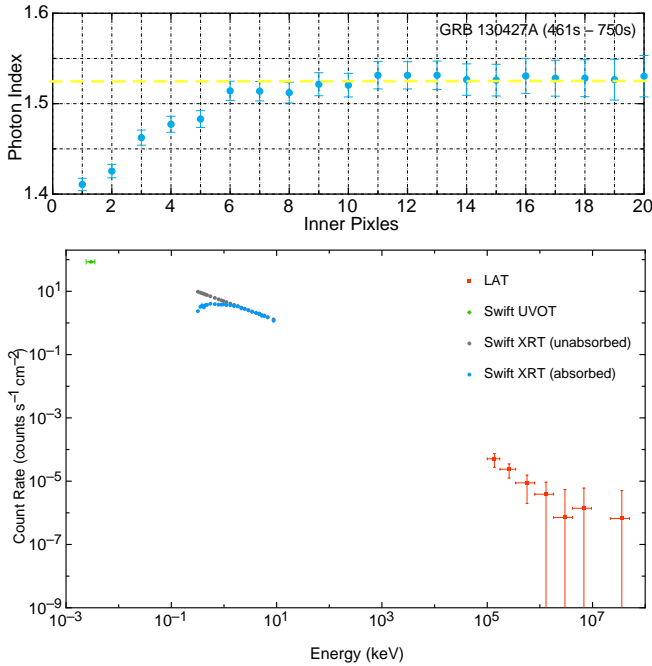


**Figure 6.** Top: Data from the *Swift*-XRT (0.3–10 keV) in the time range of 461–750 s for GRB 130427A. The data shows the photon index for different region selections after considering the pile up effect. After 6 inner pixels the photon index approaches an almost constant value of 1.52. Bottom: Spectra of GRB 130427A in the time range of 461–750 s. The green data points are from *Swift*-UVOT (Perley et al. 2013), the blue and gray points come from *Swift*-XRT and red data correspond to *Fermi*-LAT. The horizontal error bars are energy bins in which the flux is integrated and the vertical ones are  $1-\sigma$  statistical errors on the count rate. The gray data points correspond to unabsorbed *Swift*-XRT data while the blue ones are obtained with the assumption of absorption.

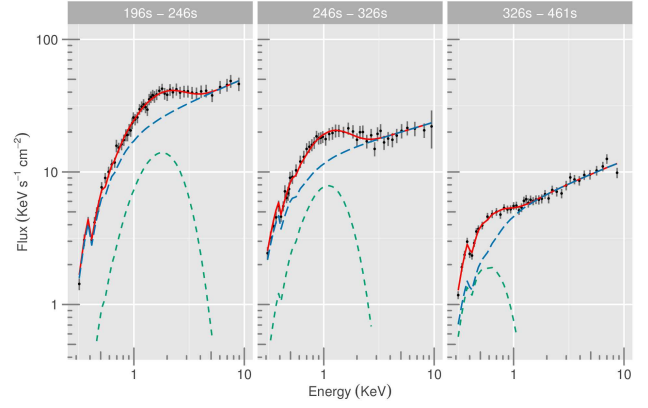


**Figure 7.** Spectral fitting of three time intervals (196s - 246s, 246s - 326s, 326s - 461s) in *Episode 3*, data come from *Swift*-XRT (0.3 keV - 10 keV, without pile-up area). Black points are the deduced data, green dashed line presents the thermal component, blue long-dashed line is the power law component, and red line shows the combination of these two components. Clearly the flux of thermal component drops and the temperature decreases along the time.

to 750 s as an example, the deviation comes from where the inner size is smaller than 6 pixels, shown in Figure 6. Then we applied the standard XRT data analyzing process (Evans et al. 2007, 2009) to obtain the spectrum, plotted in Figure 6. For the luminosity light curve, we split XRT observations in the nominal 0.3–10 keV energy range to several slices with a fixed count number, and we followed the standard procedure (Evans et al. 2007, 2009) and considered the pile-up correction. The XRT light curves of different bands are shown in Figure 5.

### 3.3. The X-ray qualification of GRB 130427A as a BdHN

Here we first focus on the extended X-ray emission of *Episode 3* which, as we have shown above, gives the qualifying features for the identification of GRB 130427A as a BdHN. We first proceed to identify the power law component of the light curve after the steep decay and the end of this plateau. This power law component, in the present case of this most energetic source GRB 130427A, has a power law index  $\alpha = -(1.31 \pm 0.01)$  and it extends all the way from 400 s to  $\sim 10^7$  s without jet breaks. These results are consistent with some previous papers (see e.g. in Perley et al. 2013; Laskar et al. 2013) which find no jet break, but differs from (Maselli et al. 2013) in which a break of the later time light curve is claimed.

We turn now to an additional crucial point: to confirm that the X-ray emission of *Episode 3* belongs to the SN ejecta and not to the GRB. To do this it is crucial, as already done for other sources (Ruffini et al. 2014b), to determine the presence of a thermal component in the early time of *Episode 3* and infer its temperature and the size of its emitter. Indeed, by analyzing the XRT data, we find that adding a blackbody component efficiently improves the fit with respect to a single power law from 196 s to 461 s. The corresponding blackbody temperature decreases in that time duration from 0.5 keV to 0.1 keV, in the observed frame. Figure 7 shows the evolution of the power law plus blackbody spectra in three time intervals, clearly the flux of thermal component drops along the time, as well as the temperature corresponding to the peak flux energy decreases. Kouveliotou et al. (2013) find that a single power law is enough to fit the *NuStar* data in the *NuStar* epochs, the reason could be that the thermal component has

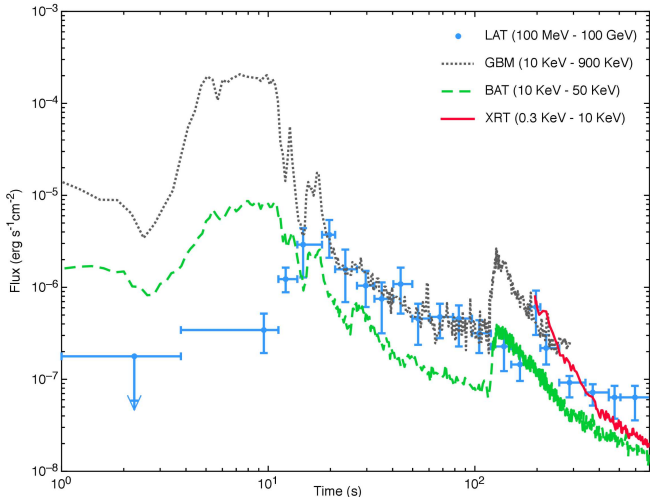


**Figure 8.** Flux of first 700 s. Blue points are the *Fermi*-LAT high energy emission from 100 MeV till 100 GeV (Ackermann et al. 2013), grey dotted line represents the *Fermi*-GBM, from 10 keV to 900 keV, green dashed line represents the photons detected by *Swift* BAT from 10 keV to 50 keV, and red solid line is the soft X-ray *Swift*-XRT detection, in the range of 0.3 KeV to 10 KeV. From this figure, clearly the *Fermi*-LAT emission reaches highest fluence at about 20 s while the gamma-ray detected by *Fermi*-GBM releases most of the energy within the first 10 s.

faded away or exceeded the observational capacity of the *Swift* satellite in the *NuStar* epochs, which start later than  $10^5$  s.

By assuming that the blackbody radiation is isotropic in the rest frame, the emitter radius along the light of sight increases from  $\sim 0.7 \times 10^{13}$  cm at 196 s to  $\sim 2.8 \times 10^{13}$  cm at 461 s in the observed frame, orders of magnitude smaller than the emission radius of the GRB, which is larger than  $10^{15}$  cm in the traditional GRB collapsar afterglow model. The size of  $10^{13}$  cm at hundreds of seconds is consistent with the observation of supernova ejecta. After considering the cosmological and the relativistic corrections,  $t_a^d \simeq t(1+z)/2\Gamma^2$ , where  $t$  and  $t_a^d$  are the time in the laboratory and observed frame respectively, and  $\Gamma$  is the Lorentz factor of the emitter, we get an expansion speed of  $\sim 0.8c$ , corresponding to Lorentz factor  $\Gamma = 1.67$ . These results contradict the considerations inferred in (Maselli et al. 2013)  $\Gamma \sim 500$ , which invoke a value of the Lorentz factor in the traditional collapsar afterglow model (see e.g. Mészáros 2006). Again in the prototypical GRB 090618, the Lorentz factors ( $1.5 \leq \Gamma \leq 2.19$ ) and emission radii ( $\sim 10^{13}$  cm) are very similar to the ones of GRB 130427A presented in Ruffini et al. (2014b). It is interesting that such a thermal component has been also found in the early parts of *Episode 3* of GRB 060729 (adopted in Fig. 4) and many other SN associated GRBs (see Ruffini et al. 2014b; Grupe et al. 2007; Starling et al. 2012).

### 3.4. Discussion of multi-wavelength observations in *Episode 3*

Now we turn to the most unexpected feature in the analysis of the optical, X-ray,  $\gamma$ -ray and very high energy emission in *Episode 3* of GRB 130427A. The optical emission was observed by *Swift*-UVOT and many ground-based telescopes (R band as an example for the optical observation). The soft X-ray radiation was observed by *Swift*-XRT (0.3–10 keV). Similarly the hard X-ray radiation was observed by *Swift*-BAT (15–150 keV) and by *NuStar* (3–79 keV). The gamma ray radiation was observed by *Fermi*-GBM (8 KeV–40 MeV), and the high energy radiation by *Fermi*-LAT (100 MeV –

100 GeV). The main result is that strong analogies are found in the late emission at all wavelengths in *Episode 3*: after 400s, these luminosities show a common power law behavior with the same constant index as in the X-ray (and clearly with different normalizations), by fitting multi-wavelength light curves together we have a power law index  $\alpha = -(1.3 \pm 0.1)$ .

Turning now to the spectrum, integrated between 461 s and 750 s, the energy range covers 10 orders of magnitude, and the best fit is a broken power law (see Fig. 6). In addition to the traditional requirements for the optical supernova emission in *Episode 4*, the much more energetically demanding requirement for the general multi-wavelength emission of *Episode 3* has to be addressed.

### 3.5. The onset of *Episode 3*

In the previous sections we have emphasized the clear evidence of GeV emission and its analogy in the late power law luminosities as functions of the arrival time for the X-ray, optical and GeV emissions. Equally important in this section is to emphasize some differences between the X-,  $\gamma$ -ray, and the high energy GeV emission, especially with respect to the onset of *Episode 3* at the end of prompt emission in *Episode 2* (see Fig. 8). We observe:

1) The  $\gamma$ -ray light curves, observed by *Fermi*-GBM and hard X-ray observed by *Swift*-BAT, have similar shapes. They reach the highest luminosity between 4 s to 10 s during the prompt emission phase of *Episode 2*.

2) The high energy ( $> 100$  MeV) GeV emission gradually rises up, just after the gamma and X-ray prompt emissions drop down at the end of *Episode-2*: the high energy GeV emission raises to its peak luminosity at about 20 s. The turn on of the GeV emission coincides, therefore, with the onset of our *Episode 3*. These considerations have been recently confirmed and extended by the earliest high energy observations in GRB 090510 (Ruffini et al. 2014, submitted to ApJL).

3) At about 100 s, the *Swift*-XRT starts to observe the soft X-ray and a sharp spike appears in the hard X-ray and gamma ray bands (see Fig. 8). Only at this point the *Swift*-XRT started to observe soft X-ray. We are currently addressing the occurrence of the spike to the thermal emission observed to follow in the sharp decay of the X-ray luminosity prior to the plateau and the above mentioned common power law decay (Ruffini et al. 2014).

The detailed analysis of the prolonged emission observed by *Fermi*-LAT in GeV enables us to set specific limits on the Lorentz factor of this high energy emission. We have analyzed the GeV emission from  $\sim 300$  s to  $2.5 \times 10^4$  s, dividing this time interval into seven sub-intervals and in each of them collecting the corresponding maximum photon energy and photon index of the spectral energy distribution, as shown in Ackermann et al. (2013, Fig. 2). We have focused our attention on the estimate on the Lorentz factor for this high energy component from the usual optical depth formula for pair creation  $\tau_{\gamma\gamma}$  (see, e.g., Lithwick & Sari 2001; Gupta & Zhang 2008). We have computed for different values of radii of the emitter, the corresponding Lorentz factors at the transparency condition, i.e.,  $\tau_{\gamma\gamma} = 1$ , see the solid curves in Figure 9. The constraints on the size of the emitting regions come from causality in the ultra-relativistic regime, i.e.,  $R_{em} = 2\Gamma^2 c \Delta t$ , where  $\Delta t$  corresponds to the duration of the time intervals under consideration (see the dot-dashed curves in Figure 9). The values of the Lorentz factor ranges between  $\sim 10$  and  $\sim 40$  and correspondingly, the radii of the emitting region at the transparency

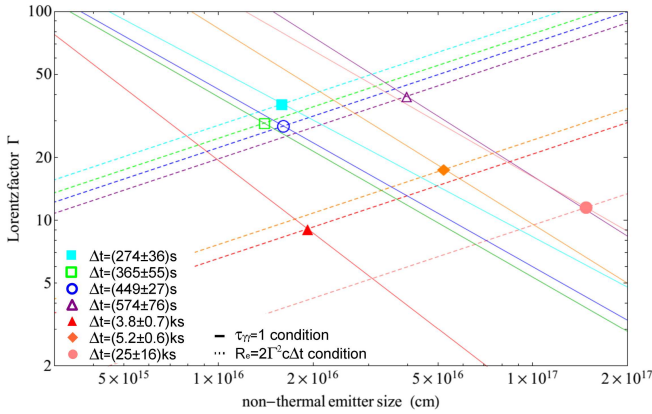


**Figure 9.** Constraints on the Lorentz factors and on the size of the GeV emitting region at the transparency point. Solid curves represent the curves defined by varying the emitting region size from the  $\tau_{\gamma\gamma} = 1$  condition; dot-dashed curves represent the radius of the emitter obtained from causality in the ultra-relativistic regime, i.e.,  $R_{em} = 2\Gamma^2 c \Delta t$ . Filled circles correspond to the solutions of both the limits. The different colors refer to the time intervals from  $\sim 273$  s to 24887 s, in the order: cyan, green, blue, purple, red, orange, and pink.

point are located between  $\sim 10^{16}$  cm and  $\sim 2 \times 10^{17}$  cm (see the filled circles in Figure 9).

### 3.6. General considerations on recent theoretical progress on BdHD

The concurrence of the above well-defined scaling laws and power law of the observed luminosities both in the X-ray and/or in the optical domains in the *Episode 3* of GRB 130427A have been considered arguments in favor for looking to the  $r$ -process and to heavy nuclei radioactive decay as the energy sources (Ruffini et al. 2014b), (see the pioneering work of Li & Paczynski 1998). The extended interaction of the  $\nu$ -NS and its binary NS companion in the SN ejecta provides environment for  $r$ -processes to create the needed neutron rich very heavy elements to attribute some of the electromagnetic energy in *Episode 3* to nuclear decay,  $\approx 10^{52}$  erg. Alternatively, we are considering emission originating from type-I and type-II Fermi acceleration mechanisms, introduced by Fermi precisely to explain the radiation process in the SN remnants (Fermi 1949). Also these processes can lead to a power law spectrum (Aharonian 2004), similar to the one presented in this article and in our recent letter (Ruffini et al. 2014b). The GRB emission of *Episode 2* interacting with the Supernovae ejecta could represent that energy injection long sought by Fermi for the onset of his acceleration mechanism (Fermi 1949).

Both of the above processes can indeed operate as energy sources for the mildly relativistic X-ray component and the relativistic GeV emission of *Episode 3*.

We are currently examining additional BdHN sources and giving particular attention to understanding the highest GeV energy emission, which is unexpected in the traditional  $r$ -process. The inferred  $\Gamma$  Lorentz factor for the GeV emission point to the possibility of a direct role of the two remaining components in the IGC paradigm: the newly born neutron star ( $\nu$ NS) and the just born Black Hole (see Fig. 1) There is also the distinct possibility that these two systems have themselves become members of a newly born binary system<sup>12</sup> (Rueda &

<sup>12</sup> Presentation of R.Ruffini in Yerevan: <http://www.icranet.org/images/stories/Meetings/meetingArmenia2014/talks/ruffini-1.pdf>

Ruffini 2012).

## 4. CONCLUSION

We have recalled that GRB 130427A is one of the most energetic GRBs ever observed ( $E_{iso} \simeq 10^{54}$  ergs), with the largest  $\gamma$ -ray fluence and the longest lasting simultaneous optical, X-ray,  $\gamma$ -ray and GeV observations of the past 40 years. For this reason we have performed our own data analysis of the *Swift* and *Fermi* satellites (see Secs. 3) in order to probe the BdHN nature of this source (see Sec. 3.3) and infer new perspectives for the IGC paradigm and the physical and astrophysical understanding of GRB.

We summarize the main results by showing how the analysis of GRB 130427A should be inserted in a wider context with three different areas: a) the formulation and the observational consequences of the IGC paradigm; b) the comprehension induced by the multi-wavelength observations of GRB130427A; c) the BDHN versus HN properties. Relevance of BDHN in establishing a new alternative distance indicator in astrophysics. Each one of these topic is going to be summarized in 3 bullets.

With reference to the formulation and observational consequences of the IGC paradigm:

1a) The IGC paradigm introduces in Astrophysics a new experience which has been already successfully applied in particle physics: to understand that a system traditionally considered elementary is actually a composed system and that new components in the system can appear at the effect of collisions or decay. Well known physical examples are represented by the introduction of the quark Aad et al. (2012), or the creation of new particles in a decay or collision of elementary particle systems: the Fermi theory of beta decay or the mesons production in an electron positron collision in storage rings are classical examples. These facts are today routinely accepted in particle physics although Fermi had to spend efforts to explain them at the time (Fermi 1934). In astrophysics this situation is new: to see that a process until recently considered elementary, as the GRB, does indeed contains four different astrophysical systems and that two of them, the FeCO core undergoing SN and the companion NS binary, interacting give origin to two different new system a  $\nu$ NS and a BH and especially that the entire process occur in less the 200 s is a totally new condition. For its understanding a new approach technically and conceptually is needed. The new style of research is more similar to the one adopted in particle physics then the one in classical astronomy, see Figure 1.

2a) Possibly the most profound novelty in this approach, for the understanding of GRBs, has been the introduction of the four episodes shortly summarized in Sec.1. The traditional GRB description corresponds to *Episode 2*. *Episode 1* corresponds to the dynamical accretion of the SN ejecta onto the companion NS. We are now considering an enormous rate of accretion of  $10^{31}$  g  $s^{-1}$ ,  $10^{15}$  times larger then the one usually considered in binary X-ray source in systems like Centaurus X-3 or Cygnus X-1 (see e.g., in Giacconi & Ruffini 1975). This process has opened a new field of research by presenting the first realization of the hypercritical accretion introduced by Bondi-Hoyle-Littleton as well the testing ground of the neutrinos emission pioneered in the Zel'dovich et al. (1972) and Ruffini & Wilson (1975), see Sec. 1. The pure analytic simplified solutions in Rueda & Ruffini (2012) have been now supported by direct numerical simulation in Fryer et al. (2014, and Fig. 1 therein).

3a) The main revolution of the IGC paradigm for GRBs

comes from the discovery of the universal laws discovered in *Episode 3* which compare and contrast to the explosive, irregular phases, varying from source to source in all observed GRBs, in their *Episode 1* and *Episode 2*. The universality of *Episode 3* as well as the precise power laws and scaling laws discovered changes the field of GRB analysis making it one of time resolved, high precision, reproducible measurements. Additional unexplored physical phenomena occurs in *Episode 3*, adding to the new ultra-relativistic regimes already observed in the *Episode 2* in previous years<sup>13</sup>, see Figure 3 and Figure 4 as well as Figure 5.

With reference to the comprehension induced by the multi-wavelength observations of GRB130427:

1b) Following the work on the *GS* (Pisani et al. 2013) and the more recent work on the nested structures (Ruffini et al. 2014b), we have first verified that the soft X-ray emission of GRB 130427A follows for time  $t \simeq 10^4$  s the power-law decay described in Pisani et al. (2013). Surprisingly in this most energetic GRB unveils such power-law behavior already exists at the early time as  $t \sim 100$  s (details in Ruffini et al. (2014b)). From the X-ray thermal component observed at the beginning of *Episode 3* following a spiked emission at  $\sim 100$  s, a small Lorentz factor of the emitter is inferred ( $\Gamma < 2$ ): this X-ray emission appear to originate in a mildly relativistic regime with a velocity  $v \sim 0.8c$ , in addition it does not appear to have substantial beaming and appears to be relatively symmetric and with no jet break, see Figure 5, and Ruffini et al. (2014b, Figure 2).

2b) We have proceeded to make a multi-wavelength analysis of *Episode 3* where we have compared and contrasted optical data from *Swift*-UVOT and ground based telescopes, X-ray data from *Swift*-XRT,  $\gamma$ -ray data from *Fermi*-GBM, as well as very high energy data in the GeV from *Fermi*-LAT. The high energy emission appears to be detectable at the end of the prompt radiation phase in *Episode 2*, when the fluence of X-ray and  $\gamma$ -ray of the prompt exponentially decrease and becomes transparent for the very high energy photons in the *Fermi*-LAT regime. From the transparency condition of the GeV emission a Lorentz Gamma factor of 10–40 is deduced. In principle this radiation, although no brake in its power law is observed, could be in principle beamed, see Figure 9.

3b) Although the light curves of X-ray and GeV emission appear to be very similar, sharing similar power-law decay index, their Lorentz  $\Gamma$  factors appear to be very different, and their physical origin are necessarily different. Within the IGC model the X-ray and the high energy can originate from the interaction of some of the physical components (e.g., neutron star and black hole) newly created in the C-matrix: the interaction of the GRBs with the SN ejecta (Ruffini et al. 2014) may well generate the X-ray emission and the associated thermal component. The high energy should be related to the novel three components, the BH, the  $\nu$ NS and the SN ejecta. From the dynamics it is likely that the  $\nu$ NS and the BH form a binary system, see e.g., Rueda & Ruffini (2012) and the presentation by one of the authors<sup>14</sup>.

With reference to the the BDHN versus HN properties:

1c) The verification of the BdHN paradigm in GRB 130427A has confirmed that for sources with isotropic energy approximately  $10^{54}$  erg, the common power law behav-

ior is attained at earlier times, i.e.,  $\sim 10^3$  s, and higher X-ray luminosities than the characteristic time scale indicated in (Pisani et al. 2013), see Figure 3. From the observation of the constant-index power law behavior in the first  $2 \times 10^4$  s of the X-ray luminosity light curve, overlapping with the known BdHNe, it is possible to have an estimate of: 1) the redshift of the source, 2) the isotropic energy of the GRB and 3) the fulfillment of the necessary and sufficient condition for predicting the occurrence of the SN after  $\sim 10$  days in the rest frame of the source, see e.g., GCN 14526. This procedure has been successfully applied to GRB 140512A (Ruffini et al. in preparation).

2c) The overlapping with the *GS* members of the late X-ray emission observed by *Swift* XRT, referred to the rest frame of the source, introduces a method to establish and independent distance estimator of the GRBs. Although this method has been amply applied (e.g. GRBs 060729, 061007, 080319, 090618, 091127, 111228A), we also declare that there are some clear outlier to this phenomenon: GRB 060614 (Ruffini et al. 2013a), 131202A (Ruffini et al. 2013c) and 140206A (Ruffini et al. 2014a). These are all cases of great interest and the solution of this contradictions may reveal to be of particular astrophysical significance. Particularly interesting is the case of GRB 060614 since the cosmological redshift has not been directly measured and there can be a misidentification of the host galaxy (Cobb et al. 2006).

3c) As first pointed out in Rueda & Ruffini (2012) and Ruffini et al. (2014b), further evidenced in Fryer et al. (2014), the crucial factor which may explain the difference between the *family 1* and *family 2* of GRBs is the initial distance between the FeCO core and its binary NS companion. The accretion from the SN ejecta onto the companion NS and the consequent emission process decrease by increasing this distance: consequently is hampered the possibility for the binary companion NS to reach its critical mass (see Fig. 3 and Fig. 4 in Izzo et al. 2012, and the discuss therein). Unlike *family 2*, in *family 1* no BH is formed, no GRB is emitted, and no *Episode 2* nor *Episode 3* exist, only a softer and less energetic radiation from the accretion onto the neutron star will be observed in these sources. The problem of explaining the coincidence between the GRB and supernova in the case of the *family 1* is just a tautology: no GRB in this family exist but only a hypernova Ruffini et al. (2014b).

This article addresses recent results on the IGC paradigm applied to long GRBs. The IGC paradigm and the merging of binary neutron stars has been also considered for short GRBs (see e.g., Muccino et al. 2013a,b, 2014; Ruffini et al. 2014b) and is now being further developed.

We acknowledge the use of public data from the *Swift* and *Fermi* data achieve. We thank Robert Jantzen for his careful reading and valuable advise. We also thank the editor and the referee for their constant attention and beneficial suggestions which largely improve this article. ME, MK and GBP are supported by the Erasmus Mundus Joint Doctorate Program by Grant Numbers 2012-1710, 2013-1471 and 2011-1640, respectively, from the EACEA of the European Commission.

## REFERENCES

<sup>13</sup> Presentation of R.Ruffini in 13th Marcel Grossmann Meeting: <http://www.icra.it/mg/mg13>

<sup>14</sup> Presentations of R.Ruffini in Yerevan: <http://www.icranet.org/images/stories/Meetings/meetingArmenia2014/talks/ruffini-1.pdf>

Aad, G., Abajyan, T., Abbott, B., et al. 2012, Phys. Lett. B, 716, 1  
Ackermann, M., Ajello, M., Asano, K., et al. 2013, Science, 343, 42  
Aharonian, F. A. 2004, Very high energy cosmic gamma radiation : a crucial window on the extreme universe  
Bernardini, C. 2004, Physics in Perspective, 6, 156

- Bloom, J. S., Perley, D. A., Li, W., et al. 2009, *ApJ*, 691, 723
- Bondi, H. 1952, *MNRAS*, 112, 195
- Bondi, H., & Hoyle, F. 1944, *MNRAS*, 104, 273
- Broderick, A. E. 2005, *MNRAS*, 361, 955
- Cobb, B. E., Bailyn, C. D., van Dokkum, P. G., & Natarajan, P. 2006, *ApJ*, 651, L85
- de Ugarte Postigo, A., Xu, D., Leloudas, G., et al. 2013, *GCN Circ.*, 14646
- Evans, P. A., Beardmore, A. P., Page, K. L., et al. 2007, *A&A*, 469, 379
- , 2009, *MNRAS*, 397, 1177
- Fermi, E. 1934, *Il Nuovo Cimento*, 11, 1
- , 1949, *Phys. Rev.*, 75, 1169
- Flores, H., Covino, S., Xu, D., et al. 2013, *GCN Circ.*, 14491
- Friis, M., & Watson, D. 2013, *ApJ*, 771, 15
- Fryer, C. L., Benz, W., & Herant, M. 1996, *ApJ*, 460, 801
- Fryer, C. L., Rueda, J. A., & Ruffini, R. 2014, *arXiv.org*, 1473
- Fryer, C. L., Woosley, S. E., & Hartmann, D. H. 1999, *ApJ*, 526, 152
- Galama, T. J., Vreeswijk, P. M., van Paradijs, J., et al. 1998, *Nature*, 395, 670
- Giacconi, R., & Ruffini, R. 1975, *Physics and Astrophysics of Neutron Stars and Black Holes*
- Grupe, D., Gronwall, C., Wang, X.-Y., et al. 2007, *ApJ*, 662, 443
- Guetta, D., & Della Valle, M. 2007, *ApJL*, 657, L73
- Gupta, N., & Zhang, B. 2008, *MNRAS*, 384, L11
- Izzo, L., Rueda, J. A., & Ruffini, R. 2012, *A&A*, 548, L5
- Kouveliotou, C., Granot, J., Racusin, J. L., et al. 2013, *ApJ*, 779, L1
- Kovacevic, M., Izzo, L., Wang, Y., et al. 2014, 1408.6227
- Laskar, T., Berger, E., Zauderer, B. A., et al. 2013, *ApJ*, 776, 119
- Levan, A. J., Cenko, S. B., Perley, D. A., & Tanvir, N. R. 2013, *GCN Circ.*, 14455
- Levan, A. J., Fruchter, A. S., Graham, J., et al. 2013a, *GCN Circ.*, 1468
- Levan, A. J., Tanvir, N. R., Fruchter, A. S., et al. 2013b, *arXiv*, 5338
- Li, L.-X., & Paczynski, B. 1998, *ApJ*, 507, L59
- Lithwick, Y., & Sari, R. 2001, *ApJ*, 555, 540
- Maselli, A., Beardmore, A. P., Lien, A. Y., et al. 2013, *GCN Circ.*, 14448
- Maselli, A., Melandri, A., Nava, L., et al. 2013, *Science*
- Mészáros, P. 2006, *Rep. Prog. Phys.*, 69, 2259
- Muccino, M., Ruffini, R., Bianco, C. L., Izzo, L., & Penacchioni, A. V. 2013a, *ApJ*, 763, 125
- Muccino, M., Ruffini, R., Bianco, C. L., et al. 2013b, *ApJ*, 772, 62
- Muccino, M., Bianco, C. L., Izzo, L., et al. 2014, *Gravitation and Cosmology*, 20, 197
- Nava, L., Sironi, L., Ghisellini, G., Celotti, A., & Ghirlanda, G. 2013, *MNRAS*, 433, 2107
- Nousek, J. A., Kouveliotou, C., Grupe, D., et al. 2006, *ApJ*, 642, 389
- Page, K. L., Starling, R. L. C., Fitzpatrick, G., et al. 2011, *MNRAS*, 416, 2078
- Penacchioni, A. V., Ruffini, R., Bianco, C. L., et al. 2013, *A&A*, 551, A133
- Penacchioni, A. V., Ruffini, R., Izzo, L., et al. 2012, *A&A*, 538, 58
- Perley, D. A., Cenko, S. B., Corsi, A., et al. 2013, *ApJ*, 781, 37
- Pian, E., Amati, L., Antonelli, L. A., et al. 2000, *ApJ*, 536, 778
- Piran, T. 2005, *RMP*, 76, 1143
- Pisani, G. B., Izzo, L., Ruffini, R., et al. 2013, *A&A*, 552, L5
- Rhoads, J. E. 1999, *ApJ*, 525, 737
- Romano, P., Campana, S., Chincarini, G., et al. 2006, *A&A*, 456, 917
- Rueda, J. A., & Ruffini, R. 2012, *ApJL*, 758, L7
- Ruffini, R., Bianco, C. L., Frascchetti, F., Xue, S.-S., & Chardonnet, P. 2001, *ApJ*, 555, L117
- Ruffini, R., Salmonson, J. D., Wilson, J. R., & Xue, S.-S. 1999, *Astronomy and Astrophysics*, 350, 334
- , 2000, *Astronomy and Astrophysics*, 359, 855
- Ruffini, R., Vereshchagin, V., & Wang, Y. 2014, In preparation
- Ruffini, R., & Wilson, J. R. 1975, *PRD*, 12, 2959
- Ruffini, R., Bernardini, M. G., Bianco, C. L., et al. 2008, *Proceeding of The Eleventh Marcel Grossmann Meeting*, 368
- Ruffini, R., Bianco, C. L., Enderli, M., et al. 2013a, *GCN Circ.*, 15560, 1
- , 2013b, *GCN Circ.*, 14526
- , 2013c, *GCN Circ.*, 15576, 1
- , 2014a, *GCN Circ.*, 15794, 1
- Ruffini, R., Muccino, M., Bianco, C. L., et al. 2014b, *A&A*, 565, L10
- Ruffini, R., Izzo, L., Muccino, M., et al. 2014, *arXiv*, 1840
- Starling, R. L. C., Page, K. L., Pe'er, A., Beardmore, A. P., & Osborne, J. P. 2012, *MNRAS*, 427, 2950
- Tanvir, N. R., Rol, E., Levan, A. J., et al. 2010, *ApJ*, 725, 625
- Tavani, M. 1998, *ApJL*, 497, L21
- Trotter, A., Reichart, D., Haislip, J., et al. 2013, *GCN Circ.*, 1466
- van Eerten, H., Zhang, W., & MacFadyen, A. 2010, *ApJ*, 722, 235
- van Eerten, H. J., & MacFadyen, A. I. 2012, *ApJ*, 751, 155
- von Kienlin, A. 2013, *GCN Circ.*, 14473
- Woosley, S. E. 1993, *ApJ*, 405, 273
- Xu, D., de Ugarte Postigo, A., Schulze, S., et al. 2013, *GCN Circ.*, 14478
- Xu, D., de Ugarte Postigo, A., Leloudas, G., et al. 2013, *ApJ*, 776, 98
- Zel'dovich, Y. B., Ivanova, L. N., & Nadezhin, D. K. 1972, *Soviet Astron.*, 16, 209